THE ROLE OF PROTEOLYTIC PROCESSING OF THE 220KDA POLYPROTEIN OF AFRICAN SWINE FEVER VIRUS AND AGGRESOMES DURING VIRION ASSEMBLY

COLIN MALCOLM HEATH

A THESIS SUBMITTED IN PARTIAL FULFILMENT

OF THE REQUIREMENTS OF THE

UNIVERSITY COLLEGE OF LONDON

FOR THE DEGREE OF

DOCTOR OF PHILOSOPHY

THE PROGRAMME OF RESEARCH WAS CARRIED OUT AT THE

INSTITUTE FOR ANIMAL HEALTH, PIRBRIGHT

JUNE 2000

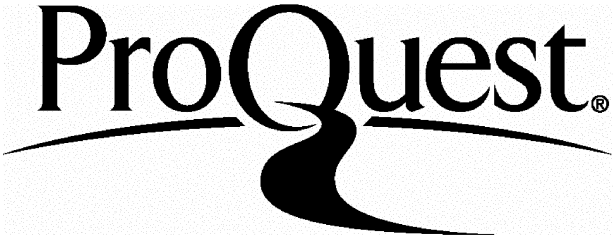

Acknowledgements

Firstly, I would like to thank Dr. Tom Wileman for his supervision and support throughout this project and for combating "thesis fatigue".

I would like to thank my two favourite "technicians", Miriam Windsor and Liz Reid, for their support in the lab and for making Pirbright so much fun. Also a special thanks to Mirrie for the excellent proof reading.

Thanks to Stephen for his friendship and the patience he had to share a house with me for the last 3½ years, only wish you could learn to wash up!

Special thanks to Paul Smith for giving me a superb aggression release and without who this may have been completed earlier.

Thanks to my personal taxi driver and for making a trip to casualty so, so entertaining. Cheers Val, I'll get you a double vodka and orange.

Thanks to Steven Archibald for the help with the images, thanks to Dr. Paul Monaghan and Hannah Cook for generating the EM images, and thanks to Sheila Shrigley and Janette Farley for my office and help with my references.

A special thanks to the two most important women in my life. Firstly my Mum, thanks for the support and for always being there. And finally, thanks to Laura for her support and especially her patience and those other things she does so well.

Abstract

African swine fever virus (ASFV) is a large double stranded DNA virus causing a lethal haemorrhagic disease in domestic pigs. The 170kbp genome encodes 150 open reading frames and virions contain more than 50 different proteins. ASFV uses a 220kDa polyprotein (pp220) to produce major structural proteins p150, p37, p34 and p14. This thesis investigates the subcellular distribution and regulation of pp220 processing. Antibodies specific for p150 and p34 were generated and characterised. Western blot analysis showed that approximately 35% of the intracellular pool of pp220 associated with membranes, the remainder was cytosolic. The membrane bound pool was processed via intermediates to p34 and p150. p34 and p150, but not the polyprotein, or the processing intermediates, were enveloped and released in virions. The cytosolic pool was processed incorrectly and failed to produce structural proteins. The correct processing of pp220 occurs at 4 Gly-Gly-X motifs, however the polyprotein contains 19 Gly-Gly-X motifs. It was concluded that membrane association is required for correct processing. In the absence of membrane association the polyprotein maybe cleaved at all 19 Gly-Gly-X motifs.

Aggresomes are a major site of proteolysis in cells and their role in ASFV assembly was investigated. Aggresomes are pericentriolar structures enriched for chaperones, proteasomes and ubiquitin. They are enclosed in a vimentin cage surrounded by mitochondria (Johnston et al, 1998. J. Cell Biol. 143:1883-1898). ASFV assembly occurs in perinuclear structures called viral factories and the possibility that these derive from aggresomes was investigated. Immunofluorescence experiments showed viral factories close to the centriole and surrounded by vimentin cages and mitochondria. Furthermore, inhibitors of

aggresome proteolysis and the over expression of misfolded proteins in the cytosol blocked viral replication. It is possible that ASFV uses aspects of the aggresomes to concentrate viral proteins during assembly.

Contents

Figures and tables.

Abbreviations

ΔF508:	Mutant cystic fibrosis transmembrane conductance regulator
α-p150C:	Antibody raised against a peptide of the p150 C-terminus
α-p150N:	Antibody raised against a peptide of the p150 N-terminus
α-p34C:	Antibody raised against a peptide of the p34 C-terminus
2D:	Two dimensional
ALLN:	Acetyl-leucyl-leucyl-norleucinal
ASF:	African swine fever
ASFV:	African swine fever virus
ATP	Adenosine triphosphate
BA71v:	Badajoz 1971 Vero adapted strain of ASFV
bp:	Base pair
BSA:	Bovine serum albumin
BSC:	Monkey African green kidney epithelial cells
BTV:	Bluetongue virus
CFTR:	Cystic fibrosis transmembrane conductance regulator
CMXRos:	Chloromethyl derivatives of X rosamine
Cos-7:	African green kidney cells
DAPI:	4'-6-Diamidino-2-phenylindole
dH_2O:	Distilled water
DMEM:	Dulbecco's modified Eagle's medium
DMSO:	Dimethyl sulphoxide
DNA:	Deoxyribonucleic acid
DTT:	Dithiothreitol
E.coli:	*Escherichia coli*

ECL:	Enhanced chemiluminescence
EDTA:	Ethylenediaminetetra-acetic acid
EEV:	Extracellular envelope virus
EM:	Electron microscopy
ER:	Endoplasmic reticulum
ERGIC:	Endoplasmic reticulum/Golgi intermediate compartment
FCS:	Foetal calf serum
FITC:	Fluorescein isothiocyanate
FMDV:	Foot and mouth disease virus
FV3:	Frog virus 3
GFP-250	Green fluorescent protein fused to C-terminus of p115
GFP:	Green fluorescent protein
Gln	Glutamine
Gly	Glycine
HCl:	Hydrochloric acid
Hdj-1:	Chaperone of the Hsp40 family
Hdj-2:	Human homolgue of DNAJ
HEK 293:	Human embryo kidney 293 cells
HEPES:	N-2-hydroxyehtylpiperazine-n'[2-ethanesulfonic acid]
hpi:	Hours post infection
HRP:	Horseradish peroxidase
Hsc70:	Constitutive 70kDa heat shock protein
Hsp70:	70kDa heat shock protein
Hsp90:	90kDa heat shock protein
HSV:	Herpes simplex virus

HSV-1:	Herpes simplex virus type 1
IBRS2:	Instituto Biol Renal Swine cells
IC:	Intermediate compartment
IEV:	Intracellular envelope virus
IF:	Intermediate filament
Ig:	Immunoglobulin
Ile	Isoleucine
IMV:	Intracellular virions
IPB:	Immunoprecipitation buffer
IPTG:	Isopropyl-β-*D*-thiogalactopyranoside
ITR:	Inverted terminal repeat
IV:	Immature virion
kbp:	Kilobase pairs
kDa:	Kilodaltons
KLH:	Keyhole limpet hemocyanin
Leu	Leucine
Met	Methionine
MOI	Multiplicity of infection
mRNA:	Messenger ribonucleic acid
MTOC:	Microtubule organising centre
NE:	Nuclear envelope
NGS:	Normal goat serum
NP40:	Nonidet P-40
NTP	Nucleotide triphosphate
ORF:	Open reading frame

p14:	14kDa final protein
p150:	150kDa final protein
p34:	34kDa final protein
p34R:	Recombinant p34
p37:	37kDa final protein
p37R:	Recombinant p34
PA28:	180kDa proteasome activator
PA700:	700kDa proteasome activator
PAGE:	Polyacrylamide gel electrophoresis
PBS:	Phosphate buffered saline
PCR:	Polymerase chain reaction
PM:	Plasma membrane
PMSF:	Phenylmethylsulfonyl fluoride
pp220:	220kDa polyprotein
RNA:	Ribonucleic acid
rpm:	Revolutions per minute
RT	Room temperature
SDS:	Sodium dodecyl sulphate
SPB:	Sample preparation buffer
SPI:	Small protease inhibitors
TBS:	Tris buffered saline
$TCID_{50}$	50% tissue culture infectious dose
TCP-1:	T-complex polypeptide 1
TGN:	*Trans* Golgi network
TMV:	Tobacco mosaic virus

Tween-20:	Polyxyethylenesorbitan monolaurate
UBC:	Ubiquitin-conjugating
UBCv1:	Ubiquitin-conjugating enzyme
Vero:	African Green monkey kidney cells
X:	Any amino acid

1. Introduction.

1.1 African Swine Fever.

African swine fever (ASF) is a highly contagious, devastating haemorrhagic disease that affects the domestic pig. The etiological agent is the large, icosahedral deoxyvirus African swine fever virus (ASFV). This disease is transmitted by soft ticks of the *Ornithodorous* species, in which the virus replicates without causing disease (Plowright, 1977). ASFV infects different species of *Suidae* mammals including warthogs (*Phacochoerus aethiopicus*), bush pigs (*Potamochoerus porcus*) and domestic pigs (*Sus scrofa*) (reviewed in Mebus, 1988). Warthogs and bush pigs are the natural hosts of ASFV in which there is no apparent infection.

The disease was first described in Kenya in 1921 (Montgomery, 1921), and was subsequently recognised in other African countries, where it is still an economically devastating disease. The disease first spread from Africa to the Iberian peninsula in 1957 and since then ASFV has been introduced into a variety of countries, including Spain (1960), France (1964, 1967, 1974), Italy (1967, 1969/70, 1983), Cuba (1971, 1984), Brazil (1978-1981), The Dominican Republic (1978), Haiti (1978), Malta (1978), Sardinia (1978), Belgium (1986), and The Netherlands (1987) (Plowright, 1984, Wilkinson, 1989).

At present, ASFV is only endemic in Sardinia and some African countries. The more persistent strains of the virus pose a permanent threat to the pig industry worldwide. The major spread of the virus through Europe is by direct contact between domestic pigs and also through their contact with infected meat. ASFV is an economically important disease and the economic problems caused by an outbreak are increased by the fact that there is currently no vaccine. As a

result a slaughter policy is the only available method to control the spread of the virus.

1.2 Pathogenicity of ASFV.

The primary route of ASFV infection is the upper respiratory tract, after which the virus replicates in pharyngeal tonsils and then spreads throughout the lymph nodes of the head into the blood stream. The virus then rapidly spreads to cells of the mononuclear phagocytic system, reticuloendothelial cells of lymphoid tissue and other organs (Wilkinson and Wardley, 1978). A fever (40-42°C) develops, which persists for about 4 days depending on the virulence of the virus strain. Clinical signs observed after the onset of the fever include weakness, coughing, loss of appetite and haemorrhaging (Plowright, 1981). Other signs may include vomiting, bleeding from nose or anus, conjunctivitis and nasal and conjunctival discharge. The highly virulent strains from Africa, such as Malawi, cause almost 100% mortality of infected pigs after 7-10 days. The less virulent strains (Malta, 1978) produce milder clinical symptoms and the pigs may recover to become virus carriers.

1.3 Classification of ASFV.

ASFV is a large, enveloped, double stranded DNA virus with icosahedral symmetry. The virus was originally classified as an iridovirus due to their morphological similarities, cytoplasmic location and large DNA genome (Mathews, 1982; Goorha and Granoff, 1979). Recent investigations into the genome structure and replication strategy of ASFV show it is more closely related to the poxviruses. For example, the genome structure contains terminal inverted

repeats, terminal cross-links and terminal hairpin loops (reviewed in Dixon et al, 1995 and Yáñez et al, 1995). Also similar to poxviruses, ASFV incorporates the enzymes required for early transcription and mRNA processing and displays a temporal regulated pattern of gene expression (reviewed in Viñuela, 1985, 1987; Wilkinson, 1989; Costa, 1990; Dixon et al, 1990). Table 1.1 shows the comparisons between ASFV, poxviruses and iridoviruses. Further examination of ASFV reveals no obvious phylogenetic relationship with the *Poxviridae* or the *Iridoviridae.* As a result ASFV has been reclassified and is currently the only member of a family of viruses known as the "African swine fever-like viruses" (Dixon et al, 1995).

1.4 Morphology of ASFV.

The mature intracellular virions, when viewed by electron microscopy, appear as ≈200nm diameter hexagons in cross section (figure 1.1). The virions are composed of a central electron-dense nucleocapsid core (the nucleoid), surrounded by an inner core shell, a double inner membrane and an outer layer (capsid) (Rouiller et al, 1998). The extracellular mature virions of African swine fever are icosahedral and measure between 172-191nm in diameter (Viñuela, 1985) and have an outer envelope, derived from budding through the plasma membrane. The overall appearance of the virus is an ordered, multi-layered structure, reminiscent of iridoviruses (Carrascosa et al, 1984).

1.5 Virus encoded proteins.

ASFV encodes for up to 200 open reading frames (ORFs), depending on the virus isolate. The proteins are classed as early, which are synthesised before

	Poxvirus	ASFV	Iridovirus
Genome structure	Unique sequence with terminal inverted repeats and hairpin loops		Circulated permuted terminal redundancy
Enzymes for RNA synthesis	Yes		No
Polyadenylate mRNA	Yes		No
Host RNA polymerase independent	Yes		No
DNA replication	[1]Cell nucleus independent	Cell nucleus dependent	
Host protein synthesis shutdown	Yes	No	Yes
Virus structure	Complex symmetry, structural glycoproteins	Icosahedral symmetry, no major structural glycoproteins	
Capsid	No	Yes	
[2]Virus envelopes	2 from IC, 2 from TGN	1 from PM, 2 from ER	One from the PM

Table 1.1: Comparison of poxviruses, ASFV and iridoviruses. The genome structure, basic factors involved in RNA synthesis and DNA replication and virus structure are shown. [1]Poxvirus DNA replication is unaffected in enucleated cells, whereas ASFV and iridovirus DNA replication does not occur. [2] IC: intermediate compartment, TGN: trans Golgi network, PM: plasma membrane, ER: endoplasmic reticulum.

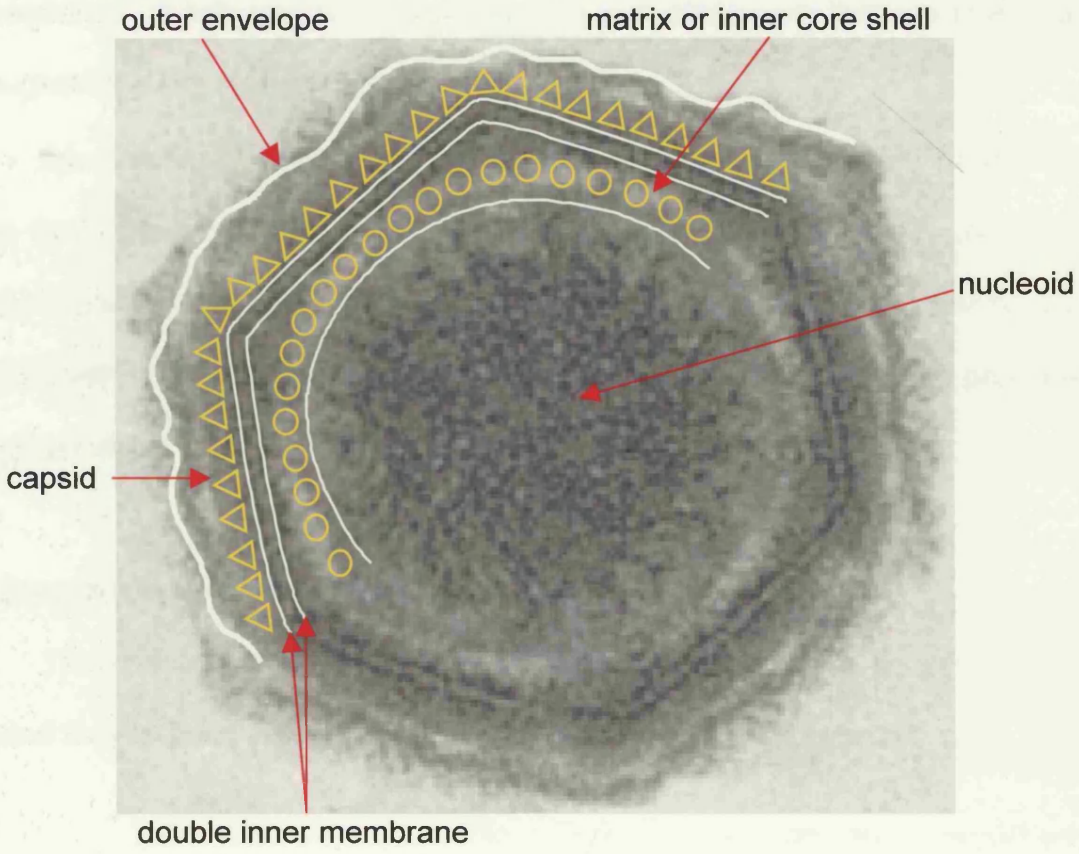

Figure 1.1: An African Swine Fever Virion.

DNA replication, or late proteins that follow DNA replication (Escribano and Tabarés, 1987). The early proteins are classed as either immediate early, which are switched off following DNA replication, or persistent early that are produced throughout the infection cycle.

54 structural proteins with molecular weights ranging from 10-150kDa have been identified in purified extracellular virions, however not all these proteins participate in virion structure (Esteves et al, 1986). 12 proteins co-migrate with host proteins, such as actin and tubulin, and are therefore probably of cellular origin.

1.6 Structural proteins of ASFV.

The characteristics of some ASFV-encoded proteins are shown in table 1.2 and their location within the mature virion is depicted in figure 1.2.

1.6.1 Major capsid proteins lacking membrane spanning domains or leader sequences.

1.6.1.1 Protein p73.

p73 is the major structural protein of ASFV and accounts for 35% of the total protein content of mature virions. It is one of the most immunogenic proteins in natural infection and was mapped to the *B646L* open reading frame (López-Otín et al, 1990; Cistué and Tabarés, 1992). The amino acid sequence of p73 shares some similarity with the major structural capsid proteins of iridoviruses and Chlorella virus PBCV-1 (Mao et al, 1996). The p73 protein is expressed late in infection and contains no putative membrane spanning domains or leader sequences (Cistué and Tabarés, 1992), however Cobbold et al (1996) have

Gene or ORF	Protein name	Molecular weight (kDa)	[1]Characteristics	[2]Location
K786	p10	10	DNA binding	Nucleoid, VF
A137R	p11.5	11.5	Late	Virion, VF
O61R	p12	12 *Predicted 6.7*	Hydrophobic central, late	VF, outer envelope
D117L (i1L)	p17	17 *Predicted 13.1*	Hydrophobic central, late	VF, internal layer
KP177R (L10L)	p22	22	N-terminal hydrophobic	Outer layers
E183L (J13L)	p54	24-28 *Predicted 19.9*	Late, N-terminal hydrophobic	VF, outer envelope
CP530R	pp62⇒p35, p15	60, 35, 15	--	--
B646L	p73	73	Late	Capsid, VF
CP2475L	pp220⇒p150, p37, p34, p14	220, 150, 37, 34, 14. *Predicted 282, 181, 41, 36, 18*	Late, myristate modified	VF, inner core shell

Table 1.2: Characteristics of a selection of ASFV encoded structural proteins. [1]hydrophobic central refers to a protein with a predicted transmembrane domain in the middle of its amino acid sequence. [2]VF – viral factory

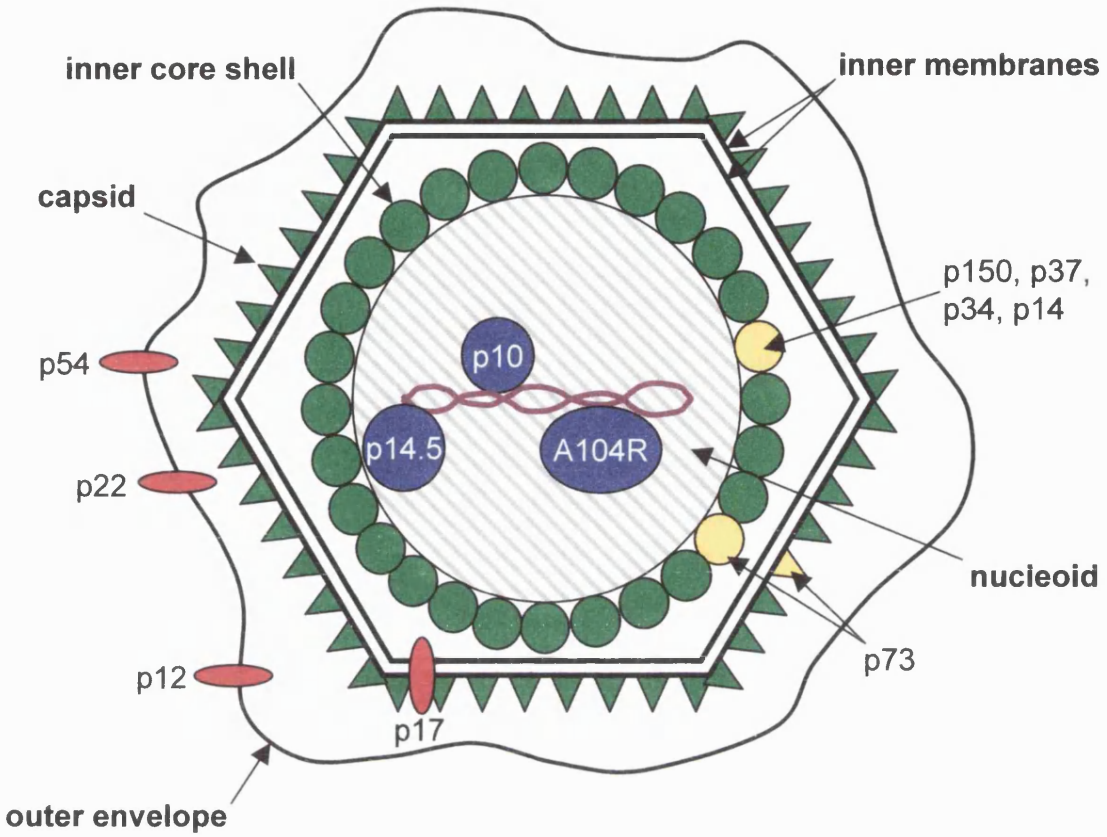

Figure 1.2: Schematic representation of the ASFV particle showing the localisation of some of the major structural proteins. The proteins in red contain putative membrane spanning domains and/or leader peptides. The blue proteins are DNA binding proteins and the proteins in yellow lack membrane spanning domains and/or leader peptides

shown that the protein is peripherally associated with the endoplasmic reticulum located in the viral factories. Electron microscopy has located the protein to the intermediate and outer layers of the intracellular virions (Carrascosa et al, 1986) and biochemical data has verified the location of the protein on either side of the inner membranes, the capsid and inner core shell (Cobbold et al, 1996).

1.6.1.2 Polyproteins of ASFV.

There are two polyproteins encoded by ASFV, which may serve to cluster genes whose products are related, allowing them to be synthesised from a single transcription and translation event. This may allow the proteins to be expressed together, both temporally and spatially. The role of polyproteins in virus replication and assembly will be reviewed later in this section.

pp220.

Simón-Mateo et al (1993) showed that the *CP2475L* ORF encoded the pp220 polyprotein. This polyprotein becomes myristylated at its N-terminus and is subsequently processed, by an ordered cascade, into four major structural proteins, p150, p37, p34 and p14 (figure 1.3A) (Simón-Mateo et al, 1993). The final structural proteins are found in mature virions in equimolar concentrations and account for 25% of the total protein content of the mature virions (Andrés et al, 1997). The polyprotein is cleaved at 4 Gly-Gly-X motifs, in a time dependent manner, to give rise to the final structural proteins, via two intermediate polyproteins, pp90 and pp55. Andrés et al (1997) showed by electron microscopy that the final structural proteins are located in a radial distribution around the inner core shell.

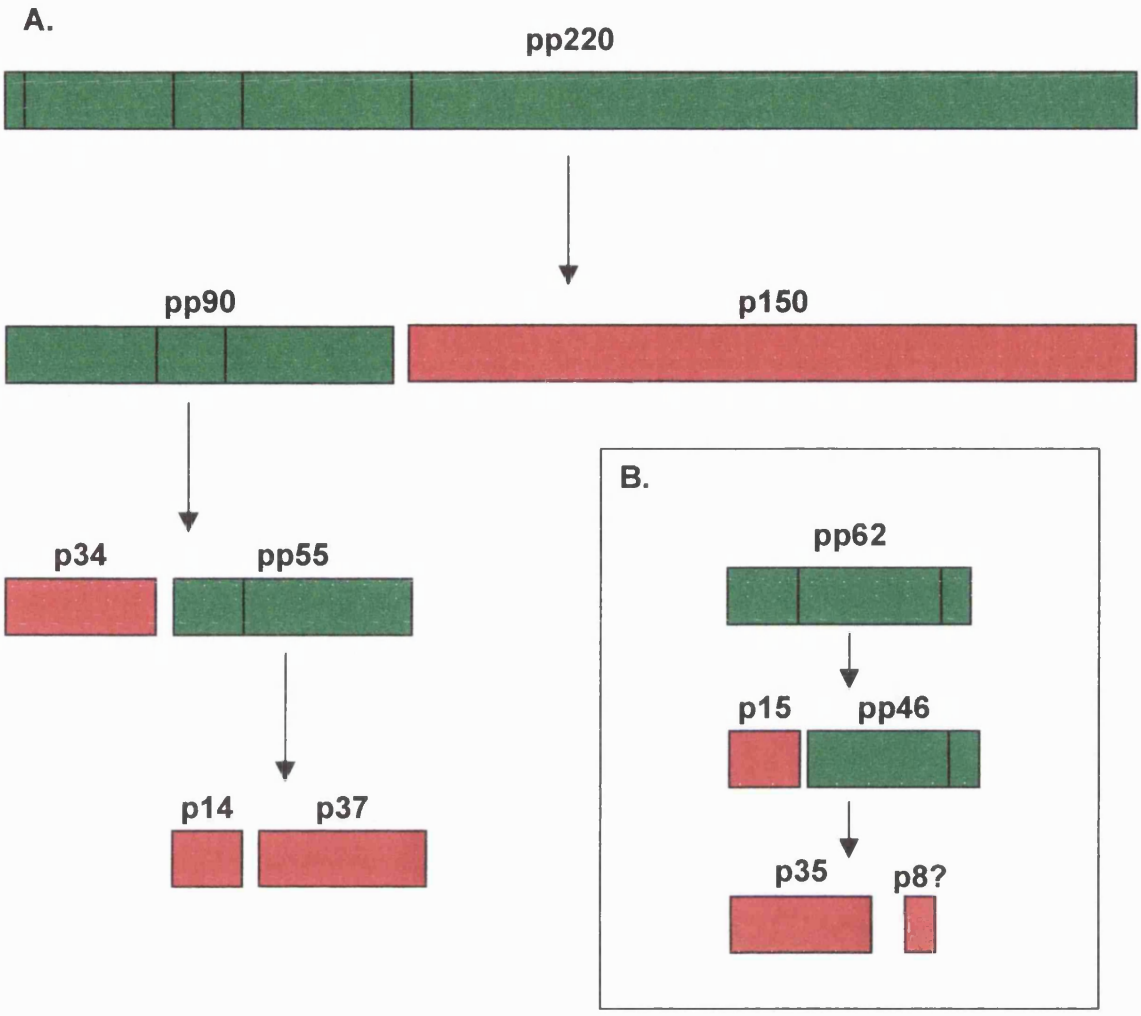

Figure 1.3: The ordered cascades of proteolytic cleavages during polyprotein processing. A. The ordered processing of pp220 polyprotein as described by Simón-Mateo et al (1993). B. The ordered processing of pp62 polyprotein as described by Simón-Mateo et al (1997). The green boxes depict the polyproteins and the red boxes represent the final structural proteins.

pp62.

The *CP530R* ORF encodes for a 62kDa polyprotein that is expressed during the late phase of virus replication. As with the pp220 polyprotein, pp62 is proteolytically processed at Gly-Gly-X motifs, via an ordered cascade, to a putative 8kDa, and a 15 and a 35kDa protein (panel B, figure 1.3) (Simón-Mateo et al, 1997). Immunofluorescence analysis locates pp62 to the viral factory and immunoprecipitation studies have shown p35 and p15 in the mature virions (Simón-Mateo et al, 1997).

1.6.2 Proteins with putative membrane spanning domains and/or leader sequences.

1.6.2.1 Protein p12.

Alcamí et al (1992) sequenced the gene, *O61R,* encoding the p12 protein and mapped it to the central region of the BA71v genome. It encodes for a 61 amino acid polypeptide that has a predicted molecular weight of 6.7kDa. The p12 protein is synthesised late in infection (Almazán et al, 1993) and has no post translation modifications, such as glycosylation, phosphorylation, or fatty acid acylation (Alcamí et al, 1992). The protein was shown to localise to the viral factories by immunofluorescence (Carrascosa et al, 1993). The protein has a stretch of 22 hydrophobic residues in the centre of the protein sequence that may serve to anchor the protein in the virus envelope.

The p12 protein forms a dimer, which is the only form present in viral particles. Dimeric p12 binds to ASFV susceptible Vero cells (Alcamí et al, 1992), suggesting a role for p12 in virus attachment.

1.6.2.2 Protein p17.

The *D117L* ORF of BA71v, or the *i1L* ORF of Malawi isolates of ASFV encode p17, a major structural protein of ASF virions. The ORF encodes a late, 117 amino acid protein that is putatively membrane-associated. It has a predicted molecular weight of 13.1kDa , but migrates at 17kDa on SDS-PAGE (Simón-Mateo et al, 1995). Immunofluorescence analysis has localised the protein to the viral factories (Sanz et al, 1985). Immunogold electron microscopy has located the protein to the intermediate layers of ASF virus that correspond to the capsid and the inner membranes (Carrascosa et al, 1986, Rouiller et al, 1998).

1.6.2.3 Protein p22.

The p22 protein is encoded for by the *KP177R* ORF (Camacho and Viñuela, 1991). The amino acid sequence contains a hydrophobic region (22 amino acids) at its N-terminus, which has signal peptide characteristics, and the protein has a molecular weight of 22kDa. Immunolabelling experiments have localised the protein to the plasma membranes of infected cells at early times after infection. In addition, detergent analysis of mature virions suggests that p22 is present in the outer layers of the virions (Camacho and Viñuela, 1991).

1.6.2.4 Protein p54.

The p54 gene, *E183L* in BA71v and *j13L* in the Malawi isolate, encodes a protein of 183 amino acids with a predicted molecular weight of 19.9kDa (Alcaraz et al, 1992;). The p54 protein is expressed late during infection and exhibits size variation, 24-28kDa, between the various ASFV isolates (Sun et al, 1995). The

protein contains a putative signal peptide cleavage site, an N-terminal transmembrane domain and a Gly-Gly-X motif, a recognition sequence for protein cleavage of several ASFV proteins. The protein was found in the viral factories and is incorporated into the external membrane of the virion (Rodríguez et al, 1994).

1.6.3 ASFV DNA binding proteins that may have a role in DNA packaging.

Esteves et al (1987) used DNA-cellulose chromatography to detect 13 major and 7 minor ASFV DNA binding proteins, of which 12 are late proteins and the remainder are early proteins. Most of the DNA binding proteins associate with both single and double stranded DNA, however only four of these are structural proteins with a putative DNA-binding capacity (Yáñez et al, 1995).

The *A104R* ORF encodes a protein that has sequence homology to bacterial histone-like proteins, which are small basic proteins that possess DNA condensing and wrapping properties (Neilan et al, 1993). The *A104R* protein is located in the nucleoid of the virion (Borca et al, 1996) indicating a possible role in DNA packaging in the virus particle. A second DNA binding structural protein is encoded by the *K78R* ORF, which encodes a 10kDa protein, p10, which binds to sequence non-specific single and double stranded DNA. p10 may also have a role in DNA packaging and/or condensation as it is located in the nucleoid of mature virions (Muñoz et al, 1993; Borca et al, 1996). The ORF *E120R* encodes the p14.5 protein, which interacts with DNA in a sequence independent manner and also interacts with a 72kDa protein, possibly the major capsid protein, p73 (Martinez-Pomares et al, 1997).

1.7 Entry of African swine fever into cells.

The first stage of the replication cycle of ASFV is cell attachment, which was initially thought to occur through the binding of the p12 protein to a saturable component on the surface of permissive cells (Alcamí et al, 1989a; 1989b; Angulo et al 1993). More recently, Gómez-Puertas et al (1996) showed that the structural proteins p54 and p73 are also involved in cell attachment, as antibodies specific for the proteins neutralise cell binding. The above observations suggest that the virus enters the cell via receptor mediated endocytosis (Valdeira and Geraldes, 1985), in addition, Makarov et al (1991) stated that the virus can enter cells by normal phagocytosis and/or Fc receptor mediated phagocytosis (figure 1.4).

Cell attachment is followed by the internalisation of the virus and the non-structural protein p30 is thought to play a role in this event, as antibodies specific for p30 prevent internalisation following attachment (Gómez-Puertas et al, 1996). After internalisation, the virions are detected in endosomes and are then transferred to lysosomes. The virus is predicted to be released from the endosomes and/or lysosomes by low pH induced fusion of viral membranes with the vesicle membranes, as lysosomotrophic agents, such as chloroquine, prevent release (Valdeira and Geraldes, 1985; Geraldes and Valdeira, 1985). The fusion of the membranes allows for the release of the viral genome into the cytoplasm.

1.8 African swine fever virus replication.

Once ASF virions have entered the cell and uncoated, viral DNA is transcribed by the RNA polymerase, which is present in the viral particle. The early proteins, some of which are enzymes required for DNA replication, are

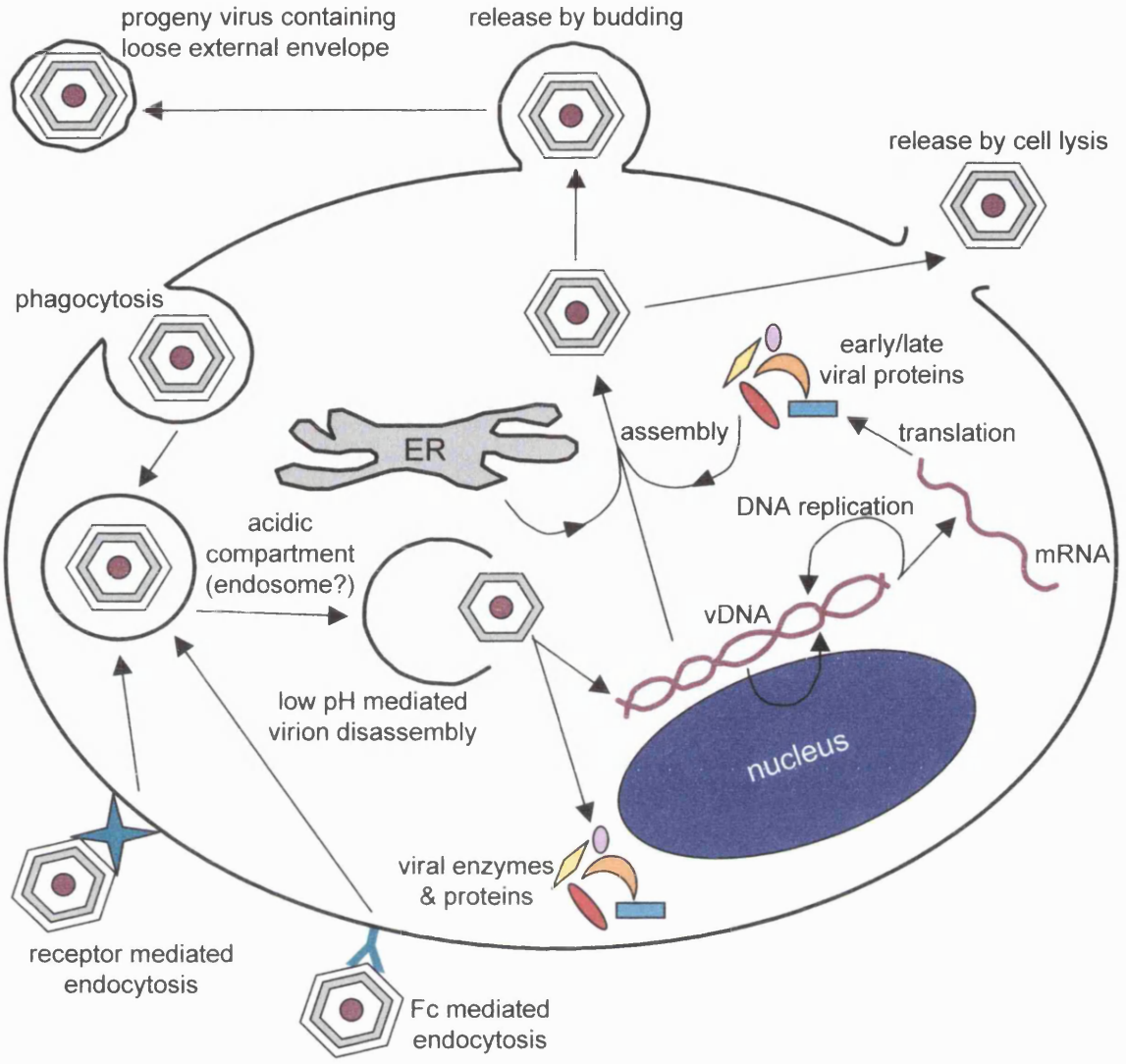

Figure 1.4: Diagrammatic representation of the replication cycle of African swine fever virus. See text for details

translated from the early mRNA transcripts. The published literature suggests that the replication of ASFV DNA requires a functional nucleus (Ortín and Viñuela, 1977) and begins within four hours. The viral DNA undergoes an early intra-nuclear stage (García-Beato et al, 1992, Rojo et al; 1999) as hybridisation experiments detected ASFV-specific DNA in the nucleus four hours after infection. Following the initial nuclear stage, the viral DNA is thought to bud through the nuclear membrane (García-Beato et al, 1992), into the cytoplasm, where it moves to a perinuclear location known as the viral factory. Viral DNA replication becomes maximal at eight hours post infection and is catalysed by the virus encoded DNA polymerase (Polatnick and Hess, 1972). The first cell-associated virions are detected at the same time and these are soon followed by the appearance of mature extracellular virions, which are released from the cell either by budding from the plasma membrane or directly by cell lysis (figure 1.4).

The transcription and replication of ASFV in the cytoplasm means that the virus must encode the enzymes required for these events. A number of the enzymes involved in the transcription and replication of the viral genome have been identified in the virions. For example, an RNA polymerase (Kuznar et al, 1980), poly-A capping polymerase and capping enzymes (Salas et al, 1981), and a single stranded DNA nuclease (Barros et al, 1986). After the early ASF genes are transcribed and translated the new virus specific DNA replication enzymes are formed, including DNA polymerase (Polatnick and Hess, 1972), thymidine kinase (Polatnick and Hess, 1970) and ribonucleotide reductase (Cunha and Costa, 1992).

1.9 Assembly of African swine fever virus.

1.9.1 Envelopment.

1.9.1.1 Nature of viral envelopes.

The number and location of viral envelopes found in the ASF virion has been a point of conflict in the published literature, Schloer et al (1985) and Arzuza et al (1992) describe two membranes in intracellular virions, which has a capsid between the two membranes. Carrascosa et al (1984) and Andrés et al (1997) describe a single membrane within the intracellular virions and two within the extracellular virions. In 1998, Rouiller et al undertook an in depth EM study to show that ASFV virions have two internal membranes sandwiched between the inner core shell and the capsid. In addition to these membranes, some of the published literature reports that ASF virions gain a single outer envelope by budding through the plasma membrane (Breese and DeBoer, 1966, 1967; Moura-Nunes et al, 1975, Breese and Pan, 1978; Arzuza et al, 1992; Brookes et al, 1996; Andrés et al, 1997), however Breese and DeBoer (1966) suggested that ASFV can exit by cell lysis. Interestingly, the external envelope is not required for the infectivity of the virus (Moura-Nunes et al, 1975; Borca et al, 1994).

1.9.1.2 Origin of membrane envelopes.

Early models of membrane acquisition suggest that ASFV acquires its membranes from newly synthesised lipids within the cytoplasm, at the same time as capsid formation, using a *de novo* mechanism (Arzuza et al, 1992). The major reason for the generation of this model was that the assembling intermediates of ASFV were not seen in continuation with cellular membrane compartments (Moura-Nunes, 1975).

This model seems to be in conflict with both cellular membrane synthesis and the envelopment of other large DNA viruses. The synthesis of lipids for cellular membrane compartments is thought to occur mainly in the endoplasmic reticulum and not the cytoplasm (reviewed in van Meer, 1993; Alb et al, 1996). Other large DNA viruses, such as herpesvirus and poxvirus, acquire their membranes from existing cellular compartments, such as the ERGIC and TGN (reviewed in Griffiths and Rottier, 1992; Pettersson, 1991; Stephens and Compans, 1988). In addition, the genome of the BA71v isolate of ASFV has been completely sequenced (Yáñez et al, 1995) and to date no enzymes required for *de novo* membrane synthesis or for the recruitment of phospholipids to the viral membranes have been identified.

1.9.1.3 Membrane wrapping.

Recently, a new model for membrane acquisition has been described for the large DNA viruses and has been termed wrapping. Wrapping is a different system compared to classical budding, as the virus acquires two lipid bilayers, and the luminal contents of the cellular compartment involved, in the process. The classical budding system, on the other hand, allows the viruses to only acquire a single lipid bilayer (figure 1.5).

Rouiller et al (1998) used electron microscopy techniques to show that the two inner membranes are in continuation with a cellular compartment and using immunogold labelling they concluded that the membranes are derived from the endoplasmic reticulum. The method for acquisition of the viral membranes was shown to be via a wrapping mechanism (figure 1.5), where the virus acquires two membranes and the lumen of the endoplasmic reticulum. This was shown by

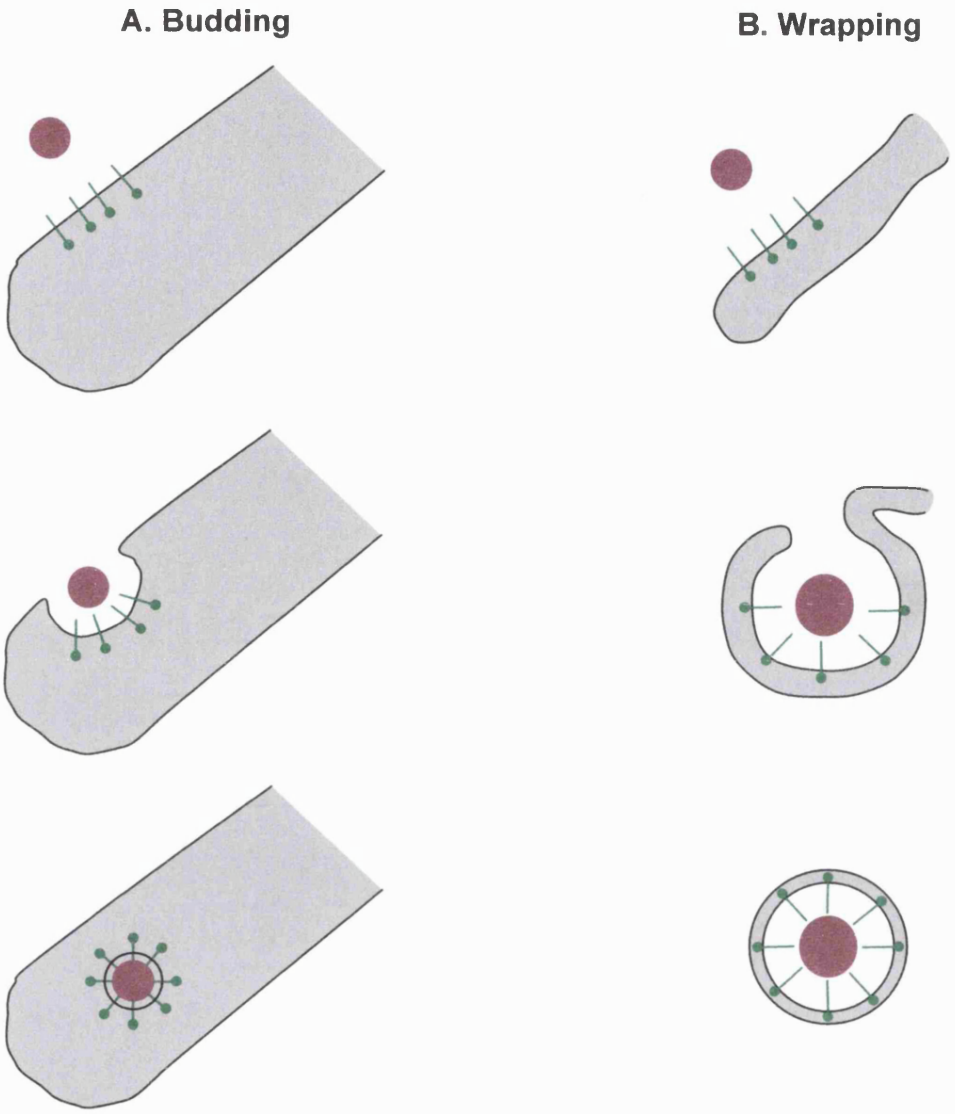

Figure 1.5: Virus budding and wrapping models. A. Viral nucleoprotein cores associate with the cytoplasmic domains of virally encode integral membrane proteins, normally viral glycoproteins. These interactions lead to the subsequent budding of the virus into the lumen of the membrane compartment. The budding event results in the acquisition of a single bilipid membrane. B. As with budding, the viral nucleoprotein core associates with the cytoplasmic domains of virally encoded integral membrane proteins. This interaction then results in the wrapping of the core by the membrane compartment, resulting in the acquisition of two bilipid membranes and the lumen of the cellular compartment. In addition the particle remains cytosolic.

immunogold labelling and Western blot analysis of purified virions, which were found to contain host cell ER luminal proteins (Rouiller et al, 1998). In addition to the host ER luminal proteins, ASFV was found to encode a viral structural protein from the XP124L ORF that localised to the lumen of the ER and was also found in purified mature virions (Rouiller et al, 1998). Further evidence for the involvement of ER membranes in ASFV morphology came from studies into the major capsid protein, p73, which was shown to associate with ER membranes (Cobbold et al, 1996).

Figure 1.6 shows the model for ASFV assembly and compares it to the wrapping models of the large DNA viruses, herpes and poxvirus. The herpesviruses require the nuclear machinery of the host cell for replication and transcription. The large double stranded DNA of the herpesviruses replicates in the nucleus and the nucleocapsid proteins are imported into the nucleus, where the nucleocapsid assembles. The nucleocapsids associate with viral glycoproteins localised to the inner nuclear membrane and then bud into the lumen of the nuclear envelope. This stage leads to the acquisition of a single bilipid membrane, which is lost when the virus buds out of the nuclear membrane into the cytoplasm, leaving "naked" nucleocapsids free in the cytosol. The "naked" nucleocapsids acquire two membranes on wrapping by the *trans* Golgi network (Gershon et al, 1994), possibly driven by the accumulation of envelope glycoproteins to the TGN (Whealy et al, 1991; Tooze et al, 1993; Zhu et al, 1995). The herpesviruses then fuse with the plasma membrane, losing the outer membrane thus releasing the virus from the cell with a single bilipid membrane.

The poxviruses are large (200-400nm diameter) DNA viruses that encode the proteins required for DNA replication and transcription. This occurs in large

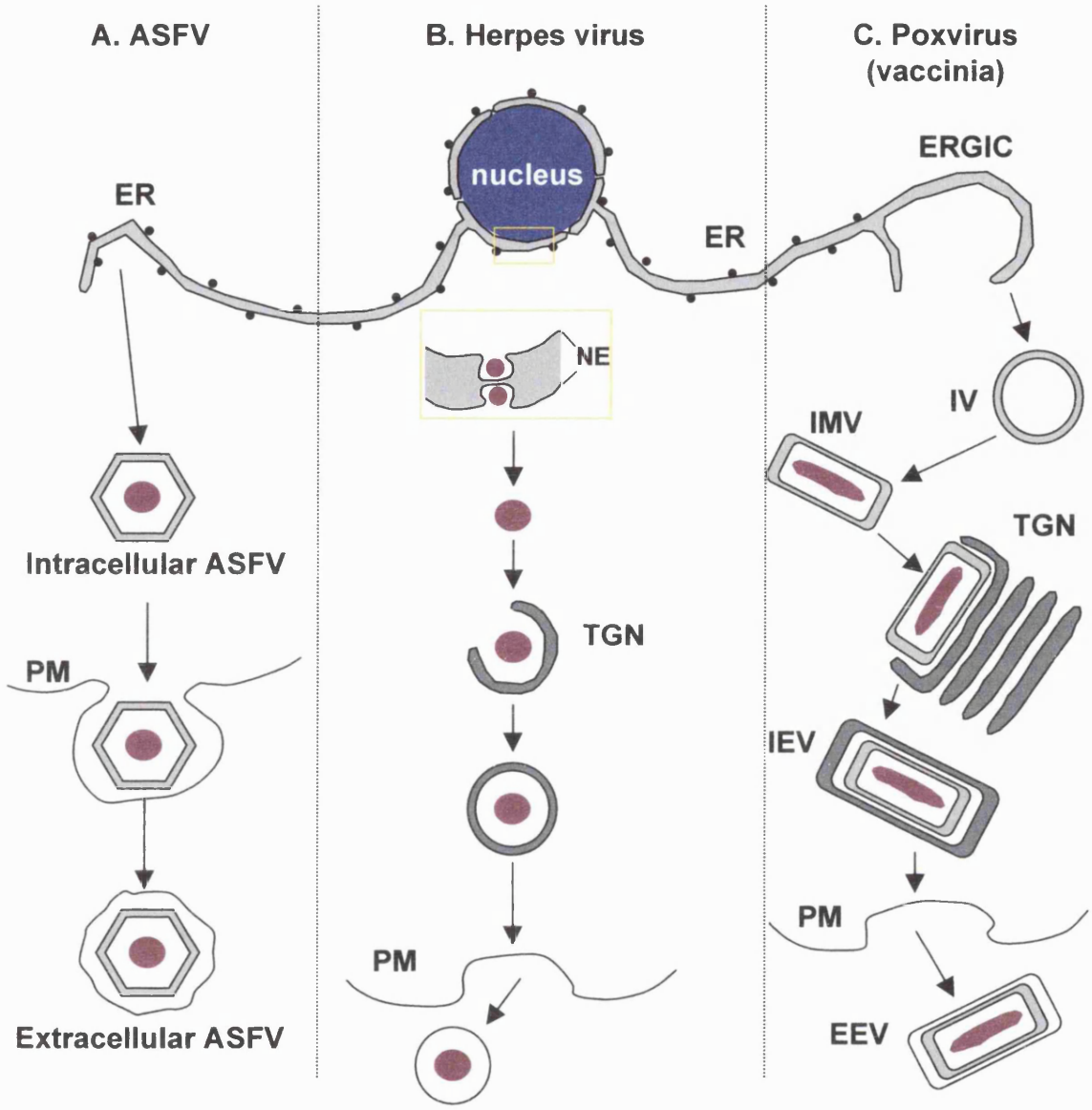

Figure 1.6: Models for the assembly of large DNA viruses. A. ASFV is wrapped by the ER, acquiring two membranes, and then it buds from the PM, gaining a third membrane. B. Herpes virus nucleoprotein core assembles in the nucleus and buds into the nuclear envelope (NE) acquiring a single membrane, which is lost on budding from the NE. The core then acquires two membranes by wrapping by the TGN, one of which is lost on budding through the PM. C. Vaccinia virus acquires its first two membranes by wrapping the ERGIC forming spherical immature virions (IV). The IV undergo additional maturation steps to form the brick shaped intracellular mature virions (IMV), which acquire an additional two membranes by wrapping by the TGN, forming the intracellular envelope virus (IEV). The external membrane is lost on budding through the plasma membrane (PM) to form the extracellular envelope virus (EEV).

cytoplasmic structures known as viral factories. The vaccinia virus model for membrane acquisition is complex as the virus interacts with two different membrane compartments to acquire four bilipid membranes. The first stage is the formation of the immature virions (IV), which have two bilipid membranes. Originally, it was thought that the membranes were acquired by *de novo* membrane synthesis (Dales and Mossbach, 1968). The evidence for this argument was largely from electron microscopy studies, which showed that the crescent shaped viral membranes did not have continuity with cellular compartments. The use of antibodies against specific cellular organelles and phospholipid analysis of purified IMV and EEV, however, suggest that the first two membranes originate from the intermediate compartment between the ER and the Golgi (ERGIC) (Sodeik et al, 1993). The IV then undergoes a maturation step to form the brick shaped intracellular mature virus (IMV), a portion of which becomes wrapped by the *trans* Golgi network (TGN) forming the four membraned intracellular envelope virus (IEV) (Tooze et al, 1993). Schmelz et al (1994) used EM immunocytochemistry using lectins, antibodies specific for endocytic markers, and recombinant vaccinia proteins to show that the TGN was enriched with virus membrane proteins, which facilitate the wrapping of the IMV to form the IEV. Finally, the IEV are propelled to the plasma membrane on actin tails (Cudmore et al, 1995), which they fuse with, losing the external membrane, and releasing the three membraned extracellular envelope virus (Griffiths and Rottier, 1992).

1.9.2 Assembly of the ASFV capsid.

The major capsid protein, p73, has been shown to localise to the inner membranes of the virions (Carrascosa et al, 1986) and has been one of the main

targets for studying the assembly of ASFV. In recent years, the assembly of the major structural protein, p73, into the capsid of ASFV has begun to be elucidated. In 1996, Cobbold et al used subcellular membrane fractionation and immunoprecipitation analysis to show that 50% of the total cellular pool of p73 peripherally associates with the membranes of the endoplasmic reticulum 15 minutes after synthesis. They used a novel protease protection assay to demonstrate that the major capsid protein is enveloped by the ER one hour after binding of p73 to the membranes. The envelopment is completed one hour before the appearance of extracellular mature virions. Sucrose density gradients and immunoprecipitation experiments were used to show that the capsid protein forms a 150-250kDa complex immediately after synthesis (Cobbold and Wileman, 1998). The *in vitro* translation of the capsid protein failed to form a complex and suggests that other cellular or viral proteins are required. During a two-hour chase period the membrane-associated p73 formed a large complex of approximately 50,000kDa and using immunoprecipitation and sucrose gradients it was shown that these large complexes form via assembly intermediates. Interestingly, the formation of these large complexes has similar kinetics to the envelopment of p73 by the ER membranes (Cobbold et al, 1996; Cobbold and Wileman, 1998). Using the protease protection assay, the large complexes were found associated with both the inside and outside of the inner viral envelope, suggesting that p73 is involved in the formation of both the inner core shell/matrix and the capsid. Recently, using depletion experiments, it was shown that the assembly and wrapping of ASFV requires ATP and is regulated by the calcium gradients present across the ER membrane cisternae (Cobbold et al, 2000).

1.10 Polyprotein processing.

Six structural proteins of ASFV are produced from the ordered processing of two polyproteins, pp220 and pp62. Together these proteins account for over 25% of the total protein content of the mature virions. Given the importance of polyprotein processing for the production of structural proteins of ASFV it is interesting to consider why viruses use polyprotein processing during replication and assembly.

The proteolytic processing of viral polypeptides, by viral proteinases, can be generally classed by the use of two different strategies. The first being the translation of the entire viral genome into a single large precursor polyprotein, which is then processed to yield diverse structural and non-structural proteins. The second is co-ordinated with morphogenesis where the proteolytic processing of structural proteins produces mature virus particles.

The first strategy appears to be restricted to the positive strand RNA viruses, such as the picornavirus super group (picorna-, como-, nepo-, poty-, and bymoviruses), flaviviruses, and retroviruses (reviewed in Kräusslich and Wimmer, 1988; Hellen et al, 1989; Ryan and Flint, 1997; Ryan et al, 1998). The main reasons for the positive stranded viruses using this system are that firstly, the eukaryotic translation machinery can only handle mono-cistronic messengers (Kozak, 1983) and secondly, the synthesis of a polyprotein in these small RNA viruses allows for genetic economy, as several proteins are produced from a single transcription/translation event. Another benefit is that it allows the expression of equimolar amounts of the proteins, however some viruses, such as the retrovirus, have different mechanisms to allow for expression of different amounts of the proteins from one polypeptide.

The second strategy plays an important role in the morphology of the viruses. The use of polyproteins allows for the equimolar expression of capsid proteins and, if processing is delayed until assembly and maturation, also allows for the delivery of equimolar ratios of the capsid proteins to the assembly and/or maturation sites. Viruses also use proteolytic processing of precursor proteins that result in the formation of a single protein as a maturation step in capsid formation.

1.10.1 Picornaviridae.

Figure 1.7 shows a schematic representation of the processing events involved in picornavirus replication (reviewed in Kräusslich and Wimmer, 1988; Wellink and van Kammen, 1988; Palmenberg, 1990; Lawson and Semler, 1990; Hellen and Wimmer, 1992; Ryan and Flint, 1997). *Picornaviridae* are a family of small positive strand RNA viruses. The genome of the picornaviruses consists of a single positive strand RNA molecule with a small protein, VPg, covalently linked to the 5' end and a poly A tail at the 3' end. For the purpose of this report the proteolytic events involved in the maturation of poliovirus, the prototypic member of the *Picornaviridae*, will be reviewed. The primary cleavage event is the separation of the capsid proteins from the non-structural proteins, which is necessary for virus replication and assembly. The initial event is the cleavage of a tyrosine-glycine bond between the P1 and P2 polyprotein (1D-2A). This reaction is catalysed in *cis* by the virally encoded 2A proteinase, which cleaves at its own amino terminus (Toyoda et al, 1986). The remaining cleavages use the viral proteinase 3C, however in the case of polioviruses these cleavage events are mediated by 3CD (Jore et al, 1988; Ypma-Wong et al, 1988). This proteinase

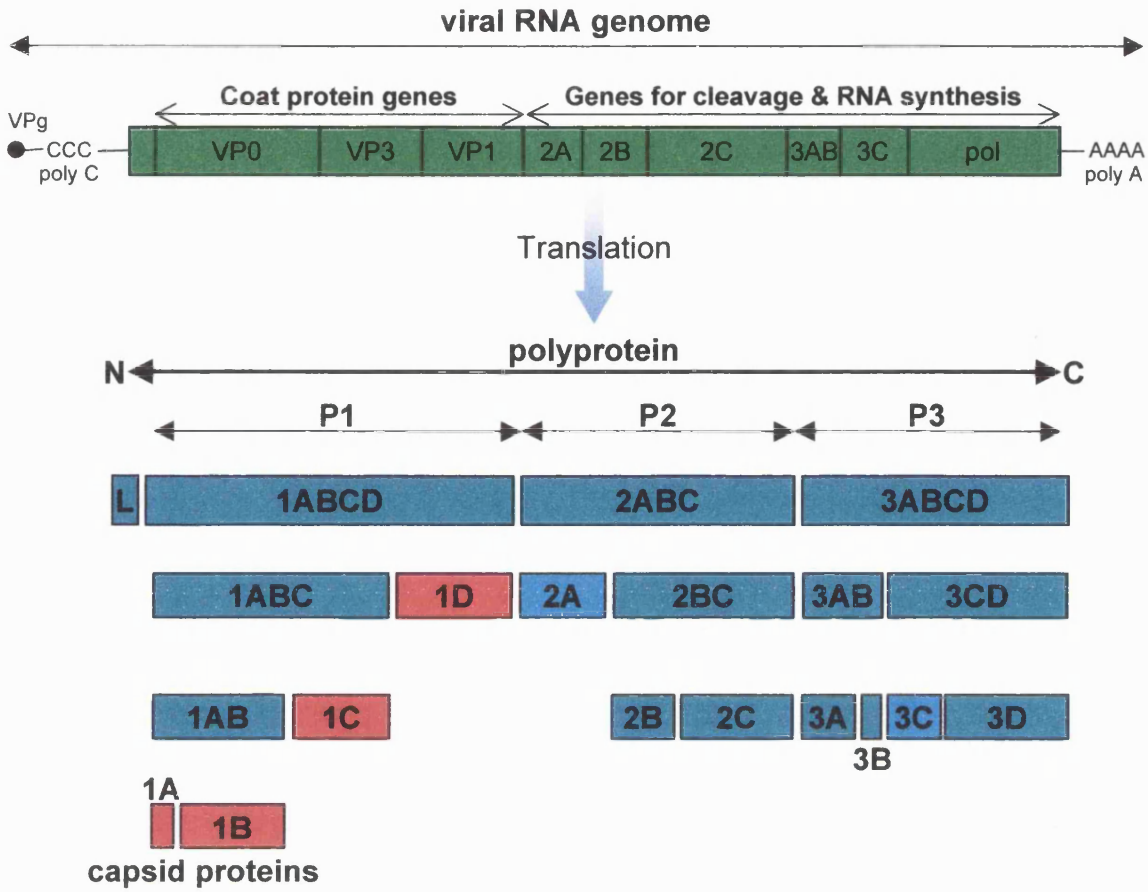

Figure 1.7:Organisation and expression of the picornaviral genome. The polyC tract, found in the 5'-nontranslated region, is found only in encephalomyocarditis-like viruses and apthoviruses. The growth machinery (proteins needed for RNA synthesis and proteinases) are encoded downstream from the capsid proteins. Cleavage of the polyprotein is carried out by the early 2A or 2AB proteinase that is inactive in apthoviruses, which uses the unique, early L proteinase, and the 3C (or 3CD) proteinase. The maturation cleavage of VP0 to VP4 and VP2 occurs only after the RNA has been packaged into the protein shell. Proteins L and 2A perform early cleavages of the polyprotein and the remaining cleavages are performed by the 3C proteinase or its precursor (3CD). Adapted from Rueckert (1996).

cleaves at Gln-Gly base pairs, however, not all these motifs found in the polyproteins are cleaved (Ryan and Flint, 1997).

The main function of proteolytic processing in picornaviruses is to allow the transcription and translation of the entire genome in a single event. The P1 polyprotein in poliovirus is myristylated and cleavage produces the four structural proteins, VP1-VP4, which make up the virus capsid and are present in equimolar amounts.

1.10.2 Adenovirus.

The adenoviruses use proteolytic processing of proteins to aid in the assembly and maturation of virus particles.

In 1976, Weber used a temperature sensitive mutant to show that the Adenovirus type 2 encodes an endoprotease required for the proteolytic processing of three viral polypeptides to form the final structural proteins (Weber, 1976). The viral proteinase, the 23kDa L3 protein (Weber, 1976; Liang et al; 1983) cleaves six proteins that include the precursors to polypeptides IIIa, VI, VII, VIII and X, which are involved in many structural aspects of the virus (Tihanyi et al, 1993). If the polyproteins are not cleaved then virus-like particles are formed, however these particles are non-infectious (Mirza and Weber; 1980; Hannan et al, 1983). The L3 proteinase functions late in the assembly process and requires the viral DNA and a fragment of another viral polypeptide as cofactors (Mangel et al, 1993, 1997). The proteinase cleaves the polyproteins, at a Leu/Met/Ile-X-Gly-Gly/X-X/Gly motif (Freimuth and Anderson, 1993), to generate the mature structural proteins that stabilise the virion structure and render the particle infectious (Shenk, 1996).

1.10.3 Retroviridae.

The retroviruses use a viral proteinase to process viral proteins during maturation. The *retroviridae* are a family of enveloped RNA viruses that differ from the positive stranded RNA viruses by replicating via a DNA intermediate. The genome of the viruses consists of three major genetic elements that are arranged as *5'-gag-pol-env-3'*. The *gag* (**g**roup-specific **a**nti**g**en) region encodes six structural proteins involved in the formation of the nucleocapsid, capsid and matrix, the *pol* region encodes the viral replication enzymes, (the proteinase, reverse transcriptase and integrase), and *env* encodes the envelope glycoproteins (Hellen et al, 1989). The *gag* polyprotein is translated as a full-length precursor polyprotein and the *pol* polyprotein is expressed as a fusion protein with *gag* (Kräusslich and Wimmer 1988). The *env* gene is silent during translation of the full-length RNA and is only translated from subgenomic, spliced mRNA. As a result the retroviruses make three polyproteins, *gag, gag-pol, env*, all of which need to be further processed. The initial cleavage of the *env* polyprotein is carried out in the cellular transport vesicles by a host protease, all the other cleavages are undertaken by a virally encoded proteinase. The viral proteinase responsible for the cleavage of *gag* and *pol* is encoded by the *pro* gene, which is expressed differently in the various retrovirus groups. For example, avian leukosis sarcoma virus (ALSV) *pro* is expressed as part of *gag*, in murine leukemia virus and HIV *pro* is in the *pol* frame and in mouse mammary tumour virus, it is in its own distinct frame (Coffin, 1996).

The precise timing of viral proteinase cleavage of the polyproteins is not full understood, however it is thought to occur late in assembly, most likely

immediately before the completion of budding and release of the virus particle. The processing of the *gag* polyprotein leads to the maturation of the virus and evidence for this has come from the various properties of proteinase deficient viruses, the correlation between uncleaved *gag* and immature particles and the effect of HIV proteinase inhibitors (Vogt, 1996). The exact role *gag* proteins play in maturation events is still unknown, but it has been suggested that they have a role in virus budding and capsid shape.

1.11 Control of proteolytic processing.

Many viruses require proteolytic processing events to produce final mature proteins; these processing events are usually an important step in the regulation of the production and activity of the viral proteins. Viruses use several different methods for the control and regulation of proteolytic processing.

1.11.1 Control through post-translational modifications.

One of the simplest methods for the control of processing of viral proteins is seen with the viral envelope proteins. These proteins are commonly processed and modified by host proteinases found in the cellular secretory pathway. For example, the *env* polyproteins of the retroviruses and the glycoproteins of the *Togaviridae*. The P62, E1 and 6K proteins contain signal peptide motifs that direct the proteins to the ER from whence they traverse the secretory pathway to the plasma membrane. These proteins acquire several modifications, such as the addition of oligosaccharides, palmitate acylation and proteolytic cleavage of P62 to E2 and E3. All these modifications are under the control of host enzymes and machinery (reviewed in Schlesinger and Schlesinger, 1996).

The other retroviral polyproteins, *gag* and *gag-pol*, also undergo post-translational modifications that help in the regulation of processing. The polyproteins are myristylated at the N-terminus and, in most cases, this allows for the concentration of the polyproteins at the plasma membrane, which results in the activation of the protease by its dimerisation (reviewed in Dougherty and Semler, 1993).

Another point of control, which may also be a regulation point for retroviruses, is based on the cellular zymogens. The retroviral PR proteases are aspartic proteases and the cellular aspartic proteases are synthesised as zymogens, which require proteolytic removal of N-terminal extensions to achieve full enzymatic activity (Davies, 1990). It is therefore speculated that the section of the polyprotein upstream from the PR region could have a similar role in inactivating the protease, however the details of this control mechanism are poorly understood, but it suggests an importance for conformational changes as a control mechanism (Vogt, 1996). These could be initiated by interaction with other proteins or association with particular cellular compartments, such as the plasma membrane.

1.11.2 Control through the action of viral cofactors.

A second point of regulation, which is important for proteolytic processing in virus maturation, is the interaction of viral proteases with other viral proteins and viral DNA/RNA as cofactors. An example of this is the activity of the adenovirus protease, which requires a viral peptide and viral DNA for its activity. The viral peptide and the viral DNA interactions may be required so that proteolytic processing of precursor proteins only occurs after virion assembly,

otherwise they may not be able to convene into a virus particle (Mangel et al, 1993, 1997). A second example is the picornaviruses, which are thought to require the packaging of the RNA before the cleavage of VP0 to VP4 and VP2 occurs (reviewed in Hellen and Wimmer, 1992b).

The retroviruses appear to have several different points of control, which appear to be connected. In most cases, the PR protease involved in the proteolysis of the polyproteins has to act as a dimer for efficient processing and formation of these dimers can be a rate-limiting step (reviewed in Dougherty and Semler, 1993).

1.11.3 Control through processing.

Another control point is during the actual formation of the mature proteins. The mature proteins can be formed in an ordered process, where a certain cleavage cannot occur until cleavages higher in the order have been carried out. This has been shown for the processing of the picornavirus polyproteins, where the primary cleavage to occur is the separation of the structural polyproteins (P1) from the replicative domains (P2 and P3). This must be carried out before the polyproteins are processed into the final mature proteins.

In many cases, the viral proteases that catalyse the cleavage of a polyprotein are actually part of the polyprotein itself. This offers an important point of regulation as these proteases can cleave intramolecularly (*cis*) and/or intermolecularly (*trans*). The *cis* cleavages are normally rapid and as the cleavage sites and protease are part of the same molecule, follow zero order kinetics. The *trans* cleavages are normally slower and follow second order kinetics.

1.12 ASFV proteolytic processing.

The processing of the pp220 and pp62 polyproteins of ASFV has not been fully elucidated, however the evidence in the published literature for ASFV and the processing of other viruses allows for the speculation of the possible roles of the polyproteins.

As stated earlier, polyprotein processing can be classified into two main areas, the use of polyproteins in genomic economy and in the assembly and morphology of the virions. As ASFV is a large DNA virus, which encodes its own transcription machinery the use of polyproteins as a genomic economy strategy seems unlikely. The large percentage of polyprotein structural proteins in the mature virions and their localisation to the viral factories suggests a likely role in assembly and morphology.

The processing of the ASFV polyproteins seems to be very similar to the processing of the P1 structural polyprotein in picornaviruses. The P1 polyprotein is not processed until late in the assembly of the virus, it is myristylated at its N-terminus and is processed into four structural proteins that are present in equimolar amounts in the virions. ASFV proteolytic processing also shares common features with the adenovirus polyproteins. Although proteolytic processing in adenoviruses is restricted to the maturation of single proteins, it still shares similar features with the processing of the ASFV polyproteins. For example, processing occurs at Gly-Gly-X motifs and occurs late in the assembly process. This provides support for the processing of ASFV polyproteins having a role in virus assembly or morphology. The retrovirus *gag* polyproteins are also myristylated and encode for six proteins involved in virus assembly and

morphology. This suggests that the myristylation site on pp220 may be important in assembly.

In conclusion, it seems that the main role for polyprotein processing in ASFV is in virus assembly and morphology. The use of the polyproteins would allow for the movement of the polyprotein to the wrapping virions, where it can be processed and therefore allow for the expression of an equimolar amount of the proteins. The myristylation site on pp220 would allow for the association of the polyprotein with the ER membranes and therefore play a role in the wrapping of the virions.

The regulation of processing and packaging of pp220 is studied during the first part of this thesis.

1.13 Assembly of cytoplasmic viruses in viral factories.

1.13.1 African swine fever virus.

As stated earlier, the DNA replication and assembly of ASF virions occurs in discrete cytoplasmic locations, known as viral factories (Moura-Nunes et al, 1975). The virus has been subjected to numerous electron microscopic studies (Alves De Matos et al, 1980; Arzuza et al, 1992; Breese and DeBoer, 1966; Brookes et al, 1996; Moura-Nunes et al, 1975; Rouiller et al, 1998; Vigario et al, 1967) and these have shown that the factories contain fully assembled virions as 200nm hexagons, some containing a dense nucleoprotein core, and membranous material. In addition, an ordered series of assembling intermediates with one to six sides of a hexagon are seen . Recent reports have shown that the membranous material is most likely derived from the endoplasmic reticulum (Rouiller et al, 1998). Figure 1.8 shows an ASFV virus assembly site,

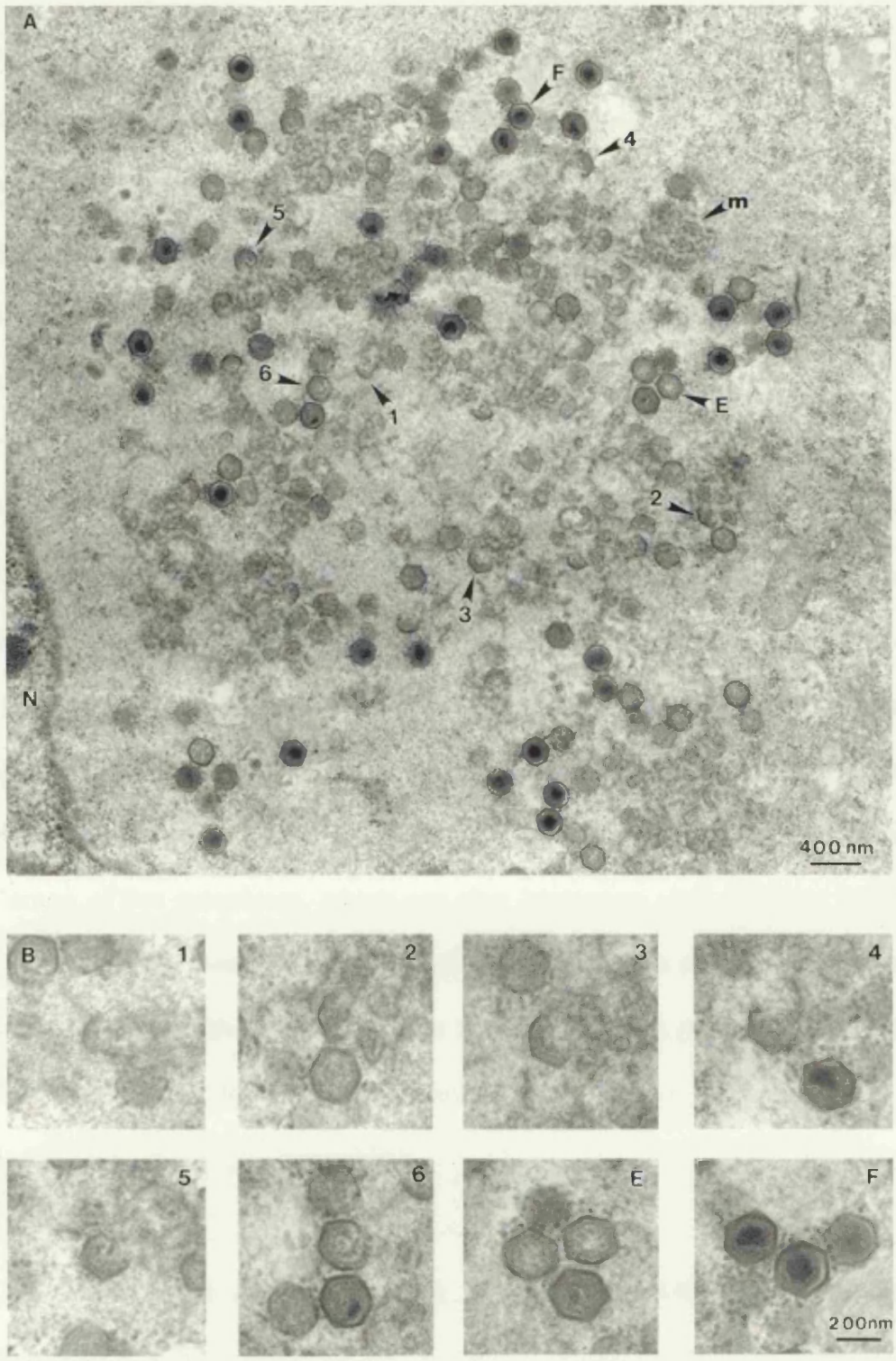

Figure 1.8: ASF virus assembly site and intermediates. A) A transmission EM of an ASFV viral factory, showing full (F) and empty (E) virions, the 1 to 6-sided intermediates (1-6) and amorphous membrane material (m). B) Selected images from panel A showing the assembling intermediates and the empty and full virions. (Adapted from Rouiller et al, 1998)

showing full and empty particles and the assembling intermediates. The published literature has shown that the viral factories use cellular proteins and mechanisms for their establishment. In 1988 Carvalho et al showed that there was an accumulation of vimentin around the factories and a possible requirement for microtubules and Rojo et al (1998) showed that the factories were surrounded by mitochondria.

1.13.2 Poxviruses.

As already stated, African swine fever virus replicates and assembles in the cytoplasm of cells, however there is strong evidence for a preceding nuclear stage (García-Beato et al, 1992, Rojo et al; 1999). The poxviruses, however, replicate and assemble entirely in the cytoplasm of the host cells. Virion replication and assemble occurs entirely within circumscribed, granular, electron-dense areas of the cytoplasm, which are also known as viral factories (Cairns, 1960). The viral factories contain 50-55nm wide membrane structures, known as caps and cupules, which develop into the immature virions (Fenner et al, 1989). These then develop as described earlier and in figure 1.6.

1.13.3 Iridoviruses.

The iridoviruses appear to have a similar replication and assembly strategy to ASFV, as the virus requires a nuclear stage, followed by assembly in cytoplasmic factories. Very little work has been carried out on the iridoviruses, however electron microscopy data has shown the viral factories have a similar morphology to African swine fever viral factories.

1.14 Aggresomes.

The above sections have briefly described subcellular cytoplasmic compartments that are the sites of virus assembly and replication, known as viral factories. Recently, a novel cellular pathway was described that created a subcellular cytoplasmic compartment for the sequestration of misfolded and aggregated proteins, which was termed the aggresome (Johnston et al, 1998) (Figure 1.9).

The aggresome pathway was first discovered by using a mutant of the cystic fibrous transmembrane conductance regulator (CFTR). The CFTR mutant, ΔF508, has a deletion of a phenylalanine residue at position 508, which can lead to the development of cystic fibrosis (Cheng et al, 1990; Thomas et al, 1992; Welsh and Smith, 1993). The mutation prevents the protein adopting its correct conformation, as a result of this, the ER "quality control" measures identify the protein as abnormal and target the protein for export from the ER and subsequent degradation by proteasomes (figure 1.9, 2,3). Johnston et al (1998) used potent inhibitors of the proteasomes to block the degradation of the wild type and ΔF508 CFTR and showed that the proteins aggregated (4,5) and were subsequently sequestered into a novel, cytoplasmic structure, known as the aggresome (7). The aggresomes were associated with the microtubule organising centre (MTOC), were highly ubiquitinated and were surrounded by a cage of the intermediate filament (IF), vimentin. Using microtubule-disrupting agents, such as nocodazole, they showed that there was an obligate requirement for the microtubule network in the formation of the aggresomes.

Similar subcellular structures have been shown using a soluble protein chimera, composed of the green fluorescent protein fused to a fragment of the

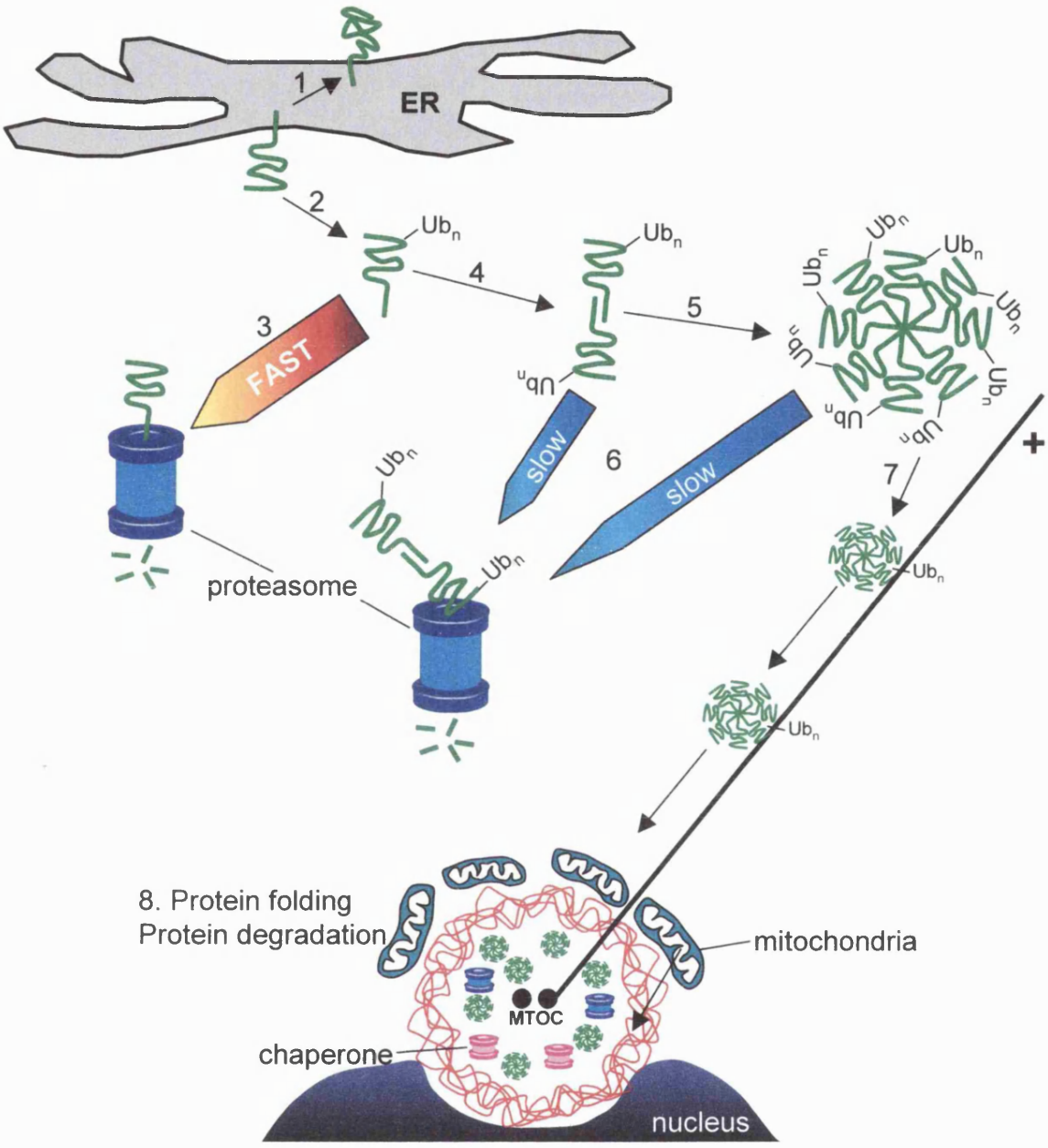

Figure 1.9: The aggresome pathway. Correctly folded proteins pass through the ER and enter the secretory pathway (1). Others misfold and are dislocated from the membrane and become ubiquitinated (2), where they can be rapidly degraded by cytosolic proteasomes (3) or aggregate (4,5). The aggregates are difficult to unfold, and as a result are likely to be slowly degraded by the proteasomes (6). Misfolded, aggregated protein is transported to the microtubule organising centre (MTOC) by the microtubules, where it becomes surrounded by collapsed vimentin and clustered mitochondria (7). Chaperones and proteasomal machinery attempt to correctly folded or degrade the aggregates (8). Adapted from Johnston et al (1998).

cytosolic protein, p115 (García-Mata et al, 1999). Further characterisation of the aggresomes showed that they were rich in proteasomal machinery and cellular chaperones, clustered mitochondria and utilised the dynein/dynactin-associated minus-end motors for the movement of aggregates along the microtubules (Wigley et al, 1999; García-Mata et al, 1999).

Interestingly, the published literature on aggresomes and ASF virus factories show some similarities between the two structures, such as their perinuclear location, rearrangement of vimentin, requirement for microtubules and clustering of mitochondria. The similarities between the cellular aggresome pathway and the viral factories suggest that ASFV may be utilising the cellular pathway to establish the factories and as a result concentrate the viral proteins in a cytosolic structure. The possible connections between these two pathways are explored in the second part of this thesis.

2. Materials and Methods.

2.1 Reagent suppliers.

Chemicals were either supplied by Sigma, Mo. USA or Merck, UK unless otherwise stated. Radioisotopes were from Amersham Pharmacia, UK. Restriction endonucleases and nucleic acid modifying enzymes, with their appropriate buffers, were purchased from Promega, UK or Boehringer Mannheim, Germany.

2.2 Media.

DMEM: Dulbecco's modified Eagle's medium supplemented with 20mM L-glutamine, 100units/ml penicillin and 100units/ml streptomycin.

Optimem: Reduced serum medium supplied by Life Technologies, MD. USA.

LB medium: 1% Bacto tryptone, 0.5% Bacto yeast extract, 86mM NaCl in dH_2O.

Agar plates: 1.5% Bacto agar in LB medium.

Ampicillin resistance: 50μg/ml ampicillin.

Kanamycin resistance: 30μg/ml kanamycin.

Versene-trypsin: 136mM NaCl, 5.3mM KCl, 5.5mM $NaHCO_3$, 0.02% trypsin, 0.01% versene (EDTA), and 0.1% phenol red.

2.3 Viruses and cells.

Vero (ECACC 84113001) African Green monkey kidney cells were obtained from the European Collection of Animal Cell Cultures (Porton Down, United Kingdom). Cells were grown at 37°C in Hepes-buffered Dulbecco's modified Eagle's medium (DMEM), supplemented with 10% foetal calf serum (FCS), 20mM L-glutamine, 100units/ml penicillin and 100units/ml streptomycin.

The attenuated, tissue culture adapted BA71v strain of ASF virus has been described previously (Carrascosa et al, 1985; Sun et al, 1995).

2.4 Virus infection protocols.

2.4.1 Virus infection.

Vero cells were infected with 5 MOI for 60 minutes at 37°C, after which fresh DMEM supplemented with 2% FCS was added and cells were incubated at 37°C for the indicated time periods.

2.4.2 Virus titration.

10-fold serial dilutions of ASFV supernatant were incubated with 80% confluent Vero cells in a 96 well plate for 16 hours at 37°C. The supernatant was removed and the plate washed gently by flooding three times with PBS. The monolayers were fixed with methanol (50µl/well) for 20 minutes at room temperature (RT) and were further washed three times with PBS. The cells were blocked with 10% FCS in PBS (50µl/well) for 20 minutes at RT, followed by a final wash in PBS. The 4H3 monoclonal antibody (anti-p73 capsid protein) was diluted with PBS, containing 10% FCS, and 50µl added to each well, and incubated at RT for 20 minutes. The plate was washed three times in PBS. A 1/500 dilution of anti-mouse HRP conjugate in 10% FCS in PBS (Southern Biotechnologies, USA) was added to each well (50µl/well) and incubated at RT for 20 minutes. The plate was washed three times in PBS and then 50µl substrate (0.4mg/ml 3-amino-9-ethylcarbazole in 0.1M acetate buffer, pH 5.2, and 0.1% hydrogen peroxide) was added and incubated at RT for 30 minutes. The plate was flooded with water and read under a light microscope. A red/brown

precipitate was formed in infected cells allowing the $TCID_{50}$ in the original supernatant to be calculated.

2.5 Antibodies.

2.5.1 ASFV antibodies.

Monoclonal antibody 4H3, recognising p73, was generated by Trevor Whittle at the Institute for Animal Health, Pirbright, UK (Cobbold et al, 1996). The mouse monoclonal antibody specific for vp30 was a generous gift from Dan Rock (Plum Island Animal Disease Centre, NY. USA) (Afonso et al, 1992). The rabbit polyclonal antibody raised against recombinant p73 protein was generated by Christian Cobbold (Institute for Animal Health, Pirbright Laboratory, UK). Rabbit polyclonal antibodies, p34R and p37R, were generated from recombinant proteins (see below). Rabbit antisera raised against the C-terminus of p34 and the N- and C-termini of p150 were generated using synthetic peptides (see below).

2.5.2 Primary antibodies.

The monoclonal antibodies anti-Hsp70, a stress induced molecular chaperone; and anti-t-complex polypeptide 1 (TCP-1) α-subunit, a 60kDa subunit of a cytosolic hetero-oligomer chaperone involved in the folding of actin and tubulin (Willison et al, 1986, 1989) were purchased from Stressgen Biotechnologies Corp, Canada. The monoclonal antibody HDJ-2/DNAJ Ab-1, a human homologue of the *Escherichia coli* DNAJ protein (Chelliah et al, 1993), was supplied by Neomarkers, CA, USA. The anti-20S proteasome, α-subunit, was supplied by Calbiochem, CA, USA. The monoclonal antibodies anti-α-

tubulin (clone B-5-1-2), anti-γ-tubulin (clone GTU-88) and anti-vimentin (clone V9) were purchased from Sigma, Mo. USA. The anti-ubiquitin antibody was supplied by DAKO, Denmark. The mouse monoclonal and rabbit polyclonal α-TCR CD3 δ-chain antibodies were a kind gift from T.Wileman and are described in Pessano et al (1985).

2.5.3 Fluorescence conjugated antibodies and dyes.

The Alexa Fluor™ 488 (green) and 594 (red) goat anti-mouse, anti-rabbit and anti-rat IgG (H+L) conjugates and the MitoTracker Red chloromethyl derivatives of X rosamine (CMXRos) were purchased from Molecular Probes, The Netherlands. The DNA stain, 4'-6-Diamidino-2-phenylindole (DAPI) was purchased from Sigma, Mo., USA. The goat anti-mouse and anti-rabbit HRP conjugates were purchased from Promega, UK.

2.6 Buffers and solutions.

All solutions were prepared in distilled water unless otherwise stated.

Phosphate buffered saline: 10mM sodium phosphate, 150mM NaCl, pH7.5.

2.6.1 DNA manipulation.

2.6.1.1 Agarose gel electrophoresis.

50X TAE buffer: 2M Tris, 4M sodium acetate, 2mM EDTA.

Ethidium bromide solution: 1.5% ethidium bromide in dH_2O.

2.6.1.2 Plasmid DNA preparation.

Suspension buffer: 50mM Tris/HCl pH 8, 10mM EDTA.

Lysis buffer: 0.2M NaOH, 1% (w/v) SDS.

Sodium acetate buffer: 3M Sodium acetate, 11% (v/v) acetic acid.

2.6.2 Protein purification buffers.

Sonication buffer: 20mM Tris, 300mM Sodium chloride.

Imidazole elution buffer: 100mM Imidazole in sonication buffer.

2.6.3 Protein analysis.

2.6.3.1 SDS-PAGE.

4X Resolving gel buffer: 1.5M Tris, 0.4% (w/v) SDS, pH 8.8.

2X Stacking gel buffer: 0.5M Tris, 0.2% (w/v) SDS, pH 6.8.

10X Running buffer: 250mM Tris, 2M glycine, 0.1% (w/v) SDS, pH 8.3.

5X Sample preparation buffer (SPB): 25% (v/v) glycerol, 7.5% (w/v) SDS, 13.5% (v/v) β-mercaptoethanol, 0.1% (w/v) bromophenol blue, 62.5mM Tris, pH 6.8.

Coomassie blue stain: 0.05% (w/v) coomassie blue, 50% (v/v) methanol, 10% (v/v) glacial acetic acid.

Destain solution: 10% (v/v) methanol, 10% (v/v) glacial acetic acid.

Enhance solution: 1M Sodium salicylate.

2.6.3.2 Immunoprecipitation buffers.

Immunoprecipitation buffer (IPB): 50mM Tris, 1mM EDTA, 0.15M NaCl, 1% (v/v) Brij-35, 10mM iodoacetamide, 1mM PMSF, 1μg/ml SPI, pH 7.8.

1000X Small protease inhibitors (SPI): 1mg/ml leupeptin, 1mg/ml pepstatin, 1mg/ml antipain, 1mg/ml chymostatin.

2.6.3.3 Western blotting buffers.

Transfer buffer: 33% (v/v) 10X running buffer.

Blocking buffer: 5% (w/v) skimmed milk powder, 0.1% (v/v) Tween-20 in PBS.

Antibody incubation buffer: 10% (v/v) normal goat serum (NGS) in blocking buffer.

Washing buffer: 0.1% (v/v) Tween-20 in PBS.

2.6.3.4 Immunofluorescence microscopy buffers.

10X Tris buffered saline (TBS): 1.55M NaCl, 200mM Tris, pH 7.5.

Blocking buffer: 0.2% (w/v) gelatin, 0.1% (v/v) Triton X-100 in TBS, 30% (v/v) NGS.

Washing buffer: 0.1% (v/v) Tween-20 in PBS.

Paraformaldehyde fixative: 4% (w/v) paraformaldehyde in PBS, pH 7.5-8.

2.6.3.5 Electron microscopy buffers.

Phosphate buffer: 0.1M $NaH_2PO_4.H_2O$, 0.1M Na_2HPO_4, pH 7.2.

Uranyl acetate: Saturated Uranyl acetate in 50% ethanol.

Blocking buffer: 1% (w/v) BSA, 5% (v/v) NGS, 10mM glycine in PBS, pH 7.4.

2.6.4 Sucrose density sedimentation.

10-40% sucrose gradients: 10-70% (w/v) sucrose in immunoprecipitation buffer.

10-70% sucrose gradients: 10-70% (w/v) sucrose in 20mM Tris, pH 7.5.

2.6.5 Subcellular membrane fractionation.

Buffered sucrose: 8% (w/v) sucrose, 1mM EDTA, 20mM Tris, pH 7.5.

2.6.6 Protease protection assay buffers.

Trypsin solution: 5mg/ml trypsin in distilled water.

10X transport buffer: 25mM magnesium acetate, 500mM potassium acetate, 250mM HEPES/KOH, pH 7.2.

Trypsin inhibitor solution: 10mg/ml trypsin inhibitor, 100mM Tris, pH 7.5.

Trypsin stop solution: 10% (w/v) trypsin inhibitor solution, 10% FCS in IPB.

2.7 Manipulation of recombinant DNA.

2.7.1 Primer design.

Oligonucleotides were purchased from MWG Biotech, NC, USA. The p37 open reading frame (ORF) was obtained from the ORF of pp220 (CP2475L), from the African swine fever virus BA71v genome using the following primers: forward *GGATCCT***GCTGCTCTCACAGTTGAAG** (genome co-ordinates (bold) 106338-106320) and reverse *GAATTC***CTTACTCAGGTTCTAGCTCATCGG** (genome co-ordinates (bold) 105250-105223). The p34 ORF was obtained from the CP2475L gene of the BA71v strain of ASFV using the following primers: forward *GGATCCG***GGGGACAAAAATCCTGTACAAC** (genome co-ordinates (bold) 107772-107751) and reverse *GAATTC***GTTATAGTGGCGTTTTCTCCTCGTC** (genome co-ordinates (bold) 106780-106801). The primers were also designed to incorporate BamH1 and EcoR1 restriction sites (italics) when used in a polymerase chain reaction (PCR).

2.7.2 Polymerase chain reaction (PCR).

The PCR reactions were set up as follows:

5µl 10X Taq buffer

4µl $MgCl_2$

2µl 5mM dNTP

2µl 100µM forward primer

2µl 100µM reverse primer

100ng DNA template

5U Taq polymerase

To 50µl with sterile double distilled water.

The reaction mixture was overlaid with 30µl mineral oil and placed in a Biometra Trio thermoblock. The following PCR cycling parameters were used:

Denature 94°C for 30 sec

Denature 94°C for 30 sec
Anneal 55°C for 30 sec
Polymerise 72°C for 30sec
} 30 cycles

Polymerise 72°C for 10 minutes

10µl aliquots of each reaction were run on a 0.7%(w/v) agarose gel and the bands were visualised by ethidium bromide staining. The PCR product was isolated using the Qiagen Qiaex II kit (Qiagen Ltd, UK) (see below).

2.7.3 Restriction digestion of DNA.

Endonuclease digestions were performed according to the manufacturers instructions, normally performed in a 37°C waterbath.

2.7.4 Purification of DNA fragments.

DNA fragments were purified by running the samples on a 1% agarose gel, containing 0.1% ethidium bromide. The DNA bands were excised from the gel and the DNA was purified from the agarose using the Qiagen Qiaex II kit. The excised DNA/agarose was placed in a sterile 1.5ml microfuge tube and three volumes of QX1 buffer was added, along with 30µl Qiaex II beads to bind the DNA. The sample was incubated at >50°C for 10 minutes to melt the agarose. The sample was centrifuged for 30 seconds at 16,000*g* and the pellet was washed once in 500µl QX1 buffer, followed by two washes in 500µl wash buffer. The pellet was air-dried, resuspended in 20µl distilled water and incubated at 50°C for 5 minutes to elute the DNA. The beads were pelleted at 16,000*g* for 30 seconds and the purified DNA was removed to a sterile tube.

2.7.5 Ligation of DNA.

Ligations were performed at 16°C overnight. Each 10µl reaction consisted of 50-100ng of linearised vector, 0.5-1µg PCR product or DNA insert, 1µl 10X ligation buffer, 1-3U T4 DNA ligase (Promega) and distilled water to the final volume.

2.7.6 Transformation of bacteria.

50µl of JM109 competent cells (Promega) was thawed on ice. 1-10µl (1-10ng) of plasmid DNA or ligation reaction was added to each tube, mixed gently, and placed on ice for 1 hour. The DNA/competent cell mix was heat shocked for 40 seconds at 42°C and placed on ice for 2 minutes. 100µl LB broth was added to the mixture and was incubated for 1 hour at 37°C. Finally 10-150µl of mixture

was plated out onto agar plates containing the appropriate antibiotic and incubated overnight at 37°C.

2.7.7 Preparation of plasmid DNA.

2.7.7.1 Minipreps.

Single colonies were picked from the agar plates and added to 5ml of LB broth, containing antibiotic, in a 20ml Universal tube. The tubes were incubated overnight in a 37°C orbital shaker at 2,000rpm. 1.5ml of culture was removed and the bacteria were pelleted for 2 minutes at 16,000*g*. The pellets were resuspended in 100µl of suspension buffer and placed on ice for 5 minutes, 200µl lysis buffer was added and the suspension was mixed by inverting the tubes 3-4 times and then incubated on ice for 5 minutes. 150µl sodium acetate buffer was added, the solution was mixed by inverting, and placed on ice for a further 5 minutes. The suspension was centrifuged for 5 minutes at 16,000*g*. The supernatant was carefully decanted onto 450µl phenol/chloroform solution and mixed by vortexing. The mixture was centrifuged for a further 5 minutes at 16,000*g* and the top layer was pipetted off, added to 1ml of ice-cold absolute ethanol and incubated at -20°C for 30 minutes. The DNA was pelleted by centrifugation at 16,000*g* for 15 minutes at 4°C. The pellet was washed in 70% ethanol and dried. The pellet was resuspended in 30µl of sterile double distilled water.

2.7.7.2 Maxiprep.

For the preparation of a large concentration of DNA the Qiagen plasmid maxi kit (Qiagen Ltd, UK) was used. A single colony was picked and added to

300ml LB broth, containing antibiotic, and placed in a 37°C orbital shaker overnight. The bacterial cells were harvested at 6000g for 15 minutes at 4°C and resuspended in 10ml P1 suspension buffer. 10ml P2 lysis buffer was added and the suspension was mixed by inverting several times and then incubated at RT for 5 minutes. 10ml of chilled P3 precipitation buffer was added, mixed and incubated on ice for 20 minutes. The lysates were centrifuged at 20,000g for 30 minutes at 4°C and the supernatant was filtered with a prewetted Millipore glass fibre prefilter. The supernatant was added to an equilibrated Qiagen-tip 500 column and allowed to pass through the resin by gravity flow. The Qiagen-tip was washed twice with Qiagen wash buffer and the DNA was eluted with 15ml QF elution buffer. The DNA was precipitated with isopropanol and immediately centrifuged for 20 minutes at 15,000g at 4°C. The pellet was washed in 70% ethanol, air-dried at RT and resuspended in 300µl sterile double distilled water.

2.8 Synthesis of recombinant proteins.

2.8.1 Vector design.

PCR was used to amplify the p34 and p37 ORFs from the BA71v genome. The PCR products were then ligated into the pT7Blue capture vector (Novagen, WI. USA) and transformed into *E.coli* JM109 competent cells and positive clones selected by enzyme digestion of minipreps. The ORFs were excised from the vector using the BamH1 and EcoR1 endonucleases and, following purification, the ORFs were ligated into the expression vector, pTrcHisB (Invitrogen, CA., USA). The pTrcHisB expression vector was designed to add six histidine residues to the recombinant protein that function as a metal binding site in the expressed protein and allows for its purification by immobilised metal affinity

chromatography. The expression vector was then transformed into Novablue DE3 *Escherichia coli* (Novagen, WI. USA).

2.8.2 Protein expression.

A single *E.coli* colony was picked and used to inoculate 100ml LB medium containing 50μg/ml ampicillin and was grown overnight at 37°C in an orbital shaker. 400ml LB medium containing 50μg/ml ampicillin was inoculated with the overnight culture and then grown at 37°C with shaking to the mid-log phase (OD_{600}=0.6). Protein expression was induced with the addition of IPTG to a final concentration of 1mM and the cells were incubated at 37°C for 4 hours.

2.8.3 Recombinant protein purification.

2.8.3.1 Preparation of *E.coli* cell lysates.

The induced cells were harvested at 4,000*g* for 10 minutes and the pellet was resuspended in 16ml sonication buffer. The cells were then lysed with the addition of 0.75mg/ml egg white lysozyme and incubated for 15 minutes on ice. The lysate was then sonicated with five 20 second bursts at a medium intensity on a Misonix microscan ultrasonic cell disruptor with incubation on ice between sonications. The insoluble debris was removed by centrifugation at 3,000*g* for 5 minutes and the lysate was then stored at -20°C until use.

2.8.3.2 Binding and elution of the recombinant protein.

The recombinant protein was purified using Talon bead columns (Invitrogen, CA., USA). The protein was added to 5ml Talon beads, prewashed twice in sonication buffer, and bound at RT with gently rocking for 20 minutes.

The beads were packed by gravity and the supernatant was removed. The beads were washed five times with 25ml sonication buffer by re-suspending the beads, rocking for two minutes and then separating the beads from the supernatant by gravity. The beads were then added to a gravity flow column and allowed to pack under gravity and the recombinant protein was eluted by the addition of 100mM Imidazole. The eluted recombinant proteins were dialysed overnight at 4°C against sonication buffer. The protein concentration was measured using the Pierce BCA-200 protein assay kit. Briefly, 10µl serial dilutions of a 2mg/ml BSA standard were prepared in a microwell plate. The protein samples were diluted (1/1, 1/10, 1/100) and 10µl was added to the plate. 200µl mix of 50 parts BCA regent A (sodium carbonate, sodium bicarbonate, BCA detection reagent and sodium tartrate in 0.1M NaOH) and 1 part BCA reagent B (4% $CuSO_4.5H_2O$) were added to the samples. The plates were incubated at 37°C for 30 minutes and the absorbance at 560nm was a read on a Titertek Multiskan Plus spectrophotometer and a standard curve was plotted and protein concentrations calculated. The total protein concentration was made up to 200µg for a course of immunisation of two rabbits.

2.9 Design of synthetic peptides.

Synthetic peptides were designed against the C-terminus of p34 and the N- and C-terminus of p150. The peptides are shown in table 2.1.

Synthetic peptides were supplied by Severn Biotech Ltd, UK. The peptides were solubilised in either 100µl distilled water (p34C, p150C) or 100µl DMSO (p150N) to a final concentration of 10mg/ml. The carrier proteins, Imject maleimide activated ovalbumin and Imject maleimide activated keyhole limpet

hemocyanin (KLH) (Pierce, IL. USA) were reconstituted in distilled water to a final concentration of 10mg/ml and used immediately. The carrier proteins were added separately to the individual peptides and incubated at RT for 2 hours. The ovalbumin/peptide and KLH/peptide conjugates were combined and made up to a volume of 1ml. The complexes were dialysed overnight against PBS in a Slide-A-Lyzer 10K dialysis cassette (Pierce, IL. USA). The conjugates were then used for the immunisation of rabbits.

	Synthetic peptides	**Position**
p34 C-terminus	EKAVNLLRQTFNERHKILENSCAKK	342-366
p150 N-terminus	DYSETEIRQLIKEINVIYQHFNLE	961-984
p150 C-terminus	TEYGFSITGPSETFSDKQYDSDIR	2450-2473

Table 2.1: The synthetic peptides used to generate antisera.

2.10 Analysis of proteins.

2.10.1 Preparation of membranes and cytosol from ASFV infected cells.

ASFV (BA71v) infected Vero cells were stripped from flasks by incubation with versene trypsin and pelleted at 3,000*g* for 5 minutes. Cells were resuspended in 8% buffered sucrose and homogenised by 20 passages through a 25-gauge needle. Whole cells and nuclei were removed by centrifugation at 3,300*g* for 2 minutes. Post nuclear supernatants were pelleted at 16,000*g* for 15 minutes at 4°C to separate membrane and cytosolic fractions.

2.10.2 Preparation of ASF virions.

BA71v infected Vero cells were cultured for 24-48 hours until an extensive cytopathic effect was observed. The culture media was removed and centrifuged for 15 minutes at 500*g* to remove cell debris and then the virus was pelleted at 30,000*g* for 1 hour at 4°C in a Beckman 50Ti rotor.

2.10.3 Metabolic labelling and immunoprecipitation.

Cells were labelled metabolically with ^{35}S methionine and cysteine using ^{35}S-Pro-mix (Amersham Pharmacia, UK). Briefly, cells were pre-incubated with methionine- and cysteine-free Eagles medium for 15-30 minutes at 37°C. After starvation the media was replaced by 1MBq/ml ^{35}S-Pro-mix in methionine-cysteine-free media for the indicated time periods at 37°C. Cells were washed twice and 'chased' in DMEM, supplemented with 10% FCS, 20mM L-glutamine, 100units/ml penicillin and 100units/ml streptomycin. At the appropriate time intervals, cells were washed once in PBS and released from the flask with versene trypsin. The cells were then lysed in immunoprecipitation buffer containing 1% Brij-35. The lysates were pre-cleared by the addition of fixed *Staphylococcus aureus* (Cowan strain) for 30 minutes at 4°C. After centrifugation lysates were immunoprecipitated at 4°C using antibodies immobilised on Protein A sepharose beads. Proteins were separated by SDS-PAGE and visualised by autoradiography as previously described (Wileman et al, 1993). Gels were fixed in destain for 30 minutes and then placed in the enhancing solution for a further 30 minutes. The gels were dried and processed for autoradiography.

2.10.4 Enhanced chemiluminescence Western blotting analysis.

Proteins were resolved by SDS-PAGE and then transferred onto Protran BA85 nitrocellulose membranes (Schleicher & Schuell, Germany) using a semi-dry Western blotter (Biometra Fast blot B33) under a constant current of 5mA/cm^2 for 20 minutes. The membrane was blocked in blocking buffer for 30 minutes at 37°C with gentle rocking. The membranes were incubated with the primary antibody diluted in the antibody incubation buffer at 37°C for 20 minutes. After 5x5 minute washes in the washing buffer the membranes were incubated with the secondary antibody (anti-rabbit/mouse-HRP) diluted in the antibody incubation buffer for 20 minutes at 37°C. The membranes were washed extensively and then incubated according to the instructions for the Super Signal kit (Pierce Chemical Co, IL. USA). After 2 minutes the membranes were wrapped with Saran wrap for fluorography.

2.10.5 Immunofluorescence microscopy.

Cells were grown on No.1 glass coverslips to approximately 70% confluency. Cells were fixed in -20°C methanol or 4% paraformaldehyde. The cells were then washed extensively in wash buffer and were then blocked in blocking buffer for 15 minutes. The cells were washed further and then incubated for 30 minutes with the primary antibodies in 0.1% Tween-20 in TBS. The cells were washed for five five-minute periods in wash buffer and then incubated with the Alexa Fluor 488 or 594 IgG conjugated secondary antibodies at a 1:500 dilution of a 2mg/ml stock. Cells were washed as before and then incubated for five minutes with a 1:10,000 dilution of a 5mg/ml stock of DAPI in 100% ethanol. Cells were washed a final time in distilled water and were mounted onto slides in

Fluoromount-G (Southern Biotechnologies, USA). The cells were viewed at 60X/1.4 NA or 100X/1.3 NA with a Nikon E800 microscope. The images were captured with a Hamamatsu C-4746A DCC camera and were deconvolved using the Improvision Openlab software. 2μm of optical sections 0.2μm thick were analysed.

2.10.5.1 Expression of the GFP-250 protein chimera.

Vero cells were grown on coverslips to 70% confluency and were then transiently transfected with the plasmid using a liposomal "Transfast" transfection system (Promega, UK). Briefly, 5μg of GFP-250 plasmid and 5μl of Transfast were added to 100μl of Optimem for each coverslip and vortexed. The mixture was incubated at RT for 15 minutes. In the meantime the cells were washed twice in Optimem and 100μl of Optimem was added to the cells. The Transfast/DNA was added to each coverslip and incubated at 37°C for one hour. The cells were then topped up with 500μl DMEM supplemented with 10% FCS and incubated for 24-48 hours.

2.10.6 Electron microscopic techniques.

Cells were harvested by scraping, fixed in 2% paraformaldehyde, 0.05% glutaraldehyde in phosphate buffer for one hour and then embedded in 8% gelatin. The gelatin blocks were infused with 2.3M sucrose in PBS, frozen in liquid nitrogen and then 75nm sections were cut at -100°C on a Leica UCT cryoultramicrotome. The sections were collected on formvar/carbon coated gold grids. The sections were incubated on drops of blocking buffer and then immunolabelled with a 1:200 dilution of α-p34R antibody in blocking buffer. The

sections were washed extensively and then incubated with a 1:30 dilution of α-rabbit Ig conjugated to 5nm colloidal gold. Sections were further washed in distilled water, contrasted with 4% aqueous uranyl acetate and embedded in 1.1% methyl cellulose containing 0.2% aqueous uranyl acetate. The sections were imaged in a JEOL 1200EX electron microscope at 80kV.

2.10.7 Sucrose density sedimentation analysis.

BA71v infected cell lysates, solubilised membranes and cytosolic fractions were prepared as previously described. 2ml of pre-cleared fractions were applied to the top of a 10ml 10-40% sucrose gradient layered over a 1ml 70% sucrose cushion. Sucrose gradients were prepared by making step gradients containing 2ml each of 10, 20, 30, 35 and 40% sucrose in IPB. Gradients were left overnight at 4°C to equilibrate. The gradients were centrifuged at 200,000*g* for 20 hours at 4°C and then collected into 10 fractions. Continuous 10 to 70% gradients were prepared by making step gradients containing 2ml each of 10, 20, 30, 40, 50 and 70% sucrose dissolved in 20mM Tris pH 7.5. Gradients were left overnight at 4°C to equilibrate. The sample was then loaded onto the gradient and centrifuged at 79,000*g* for 2.5 hours at 4°C. The gradients were collected into 1.2ml fractions.

3. Characterisation of antibodies specific for the products of the pp220 polyprotein.

3.1 Generation of antigens.

3.1.1 Production of recombinant proteins.

Antibodies recognising structural proteins are a valuable tool for the study of virus biosynthesis, assembly and localisation studies. One method for obtaining such antibodies is to synthesise recombinant proteins, and use these to raise antisera in rabbits.

p37 and p34 were chosen as targets for antibody production as these were shown conclusively by NH_2-terminal sequencing to be final products of pp220 processing (López-Otín et al, 1989; Simón-Mateo et al 1993). The p150 protein was also shown to be a final product of pp220 processing, but due to the size of the reading frame (4746bp) it was anticipated that there may be difficulty in obtaining a full length PCR product. For this reason synthetic peptides were chosen as a means of raising antibodies (see below). The pp220 polyprotein is encoded by the open reading frame CP2475L. Synthetic oligonucleotide primers were designed to extract the reading frames of p37 and p34 from the CP2475L gene by PCR. The primers were designed with unique restriction sites to allow in frame cloning into the expression vector, pTrcHisB, a vector with a *trc* (*trp-lac*) promoter (Amann et al, 1983) and which attaches an affinity tag of six histidine residues to the N-terminus of translated proteins (Figure 3.1). PCR was carried out using the primers described in the materials and methods, the PCR product was then ligated into pT7blue, a capture vector. Endonuclease digestions and fragment analysis were carried out to ensure that the vector had ligated an insert of the correct size. The correct reading frame was confirmed by sequencing

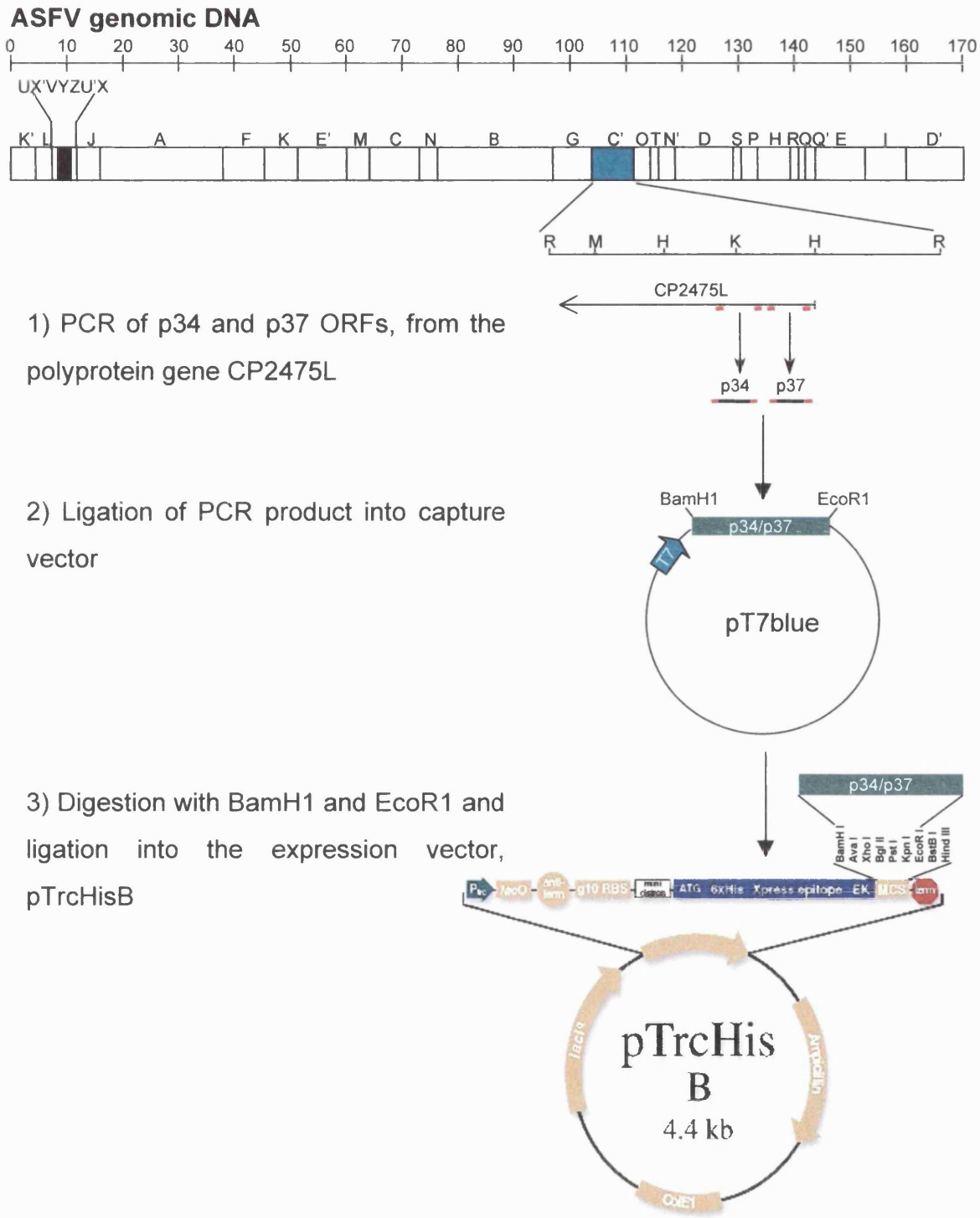

Figure 3.1: The cloning strategy for the expression of recombinant p34 and p37. The ASFV genomic DNA, showing the location of the 220kDa polyprotein gene, CP2475L (adapted from Yáñez et al, 1995). The ORFs for p34 and p37 were extracted by PCR and then ligated into the capture vector, pT7blue. The vector was digested with BamH1 and EcoR1 and the ORFs were ligated into the multiple cloning site of pTrcHisB.

(data not shown). The reading frame was cut from the capture vector, using BamH1 and EcoR1, and was ligated into the expression vector, pTrcHisB. Novablue DE3 *Escherichia coli* were transformed with the construct and grown to log phase at 37°C. Protein expression was induced by the addition of 1mM IPTG and the bacteria were incubated at 37°C for a further 4 hours. The pelleted bacteria were lysed with by addition of 100µg/ml lysozyme, followed by two cycles of freeze/thawing. Following sonication, cell debris was removed by centrifugation and the supernatant was added to a nickel column to bind the His-tagged protein. The column was washed and the bound proteins were eluted with 100mM imidazole. The purified proteins were resolved on a 10% SDS-PAGE. Figure 3.2 shows the purified recombinant proteins, p34 and p37, the proteins were resolved with molecular weights of 39 and 43kDa; the actual molecular weights for p34 and p37 are 36.3kDa and 41.5kDa respectively (Yáñez et al, 1995, Andrés et al, 1997). This difference in molecular weight is due to the N-terminal His_6 modification added to the proteins by the pTrcHisB vector, which increase the molecular weight of the protein by approximately 3kDa. The recombinant proteins were then used in the immunisation of rabbits. The sera was collected and tested by Western blotting and immunoprecipitation.

3.1.2 Design of synthetic peptides.

A second method for making antibodies for viral proteins is to design peptides containing amino acid sequences corresponding to the amino acid sequence of the protein of interest, which can then be used to immunise animals. The major advantage of this approach is that the epitope for the antisera is known, whereas immunisation of rabbits with the recombinant protein produces

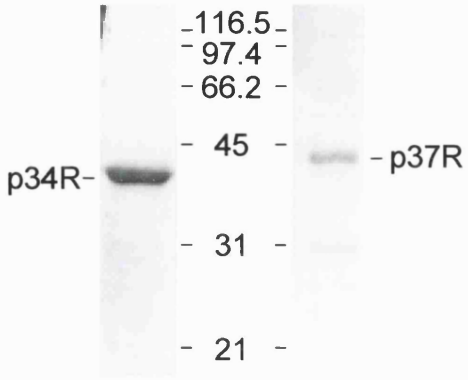

Figure 3.2: SDS-PAGE analysis showing the final purified p34 and p37 recombinant proteins. Using PCR, the open reading frames (ORF) for p34 and p37 were transcribed from the CP2475L gene. The ORFs were ligated into the pTrcHis expression vector and *E.coli* were then transformed with the plasmid. Protein expression was induced by IPTG and the recombinant proteins were purified from cell lysates using nickel columns. A representative sample of the purified recombinant protein was resolved on a 10% SDS-PAGE and visualised by staining with coomassie blue.

antisera possibly recognising epitopes throughout the protein. p34 has 4 Gly-Gly-X sites near its C-terminus and it was decided to design a peptide on the N-terminal side of these sites to ensure that the epitope was not cleaved during processing (Figure 3.3A). Antisera were raised against peptides from the N- and C-termini of the p150 protein to allow the distribution and role of the largest product of pp220 processing to be studied. Figure 3.3 shows the location and design of the synthetic peptides. The peptides were bound to carrier proteins, ovalbumin and keyhole limpet hemocyanin, and then used in the immunisation of rabbits. The resulting sera were characterised using Western blot and immunoprecipitation analysis.

3.2 Characterisation of the antisera.

As already stated the initial work on the characterisation of the polyprotein and its processing to the four structural proteins was undertaken by Simón-Mateo et al (1993). The polyprotein, intermediates and structural proteins were named according to their migration on SDS polyacrylamide gels. On examination of the amino acid sequence, however, the predicted molecular weights are different from those reported by Simón-Mateo et al (1993). The predicted molecular weights for the polyprotein and structural proteins are 281.5 (pp220), 181.1 (p150), 41.5 (p37), 36.3 (p34), and 17.8kDa (p14) (Yáñez et al, 1995; Andrés et al, 1997). To avoid confusion, the same nomenclature, described by Simón-Mateo et al (1993) was used throughout this report, but it should be appreciated that the proteins migrate slower than expected. The major difference between the predicted and apparent molecular masses of the polyprotein could be explained by deviations in the molecular weight estimation by SDS-PAGE,

A.

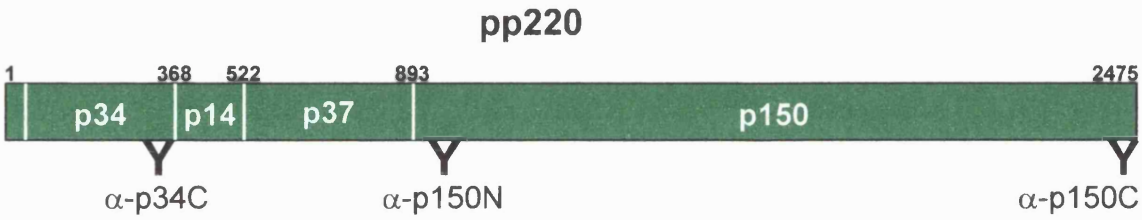

B.

	Synthetic peptides	Position
p34 C-terminus	EKAVNLLRQTFNERHKILENSCAKK	342-366
p150 N-terminus	DYSETEIRQLIKEINVIYQHFNLE	961-984
p150 C-terminus	TEYGFSITGPSETFSDKQYDSDIR	2450-2473

Figure 3.3: The location (A) and design (B) of the synthetic peptides used in the production of antibodies against pp220, p34 and p150.

especially for the polyprotein and p150 protein. On any given gel concentration the relationship between log_{10} molecular mass and relative mobility is linear only over a limited range of molecular mass. The linear relationship holds true over the following ranges: 5% SDS-PAGE, 25-200kDa; 10% SDS-PAGE, 15-70kDa; 15% SDS-PAGE, 12-45kDa (Hames, 1990), therefore using 5 or 7.5% SDS-PAGE to resolve pp220 and p150 will be prone to produce inaccurate molecular weight determinations. This would mean that the molecular weights described for these proteins may vary slightly during the course of this report, however the proteins will be clearly described in each section, using the Simón-Mateo nomenclature.

3.2.1 Analysis by Western blotting.

3.2.1.1 Purified virions.

The rabbit antisera raised against the recombinant proteins and against the synthetic peptides were first tested by Western blot analysis of purified virions. Andrés et al (1997) reported that the final products of processing were present in equimolar amounts in mature virions and accounted for 25% of the total protein content of the virions. BA71v infected Vero cells were cultured until an extensive cytopathic effect was observed, cell debris was removed by centrifugation at 500*g* for 15 minutes and a crude virus preparation was generated by pelleting at 30,000*g* for 1 hour. The pellet was lysed in sample preparation buffer, resolved by SDS-PAGE, transferred to nitrocellulose and probed with the antisera. Figure 3.4A shows the blot probed with the antibodies raised against the recombinant p34 or p37 proteins. The two antisera raised against p34 showed very strong cross reactivity with a band at approximately

34kDa. The same band was present at lower intensity, when the blot was probed with the preimmunisation sera. This band is most likely the result of spill over of the antibody specific for p34 into the lanes during the preparation of the blot. The first antisera raised against the p37 recombinant protein reacted with a band migrating at approximately 37kDa. The pre-immune sera detected bands at 34kDa, which are probably a result of spill over of the antibody specific for p34.

Figure 3.4B showed that the two antibodies raised against a peptide corresponding to the C-terminus of p34 bound to proteins within the virus. The same proteins were recognised by the pre-immune sera. Unfortunately none of the bands were of the correct molecular weight to be p34, so the immunisations were unsuccessful.

Figure 3.4C showed that the antisera raised against the synthetic peptides for the N- and C- termini of p150 cross-reacted with a ≈180kDa band, which is the correct molecular weight of the p150 protein. The intensity of signal varied between antisera. The strongest reacting antibodies were chosen for further studies.

3.2.1.2 Cell lysates.

The rabbit antisera raised against the recombinant proteins and the synthetic peptides were further characterised by probing Western blots of cell lysates prepared from infected cells. Cell lysates were prepared from uninfected and BA71v infected cells and were resolved by SDS-PAGE, transferred to nitrocellulose membranes and probed with the different antisera.

Figure 3.5A shows the analysis of lysates prepared from control (uninfected) cells. The first antiserum raised against the p34 recombinant protein

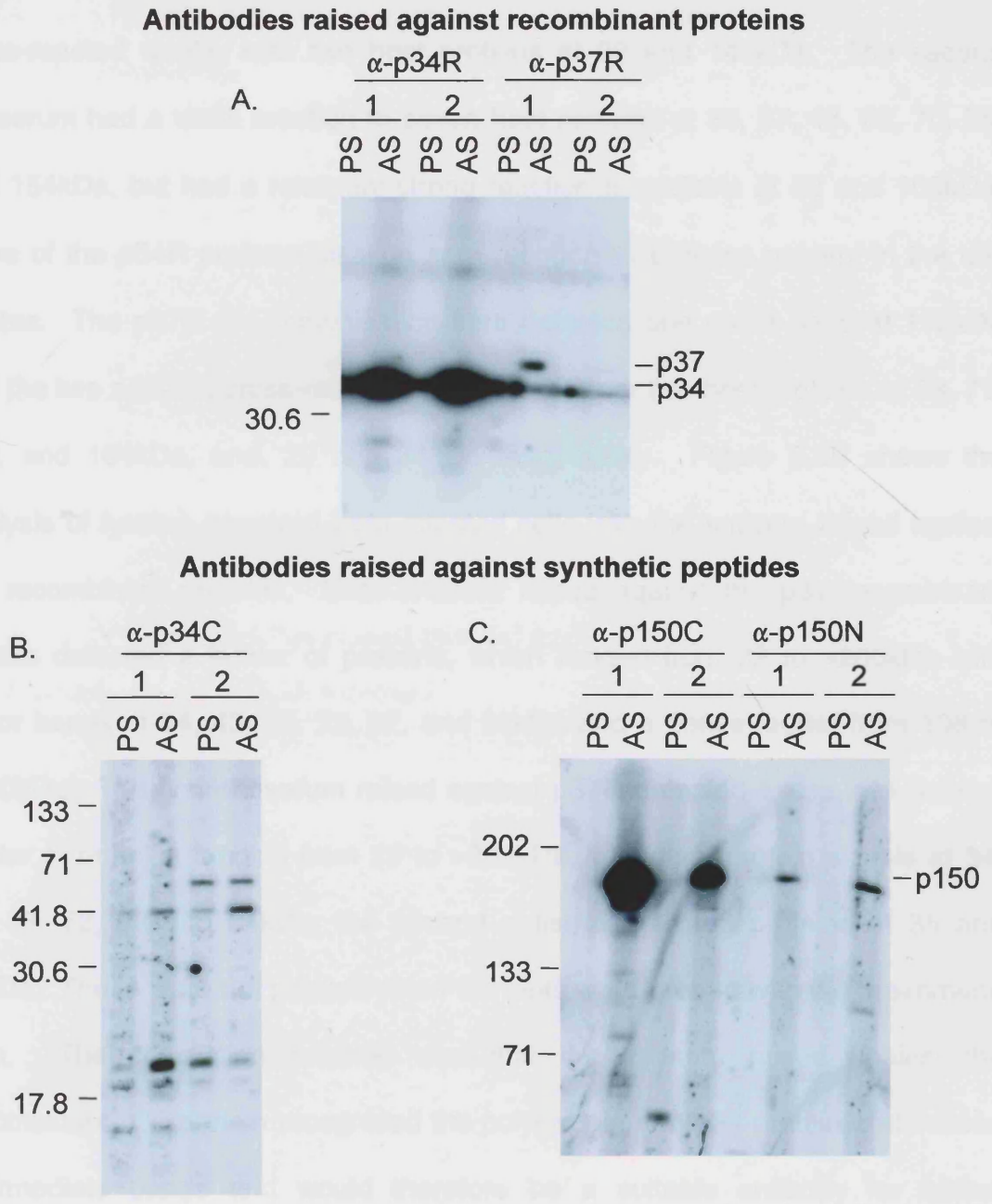

Figure 3.4: Characterisation of antibodies raised against the polyprotein products p34, p37 and p150 by Western blots of purified virions. BA71v infected Vero cells were cultured until an extensive cytopathic effect was observed, cell debris was removed by centrifugation at 500*g* for 15min and the virus was pelleted at 30,000*g* for 1h and lysed. The lysates were resolved on a 12.5% (A,B) or a 7.5% (C) SDS-PAGE, Western blotted and probed with either the pre-immunisation sera (PS) or the antibodies (AS) against p34R (A), p37R (A), p34C (B), p150C (C), or p150N (C).

cross-reacted weakly with two host proteins at 92 and 142kDa. The second antiserum had a weak reaction to seven host proteins at 30, 37, 48, 60, 70, 75, and 154kDa, but had a relatively strong reaction to proteins at 82 and 108kDa. None of the p34R preimmunisation sera recognised proteins present in the cell lysates. The p37R pre-immunisation sera detected one major band at 112kDa and the two antisera cross-reacted with either four or two host proteins at 53, 71, 109, and 164kDa, and, 29 and 34kDa respectively. Figure 3.5B shows the analysis of lysates prepared from infected cells with the antisera raised against the recombinant proteins. Both antisera raised against the p34 recombinant protein detected a ladder of proteins, which ranged from 32 to >200kDa with major bands at 34, 43, 55, 72, 82, and 98kDa and a dense ladder from 108 to >200kDa. The first antiserum raised against p37R detected a less well defined ladder of proteins ranging from 29 to >202kDa, with clear protein signals at 34, 37, 48, 72, 83 and 94kDa; the second antisera detected proteins at 35 and 57kDa. These were not present when the blots were probed with the preimmune sera. The conclusion reached was that the antisera raised against the recombinant p34 protein recognised the polyprotein, the p34 protein and several intermediate bands and would therefore be a suitable antibody for further investigations. The first antiserum was chosen as there was very little cross-reactivity with cellular proteins. The antibodies raised against the recombinant p37 protein failed to detect the polyprotein or the p37 protein and were therefore of no further use.

Figure 3.5C shows the results of using the antisera raised against the C-terminus of p34 to probe lysates from infected cells. The first antiserum detected a single protein at 133kDa, which was present in both the pre-immunisation

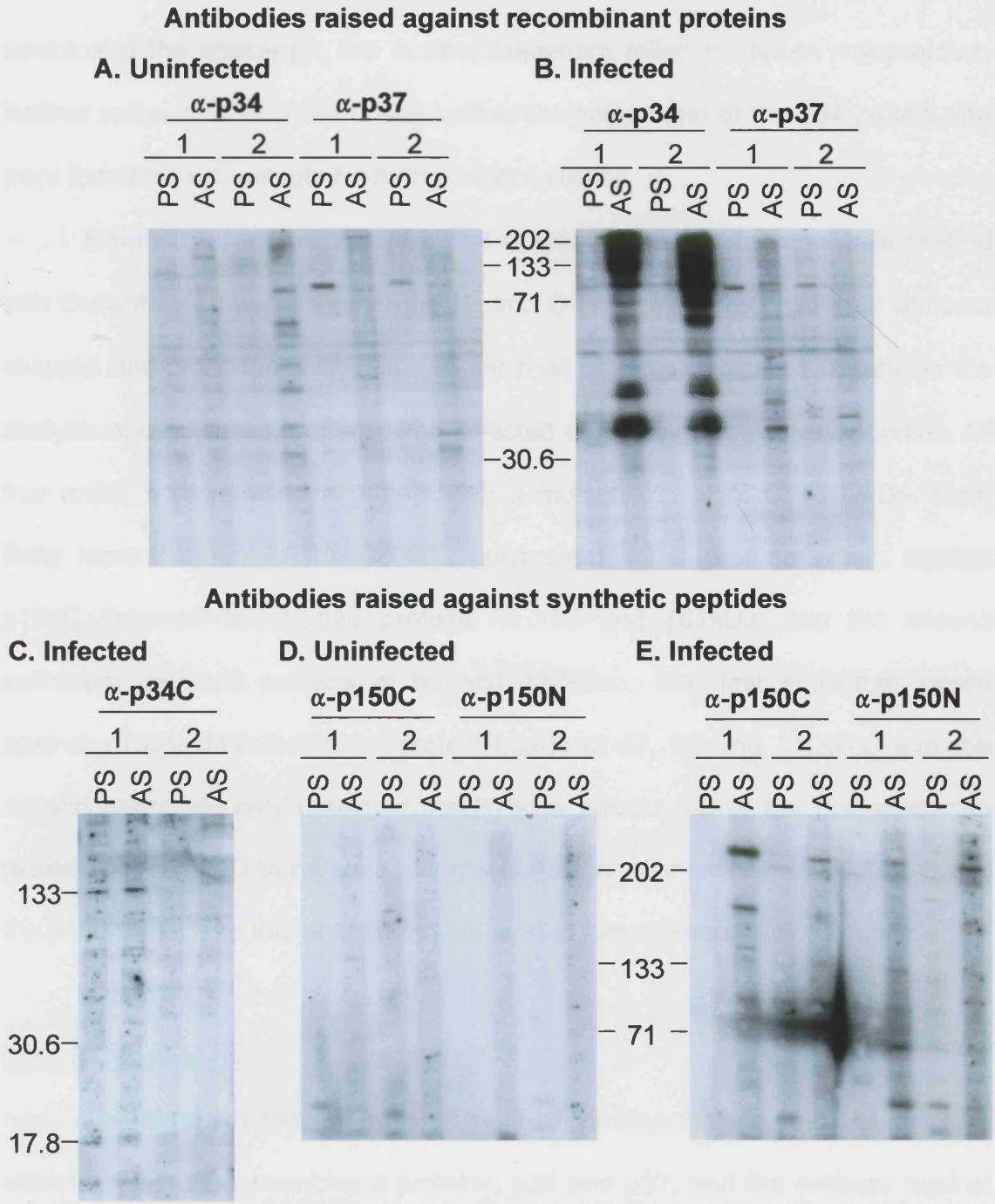

Figure 3.5: Characterisation of antibodies raised against the polyprotein products p34, p37 and p150 by Western blots of lysate taken from infected cells. Vero cells were mock infected (A,D) or infected for 16 hours with BA71v (B,C,E) and lysates were prepared. The lysates were resolved on a 12.5% (A,B,C) or a 7.5% (D,E) SDS-PAGE, Western blotted and probed with either the pre-immunisation sera (PS) or the antibodies (AS) against p34R (A,B), p37R (A,B), p34C (C), p150C (D,E), or p150N (D,E).

serum and the antiserum, the second antiserum failed to detect any proteins. Neither antisera were able to detect either the polyprotein or the p34 protein and were therefore not suitable for further investigations.

Figure 3.5D shows Western blot of lysates from uninfected cells probed with the antisera raised against the N- and C-termini of p150. All four antisera showed little cross-reactivity with cellular host proteins. Figure 3.5E shows the analysis of cell lysates prepared from infected cells using the same antibodies. All four antisera recognised a protein with a molecular weight of >202kDa, most likely representative of the 220kDa polyprotein. The first antiserum against p150C detected two further proteins at 135 and 161kDa, and the second antiserum detected proteins at 86 and 122kDa. The first antiserum raised against p150N detected minor protein bands at 47, 68 and 112kDa, with the second antiserum only detecting the 200kDa protein. Only the first antiserum raised against the C-terminus peptide was able to react with the polyprotein and the p150 protein, so this antiserum was used in further investigations.

3.2.1.3 Conclusions.

The Western blot analysis of purified virions showed that the antisera raised against the recombinant proteins, p34 and p37, and the antisera against the N- and C-terminus of p150 were able to detect proteins of the correct sizes representative of the final proteins produced from processing of the polyprotein. The antibodies specific for the recombinant p34 and C-terminus of p150 were also able to recognise the polyprotein and the final proteins, p34 and p150, when used to probe blots of infected cell lysates. However, when the α-p37R and α-p150N antibodies were used to probe blots of infected cell lysates it was difficult

to detect either the polyprotein or the final products and therefore meant these antibodies were not suitable for Western blot analysis. The antibodies specific for the recombinant p34 and C-terminus of p150 produced an interesting observation about the processing of pp220. Simón-Mateo et al (1993) showed that processing of the polyprotein was by an ordered process, but these antisera recognised several more bands than would be predicted from the work of Simón-Mateo et al (1993). This observation will be further explored in later sections.

3.2.2 Analysis by immunoprecipitation.

The antisera raised against the recombinant proteins, p34 and p37, and against the synthetic peptides were also tested using immunoprecipitations. Vero cells were infected with the attenuated BA71 strain of ASFV for 16 hours, the cells were then metabolically labelled for 2 hours and whole cell lysates were prepared. The lysates were then immunoprecipitated with the relevant antisera. Figure 3.6 shows that the SDS-PAGE analysis of the immunoprecipitations. Figure 3.6A shows the two antisera raised against the recombinant p34 protein immunoprecipitated a major band with a molecular weight of >220kDa, which corresponds to the pp220 polyprotein. This band was not recognised by the preimmunisation sera. The two antisera raised against the p37 recombinant protein also detected a band of >220kDa, which was not recognised by the preimmunisation sera. As seen for the Western blots the second antisera gave a weaker signal than the first. The two antisera recognising p34R and the first antisera raised against p37R were used in a second immunoprecipitation experiment, which was resolved on a 12.5% SDS-PAGE in an attempt to visualise the final products of pp220 processing (Figure 3.6B). After a 2 hour

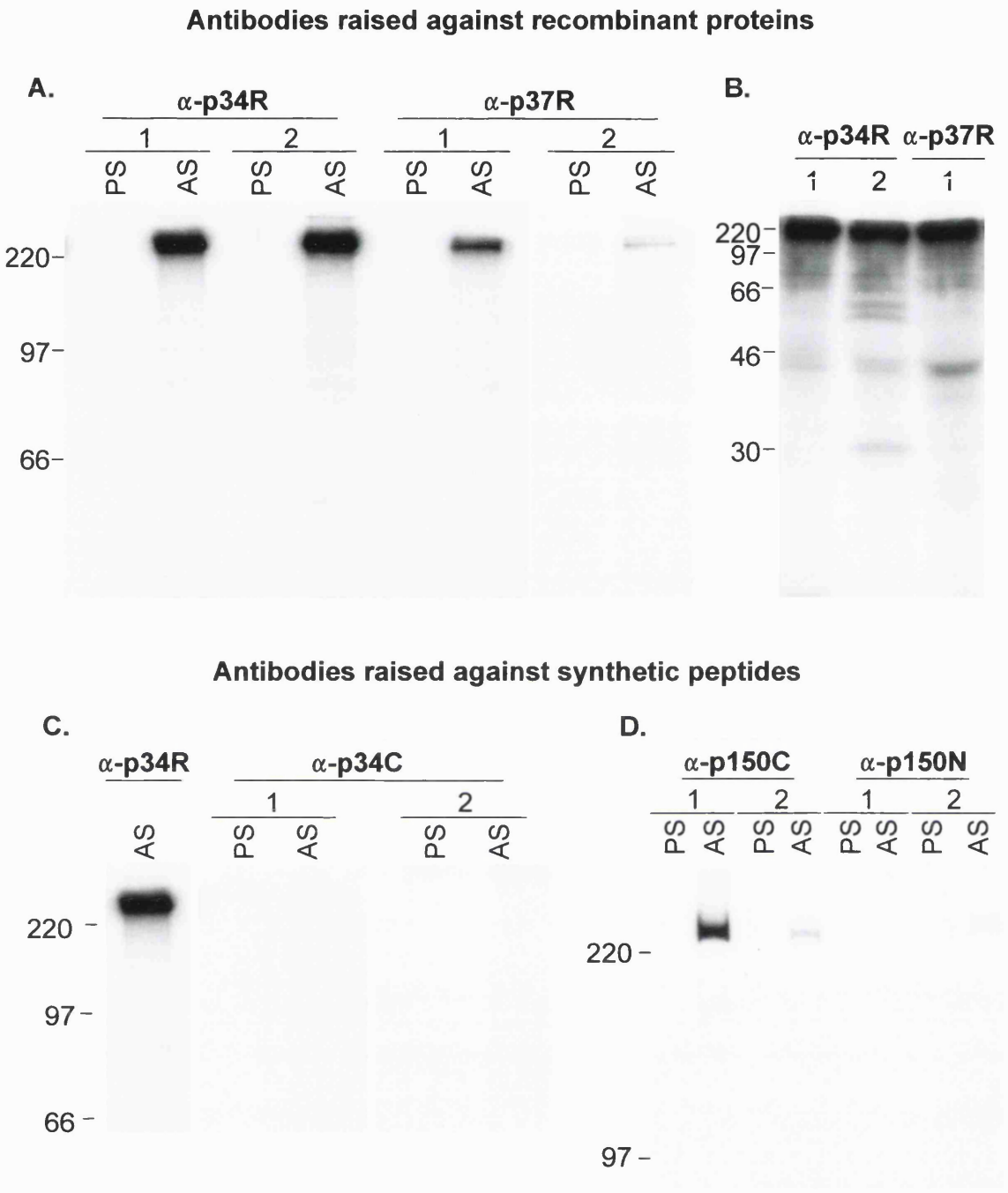

Figure 3.6: Characterisation of antibodies raised against polyprotein products p34, p37 and p150 by immunoprecipitation of infected cells. Vero cells were infected for 16h with BA71v, metabolically labelled for 2h and lysed. Levels of the polyprotein and products were determined by immunoprecipitation using the pre-immunisation sera (PS) or the α-p34R (A,B,C), α-p37R (A,B), α-p34C (C), α-p150C (D), or the α-p150N (D) antibody (AS). The immunoprecipitated proteins were resolved on 5% (A, C, D) or 12.5% (B) SDS-PAGE.

pulse all three of the antisera detected the 220kDa polyprotein, a dense ladder of proteins descending to 67kDa and a band at 41kDa. The second p34 antiserum detected a doublet at 55 and 60kDa and a weak band of 30kDa, which may correspond to the final product of pp220 processing to p34, but appears to migrate faster than the p34 band visualised in the Western blots (Figures 3.4 and 3.5). Figure 3.6C shows the immunoprecipitation of infected cell lysates with the antisera raised against the C-terminus of p34. The first lane shows the immunoprecipitation with the α-p34R antibody as a control for infection. The antisera raised against the p34 C-terminus peptide failed to immunoprecipitate any proteins, as visualised by PAGE. This is consistent with the results of Western blot analysis for these antibodies. Figure 3.6D shows the proteins immunoprecipitated with the antisera raised against the N- and C- termini of the p150 protein. The antipeptide antisera were also characterised by immunoprecipitation. The antisera raised against the C-terminus of p150 detected a band of >220kDa, with the first antisera giving a much stronger signal, whereas the antisera raised against the N-terminus failed to immunoprecipitate any proteins.

The characterisation of the antibodies by immunoprecipitation has shown that the antisera raised against the p34 and p37 recombinant proteins and against the C-terminus of p150 were able to immunoprecipitate a major protein of ≥220kDa. This protein is the pp220 polyprotein, which has a predicted molecular weight of 281kDa (Yáñez et al, 1995) and therefore is very difficult to resolve accurately by SDS-PAGE (Hames, 1990). The second α-p34R antibody detects a protein at 30kDa, which is smaller than the size of p34 seen in the Western blots, but may still be a product of proteolytic processing and will be further

investigated. These antibodies, although they do not recognise a well-defined product of processing, will be of use in study of the distribution and processing of the polyprotein. The antisera raised against the peptides for the p34 C-terminus and p150 N-terminus were unable to immunoprecipitate any proteins and were not used in subsequent investigations.

3.3 Summary.

In summary, antibodies were raised that recognised p34, p37 and p150. Proteins of the anticipated size were detected in purified virions. Analysis of cell lysates by Western blot or immunoprecipitation detected the polyprotein of the predicted size. Interestingly, analysis of cells infected with ASFV, by Western blot analysis, revealed a ladder of proteins of sizes not anticipated from the processing cascade described by Simón Mateo et al (1993). These results suggest that aberrant processing of pp220 may take place in cells. It was also possible to detect proteins of approximately 34 and 150kDa in the cell lysates and crude virus preparations by Western blot, however not by immunoprecipitation analysis.

4. The distribution of the pp220 polyprotein and the 34kDa processing product in cells and virions.

4.1 Introduction.

The use of proteolytic processing in the maturation of single proteins in DNA viruses has been shown to play a role in viral morphogenesis, for example in adenoviruses type 2 (Rashid Bhatti and Weber, 1979), herpesvirus (Liu and Roizman, 1991) and poxvirus (Katz and Moss, 1970). Polyproteins also give rise to structural proteins in RNA viruses (Hellen and Wimmer, 1992), such as polyprotein P1 of picornaviruses, which is processed into four structural proteins. In 1993 Simón-Mateo et al suggested that the ASFV polyprotein, pp220, and its products (p150, p37, p34 and p14) could play a role in viral morphogenesis and suggested that the polyprotein may act as a scaffolding protein. In 1997 Andrés et al undertook an investigation to determine the role of the 220kDa polyprotein in the assembly of African swine fever virus. They showed that the final products of pp220 accounted for 25% of the total content of the ASF virions and were present in equimolar amounts. Electron microscopic data demonstrated the association of pp220 with the membranous structures seen in viral factories and also with all the assembly intermediates of the virions (Andrés et al, 1997). They went on to show that pp220 was localised to the inner core shell of the virion and suggested that pp220 may function as an internal protein scaffold which would mediate the interaction between the nucleoid and the outer layers. The morphological approach of Andrés et al (1997), which used antibodies that could not distinguish between parental polyprotein, and mature processing products, was limited in that it could not differentiate between the distribution of the polyprotein, intermediates and/or the final products of processing.

The next stage of this investigation was to use biochemical techniques in an attempt to overcome this limitation.

4.2 The expression of pp220 and production of p34 in ASFV infected cells.

The 220kDa polyprotein is a late viral protein and synthesis begins after DNA replication (Andrés et al, 1993; Simón-Mateo et al, 1993), which starts at 4-6 hours post infection (Tabarés et al, 1980). In the first experiment the antibody raised against recombinant p34 protein was used to determine the time course of expression of the polyprotein and production of p34 during the infection cycle. The time course began at eight hours post infection. Vero cells infected with BA71v were lysed at time points between 8 and 16 hours post infection and probed by Western blot. Figure 4.1 shows that low levels of protein were recognised by the antibody at 8 hours. pp220 was first detected in cells 8 hours post infection and the relative levels of the polyprotein increased throughout the time course. These results are consistent with the polyprotein being a late protein. At 10 hours post infection a ladder of proteins was observed and at 12 hours post infection there is an increase in the relative levels of the ladder, which extends down to 32kDa, with the appearance of three doublets at 32, 35 and 43kDa. These results were surprising because the work of Andrés et al (1997) and Simón-Mateo et al (1993) predicted that an antibody specific for pp220/p34 should Western blot proteins of 220, 90 and 34kDa (Figure 4.2). Simón-Mateo et al (1993) carried out pulse-chase immunoprecipitation experiments and showed the appearance of the 90kDa polyprotein (pp90) thirty minutes after the synthesis of the 220kDa polyprotein, with the cleavage of pp90 to produce p34 2-3 hours after pp220 synthesis. A surprising observation in figure 4.1 is that the antibody

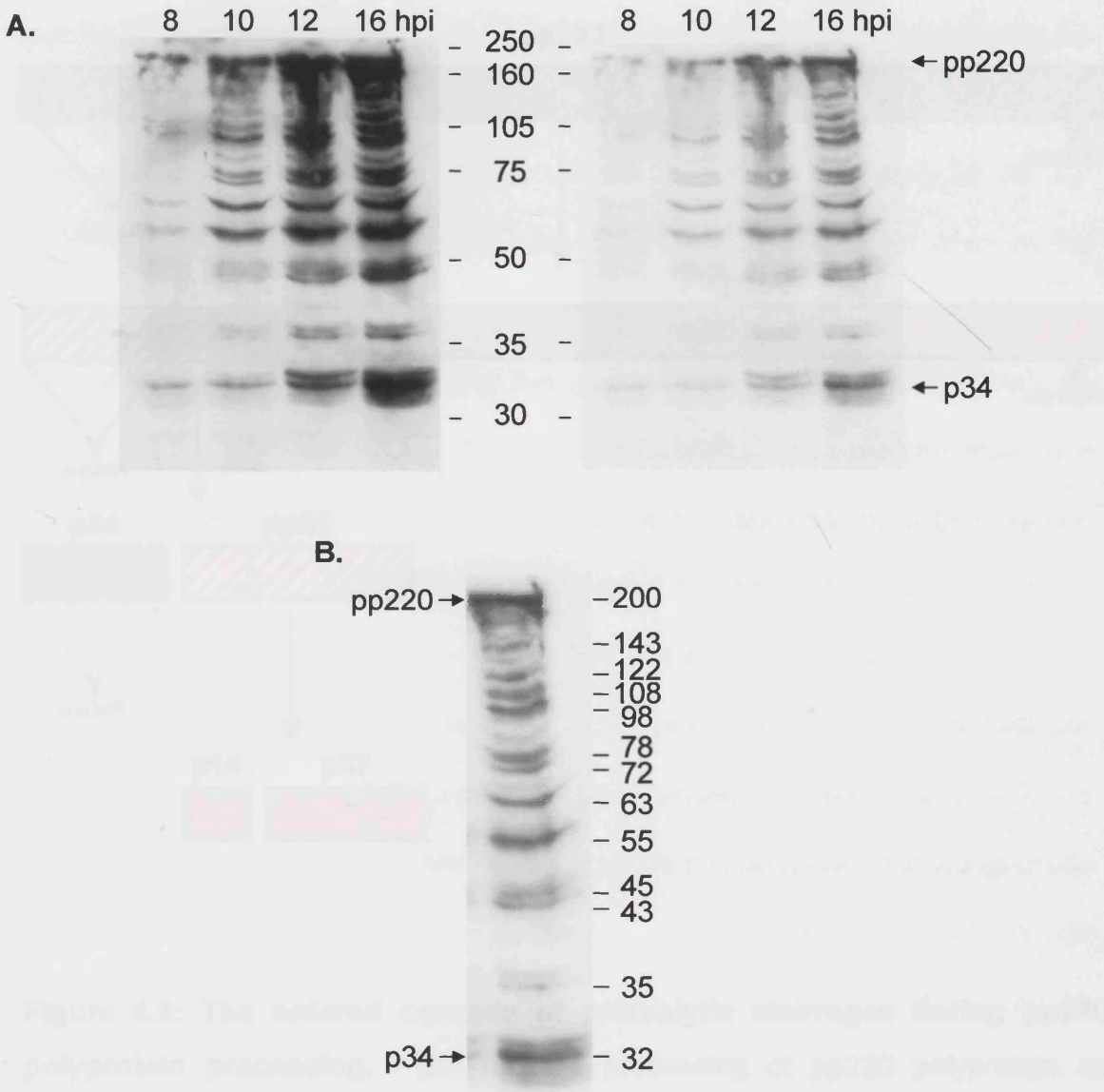

Figure 4.1: Time course of expression of pp220 and p34. At the indicated time intervals after infection with BA71v, Vero cells were lysed and the levels of pp220 and p34 determined by Western blotting using the antibody specific for p34, A) Two different exposures are depicted. Molecular weight markers are shown in the middle in kilodaltons. B) An enlarged view of the 16 hours post infection. The interpolated molecular sizes are shown on the right. pp220 and p34 are indicated by arrows.

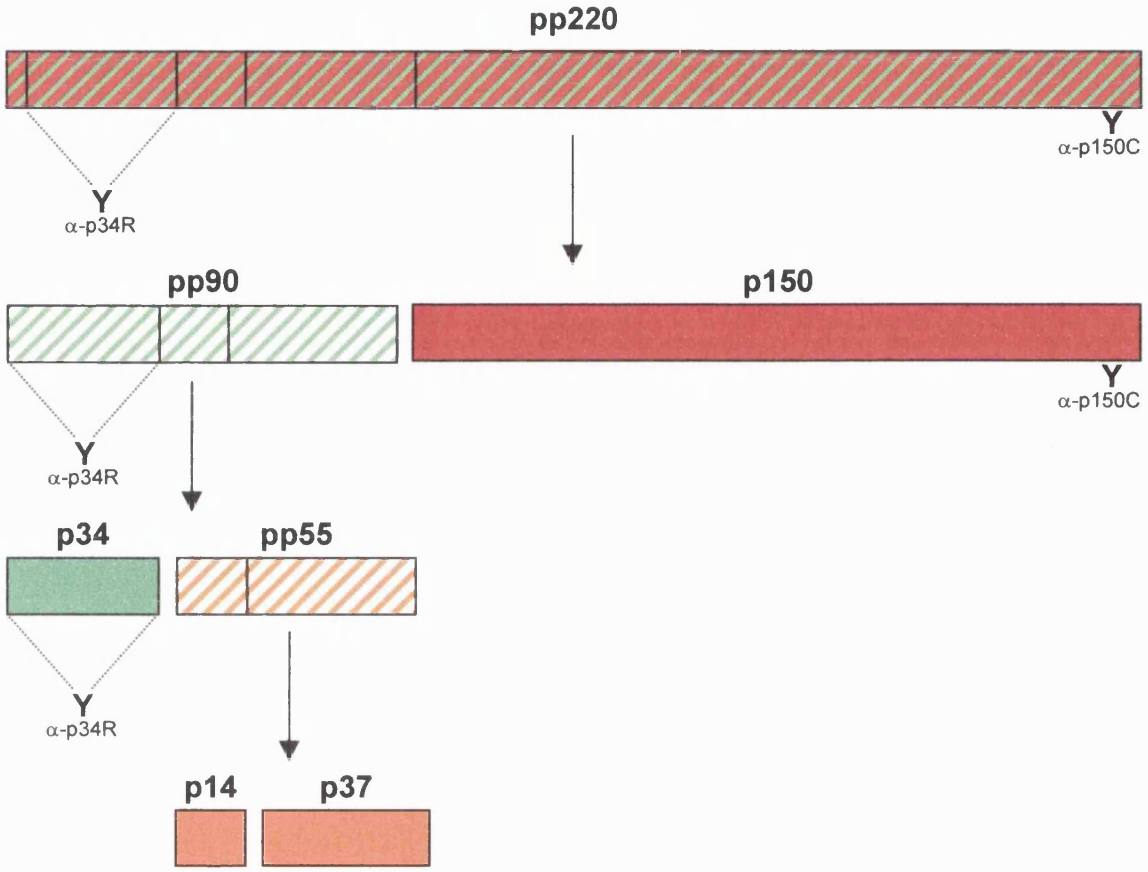

Figure 4.2: The ordered cascade of proteolytic cleavages during pp220 polyprotein processing. The ordered processing of pp220 polyprotein as described by Simón-Mateo et al (1993). The green boxes depict the proteins that would be recognised by an antibody against p34, the red boxes depict proteins that would be recognised by an antibody raised against p150 and the solid boxes represent the final proteins produced in proteolytic processing.

specific for p34 cross-reacted with a ladder of proteins, rather than the three proteins described by Simón-Mateo at al (1993). At 8 hours post infection several proteins can be seen with molecular weights of approximately 32, 35, 43, 45, 55, 63, 72, 98, 108 and 200kDa, during the increasing times of infection the relative levels of the proteins appear to change. In addition, proteins of 78, 122 and 143kDa also appeared during the infection period. Panel B shows an enlargement of the proteins described. The unpredicted extra proteins may be a result of random proteolysis of the polyprotein in the cell lysates, or they may in fact be intermediates of processing, which have not been previously described. The random proteolysis of the protein in the cell lysates is unlikely as the cells were lysed in IPB, which contains a cocktail of protease inhibitors, and then the lysates were boiled in SPB, which contains β-mercaptoethanol and SDS, to denature the proteins. Simón-Mateo et al (1993) described an ordered cascade of proteolysis occurring at four Gly-Gly-X cleavage sites, however the amino acid sequence predicted by the CP2475L gene shows that the polyprotein contains 19 Gly-Gly-X cleavage sites (Yáñez et al, 1995) (Figure 4.3A). If cleavage occurred at all 19 sites then the antibody specific for p34 would recognise approximately 34 proteins, depending on the resolution of the polyacrylamide gels (Figure 4.3B), with the smallest protein in the ladder being p34. The Western blot is consistent with cleavage at several Gly-Gly-X sites and there was little evidence for proteins smaller than ≈34kDa.

A.

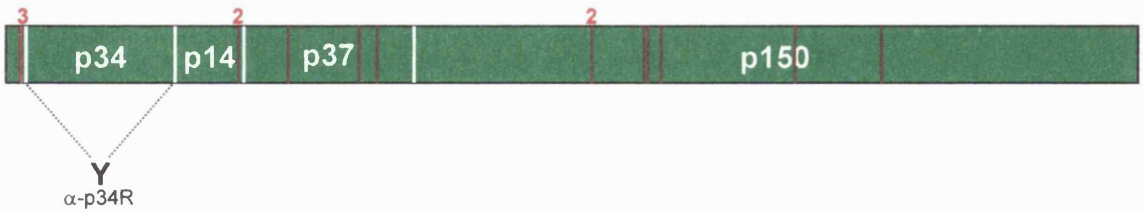

B.

Predicted molecular weights of the proteins recognised by the α-p34R antibody (kDa)			
282	163	100	58
278	160	96	55
277	159	92	54
218	158	87	53
214	156	83	41
213	155	82	37
196	154	69	36
192	146	65	
191	141	59	

Figure 4.3: The possible proteins formed by proteolytic cleavage of all 19 Gly-Gly-X cleavage sites. A) Schematic showing the 19 Gly-Gly-X cleavage sites, the white lines are those described by Simón-Mateo et al (1993) for ordered proteolysis and the red lines are the remaining sites. B) Predicted molecular weights of possible proteins formed by the cleavage of the 19 sites, which would be recognised by the α-p34R antibody.

4.3 p34, but not the polyprotein or the intermediates, is found in purified virions.

The next stage was to investigate how many of the proteins recognised by the antiserum were incorporated into mature virions. Andrés et al (1997) showed that antibodies specific for p34 bound to the inner core of the mature virions. The nature of their experiment meant however, that they were unable to determine whether both the polyprotein and/or the p34 product were present. A crude virus preparation was made by culturing BA71v infected Vero cells until an extensive cytopathic effect was observed. The culture media was centrifuged for 15 minutes at 500*g* to remove cell debris, and the virus was pelleted at 30,000*g* for 1 hour. The virions and infected cell lysates were compared using Western blots, probed with the antibody raised against p34, however the comparison was not quantitative since the virus was concentrated by centrifugation. Figure 4.4 shows that the antibody recognised a ladder of proteins ranging from 32kDa up to 220kDa in the cell lysate, which is similar to the ladder seen for the 16 hours post infection visualised in figure 4.2. The crude preparation of ASF virions contained a single reactive band at 32kDa, which is concluded to be p34. The lowest band of the ladder in the cell lysate migrated at the same position as p34 detected in virions. This suggests processing to p34 and no further. This data also suggests that the polyprotein was processed into several proteins in the cell, but only the 34kDa protein was incorporated into the mature virions.

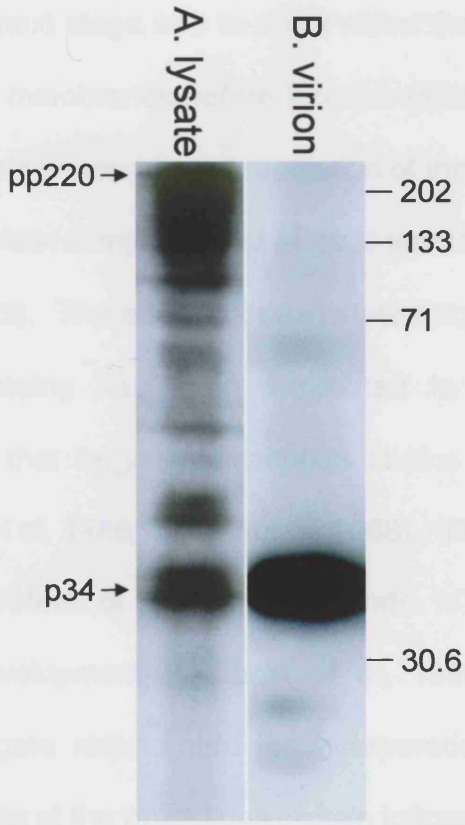

Figure 4.4: Distribution of pp220 and p34 in cell lysates and crude virus preparations. A. Vero cells were infected with BA71v for 16h and lysed in IPB. B. BA71v infected Vero cells were cultured until an extensive cytopathic effect was observed, cell debris was removed by centrifugation at 500*g* for 15min and the virus was pelleted at 30,000*g* for 1h. The pellet was lysed and both lysates were resolved on a 12.5% SDS-PAGE, Western blotted and probed with α-p34R antibody. The molecular markers are shown on the right in kilodaltons and pp220 and p34 are indicated by arrows.

4.4 The intracellular pool of p34 associates with membranes.

Having established that p34, but not the precursor pp220, is present in virions (Figure 4.4) the next stage was to see if either the polyprotein or p34 was associated with cellular membranes before incorporation into virions. There are two reasons for proposing a membrane association of the polyprotein. The first is that the 220kDa polyprotein is myristylated at its N-terminus (Aguado et al, 1991; Simón-Mateo et al, 1993). The addition of myristate through amide bonds to the amino-terminus of proteins has been implicated in mediating protein-lipid interactions, a system that targets polypeptide chains to cellular membranes (Grand, 1989; Schultz et al, 1988; Towler et al, 1988). The second reason is that the major structural protein of ASFV, p73, binds to endoplasmic reticulum membranes before envelopment (Cobbold et al, 1996), and binding to ER membranes is an obligate requirement for incorporation into virions. It was possible that the products of the pp220 polyprotein followed a similar pathway.

Vero cells were infected with BA71v for 16 hours, were homogenised by 20 passages through a 25-gauge needle and centrifuged at 3,300*g* for 2 minutes to prepare postnuclear supernatants. The postnuclear supernatants were centrifuged to produce a pellet of postnuclear membranes, and a supernatant containing the cell cytosol. The membrane and cytosolic fractions were resolved on a 12.5% SDS-PAGE, transferred to nitrocellulose membranes and probed with the antibody specific for p34. Figure 4.5 shows the distribution of pp220, intermediates and p34 between the membrane and cytosolic fractions of the cell exposed for differing times. As described above, the cytosolic fraction contained a ladder of bands ranging from approximately 220kDa down to 70kDa, with less compact bands extending to approximately 50kDa. Interestingly, there was no

visible band representative of p34 in the cytosol. The membrane fraction contained a less densely compact ladder of proteins ranging from 220kDa to 34kDa. The ladder was made up of about 10 bands of varying intensity, with major bands seen at 32, 50, 72, 78, 98, 122, 143 and 220kDa. Significantly, the major difference between the membrane and cytosolic fractions was that the final product, p34, was only found in the membrane fraction. In addition, the reactive bands seen in each fraction were different. The cytosolic fraction had more reactive protein, the majority of which migrated above 70kDa. In the membrane fraction major bands were seen at 32, 45 and 122kDa. Interestingly, the 32 and 50kDa proteins would be formed by cleavage at the major Gly-Gly-X sites, described by Simón-Mateo et al (1993), however the 122kDa protein could only be formed by cleavage of the p150 protein. This was a surprising result as the published literature suggests that pp220 is processed into the four structural proteins, which are then incorporated into mature virions in equimolar concentrations (Simón-Mateo et al, 1993; Andrés et al, 1997). The appearance of a ladder of proteins in the cytosolic and membrane fractions suggests that either random proteolysis is occurring in both fractions or the processing pathway is different from that described by Simón-Mateo et al (1993).

4.5 p34, but not pp220, is enveloped by the membrane.

Cobbold et al (1996) used a protease protection assay to show that the membrane associated intracellular pool, but not the cytosolic pool, of p73 was enveloped by membranes of the endoplasmic reticulum. The protease protection assay was based on the premise that viral proteins enveloped by a membrane would be protected from proteolysis by exogenous proteases added to the

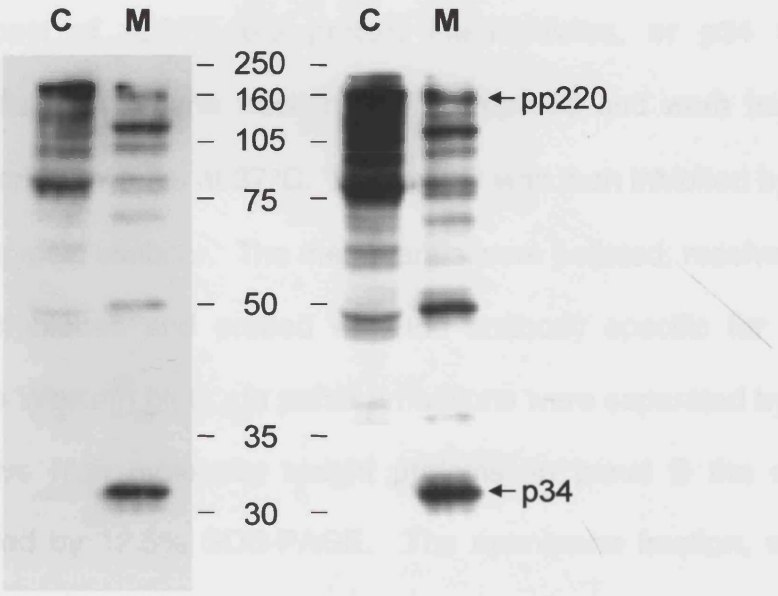

Figure 4.5: Distribution of pp220 and p34 between cellular cytosolic and membrane fractions. Vero cells were infected for 16h with BA71v. Postnuclear membrane (M) and cytosolic (C) fractions were prepared. The fractions were resolved on a 12.5% SDS-PAGE, Western blotted and probed with the α-p34R antibody. Two different exposures are depicted. The molecular markers are shown in the middle in kilodaltons and pp220 and p34 are depicted by arrows.

membrane fractions prepared from infected cells (Figure 4.6). The next stage of the investigation was to use the protease protection assay to see if the membrane bound pool of pp220, the protein intermediates, or p34 were enveloped. Postnuclear membrane fractions were prepared and were treated with 5mg/ml trypsin for 30 minutes at 37°C. Proteolysis was then inhibited by the addition of 10mg/ml trypsin inhibitor. The membranes were pelleted, resolved by SDS-PAGE, Western blotted and probed with the antibody specific for p34. Figure 4.7 shows two Western blots. In panel A fractions were separated by 5% SDS-PAGE to resolve high molecular weight proteins; in panel B the small proteins were resolved by 12.5% SDS-PAGE. The membrane fraction, which was not treated with trypsin (left lane), showed the familiar ladder of bands ranging from 34-220kDa, believed to represent the processing of the polyprotein via several intermediates to the final p34 protein. The membrane fraction treated with the protease (right lane) showed a loss of the polyprotein and intermediates, and only a single band of 34kDa was resolved. The results suggested that the p34 protein was enveloped because it was protected from trypsin. The polyprotein and intermediates were not protected and therefore not enveloped. The results demonstrated that even though pp220 and intermediates bound the membranes, only p34 was enveloped.

4.6 The bulk of the cellular pool of p34 is not present as a monomer, but assembles into a large complex.

As already stated, the products of pp220 have a suggested role as scaffolding proteins (Andrés et al, 1997; Simón-Mateo et al, 1993) in the formation of the ASF capsid layer. Scaffolding proteins act as an assembly

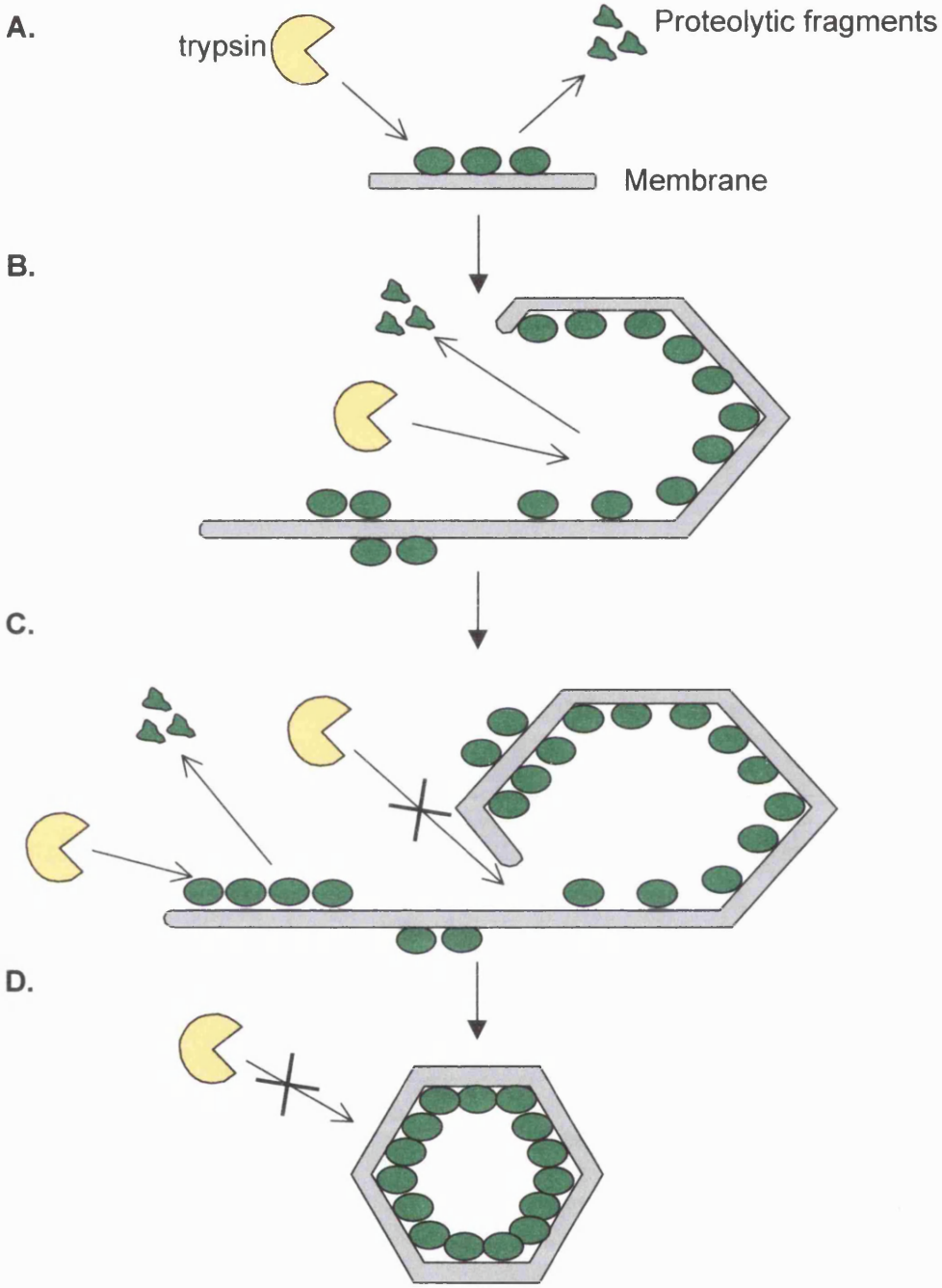

Figure 4.6: Schematic representation of the protease protection assay. Viral proteins bind to the membranes after synthesis in the cytoplasm. A. At this stage the proteins are susceptible to proteolytic degradation by the protease. B. As the wrapping process proceeds the viral proteins are still susceptible to protease digestion, however at later stages in assembly viral proteins become protected from proteolysis by the surrounding membrane (C). Finally, the mature virions provide total protection from protease action (D).

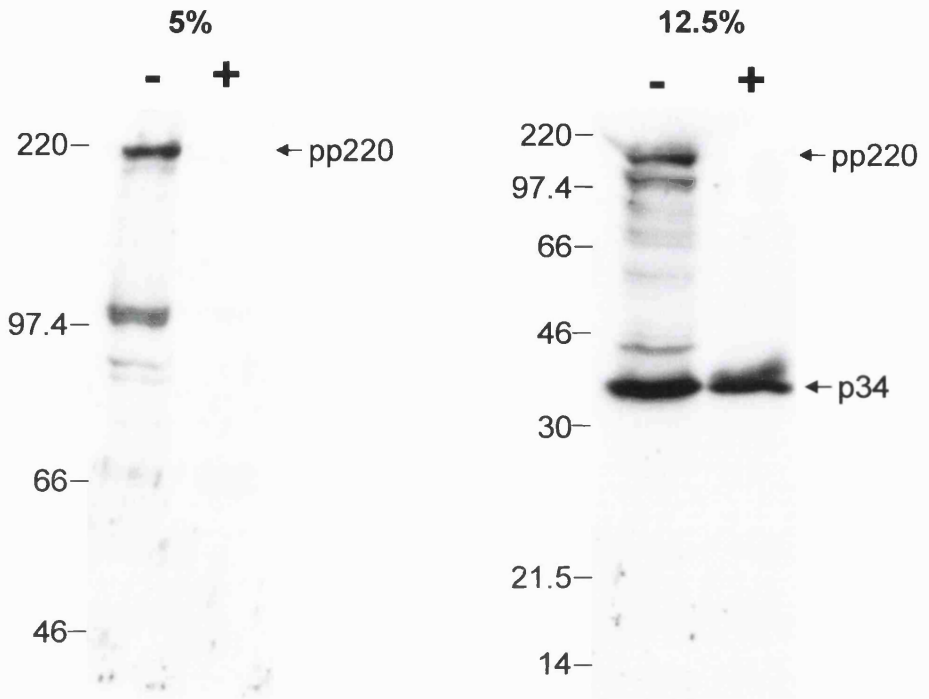

Figure 4.7: p34, but not the polyprotein or intermediates, was enveloped. Vero cells were infected for 16 hours with BA71v. Postnuclear membrane fractions were prepared and were incubated in the absence (-) or presence (+) of 5mg/ml trypsin for 30 minutes at 37°C. Proteolysis was inhibited by the addition of 10mg/ml of trypsin inhibitor. The membranes were pelleted, resolved on 5% or 12.5% SDS-PAGE as indicated, Western blotted and probed with the α-p34R antibody. The molecular weight markers are shown on the left of the blots and are in kilodaltons. pp220 and p34 are depicted by arrows.

template for the capsid of viruses, such as the herpes viruses, and tailed phages (Casjens, 1997). These scaffolding proteins are characterised by their requirement to be removed from precursor viral structures prior to DNA packaging, either as intact disassembled polypeptides or after limited proteolysis during viral maturation (Casjens and Hendrix, 1988). The results above show that the 220kDa polyprotein and the intermediates involved during the processing to the p34 protein are not found in mature virions. The question arising from these observations is whether or not the polyprotein and intermediates act as scaffolding proteins for the assembly of ASFV and are ejected at a later stage of assembly. In order to investigate this possibility, sucrose gradients were used to see if the polyprotein, the processing intermediates or the p34 protein formed large complexes indicative of procapsids during the assembly of ASFV. A large complex would be indicative of a scaffold since scaffolding proteins oligomerise into large structures around which capsids can form (Casjens, 1997). Vero cells were infected with BA71v for 16 hours and a cell lysate was solubilised in immunoprecipitation buffer containing 1% Brij-35. The lysate was floated on a 10 to 40% sucrose gradient and centrifuged at 200,000*g* for 20 hours at 4°C. The gradients were separated into 1.2ml fractions, resolved on a 12.5% SDS-PAGE, Western blotted and probed with the α-p34R antibody. The sucrose gradients were calibrated using marker proteins; carbonic anhydrase - 30kDa, BSA - 66kDa, β-amylase - 200kDa, apoferritin - 473kDa (Figure 4.8B). Figure 4.8 shows that the bulk of pp220 and the intermediates were found mainly in fractions 6, 7 and 8, which have estimated molecular weights of 200, 170 and 70kDa respectively. A small amount of the intermediates were also located in fraction 9. Given that migration on the gradients correlated with predicted size it

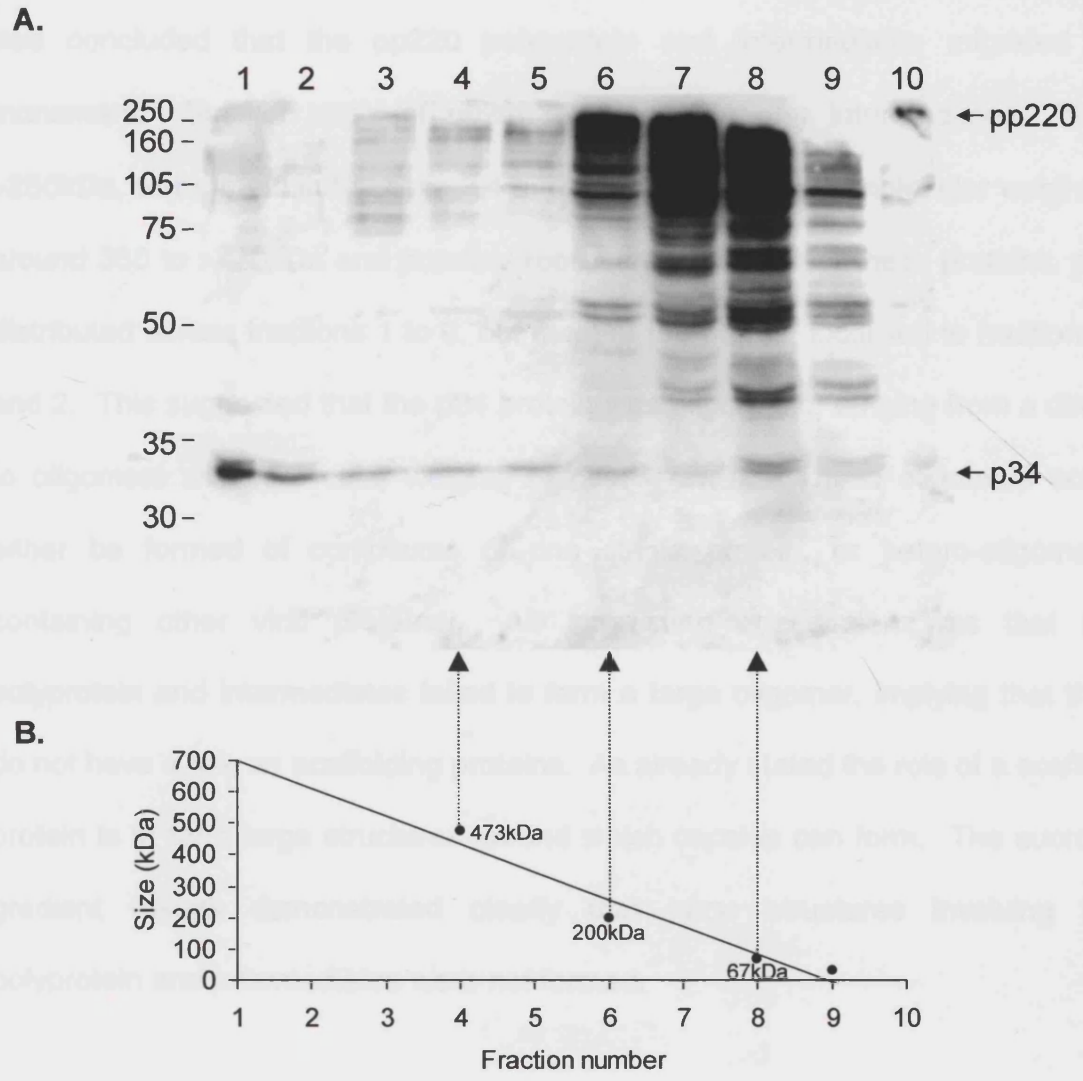

Figure 4.8: pp220, the processing intermediates and p34 assembled into a large complex. A. Vero cells were infected with BA71v for 16 hours and a cell lysate was solubilised in immunoprecipitation buffer containing 1% Brij-35. The lysate was floated on a 10 to 40% sucrose gradient and centrifuged at 200,000*g* for 20 hours at 4°C. The gradients were separated into 1.2ml fractions, resolved on a 12.5% SDS-PAGE, Western blotted and probed with the α-p34R antibody. The molecular markers are shown on the left in kilodaltons and pp220 and p34 are indicated with arrows. B. The location of the peak fractions containing the marker proteins (Carbonic anhydrase-30kDa, BSA-66kDa, β-amylase-200kDa and apoferritin-473kDa) were plotted against their molecular weight (kDa) and a best fit line was extrapolated.

was concluded that the pp220 polyprotein and intermediates migrated as monomers. Smaller pools of pp220 and some of the intermediates, 75 to >250kDa, were found in fractions 3,4 and 5 and these have a molecular weight of around 350 to >473kDa and possibly represent oligomers of these proteins. p34 distributed across fractions 1 to 9, but most of the protein localised to fractions 1 and 2. This suggested that the p34 protein was oligomeric, ranging from a dimer to oligomers with molecular weights of over 473kDa. These oligomers could either be formed of complexes of one single protein, or hetero-oligomers, containing other viral proteins. An interesting observation was that the polyprotein and intermediates failed to form a large oligomer, implying that they do not have a role as scaffolding proteins. As already stated the role of a scaffold protein is to form large structures around which capsids can form. The sucrose gradient results demonstrated clearly that large structures involving the polyprotein and intermediates were not formed.

4.7 The large complex of p34 is associated with the membranes.

In the previous experiment whole cell lysates were analysed by sucrose gradient sedimentation. In the next experiment membrane and cytosol fractions were analysed separately. Figure 4.9 shows again that the p34 protein was found solely in the membrane fractions as different sized oligomers, ranging from dimers (fraction 6) to oligomers, migrating to the bottom of the gradient, with molecular weights in excess of 473kDa. In panel A the distribution of the different pp220, intermediates and p34 oligomers associated with membranes could be visualised. The bulk of the pp220 and intermediates were present in fractions 6,7 and 8, which were representative of the monomeric forms of the proteins. Panel

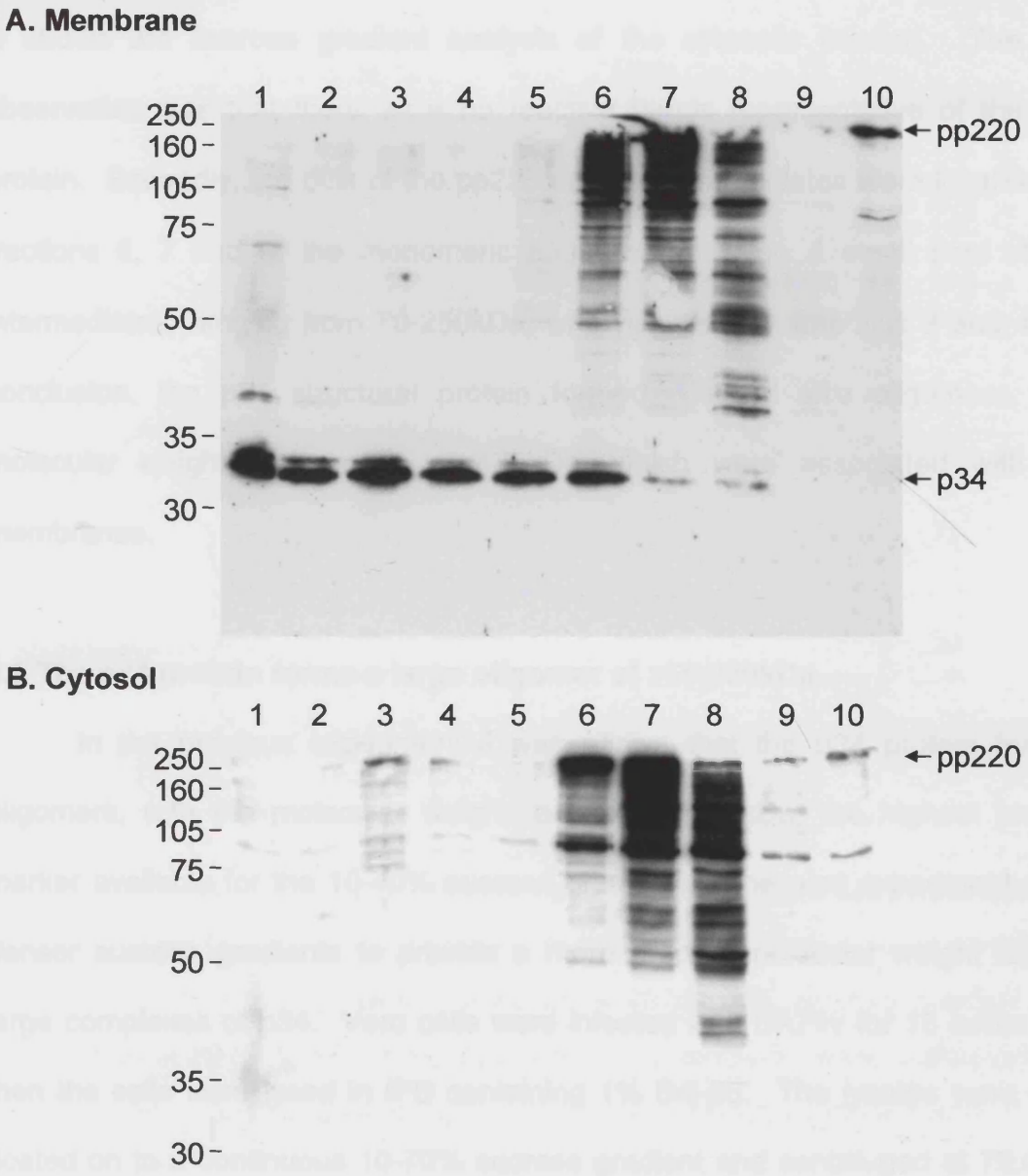

Figure 4.9: Membrane associated p34 formed a large complex. Vero cells were infected with BA71v for 16 hours and membrane and cytosolic fractions were prepared and solubilised in immunoprecipitation buffer containing 1% Brij-35. The membrane and cytosolic fractions were floated on a 10 to 40% sucrose gradient and centrifuged at 200,000*g* for 20 hours at 4°C. The gradients were separated into 1.2ml fractions, resolved on a 12.5% SDS-PAGE, Western blotted and probed with the α-p34R antibody. The molecular markers are shown on the left in kilodaltons and pp220 and p34 are indicated with arrows.

B shows the sucrose gradient analysis of the cytosolic fraction. The first observation was that there were no reactive bands representative of the p34 protein. Secondly, the bulk of the pp220 and the intermediates were localised to fractions 6, 7 and 8, the monomeric fractions, however, a small pool of the intermediates, ranging from 70-250kDa, was visualised in fractions 3 and 4. In conclusion, the p34 structural protein formed different size oligomers, with molecular weights in excess of 473kDa, which were associated with the membranes.

4.8 The p34 protein forms a large oligomer of >59,000kDa.

In the previous experiment it was shown that the p34 protein formed oligomers, with the molecular weighs exceeding 473kDa, the highest protein marker available for the 10-40% sucrose gradients. The next experiment used denser sucrose gradients to provide a more precise molecular weight for the large complexes of p34. Vero cells were infected with BA71v for 16 hours and then the cells were lysed in IPB containing 1% Brij-35. The lysates were then floated on to a continuous 10-70% sucrose gradient and centrifuged at 79,000*g* for 2.5 hours at 4°C. The gradients were separated into 1.2ml fractions, resolved on a 12.5% SDS-PAGE, transferred to nitrocellulose and probed with the antibody raised against p34. The 10-70% velocity gradients were calibrated by observing the migration of foot and mouth disease virus (FMDV) and bluetongue virus (BTV) core particles. The structures of FMDV and BTV cores are known and have approximate molecular masses of 7,600 and 59,000kDa, respectively (Acharya et al, 1989; Grimes, 1998; Gouet et al, 1999). Figure 4.10 shows the distribution of the p34 oligomers on the 10-70% sucrose gradients. The

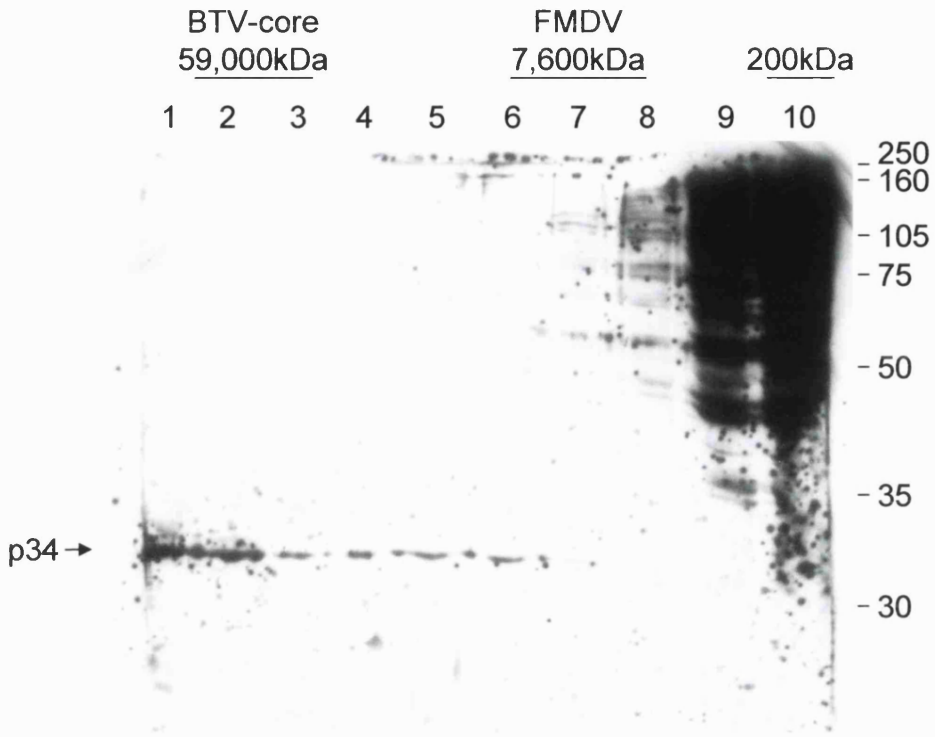

Figure 4.10: p34 complexes migrated at 50,000kDa. Vero cells were infected with BA71v for 16 hours and solubilised in immunoprecipitation buffer containing 1% Brij-35. The lysates were floated on a 10 to 70% sucrose gradient and centrifuged at 79,000*g* for 2.5 hours at 4°C. The gradients were separated into 1.2ml fractions, resolved on a 12.5% SDS-PAGE, Western blotted and probed with the α-p34R antibody. The molecular markers are shown on the right in kilodaltons and p34 is indicated by an arrow.

polyprotein and intermediates remained at the top of the gradients, mainly in fractions 9 and 10. This was consistent with the migration of the polyprotein and intermediates at 150 to 250kDa in the previous experiments. The most striking observation was the distribution of the p34 protein, which was found in fractions 1 to 7, with most of the protein localising in fractions 1 and 2. This showed that at steady state the p34 protein was found as different size oligomers with molecular weights ranging from 7,600kDa to over 59,000kDa. This observation was in agreement with the published data on the major ASFV capsid protein, p73, (Cobbold and Wileman, 1998). In their work they showed that the major capsid protein formed a large 50,000kDa complex, that assembled via intermediates on the membranes. They went onto show that the large oligomer was present in the mature virions.

4.9 pp220/p34 localises to the viral factory at 12 hours post infection.

The above experiments have demonstrated that pp220 was located in a cytosolic and membrane pool and that p34 was solely membrane associated. The experiment also showed selective envelopment of p34. The next experiment used indirect immunofluorescence to visualise the subcellular location of the polyprotein, and p34. Unfortunately the antibody raised against the recombinant p34 protein recognised the polyprotein, intermediates and p34 and was therefore unable to determine the differences between the subcellular distribution of the polyprotein or p34. A monoclonal antibody raised against the major capsid protein, p73, was also used as a marker for the ASF viral factories and virions. Vero cells were infected for 12 hours and then fixed and permeabilised as described in the materials and methods. The cells were then labelled with the

antibodies specific for p34 and p73 and visualised using Alexa Fluor α-IgG conjugates. The viral and cellular DNA were stained with DAPI and the cells were imaged as described in the materials and methods. Figure 4.11 shows the distribution of pp220/p34 and p73 at 12 hours post infection. Panel A shows a cell stained for the polyprotein and p34, and panel B shows cells stained for p73. Panel C shows the nucleus and extra-nuclear viral DNA and panel D is a digital overlay of the three images. All the panels contain an insert showing a digital enlargement of the viral factory. The antibody specific for p34 stained a large amorphous perinuclear structure brightly, and also gave a weaker cytoplasmic staining. The antibody against the major capsid protein stained a single structure, the enlargement of which showed it to consist of several small punctate, spherical structures. These structures are probably individual ASF virions (Cobbold et al, 1996). Panel C shows that DAPI stained nuclei, as well as a small perinuclear region in the infected cell, which represents the viral DNA located in the viral factory. The images were digitally merged (Panel D) and this showed that the virions and viral DNA co-localised with the amorphous staining of pp220/p34 at a perinuclear site, known as the viral factory. The enlargement of the viral factory in panel D showed that there was an amorphous pool of protein reactive with the antibody raised against p34, in which there were several well-defined virions labelled with the antibody specific for p73. This was surprising as the above data showed that p34 was selectively enveloped and assembled into oligomeric structures indicative of virions, however it is not known why p34 staining failed to give a punctate stain.

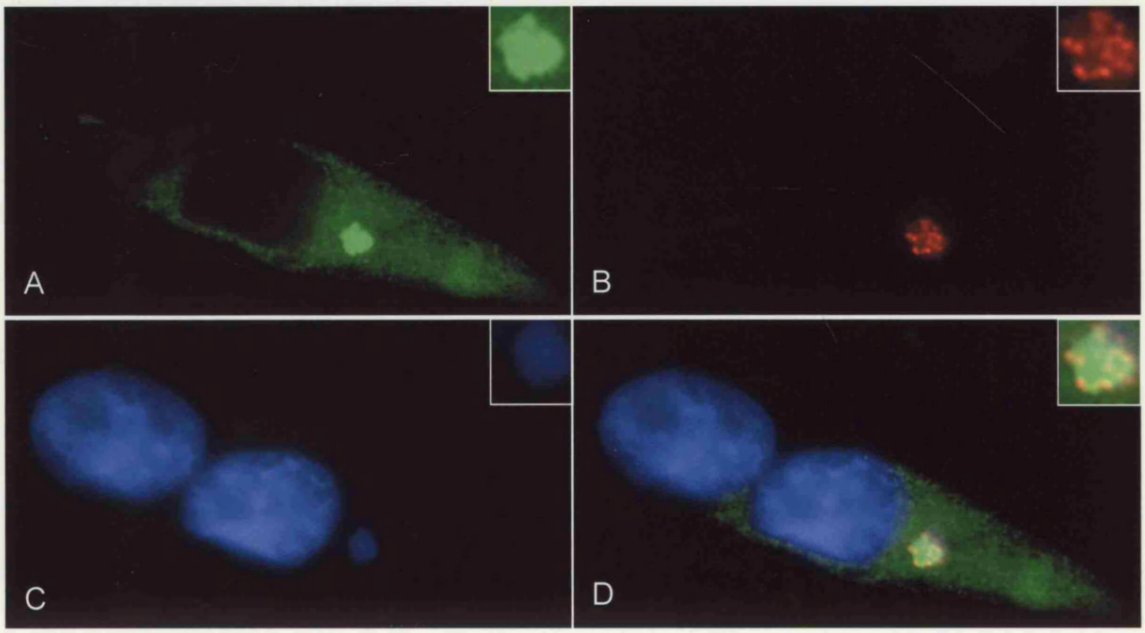

Figure 4.11: pp220/p34 localised at a perinuclear site at 12hpi. At 12 hours after infection with BA71v, Vero cells were fixed with ice-cold methanol, permeabilised with 0.1% Triton X-100 and incubated with the rabbit antibody specific for p34 (A) and a mouse monoclonal antibody specific for p73 (B). The distribution of the proteins was visualised by using the Alexa Fluor 488 (green) anti-rabbit and 594 (red) anti-mouse IgG conjugates. The cellular and viral DNA was labelled with DAPI (blue) (C). Cells were viewed at 60X and images captured as described in the materials and methods. The images were digitally deconvolved, using the Openlab system and p34, p73, and DAPI were digitally overlaid (D). The inserts are a digital enlargement of the viral factory.

4.10 pp220/p34 are not found on the surface of virions.

Cobbold et al (1996) showed that the virions produced in the viral factories at 12 hours post infection migrated away from the assembly sites, into the cytoplasm and to the periphery of the cell. The next experiment was to visualise the distribution of pp220/p34 at 16 hours post infection to see if the proteins localise to virions and to determine the fate of the amorphous pool of the protein reactive with the antibody raised against the recombinant p34 protein. Figure 4.12 shows the distribution of the major capsid protein and the pp220/p34 proteins at 16 hours post infection. The distribution of the pp220/p34 proteins at 16hpi (panel A) was very similar to that seen at 12 hours post infection. There was an amorphous perinuclear structure surrounded by a weak cytoplasmic staining, however the only difference was that the amorphous structure appeared to have fragmented into three pools of protein. The major capsid protein co-localised with the viral factory, and individual virions could be seen throughout the cytoplasm (Panel B). The merge of the images showed the amorphous pp220/p34 structure decorated with small spherical virions, stained by the antibody specific for p73. Interestingly, virions that were located outside the viral factory only stained with the antibody specific for p73 and not the antibody specific for p34 (see insert at bottom right). This was surprising because the biochemical data had shown that p34 was located in virions. The results suggest that the p34 is masked from detection by immunofluorescence in cells, and therefore implies that p34 is located deep inside the mature virions.

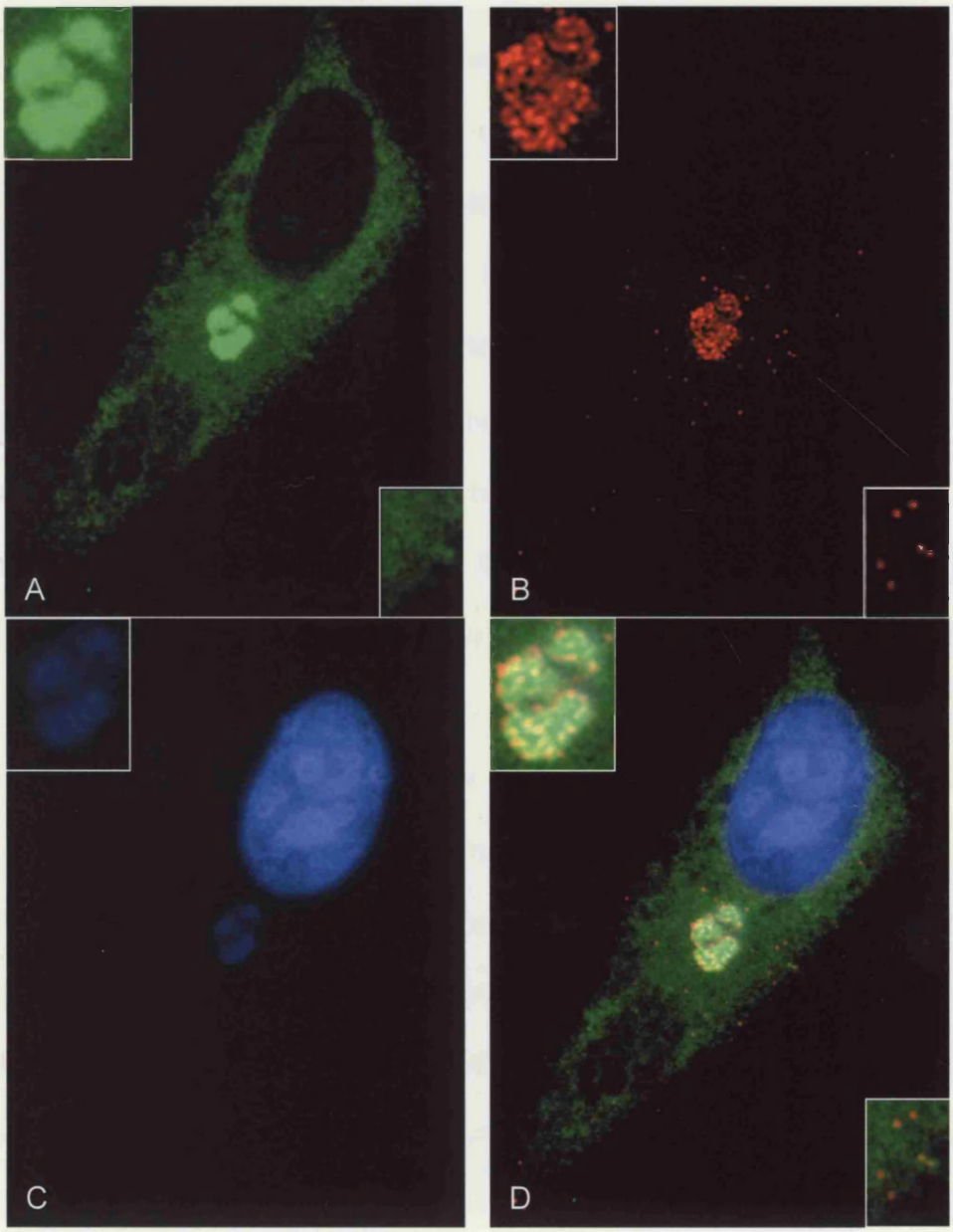

Figure 4.12: pp220/p34 were not located on the surface of virions. Vero cells were infected for 16 hours and fixed with ice-cold methanol, permeabilised with 0.1% Triton X-100 and incubated with the rabbit antibody specific for p34 (A) and a mouse monoclonal antibody specific for p73 (B). The distribution of the proteins was visualised by using the Alexa Fluor 488 (green) anti-rabbit and 594 (red) anti-mouse IgG conjugates. The cellular and viral DNA was labelled with DAPI (blue) (C). Cells were viewed at 60X and images captured as described in the materials and methods. The images were digitally deconvolved, using the Openlab system and p34, p73, and DAPI were digitally overlaid (D). The inserts are a digital enlargement of the viral factory and mature virions.

4.11 p34 is located in the nucleoid of the virions.

The previous sections showed that by Western blot analysis, the p34 protein was found in mature virions (figure 4.4), however the immunofluorescence analysis of mature virions was unable to detect p34 on virions. This implied that the antigenic site of p34 was masked in mature virions and suggested that p34 was located inside the virion. The next experiment used electron microscopy to elucidate the subcellular and subviral location of p34. Vero cells were infected for 16 hours, fixed, then embedded and thin cryo-sections were prepared and imaged as described in the materials and methods. Figure 4.13 shows the subcellular and subviral distribution of pp220 and p34. Panel A shows a section through a viral assembly site and panel B depicts a mature cytoplasmic virion at the plasma membrane. The cryo-section in panel A shows ASFV virions surrounded by membranous material. The distribution of the gold beads showed that the pp220/p34 proteins were closely associated with the membranes, which was in agreement with figure 4.5 that showed that pp220, intermediates and p34 were associated with membranes. Some virions depicted had electron-dense centres, which suggested the presence of a nucleoprotein core, whereas others appeared empty. Interestingly, the gold beads localised to the area of the dense nucleoid. This was more clearly visualised in panel B, which shows a mature virion with its condensed nucleoid. The gold beads on the mature virion were solely localised to the nucleoid. These gold beads are assumed to be labelling p34, as figure 4.4 shows that only p34 was present in the mature virions. The cryo-electron micrographs show that the p34 was located in the core of virions, and therefore provides support for the hypothesis that the epitopes are masked during the immunofluorescence analysis of virions.

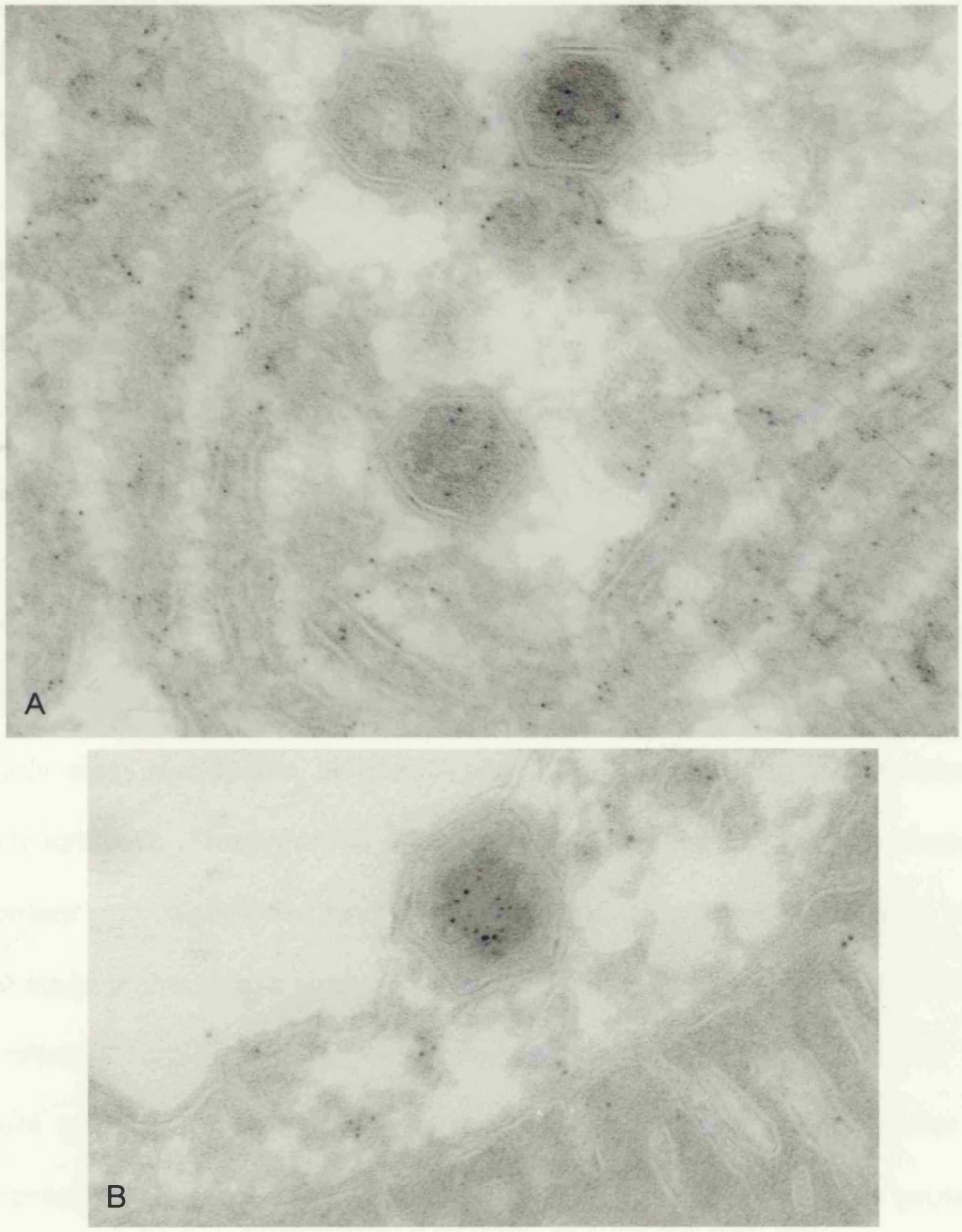

Figure 4.13: p34 was located in the nucleoid of virions. Vero cells were examined 16 h after infection with BA71v. The cells were fixed in 2% paraformaldehyde, 0.05% glutaraldehyde in phosphate buffer and embedded in 8% gelatin. 75nm cryosections were cut and incubated with α-p34R antibody. The proteins were detected with α-rabbit IgG conjugated to 5nm colloidal gold. Sections were contrasted and supported in uranyl acetate/methyl cellulose and imaged in a JEOL 1200EX electron microscope at 80kV. The images were selected from thin cryosections taken through virus assembly sites (A) or mature intracellular virions (B).

4.12 A kinetic analysis of proteolytic processing of the pp220 polyprotein.

4.12.1 The time course of expression of pp220 and its subsequent processing.

Using the antibody specific for p34 and the Western blotting technique it was demonstrated that pp220 and several intermediates were found in the cell as both a membrane and cytosolic pool, but the p34 protein was solely membrane-associated. Although pp220, the intermediates and p34 associated with the membrane, only the p34 protein was enveloped by the membrane, and found in mature virions. The Western blot analysis also demonstrated the presence of large membrane-associated oligomers of p34 with a molecular mass of >59,000kDa. The limitation of the Western blotting results was that they showed the steady state distribution of pp220 and p34, and gave no insight into the assembly kinetics. Therefore, to investigate the kinetics of pp220 processing, envelopment and oligomerisation pulse-chase immunoprecipitations were used. The first stage in the kinetic analysis of polyprotein processing was to pulse-label BA71v infected Vero cells for 30 minutes and then chase for up to 16 hours. The cells were lysed at the indicated time points in immunoprecipitation buffer and immunoprecipitated using the antibody specific for p34 bound to protein-A sepharose beads. Figure 4.14 shows the protein immunoprecipitated throughout the time course, resolved on a 12.5% SDS-PAGE. The major band on the gel had a molecular weight characteristic of the pp220 polyprotein. The intensity of this band increased two hours into the chase period. It is not known why the levels increased, but one possibility maybe that the polyprotein changes conformation allowing presentation of the antigenic site for the antibody specific for p34. This was a surprising result but was highly reproducible. The levels of the pp220 polyprotein then begin to decrease in intensity as the chase period

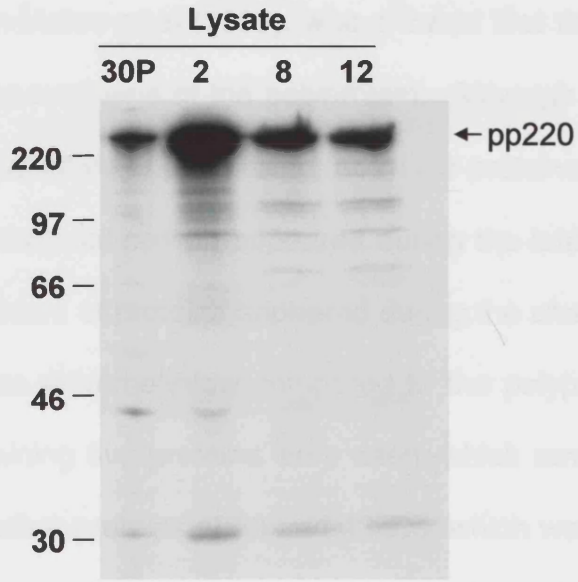

Figure 4.14: Kinetics of proteolytic processing of pp220 to p34. Vero cells were infected for 16h with BA71v. Cells were metabolically labelled for 30min, chased for the indicated time periods and then lysed in immunoprecipitation buffer. The lysates were incubated overnight with α-p34R, bound to protein-A sepharose beads, and then boiled in SPB and resolved on a 12.5% SDS-PAGE and visualised by autoradiography. Molecular markers are shown on the left in kilodaltons and pp220 is indicated by an arrow.

proceeded to 8 and then 12 hours. This decrease in intensity would be expected, if the polyprotein were to be proteolytically degraded to the various intermediates and the final p34 protein. The decrease in the levels of pp220 were much slower than described by Simón-Mateo et al (1993), who showed that the levels began to decrease an hour after synthesis of the polyprotein. Although the loss of the pp220 polyprotein was indicative of processing, no major proteins representative of the intermediates, or the final protein appeared during the later stages of the time course. Several ladders of proteins appeared during the chase periods, but their relative intensity was extremely low compared to the polyprotein. After 2 hours faint ladders containing five proteins were seen, which ranged from 85 to 120kDa, as well as two other proteins at 30 and 43kDa, which were also present after the 30-minute labelling. The 30kDa protein appeared to migrate faster than the p34 protein seen in the Western blot analysis and its identity is unknown. As the chase period continued the relative intensity of these bands decreased and proteins of 68, 144 and 176kDa appeared, with similar intensity to the other proteins in the ladder. Although there are ladders of proteins that could be described as intermediates there was no increase in intensity, suggestive of precursor/product relationship, of any of these proteins as the levels of the polyprotein decreased. In summary, the antibody specific for the p34 protein was able to immunoprecipitate the polyprotein and the levels of the polyprotein decreased with time, indicative of processing, but the antibody was not able to detect the appearance of the final p34 protein.

4.12.2 The subcellular distribution of the pp220 polyprotein with time.

The next stage of the investigation was to determine the time course of membrane association of the polyprotein. Vero cells were infected with BA71v for 16 hours, pulse-labelled for 30 minutes and then chased for the indicated time periods. Postnuclear supernatants were prepared and separated into membrane and cytosolic fractions, as previously described, and the fractions were solubilised in IPB containing 1% Brij-35 and then immunoprecipitated with the antibody specific for p34. Figure 4.15 shows the distribution of the immunoprecipitated proteins between the membrane and cytosolic fractions. The major protein immunoprecipitated by the antibody was again a protein of 220kDa, which was characteristic of the pp220 polyprotein, several other bands were also immunoprecipitated, however their levels were very low and were probably non-specific background proteins. As before, there was an increase in levels of the total pool of the polyprotein during the first two hours of the chase period, suggesting a conformational change in the protein. As expected from the Western blot data the pp220 polyprotein was found in both the membrane and cytosolic pool, but most strikingly there was a marked difference in the distribution of the pp220 with time. After the cells were metabolically labelled for 30 minutes the largest pool, 83%, of the polyprotein was found in the cytosolic fraction. After the cells had been chased for 2 hours the distribution of the pp220 polyprotein had changed to an even 50:50 distribution. As the time course continued the distribution of the pp220 polyprotein shifted more towards the membrane fraction, with 60% of the total pool of pp220 becoming membrane associated (Figure 4.15B). As already stated the antibody specific for p34 was unable to immunoprecipitate the final p34 protein, however a faint band at 30kDa

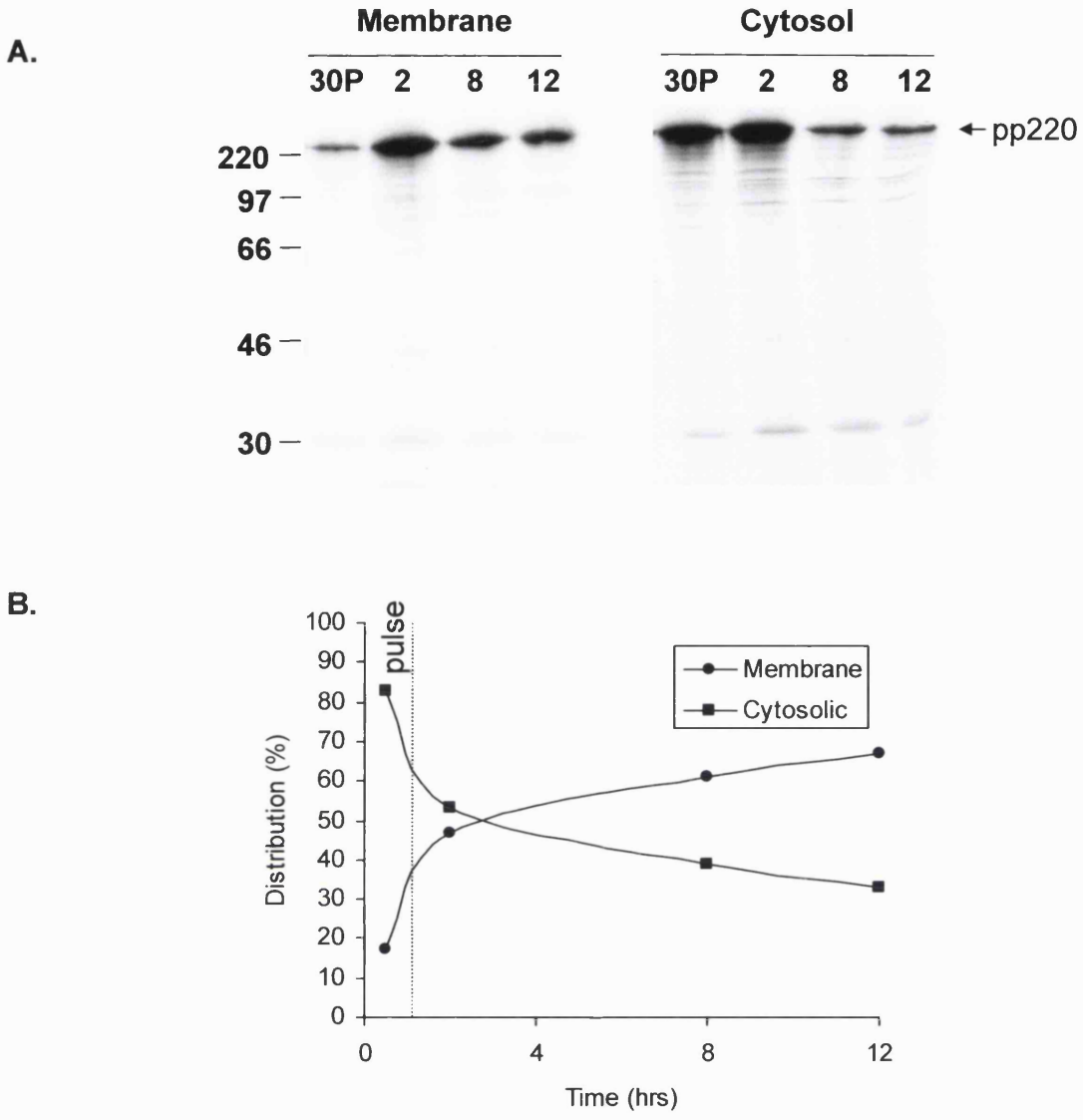

Figure 4.15: The subcellular distribution of pp220 with time. Vero cells were infected for 16h with BA71v. The cells were metabolically labelled for 30 minutes and chased in complete media for the indicated times. Postnuclear membranes and cytosolic fractions were prepared. The fractions were immunoprecipitated overnight with the α-p34R antibody, boiled in SPB and resolved on a 12.5% SDS-PAGE. The proteins were visualised on an autoradiograph (A). B) The protein bands were quantified by scanning densitometry and the percentage distribution of the pp220 protein was depicted. Molecular markers are shown on the left in kilodaltons and pp220 is indicated by an arrow.

was visualised in both the membrane and cytosolic fractions. The distribution of this protein was in conflict with the Western blot data and it migrated faster than p34, therefore it was taken that the 30kDa protein was not p34. In summary, the immunoprecipitation showed that there was a time dependent association of the polyprotein with the membranes and that there was slow processing of the polyprotein, however no end product of processing was detected.

5. The distribution of pp220 polyprotein and the p150 protein in cells and virions.

5.1 Introduction.

Having demonstrated a need for membrane association for the correct processing and packaging of p34, similar methods were used to follow the processing of pp220 to p150. The main aim of studying p150 was to see if it followed the same pathway as p34. If so, this would suggest that co-ordinated processing of pp220 does indeed allow proteins to be produced in a stoichiometric manner suitable for packaging and assembly.

5.2 The expression of the polyprotein and production of p150 in ASFV infected cells.

In the first experiment the antibody generated against a peptide representing the C-terminus of p150 was used to determine the time course of expression of the polyprotein and p150 during the infection cycle. Vero cells were infected for increasing times with BA71v and cell lysates were analysed by Western blotting. Panel A of figure 5.1 shows blots developed for different times. The major protein band was seen to migrate at >250kDa, which was thought to be representative of the pp220 polyprotein. The relative levels of the polyprotein increased with time as demonstrated in the previous section for blots probed with antibodies specific for p34 (Figure 4.1). The longer exposure on the right shows a second major protein band, at 8 hours, migrating at 160kDa. This protein was representative of the p150 protein. The relative levels of p150 increased over the time course and appeared very similar to the expression of pp220 polyprotein and the appearance of the 32kDa protein in figure 4.1. In addition to these two

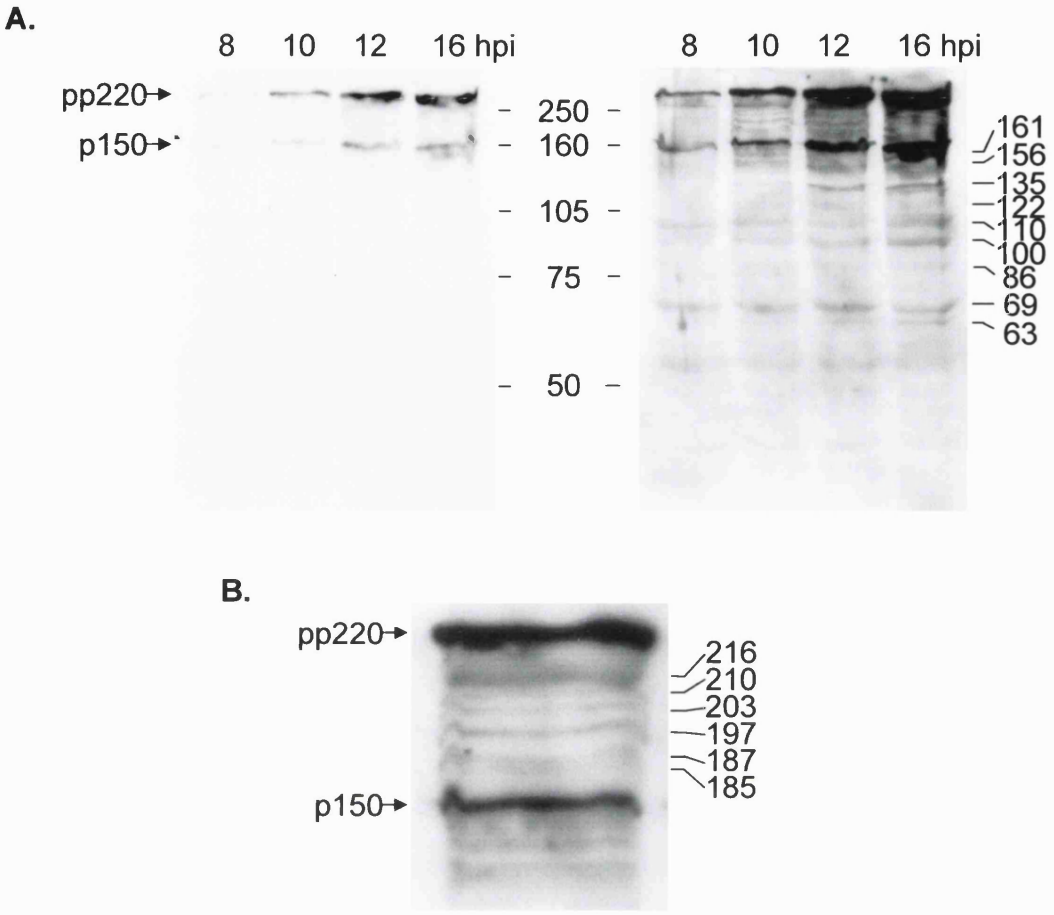

Figure 5.1: Time course of expression of pp220 and p150. At the indicated time intervals after infection with BA71v, Vero cells were lysed and the levels of pp220 and p150 determined by Western blotting using α-p150C. A. Different exposures of the blots are depicted. B. An enlarged view of the six protein ladder found at 10 hours post infection. Molecular weight markers are shown in the middle of panel A and interpolated molecular sizes are shown on the right in kilodaltons. pp220 and p150 are indicated by arrows.

major proteins, the antibody raised against the C-terminus of p150 also detected low levels of other proteins. At 8hpi faint protein bands were visible at 69, 100 and 110kDa. There was a slight increase in the relative levels of these proteins during the time course, but the major difference was the appearance of a ladder of six proteins between the polyprotein (>280kDa) and product (160kDa), with molecular weights of 185, 187, 197, 203, 210 and 216kDa at 10 hours post infection (Figure 5.1B). At 12 hours post infection the antibody against p150 C-terminus was able to detect more proteins, which migrated below p150 at 63, 86, 122 and 135kDa.

Interestingly, the antibody against the p150 C-terminus detected a ladder of proteins. As seen for p34, Simón-Mateo et al (1993) showed that an antibody raised against the p150 protein, only reacted with the polyprotein and the p150 protein (Figure 4.2). As already stated Simón-Mateo et al (1993) deduced this hypothesis by describing an ordered cascade of proteolysis occurring at four Gly-Gly-X sites. If proteolysis occurs at all 19 Gly-Gly-X sites then approximately 16 proteins would be detected by the antibody specific for the C-terminus of p150 (Figure 5.2), depending on the resolution of the SDS-PAGE.

5.3 p150, but not the polyprotein or the intermediates, is found in purified virions.

It has already been demonstrated that p34, but not pp220 and its intermediates, were present in mature virions (figure 4.4). In the next experiment lysates from infected cells and a crude virus preparation were prepared as described in section 5, resolved on a 7.5% SDS-PAGE, transferred to nitrocellulose and probed with the antibody against p150. Figure 5.3 shows that

A.

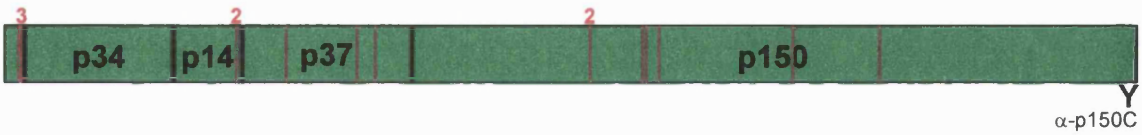

B.

Predicted molecular weights of the proteins recognised by the α-p150C antibody (kDa)			
282	224	190	122
278	223	181 (p150)	119
277	212	136	86
241	195	123	64

Figure 5.2: The possible proteins formed by proteolytic cleavage of all 19 Gly-Gly-X cleavage sites. A) Schematic showing the 19 Gly-Gly-X cleavage sites, the black lines are those described by Simón-Mateo et al (1993) for ordered proteolysis and the red lines are the remaining sites. B) Predicted molecular weights of possible proteins formed by the cleavage of the 19 sites, which would be recognised by the α-p150C antibody.

the cell lysates contained a ladder of proteins ranging from 57 to 212kDa, the ladder contained major proteins at 57, 63, 69, 74, 78, 86, 110, 135, 161, 185, 197 and 220kDa. This was a similar ladder to that seen for the 16 hours post infection visualised in figure 5.1. This ladder suggested processing of pp220 to p150 via several intermediates and further processing of p150 at internal Gly-Gly-X sites. The crude preparation of ASF virions contained a single major band, which corresponded to p150. These data suggest that the polyprotein was processed at all the Gly-Gly-X sites, producing the final p150 product, and also smaller proteins, formed by cleavage of the p150 protein at internal Gly-Gly-X sites. This was different from the processing seen for the p34 protein, as the p34 protein has no internal Gly-Gly-X motifs (figure 5.2); therefore p34 was the end product of processing. This difference suggests that processing was occurring at all 19 Gly-Gly-X sites. Interestingly, although a high number of proteolytic intermediates and products were formed, only the correct final product, p150, was found in the virions.

5.4 The intracellular pool of p150 associates with membranes.

Figure 4.5 showed that p34 was found solely in the membrane fraction, but another interesting aspect of the figure was that different proteins were located in the cytosolic and membrane fractions. In the next experiment Vero cells were infected with BA71v for 16 hours and postnuclear supernatants were prepared following homogenisation of cells by 20 passages through a 25-gauge needle. The postnuclear supernatants were centrifuged to produce a pellet of postnuclear membranes and a supernatant containing the cell cytosol. Figure 5.4 shows the distribution of pp220 and p150 between the membrane and cytosolic fractions of

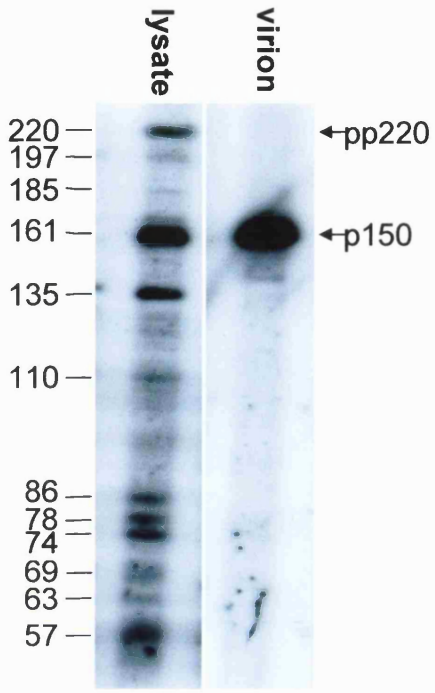

Figure 5.3: p150, but not the polyprotein or the intermediates, were found in purified virions. Vero cells were infected with BA71v for 16h and the cells were lysed. BA71v infected Vero cells were cultured until an extensive cytopathic effect was observed, cell debris was removed by centrifugation at 500*g* for 15min and the virus was pelleted at 30,000*g* for 1h. The pellet was lysed and both lysates were resolved on a 7.5% SDS-PAGE, Western blotted and probed with α-p150C antibody. Interpolated molecular sizes are shown on the right in kilodaltons and pp220 and p150 are indicated by arrows.

the cell. The cytosolic fraction contained a single high intensity band at 282kDa, with a weaker band visualised at 186kDa, which was representative of the pp220 polyprotein and very low levels of p150. The membrane fraction contained a ladder of six proteins of 135, 187, 239, 252 and 282kDa, the 187 and 278kDa proteins are the major bands visualised on the gel and represent pp220 and p150 respectively. The increase in the molecular weight assigned to the polyprotein and p150 protein, compared to figure 5.1 and 5.3, was due to an improved resolution on the SDS-PAGE and therefore more accurate molecular weight estimation. The distribution of pp220 between the two fractions was 62% in the soluble cytosolic pool and 38% in the membrane fraction. This level of distribution was very similar to that found for p34 (65%: 35%; figure 4.5). One difference between p34 and p150 in their cellular distribution is that 15% of the total cellular pool of p150 was found in the cytosolic fraction, but no p34 was visualised in the cytosolic fraction. Interestingly, all the proteins recognised by the antibody specific for the C-terminus of p150, with the exception of the polyprotein, would not have an N-terminal myristylation site. This suggests that membrane-association was not a result of myristylation, but possibly due to association with other proteins.

The cytosolic fraction contained only two protein bands, representative of pp220 and p150, whereas the antibody specific for p34 detected a dense ladder of proteins in the cytosol. This was a surprising result as the same fractions were used for both experiments. The antibody specific for p34 was generated from the recombinant protein and therefore a polyclonal serum recognising several epitopes would be generated. The antibody against p150 was generated from a C-terminal peptide. This would be expected to recognise fewer epitopes and

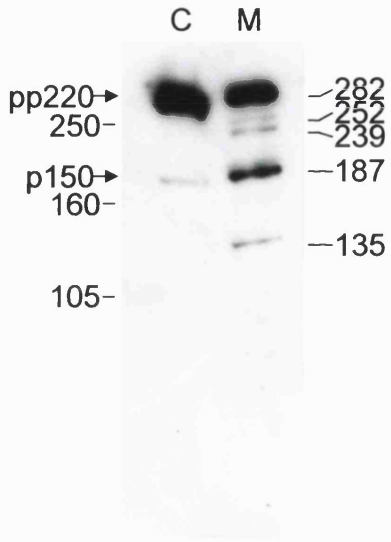

Figure 5.4: pp220 and p150 associated with the cytosolic and membrane fractions. Vero cells were infected for 16h with BA71v. Postnuclear membrane (M) and cytosolic (C) fractions were prepared. The fractions were resolved on a 7.5% SDS-PAGE, Western blotted and probed with the α-p150C antibody. Molecular weight markers are shown on the left and interpolated molecular sizes are shown on the right in kilodaltons. pp220 and p150 are indicated by arrows.

may therefore recognise fewer proteins. In addition the C-terminus of p150 could be removed by proteolysis during random cleavage resulting in the loss of the epitope.

5.5 The membrane envelops p150, but not pp220.

The protease protection assay described in section 5.5 had already shown that p34 was enveloped. The experiment was therefore repeated for p150. Figure 5.5 shows the postnuclear membrane fractions after incubation in the absence or presence of trypsin respectively. The untreated membrane fraction contained two proteins binding the antibody, these were pp220 and p150. In contrast the trypsin treated membrane fraction shows a single reactive band, which was the p150 protein. Again the results show the selective envelopment of the structural proteins and not the polyprotein precursor.

A surprising result was that the untreated membrane fraction contained only the pp220 polyprotein and p150, whereas figure 5.4 shows the membrane fraction had six proteins associated. A major difference between figures 5.4 and 5.5 were the relative levels of the pp220 polyprotein and the p150 protein. In figure 5.5 the proteins may be present, but due to the decreased signal, they are no longer visible.

5.6 pp220 and p150 assemble in to a large complex.

In the previous chapter, which followed the processing of pp220 to p34, sucrose gradients showed that membrane associated pool of p34 was present in a complex in excess of 59,000kDa. The next experiments explored the possibility that p150 was incorporated into a similar complex. Vero cells were infected with

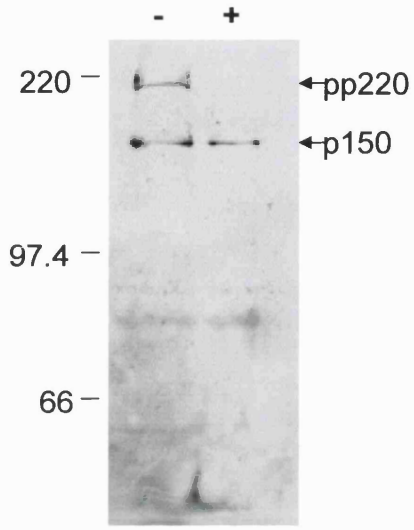

Figure 5.5: p150, but not the polyprotein, was enveloped. Vero cells were infected for 16 hours with BA71v. Postnuclear membrane fractions were prepared and were incubated in the absence (-) or presence (+) of 5mg/ml trypsin for 30 minutes at 37°C. Proteolysis was inhibited by the addition of 10mg/ml of trypsin inhibitor. The membranes were pelleted and were resolved on a 5% SDS-PAGE, Western blotted and probed with the α-p150C antibody. Molecular weight markers are shown on the left in kilodaltons. pp220 and p150 are indicated by arrows.

BA71v for 16 hours and a cell lysate was solubilised in immunoprecipitation buffer containing 1% Brij-35. The lysate was floated on a 10 to 40% sucrose gradient and centrifuged at 200,000*g* for 20 hours at 4°C. The gradients were separated into 1.2ml fractions, resolved on a 7.5% SDS-PAGE, Western blotted and probed with the antibody specific for the C-terminus of p150. The sucrose gradients were calibrated using marker proteins; carbonic anhydrase - 30kDa, BSA - 66kDa, β-amylase - 200kDa, apoferritin - 473kDa. Figure 5.6 shows that a major reactive protein of >250kDa was detected in fractions 3 through to 8, this protein was characteristic of the 220kDa polyprotein. The bulk of this protein was visualised in fractions 6 and 7, and therefore migrated at ≈200kDa and was therefore a monomeric form of the polyprotein. Fractions 6 and 7 also contained a ladder of proteins ranging from the polyprotein down to a protein of 90kDa; this ladder was very similar to that seen in figure 5.1. The reactive proteins in fractions 6 and 7 were concluded to be monomers of the proteins formed in the proteolytic processing of the polyprotein. Fractions 3 to 5 contained a strong reactive band characteristic of the pp220 polyprotein, and also a weaker reactive band migrating at 177kDa, which was representative of the final p150 protein. These reactive proteins were migrating with molecular weights characteristic of dimeric and possibly trimeric forms of the polyprotein and p150 protein. The majority of p150 however, was found in fraction 1, showing that the final p150 protein migrated on the 10-40% sucrose gradients as a large complex of over 473kDa. In contrast, the bulk of the polyprotein migrated as a monomer.

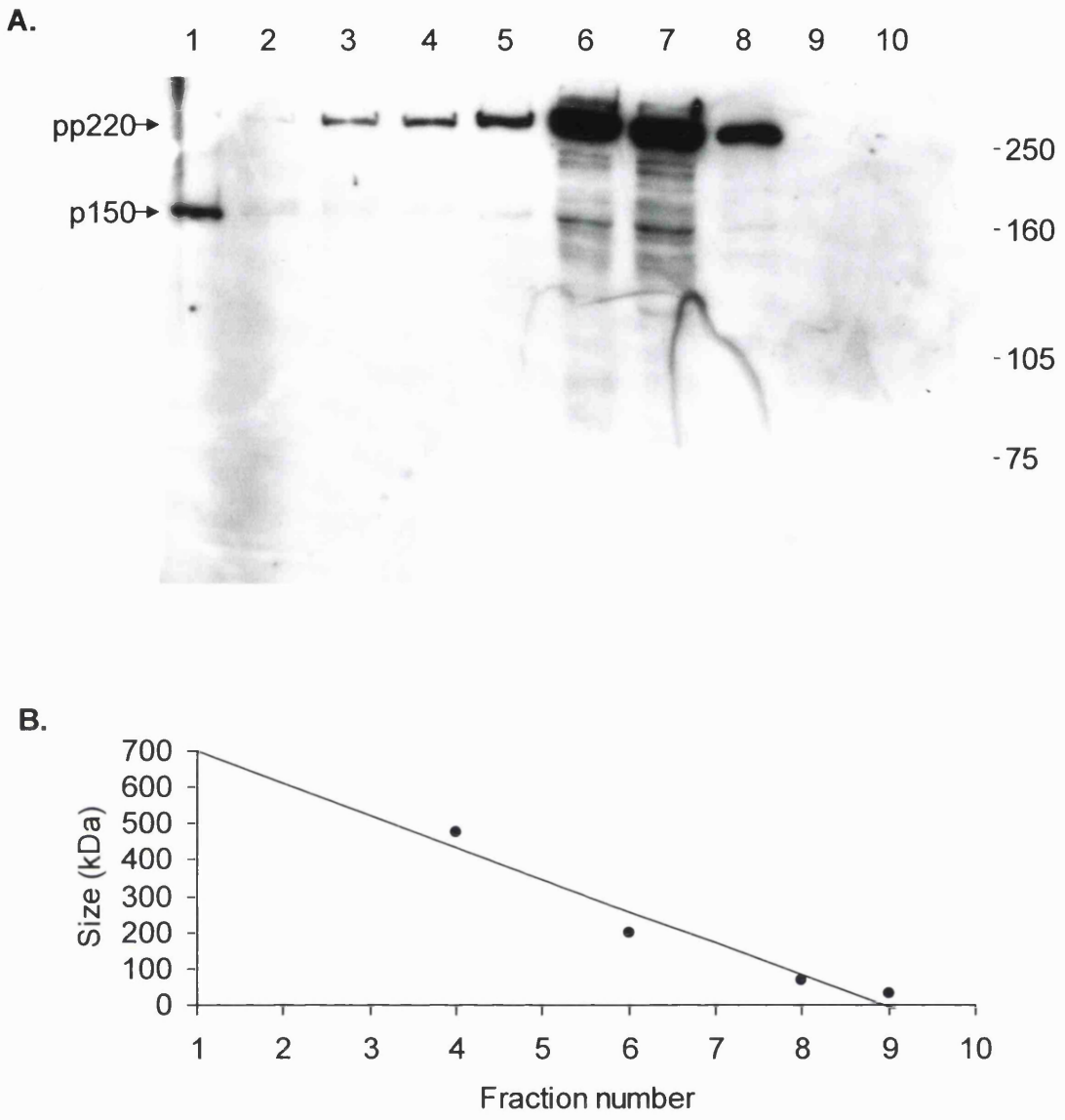

Figure 5.6: p150 assembled into a large complex. A. Vero cells were infected with BA71v for 16 hours and a cell lysate was solubilised in immunoprecipitation buffer containing 1% Brij-35. The lysate was floated on a 10 to 40% sucrose gradient and centrifuged at 200,000*g* for 20 hours at 4°C. The gradients were separated into 1.2ml fractions, resolved on a 7.5% SDS-PAGE, Western blotted and probed with the α-p150C antibody. Molecular weight markers are shown on the right in kilodaltons. pp220 and p150 are indicated by arrows. B. The location of the peak fractions containing the marker proteins (Carbonic anhydrase-30kDa, BSA-66kDa, β-amylase-200kDa, apoferritin-473kDa) were plotted against their molecular weight (kDa) and a best fit line was extrapolated.

5.7 Large oligomers of p150 are found in the membrane fraction.

In the next experiment cytosol and membrane fractions were prepared before sucrose gradient sedimentation. The fractions were solubilised in IPB containing 1% Brij-35 and then floated on to 10-40% sucrose gradients. The gradients were centrifuged at 200,000*g* for 20 hours at 4°C. The gradients were separated into 1.2ml fractions, resolved on a 7.5% SDS-PAGE, transferred to nitrocellulose and probed with the antibody raised against p150. Figure 5.7 compares the size distribution of the polyprotein and p150 structural protein within membrane and cytosolic fractions. Panel A shows that the membrane-associated polyprotein was found in fractions 5, 6 and 7 and migrated at ≈200kDa indicating a monomer. As seen above, the bulk of the final p150 structural protein was found at the bottom of the gradient.

Panel B shows the distribution of the cytosolic proteins across a 10-40% velocity gradient. The bulk of the polyprotein was shown to be located to fractions 6 and 7, representative of pp220 monomers. There was also a small amount of the polyprotein in fractions 3-5, as seen for the whole cell lysates. p150 was absent from the heavy fractions but there was a small cytosolic pool of p150 migrating at ≈200kDa. The subcellular fractionation of the cells again lead to the loss of the minor proteins visualised in whole cell lysates; this will be discussed later. In conclusion, the membrane-associated pool of p150 formed the large oligomeric structures. Interestingly, it appears that membrane association is an important factor in oligomerisation, as the cytosolic p150 was monomeric.

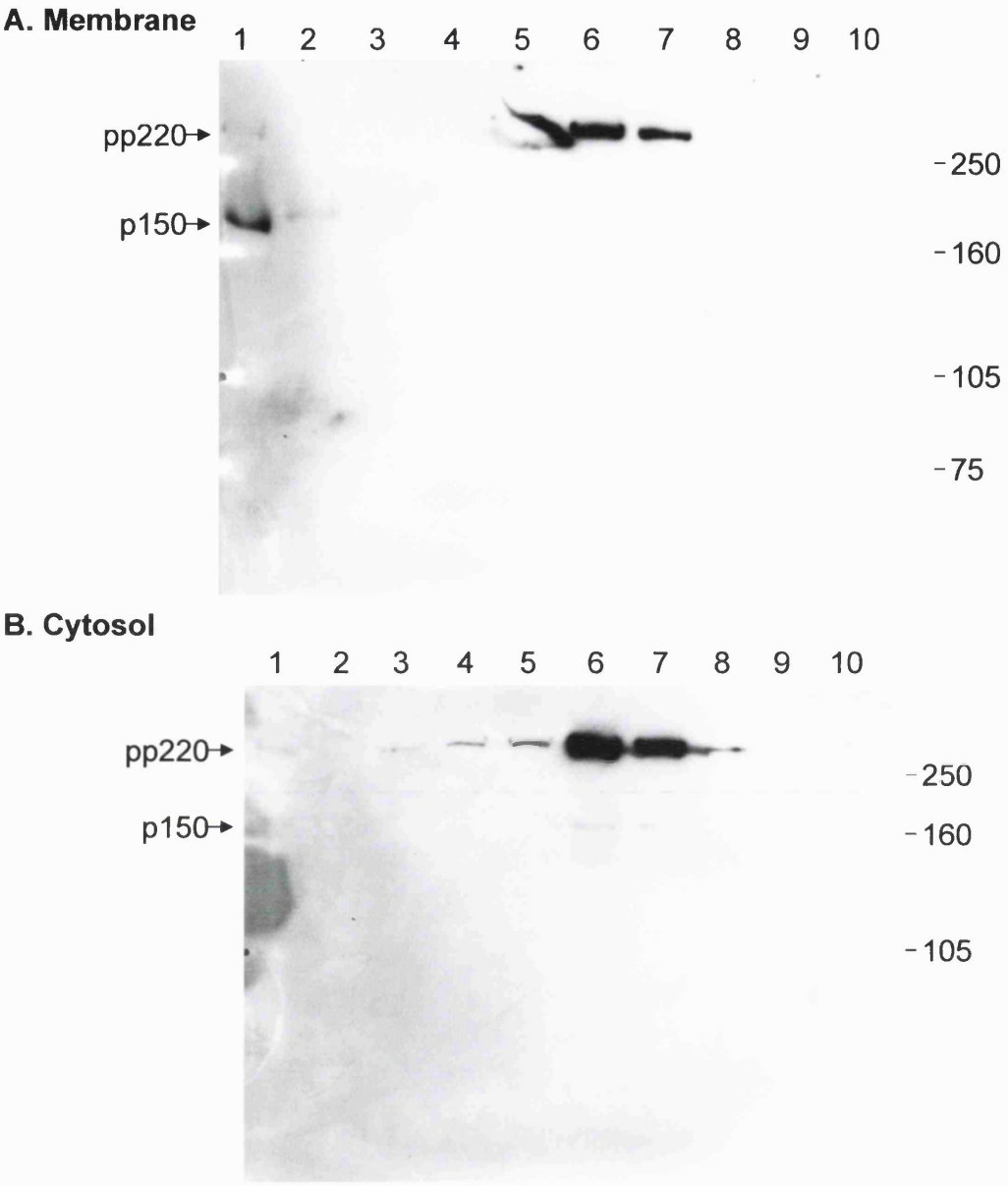

Figure 5.7: Membrane associated p150 formed a large complex. Vero cells were infected with BA71v for 16 hours and membrane and cytosolic fractions were prepared and solubilised in immunoprecipitation buffer containing 1% Brij-35. The membrane and cytosolic fractions were floated on a 10 to 40% sucrose gradient and centrifuged at 200,000*g* for 20 hours at 4°C. The gradients were separated into 1.2ml fractions, resolved on a 7.5% SDS-PAGE, Western blotted and probed with the α-p150C antibody. Molecular weight markers are shown on the right in kilodaltons. pp220 and p150 are indicated by arrows.

5.8 The p150 protein forms an oligomer with a molecular mass of >59,000kDa.

In the study of the p34 structural protein it was shown that the protein formed a large membrane associated oligomer of over 59,000kDa, a 10-70% continuous sucrose gradient was therefore used to determine the molecular mass of the p150 oligomers. Vero cells were infected for 16 hours, lysed in IPB containing 1% Brij-35, floated on a 10-70% continuous sucrose gradient and then centrifuged at 79,000*g* for 2.5 hours at 4°C. Figure 5.8 shows that the polyprotein and intermediates remained localised at the top of the gradient, in fractions 8, 9 and 10. This would represent the pool of proteins migrating at approximately 150 to 250kDa in the previous experiments. A small pool of the p150 protein migrated at the bottom of the gradients in fractions 1 to 4, which have a molecular mass of approximately 59,000kDa. Strangely, there was only a small pool of the p150 protein at the bottom of the gradient, but this could have been as a result of the disruption of the p150 oligomers in the preparation and centrifugation of the samples. Unfortunately, due to the high concentration of proteins at the top of the gradient it was difficult to visualise any p150 protein, indicative of disrupted complexes. So, both the p34 and p150 proteins migrated as oligomers of approximately 50,000kDa.

5.9 pp220/p150 localised to the viral factory 12 hours post infection.

The next experiment used indirect immunofluorescence to visualise the subcellular location of the polyprotein and p150, using the antibody specific for p150. As before this antibody was unable to determine the differences between the subcellular distribution of the polyprotein and p150, as it recognises both

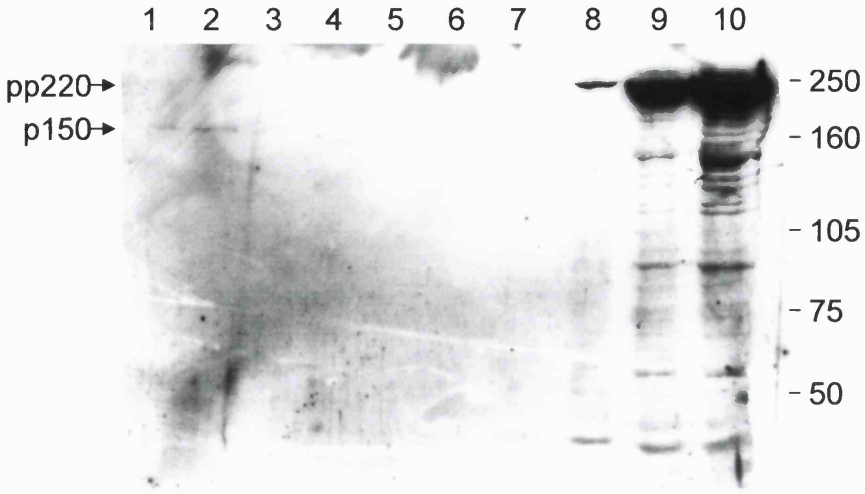

Figure 5.8: p150 complexes migrated at 50,000kDa. Vero cells were infected with BA71v for 16 hours and solubilised in immunoprecipitation buffer containing 1% Brij-35. The lysates were floated on a 10 to 70% sucrose gradient and centrifuged at 79,000*g* for 2.5 hours at 4°C. The gradients were separated into 1.2ml fractions, resolved on a 7.5% SDS-PAGE, Western blotted and probed with the α-p150C antibody. Molecular weight markers are shown on the right in kilodaltons. pp220 and p150 are indicated by arrows.

proteins. The monoclonal antibody raised against the major capsid protein, p73, was used as a marker for the ASF viral factories and virions. Vero cells were infected for 12 hours and then fixed and permeabilised as described in the materials and methods. Figure 5.9 shows the distribution of the pp220/p150 and p73 proteins at 12 hours post infection. Panel A shows a cell stained for the pp220/p150 proteins, panel B shows staining for the major capsid protein, p73, panel C shows the staining of the cellular and viral DNA with DAPI and panel D shows a digital merge of the three images. All the panels contain an insert showing a digital enlargement of the viral factory. Panel A shows that the antibody raised against p150 labelled a large amorphous pool of proteins at the site of the viral factory, as well as a very weak cytoplasmic stain. The monoclonal antibody raised against the major capsid protein labelled a similar area, however the enlargement shows that the area consisted of clusters of well defined spheres, representative of virions. The merge of the images (Panel D) shows that the area labelled by the antibodies specific for p150 and p73 co-localised with the viral DNA and was situated at a perinuclear location, characteristic of the viral factories. The insert of the merged images appeared to contain some areas of co-localisation between the pp220/p150 and p73 proteins, however on closer inspection of panels A and B the co-localisation appeared to be where the p73 virions were found over the pool of p150C. The virions on the edge of the pool show no co-localisation. The pp220/p150C proteins were found at the viral factories, but the stain lacked a structure, especially the spherical, punctate staining of virions. This was surprising since studies using immunogold electron microscopy have localised pp220/p150 to virions (Carrascosa et al, 1986; Andrés et al, 1997).

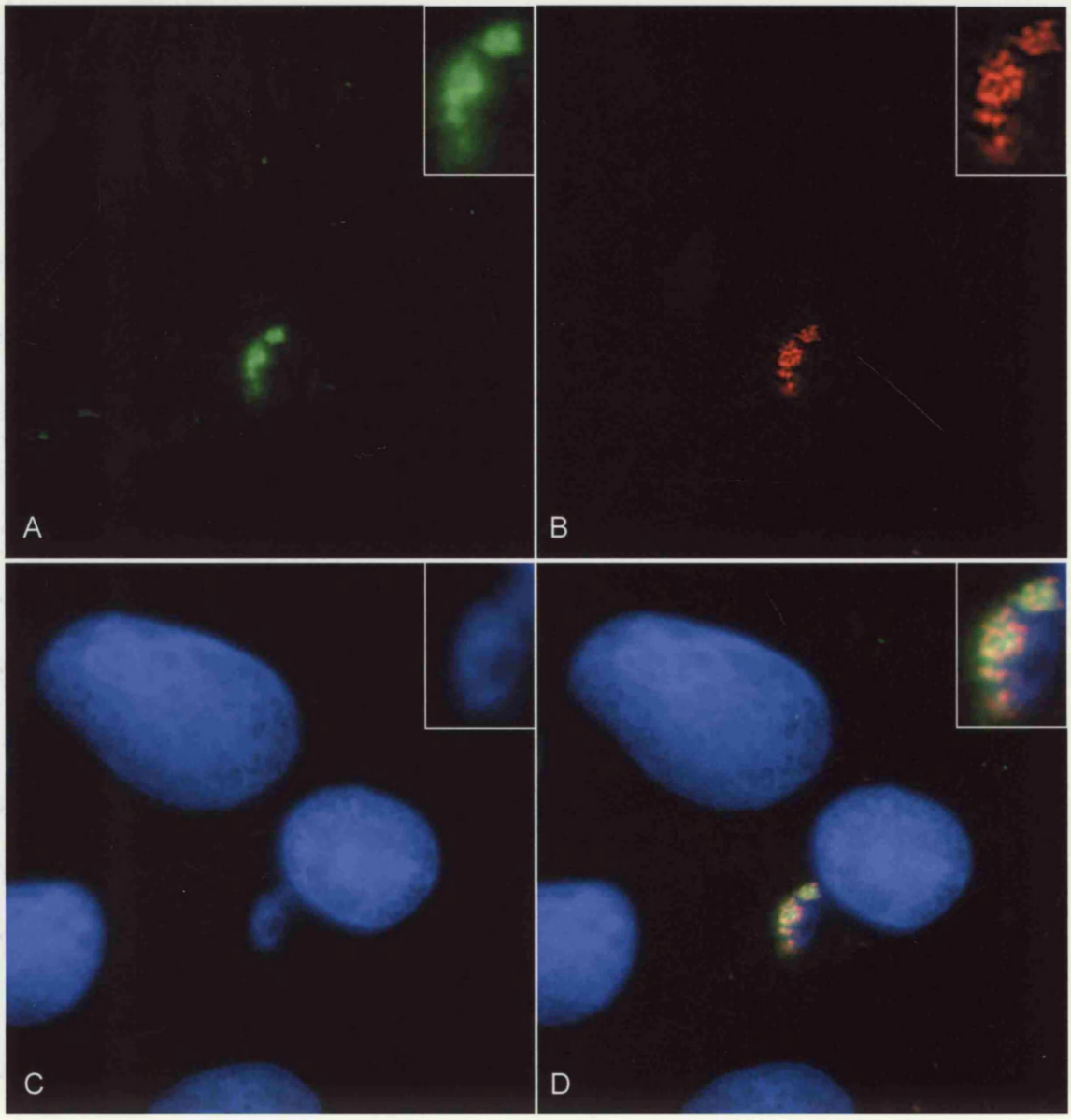

Figure 5.9: pp220/p150 localised at a perinuclear site at 12hpi. At 12 hours post infection with BA71v, Vero cells were fixed with ice-cold methanol, permeabilised with 0.1% Triton X-100 and incubated with the rabbit antibody specific for p150 (A) and a mouse monoclonal antibody specific for p73 (B). The distribution of the proteins was visualised by using the Alexa Fluor 488 (green) anti-rabbit and 594 (red) anti-mouse IgG conjugates. The cellular and viral DNA was labelled with DAPI (blue) (C). Cells were viewed at 60X and images captured as described in the materials and methods. The images were digitally deconvolved, using the Openlab system and p150, p73, and DAPI were digitally overlaid (D). The inserts are a digital enlargement of the viral factory.

5.10 pp220/p150 were not localised to the surface of virions.

The distribution of the pp220/p150 proteins was investigated at 16 hours post infection, at this time point many virions have left the viral factory, therefore allowing for better resolution in co-localisation studies. Panel A of figure 5.10 shows the distribution of the pp220/p150 proteins, panel B shows the distribution of the major capsid protein, p73, panel C shows the viral and cellular DNA and panel D shows a digital merge of the images. The images contain two inserts containing a digital enlargement of the viral factory and mature cytoplasmic virions. The antibody raised against the C-terminus peptide of p150 stained a large structure at a perinuclear location, as well as a granular stain in the cytoplasm. On closer inspection of the perinuclear structure there appeared to be a more defined structure than seen for the viral factory at 12 hours post infection. The large pool of the pp220/p150 proteins contained small punctate structures, possibly virions, and there also appeared to be some small spherical structures in the cytoplasm. The major capsid protein was largely concentrated at the viral factory, which consisted of a diffuse stain decorated with the punctate staining for virions; in addition there were a large number of virions in the cytoplasm, largely localised to the periphery of the cell. The digital merge of the viral factory showed that there was some co-localisation of the punctate structures, suggesting that the p150 epitope was accessible to the antibody. However on examination of the mature virions in the cytoplasm (lower right insert), only the major capsid protein was localised to the virions. This suggested that the small punctate structures at the viral factory might be assembly intermediates, which had some structure but had not full closed allowing the internal p150 to be labelled.

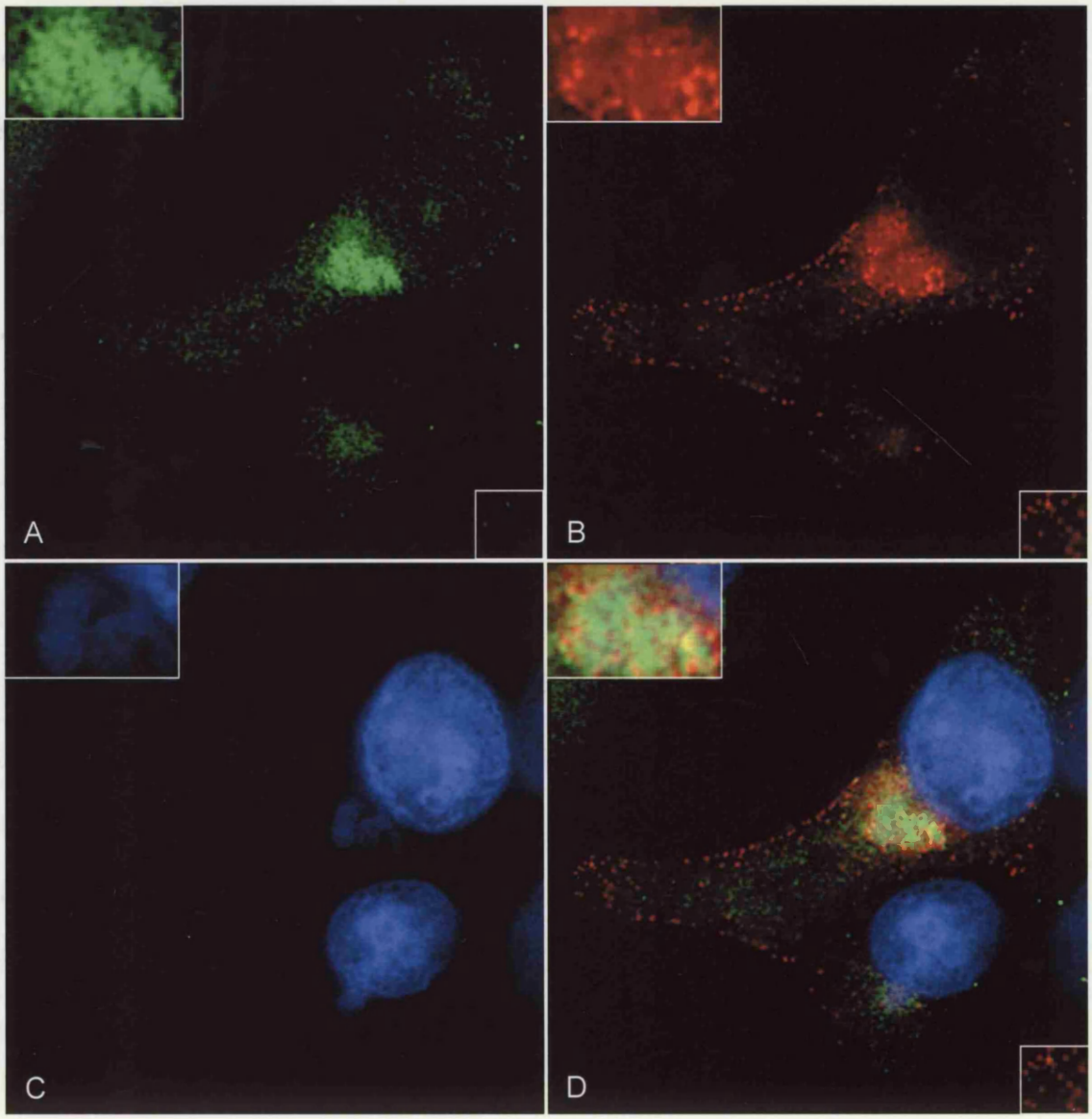

Figure 5.10: pp220/p150 were not located on the surface of virions. Vero cells were infected for 16 hours and fixed with ice-cold methanol, permeabilised with 0.1% Triton X-100 and incubated with the rabbit antibody specific for p150 (A) and a mouse monoclonal antibody specific for p73 (B). The distribution of the proteins was visualised by using the Alexa Fluor 488 (green) anti-rabbit and 594 (red) anti-mouse IgG conjugates. The cellular and viral DNA was labelled with DAPI (blue) (C). Cells were viewed at 60X and images captured as described in the materials and methods. The images were digitally deconvolved, using the Openlab system and p150, p73, and DAPI were digitally overlaid (D). The inserts are a digital enlargement of the viral factory and mature virions.

5.11 The kinetic analysis of the proteolytic processing of the 220kDa polyprotein to the 150kDa structural protein.

5.11.1 The proteolytic processing of pp220 to p150.

The above sections demonstrated that the pp220 polyprotein was present in both cytosolic and membrane fractions, and was proteolytically processed to produce p150. Although the polyprotein, several intermediates and the p150 protein associated with the membranes, only the p150 structural protein became enveloped by the membranes and was found in the purified virions. These findings were similar to those seen for the proteolytic processing of the polyprotein to the final p34 protein. The kinetic analysis of the processing of the polyprotein to p34 was hindered by the fact that the antibody specific for p34 was unable to immunoprecipitate p34, the final product of processing. The kinetic studies did demonstrate, however, a time dependent loss of the polyprotein from cell lysates. The next experiments followed a similar strategy to follow the kinetics of processing of the polyprotein to p150. Vero cells were infected with BA71v for 16 hours, metabolically labelled for 30 minutes and then chased for various time intervals up to 12 hours. The cells were then lysed in IPB containing 1% Brij-35 and immunoprecipitated with the antibody specific for p150. Figure 5.11 shows the proteins immunoprecipitated at the various time points. As before, the major protein visualised had a molecular weight characteristic of the pp220 polyprotein. The relative intensity of the polyprotein increased slightly during the two-hour chase period, after which the levels of polyprotein decreased. This was similar to the result seen with the antibody specific for the p34 protein, and suggests that the antigenic site for the antibody recognising p150 required folding of the protein to form the correct binding site. The slight decrease in the

levels of the polyprotein was expected, as the polyprotein would be proteolytically processed into the final proteins. As with the antibody specific for p34, the levels of loss of the polyprotein were very low, and in contrast to the rate of processing described by Simón-Mateo et al (1993). Interestingly, a 161kDa protein was present in the pulse, which increased slightly during the first chase period, but then gradually decreased during the remaining chase period. In parallel to the decrease in the levels of the 161kDa protein, a 135kDa protein appeared during the first 2 hours of the chase period and gradually increased in intensity throughout the chase period, suggesting a precursor/product relationship. Interestingly, two proteins with the same molecular weights were seen in the Western blots shown in figure 5.1, where a 161kDa protein was first detected at 8 hours post infection and the levels increased during the time course of expression. This protein was predicted to be the p150 protein. A protein of 135kDa appeared at 12 hours post infection. So, the results suggested that the polyprotein was highly abundant in infected cell lysates. Processing to the p150 protein was seen during the pulse and throughout the chase period, however the levels of p150 were very low. Interestingly, at later times during the chase period it seems that the p150 protein began to be degraded, leading to the formation of the 135kDa protein. This may be a result of cleavage of the first N-terminal Gly-Gly-X site in p150, which would produce a 136kDa protein (figure 5.2).

5.11.2 Membrane association was required for the correct processing of pp220 to p150.

The Western blot analysis showed that the pp220 polyprotein associated with both the membrane and cytosolic fractions, with 38% of the polyprotein

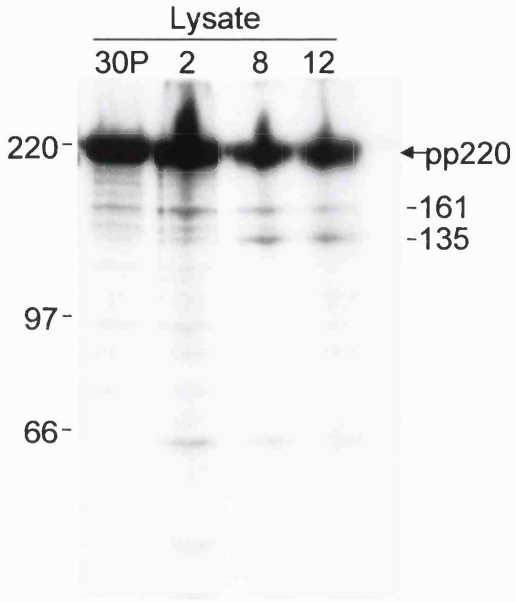

Figure 5.11: Kinetics of proteolytic processing of pp220 to p150. Vero cells were infected for 16h with BA71v. Cells were metabolically labelled for 30min, chased for the indicated time periods and then lysed in immunoprecipitation buffer. The lysates were incubated overnight with antibody specific for p150, bound to protein-A sepharose beads, and then boiled in SPB and resolved on a 7.5% SDS-PAGE and visualised by autoradiography. Molecular weight markers are shown on the left and interpolated molecular sizes are shown on the right in kilodaltons. pp220 is indicated by an arrow.

associating with a membrane pool, at steady state. The majority of the final p150 protein associated with the membranes. The kinetic analysis of the polyprotein, using the antibody against p34, showed that there was a time dependent distribution between the membrane and cytosolic fractions. The next stage of the investigation was to repeat this experiment using the antibody specific for p150 and determine the time course of membrane association of the polyprotein and p150 protein. Figure 5.12 shows the distribution of the immunoprecipitated proteins between the membrane and cytosolic fractions. The major protein immunoprecipitated by the antibody was again a protein of ≈220kDa, which was characteristic of the pp220 polyprotein, several minor bands were also immunoprecipitated, and also the 135 and 161kDa proteins. As expected from the experiments with the antibody for p34, the pp220 polyprotein was found in both the membrane and cytosolic fractions, and as before there was a marked difference in the distribution of the pp220 with time. Following the 30-minute pulse 86% of the total pool of the polyprotein was located in the cytosol, and the polyprotein became membrane-associated during the chase period. After 2 hours the pp220 polyprotein was evenly distributed and at 8 and 12 hours 60% of the polyprotein was recovered from the membrane fraction (Figure 5.12B). As before the total levels of the polyprotein increased during the 2-hour chase period indicative of a conformational change. The levels of the metabolically labelled p150 were considerably lower than in the Western blot analysis. This suggests that processing of the polyprotein to p150 was very slow, as the levels of the polyprotein are similar in both the Western blots and immunoprecipitations. An alternative possibility could be that the some of the epitopes recognised by the

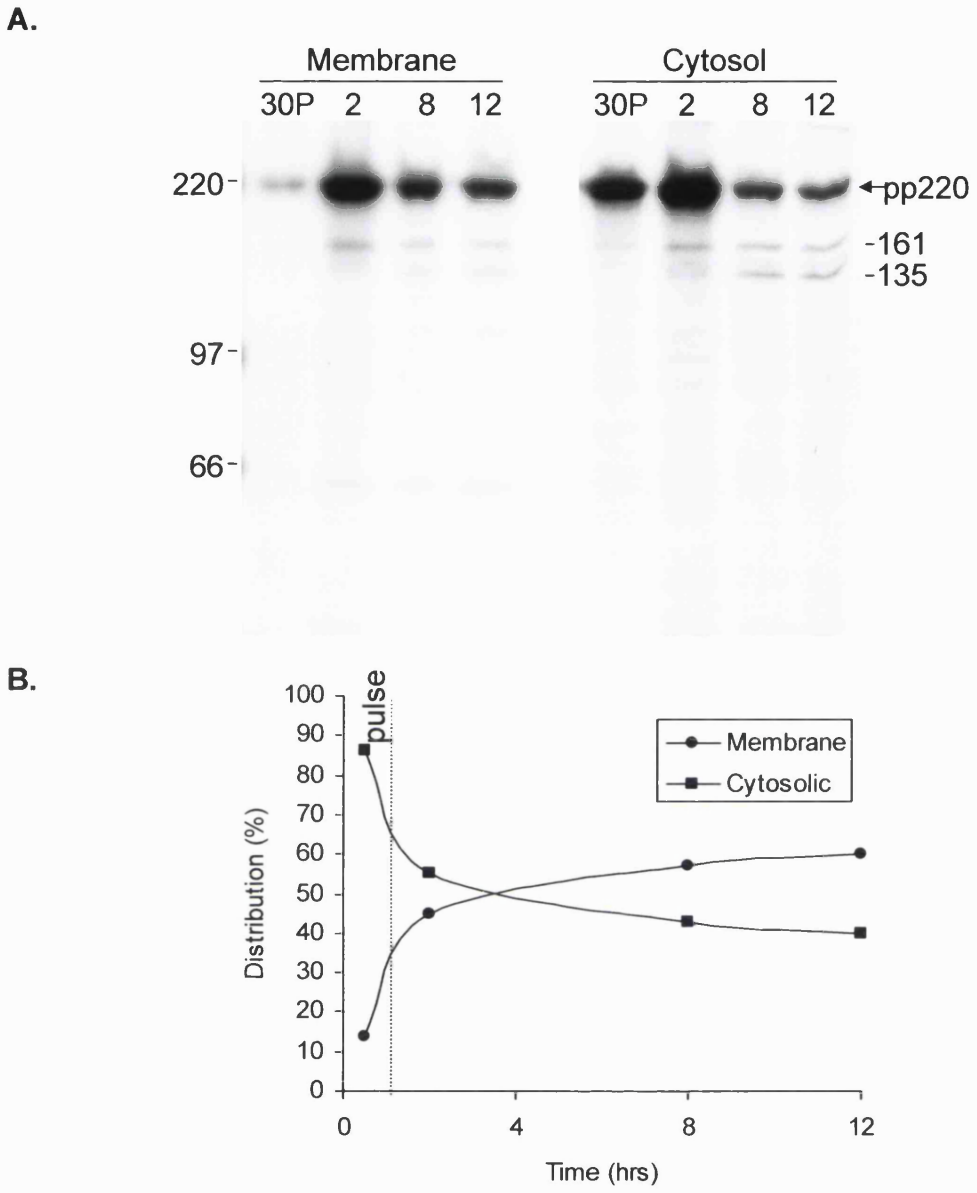

Figure 5.12: The subcellular distribution of pp220 with time. Vero cells were infected for 16h with BA71v. The cells were metabolically labelled for 30 minutes and chased in complete media for the indicated times. Postnuclear membranes and cytosolic fractions were prepared. The fractions were immunoprecipitated overnight with the antibody specific for p150, boiled in SPB and resolved on a 7.5% SDS-PAGE. The proteins were visualised on an autoradiograph. Molecular weight markers are shown on the left and interpolated molecular sizes are shown on the right in kilodaltons. pp220 is indicated by an arrow. (A). B) The protein bands were quantified by scanning densitometry and the percentage distribution of the pp220 protein was depicted.

antibody for p150 in the Western blot analysis are blocked by steric hindrance in the immunoprecipitations.

6. The role of the aggresome pathway in the assembly of ASFV.

6.1 Introduction.

In 1998 Johnston et al described a novel cellular pathway which sequesters misfolded integral membrane proteins within a pericentriolar site. This was named the aggresome pathway. They discovered this pathway through studies of a mutant form of the cystic fibrosis transmembrane conductance regulator (CFTR), ΔF508, which was unable to fold correctly (Ward and Kopito, 1994). CFTR is a 165kDa polytopic glycoprotein, which encodes a Cl^- ion channel in the plasma membrane of epithelial cells (Riordan et al, 1989). The ΔF508 mutant has a deletion of phenylalanine at residue 508, which prevents the protein adopting its correct conformation. This, in turn, is recognised as abnormal by the endoplasmic reticulum "quality control" mechanisms, which mark the protein for degradation rather than for movement to the plasma membrane, and ultimately leads to cystic fibrosis (Cheng et al, 1990; Thomas et al, 1992; Welsh and Smith, 1993). Misfolded proteins are targeted to the proteasome by ubiquitination, where they are degraded. Johnston et al inhibited degradation using proteasome inhibitors and showed that the misfolded proteins aggregate and are sequestered into a novel structure, which they termed the aggresome. They went on to show that the aggresome was associated with the microtubule organising centre (MTOC), was highly ubiquitinated, and was surrounded by a cage of the intermediate filament (IF) protein, vimentin.

In 1999 Wigley et al described a structure associated with the centrosome that was enriched for proteasomal components (the 20S proteasome, ubiquitin and the 700 and 180kDa proteasome activator complexes, PA700 and PA28 respectively) and cell stress chaperones (the 70 and 90kDa heat shock proteins,

Hsp70 and Hsp90). They concluded that the centrosome acts as a scaffold, which concentrates and recruits the systems that act as sensors and modulators of the balance between folding, aggregation and degradation. In 1999 García-Mata et al further characterised the aggresome by using a protein chimera (GFP-250) composed of the green fluorescent protein (GFP) fused at its C-terminus to a 250 amino acid fragment of the cytosolic protein, p115. p115 is peripherally associated with Golgi membranes and acts as a membrane transport factor involved in vesicle docking (Waters et al, 1992; Nakamura et al, 1997). They showed that GFP-250 would form aggresomes in cells without the need for proteasome inhibition, and aggresomes could be viewed using indirect immunofluorescence microscopy. They were able to demonstrate that aggresomes contained three chaperones; Hsc70 and two Hsp40 members, Hdj-2 (the human homologue of DNAJ) and Hdj-1, and one chaperonin, TCP1. They also showed that the aggresomes contained the 20S proteasome and in contradiction to Johnston et al (1998) the aggresomes were not ubiquitinated. Ultrastructural examination of the aggresomes showed that they were interspersed with, and surrounded by, subcellular organelles, which appeared to be predominately mitochondria and lysosomes.

Both groups (Johnston et al, 1998; García-Mata et al, 1999) reported that the microtubule network was required for the formation and integrity of aggresomes. The requirement for the microtubule network was first shown by disrupting the microtubules with the drug nocodazole, which completely abrogated the accumulation of the ΔF508 protein at a single juxtanuclear position. Instead the protein was observed at multiple sites throughout the cytoplasm (Johnston et al, 1998). Secondly, García-Mata et al (1999) used time-

lapse techniques in live cells to follow the formation of GFP-250 aggresomes in cells in the presence or absence of nocodazole. They showed that in the absence of nocodazole the GFP-250 aggregates formed at the periphery of the cell and moved to the MTOC over time. However, in the presence of nocodazole the speed of movement of the small aggregates was greatly reduced and had become non directional. In addition, they used the overexpression of p50/dynamitin to experimentally inhibit the microtubule associated minus-end-directed dynein/dynactin motors. They showed that on inhibition of the motors GFP-250 aggresomes did not form and small aggregates of the protein were seen throughout the cell.

A review of the literature concerning the sites of ASFV assembly produced some interesting similarities between the assembly pathways of ASFV and aggresomes. The assembly of ASFV takes place in the cytoplasm in perinuclear locations called viroplasm or viral factories (Breese and DeBoer, 1966; Vigario et al, 1967; Moulton and Coggins, 1968; Moura-Nunes et al, 1975; Pan et al, 1980). In 1988 Carvalho et al showed that there was an accumulation of vimentin filaments around viral factories and they also showed that colchicine inhibited viral factory formation, suggesting a function for microtubules. An intact microtubule network was shown to be essential in the movement of mature virions from the viral factories to the cell periphery (Alves de Matos and Carvalho, 1993). In 1995 Hingamp et al showed that the viral factories contained ubiquitin conjugates and recently the factories were shown to be surrounded by mitochondria (Rojo et al, 1998).

The next stage of this investigation was to revisit some of this earlier work and carry out a detailed comparison of aggresomes and ASFV assembly sites. If

an aggresome and a viral factory were present in the same cell there could be three possible outcomes. 1) The factory could co-localise with the aggresome demonstrating convincingly the close relationship between aggresomes and viral factories. 2) Aggresomes would not co-localise with factories suggesting a degree of independence. 3) The two pathways would compete with one another, possibly for energy or microtubule transport, in which case viral factories would not be found in cells with aggresomes.

6.2 Characterisation of aggresomes containing TCR CD3 δ-subunits.

6.2.1 Introduction.

The initial question to be explored was whether or not ASFV used the aggresome pathway to aid assembly. One way to explore this question would be to induce aggresomes in cells and then infect with ASFV and compare the subcellular location of the aggresomes and viral factories in cells. The first aim was to generate aggresomes in cell lines susceptible to infection by ASFV. This was achieved by repeating the work of Johnston et al (1998), who generated aggresomes by expressing a mutant CFTR protein and inhibiting proteasomes, but using a different protein for the generation of aggresomes.

6.2.2 Generation of aggresomes containing misfolded TCR CD3 δ-subunits.

The first experiment investigated the possibility of generating aggresomes in cells expressing a single subunit of a hetero-oligomeric protein, which is subject to endoplasmic reticulum to cytosol degradation. The T-cell receptor (TCR) is an octomeric protein complex made from six distinct integral membrane proteins (α, β, γ, δ, ε and ζ) (Weissman, 1994). The TCR is assembled in the

endoplasmic reticulum and correct assembly is required for the transport of the TCR to the plasma membrane. Single subunits and partial complexes are retained in the endoplasmic reticulum until they are exported to the cytosol where they are targeted, by the addition of ubiquitin, for degradation by the proteasomes (reviewed in Bonifacino and Weissman, 1998; Bonifacino et al, 1989, 1990; Manolios et al, 1990; Wileman et al, 1990, 1993, Yang et al, 1998). A CHO cell line expressing the TCR CD3 δ-chain (Wileman et al, 1990) was grown to approximately 70% confluency on glass cover slips and incubated for 12 hours at 37°C in the presence or absence of the proteasome inhibitor, MG132. The cells were fixed, permeabilised and washed and then incubated with the primary antibody specific for the TCR CD3 δ-subunit. The antibody was visualised by incubation with the Alexa Fluor 488 goat α-mouse IgG conjugate and the DNA was labelled with DAPI. Figure 6.1 shows the effects of proteasome inhibition by MG132 on the distribution of the TCR CD3 δ-subunit in CHO cells. Panel A shows the distribution of the TCR CD3 δ-subunit in CHO cells in the absence of the proteasome inhibitor. The TCR CD3 δ-subunit was localised to a reticular structure spreading throughout the cytoplasm of the cell, which was expected as the single subunit expressed in CHO cells would not be transported to the plasma membrane, but retained in the endoplasmic reticulum. Panel B shows the distribution of the TCR CD3 δ-subunit in cells treated with the proteasome inhibitor. A striking difference in the distribution of TCR CD3 δ-subunit was seen. The δ-subunit lost the characteristic reticular staining and the majority of the δ-subunit was now found in a large juxtanuclear structure, which appeared to encroach on the nucleus, and distort the nuclear envelope (panel D). A small

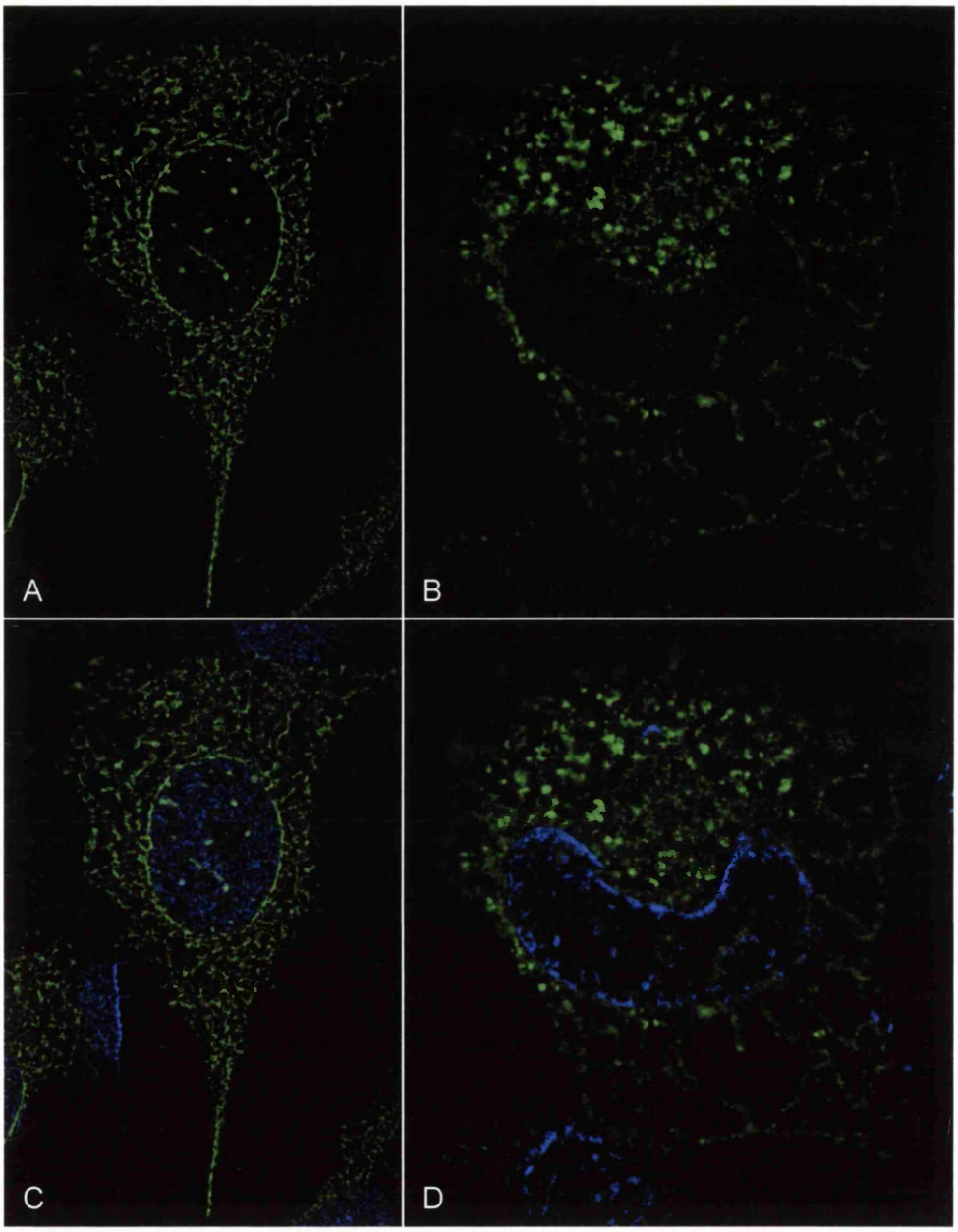

Figure 6.1: Proteasome inhibitors induced the formation of aggresomes. A CHO cell line expressing the TCR CD3 δ-chain was incubated for 12 hours at 37°C in the absence (A,C) or presence (B,D) of 25μM proteasome inhibitor, MG132. The cells were fixed with ice-cold methanol, permeabilised with 0.1% Triton X-100 and incubated with the mouse antibody specific for the TCR CD3 δ-chain. The antibody was visualised by incubation with the Alexa Fluor 488 (green) goat α-mouse IgG conjugate and then labelled with DAPI (blue). Cells were viewed at 60X and images captured as described in the materials and methods. The images were digitally deconvolved, using the Openlab system and the TCR CD3 δ-chain and cellular DNA distribution were digitally overlaid (C,D).

amount of staining for the δ-subunit was seen in the cytoplasm. The staining pattern for the δ-subunit showed many small irregular substructures of variable size, possible aggregates of the δ-subunit. The position of the δ-subunit immunofluorescence signal and its encroachment on the nuclear membrane was similar to the aggresomes reported by Johnston et al (1998) and García-Mata et al (1999). The structure however, was larger than those reported for aggresomes containing ΔF508 and GFP-250 (Johnston et al, 1998; García-Mata et al, 1999).

6.2.3 Distribution of vimentin in cells containing aggresomes.

One of the most striking characteristics of aggresomes is the collapse of the intermediate filament from its long, mesh-like filamentous structure (Franke et al 1978; Rosevear et al 1990) to a halo-like cage around the aggresome (Johnston et al, 1998; García-Mata et al, 1999). The distribution of the vimentin around aggresomes containing the CD3 δ-subunit was therefore studied. Figure 6.2 shows the rearrangement of vimentin in CHO cells expressing the TCR CD3 δ-subunit in the presence of proteasome inhibitor. Panels A and D show examples of two different cells expressing the TCR CD3 δ-subunit, and panels B and E show the distribution of vimentin. In each cell the vimentin intermediate filament rearranged from a normally long, fibrous, mesh-like structure to a collapsed ring-like structure in the area of the aggresomes. Panels C and F show a digital merge of the δ-subunit, vimentin and DAPI stained cells. In these images it can clearly be seen that the vimentin formed a cage around the aggresomes, which were seen to impinge on the nuclear membrane. This experiment established that aggresomes could be created in CHO cells by inhibiting the degradation of the TCR CD3 δ-subunit with MG132.

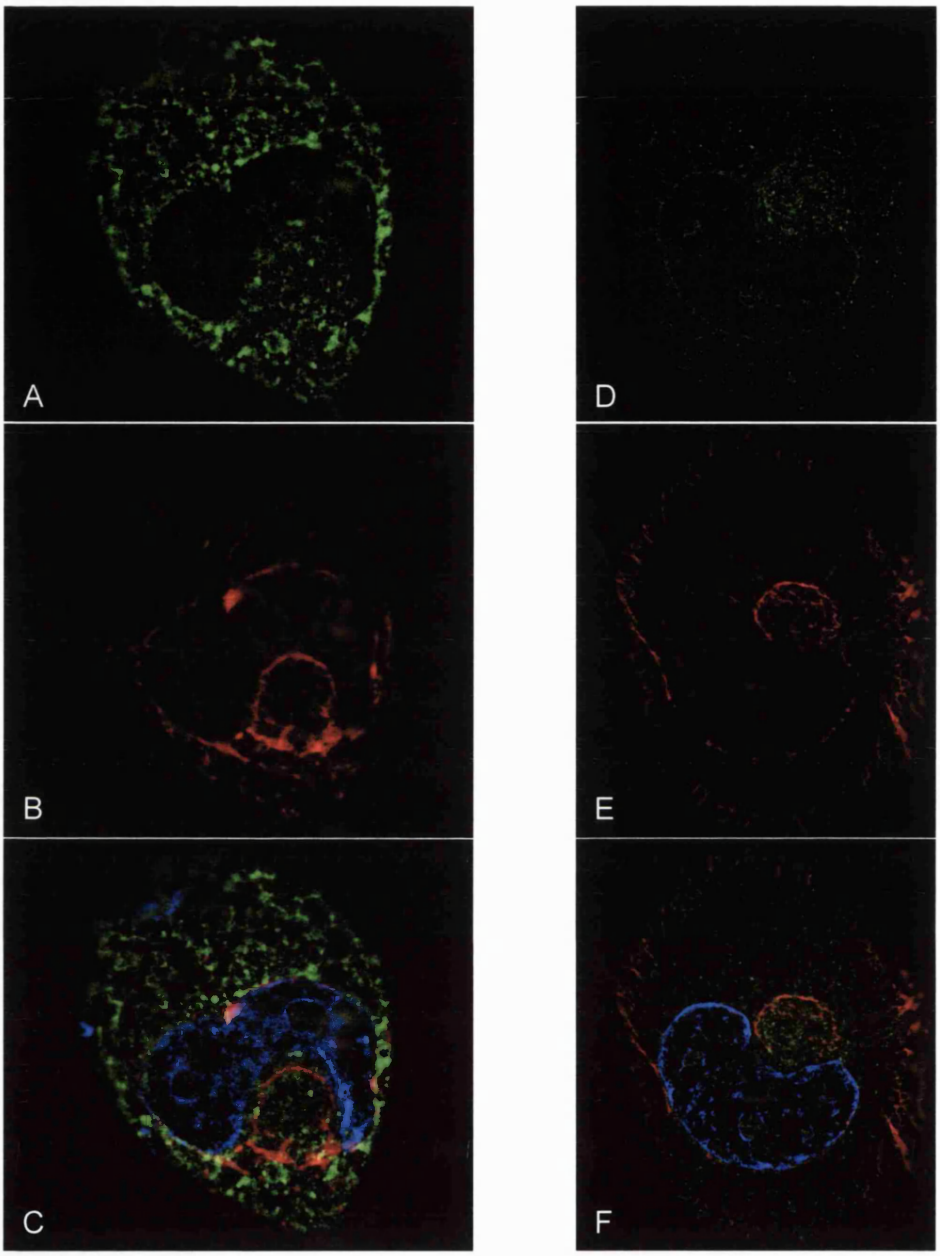

Figure 6.2: The TCR δ-chain aggresomes caused the collapse of vimentin. A CHO cell line expressing the TCR δ-chain was incubated for 12 hours at 37°C with 25μM proteasome inhibitor, MG132. The cells were fixed with ice-cold methanol, permeabilised with 0.1% Triton X-100 and incubated with a rabbit antibody specific for the δ-chain (A,D) and a mouse monoclonal specific for vimentin (B,E). The proteins were visualised by using the Alexa Fluor 488 (green) anti-rabbit and 594 (red) anti-mouse IgG conjugates and then labelled with DAPI (blue). Cells were viewed at 60X and images captured as described in the materials and methods. The images were digitally deconvolved, using the Openlab system and the TCR δ-chain, vimentin and DNA distribution were digitally overlaid (C, F).

6.2.4 Distribution of ubiquitin in cells containing aggresomes.

Ubiquitination of misfolded proteins is a signal for the protein to be targeted to proteasomes for degradation. Two studies have shown strong labelling of aggresomes with ubiquitin (Johnston et al, 1998; García-Mata et al, 1999). The next stage was to determine whether ubiquitin was present in aggresomes containing TCR CD3 δ-subunit. Panel A of figure 6.3 shows an aggresome labelled with antibodies specific for CD3 δ-subunit and panel B shows the distribution of ubiquitin in the same cell. A digital overlay is shown in panel C. There was not total co-localisation of the two proteins as the aggresome site still has clear areas of red and green, although there was some co-localisation as seen by the overall hint of a yellow colour. This experiment has not demonstrated that the δ-subunit was ubiquitinated, only that the area of the aggresome contained ubiquitin. However, in very similar experiments Yang et al (1998) showed, by immunoprecipitation and immunoblots, that the δ-subunit was ubiquitinated in cells incubated with MG132. In conclusion, the above experiments demonstrated that it is possible to produce aggresomes in CHO cells, with characteristics similar to those reported in the literature for blocked CFTR degradation (Johnston et al, 1998; Wigley et al, 1999; García-Mata et al, 1999).

6.3 Characterisation of aggresomes formed by the overexpression of protein chimera GFP-250.

6.3.1 Introduction.

A second means of producing aggresomes has been described (García-Mata et al, 1999), whereby overexpression of a cytosolic protein chimera (GFP-

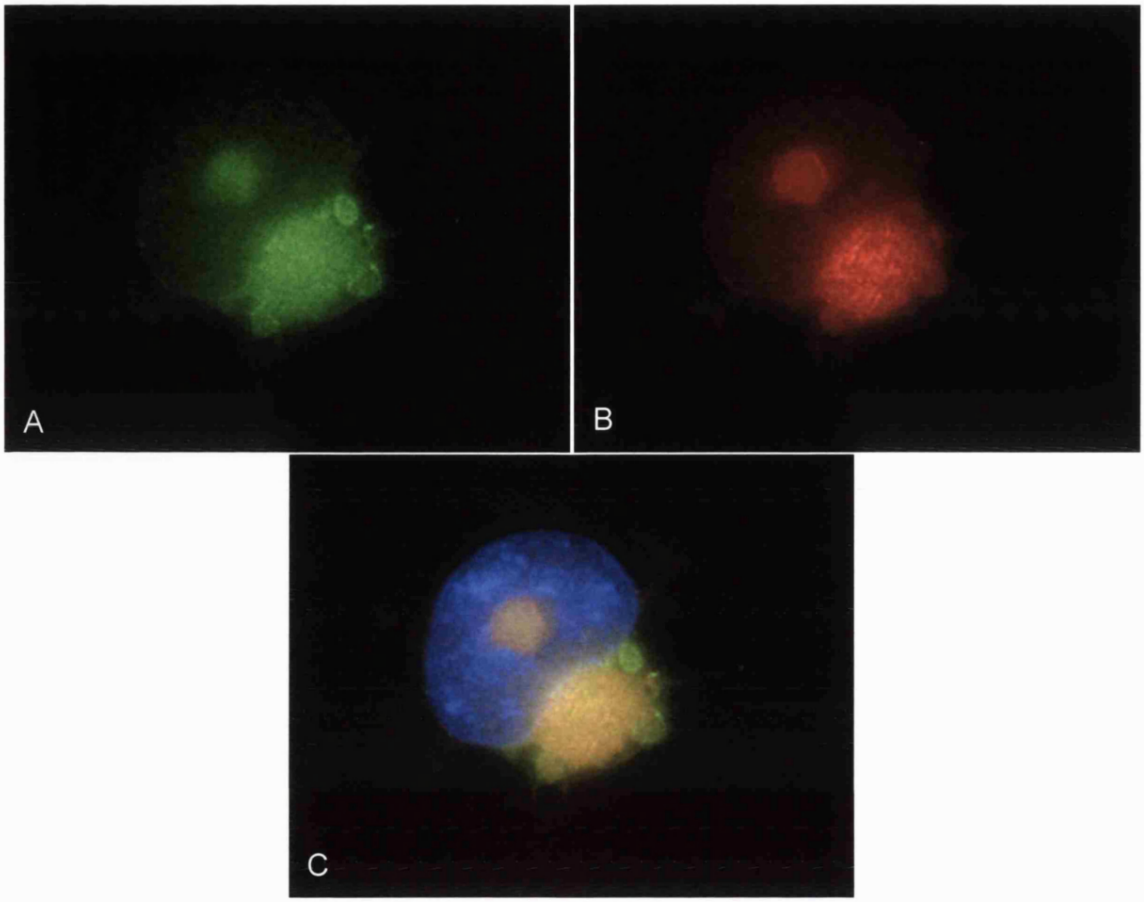

Figure 6.3: TCR CD3 δ-chain aggresomes were ubiquitinated. A CHO cell line expressing the TCR CD3 δ-chain was incubated for 12 hours at 37°C in the presence of the proteasome inhibitor, MG132. The cells were fixed with ice-cold methanol, permeabilised with 0.1% Triton X-100 and incubated with the mouse monoclonal antibody specific for the TCR CD3 δ-chain (A) and a rabbit antibody specific for ubiquitin (B). The distribution of the proteins was visualised by using the Alexa Fluor 488 (green) anti-mouse and 594 (red) anti-rabbit IgG conjugates and then labelled with DAPI (blue). Cells were viewed at 60X and images captured as described in the materials and methods. The images were digitally deconvolved, using the Openlab system and the TCR CD3 δ-chain, ubiquitin and cellular DNA distribution were digitally overlaid (C).

250) produces aggresomes without the need for proteasome inhibition. The GFP-250 chimera protein is composed of the entire GFP protein fused at its C-terminus to a 250 amino acid fragment of the cytosolic protein, p115. A cDNA encoding the chimera was obtained from Elizabeth Sztul (University of Alabama, Birmingham, AL. USA). The first stage of the investigation was to express the GFP-250 construct in a cell line susceptible to ASF infection.

6.3.2 Generation of aggresomes containing GFP-250.

Vero cells grown on coverslips to 70% confluency were transfected transiently with the plasmid encoding the GFP-250 chimera using the liposomal "Transfast" transfection system (Promega, UK), as described in the materials and methods, for 48 hours. The cells were fixed, permeabilised and then stained with DAPI. Figure 6.4 shows the formation of an aggresome by the over expression of the GFP-250 protein chimera. Panel A shows that the majority of the GFP-250 protein localised to a large juxtanuclear area, with the remainder of the protein being distributed throughout the cytoplasm as small granules. García-Mata et al (1999) used time-lapse imaging techniques in living cells to follow the formation of aggresomes. They showed that small aggregates formed at the periphery of the cell and then moved to the MTOC forming the aggresome. The cytoplasmic granules visualised in panel A were probably small aggregates of GFP-250, which had not yet been translocated to the aggresome. Panels B and C show that the aggresome was impinging on the nucleus. This experiment demonstrated that aggresomes could be produced in Vero cells, cells permissive for infection by ASFV.

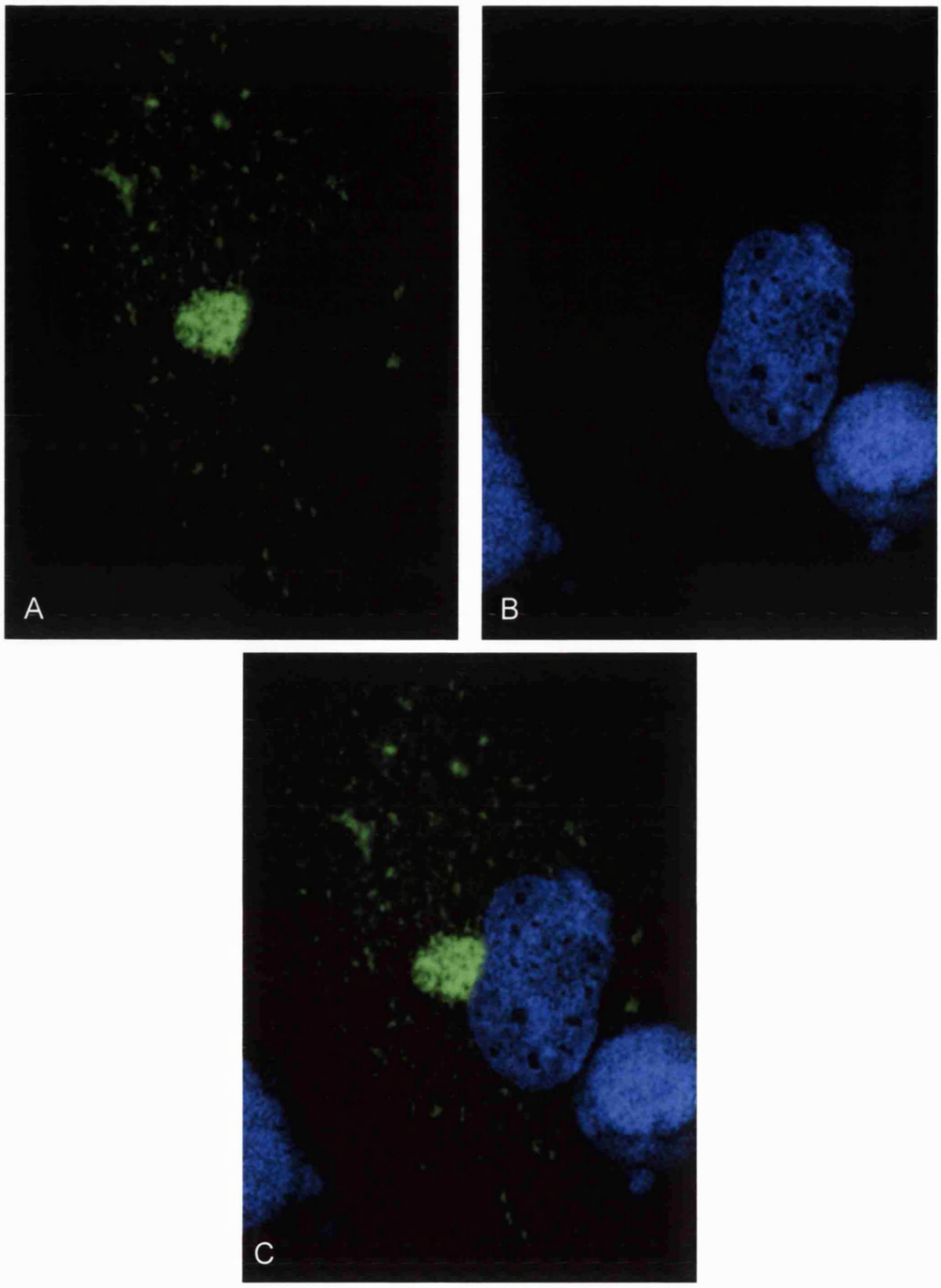

Figure 6.4: The overexpression of the GFP-250 protein chimera led to aggresome formation. Vero cells were transfected with the GFP-250 plasmid (A) and grown at 37°C for 48 hours. The cells were fixed with ice-cold methanol, permeabilised with 0.1% Triton X-100 and labelled with DAPI (blue) (B). Cells were viewed at 60X and images captured as described in the materials and methods. The images were digitally deconvolved, using the Openlab system and the GFP-250 protein and cellular DNA distribution were digitally overlaid (C).

6.3.3 Distribution of vimentin in cells containing aggresomes.

In the next experiment the arrangement of the vimentin filaments in Vero cells was studied. Panels A and D of figure 6.5 show two different large perinuclear aggresomes, with panel A also showing smaller aggregates in the cytoplasm. The distribution of vimentin is shown in panels B and E, and the vimentin filaments had collapsed around the site of the aggresome, forming a ring-like structure. In panel B some of the vimentin filaments had also collapsed around some of the smaller aggregates present in the cytoplasm. The digital overlays showed that the aggresomes were surrounded by the vimentin and that they were located at a perinuclear site.

6.3.4 The GFP-250 protein chimera forms aggresomes at the MTOC.

The published literature (Johnston et al, 1998; García-Mata et al, 1999; Wigley et al, 1999) has shown that aggresomes form at the microtubule organising centre (MTOC), so the next experiment was to locate the MTOC using a monoclonal antibody specific for γ-tubulin, an established marker for the MTOC. Panels A and B of figure 6.6 compare the distribution of γ-tubulin and GFP-250 in the same cell and panel C shows a digital merge of these two images. All the panels contain an insert showing a higher magnification view of the aggresome. The γ-tubulin antibody stained two bright spots representative of the centrioles, surrounded by a diffuse staining in the area of the aggresome and then a weaker cytoplasmic stain. The diffuse γ-tubulin staining in the area of the aggresome may have been caused by some disruption of the MTOC by the aggresome, as already described by Johnston et al (1998). Panel C shows a merge of the GFP-250 and γ-tubulin fluorescence, with a DAPI stain, and it can clearly be seen,

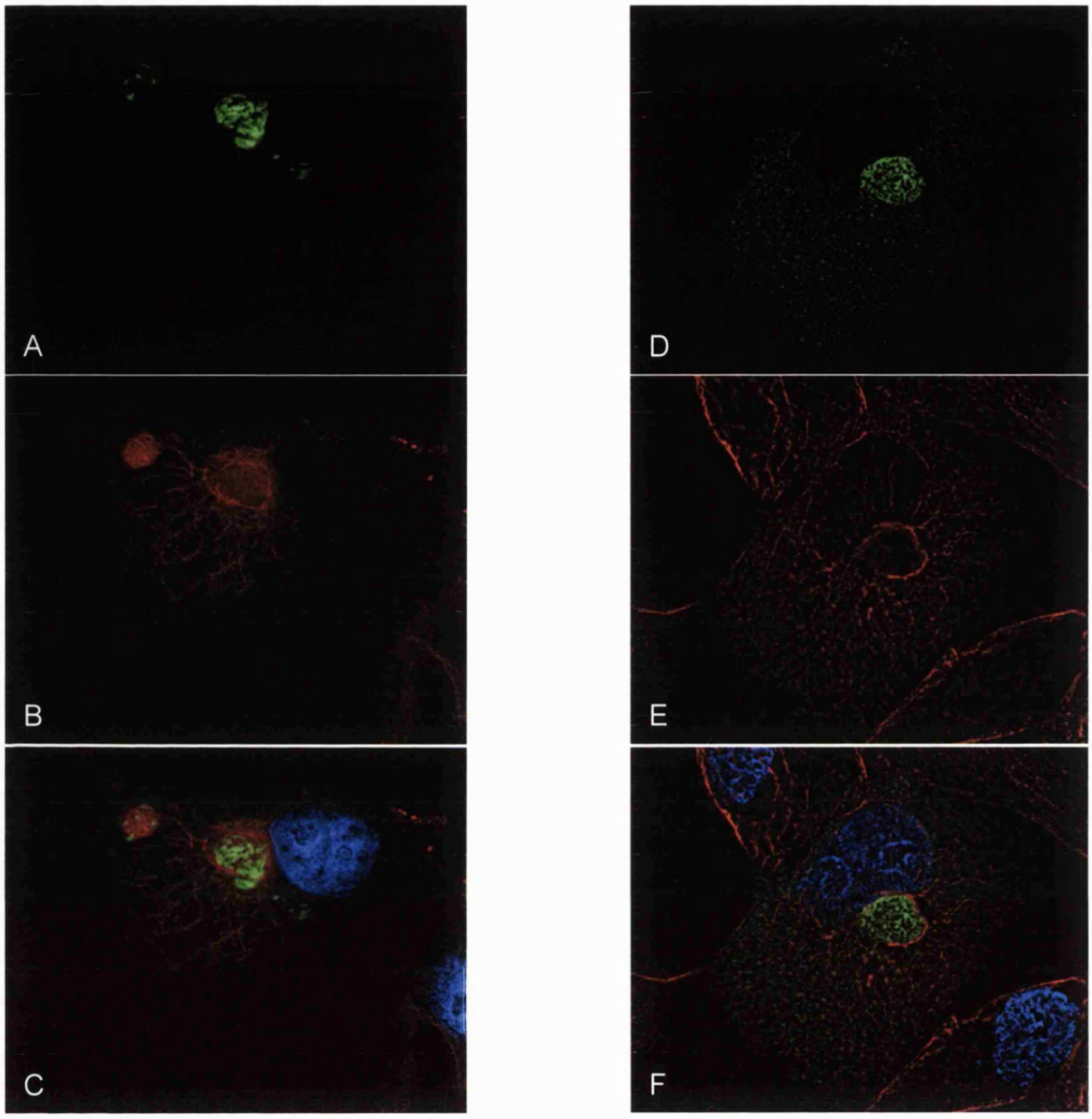

Figure 6.5: The GFP-250 aggresomes caused the collapse of the vimentin filaments. Vero cells were transfected with the GFP-250 plasmid (A,D) and grown at 37°C for 48 hours. The cells were fixed with ice-cold methanol, permeabilised with 0.1% Triton X-100 and incubated with a mouse antibody specific for vimentin (B, E). The distribution of the vimentin was visualised by using the Alexa Fluor 594 (red) anti-mouse IgG conjugate and the DNA was labelled with DAPI (blue). Cells were viewed at 60X and images captured as described in the materials and methods. The images were digitally deconvolved, using the Openlab system and the GFP-250 protein, vimentin and cellular DNA distribution were digitally overlaid (C, F).

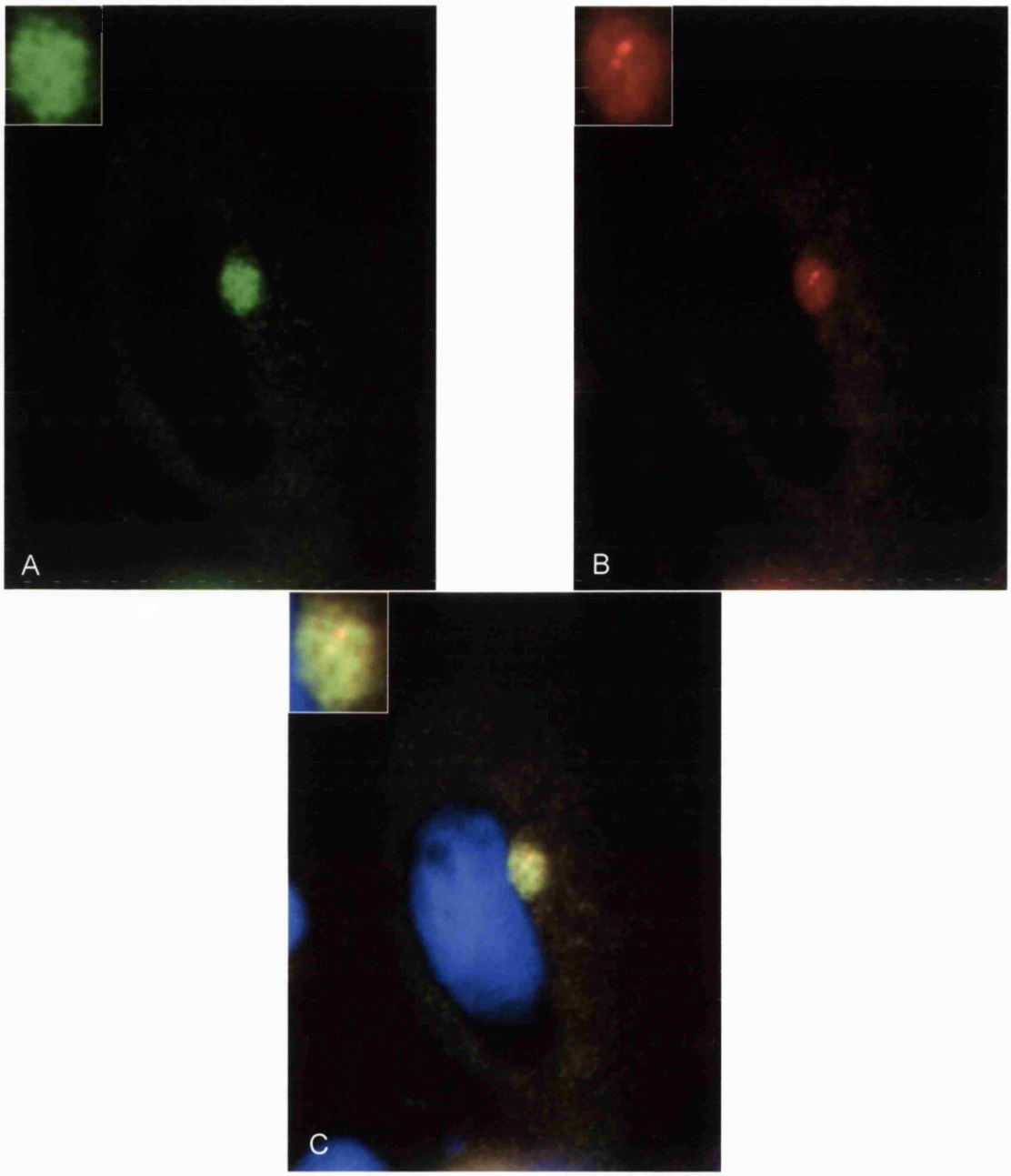

Figure 6.6: The GFP-250 aggresomes associated with the MTOC. Vero cells were transfected with the GFP-250 plasmid (A) and grown at 37°C for 48 hours. The cells were fixed with ice-cold methanol, permeabilised with 0.1% Triton X-100 and the MTOC was labelled with a mouse antibody specific for γ-tubulin (B). The MTOC was visualised by using the Alexa Fluor 594 (red) anti-mouse IgG conjugate and the DNA was labelled with DAPI (blue). Cells were viewed at 60X and images captured as described in the materials and methods. The images were digitally deconvolved, using the Openlab system and the GFP-250 protein, the site of the MTOC and cellular DNA distribution were digitally overlaid (C).

especially in the insert, that the GFP-250 aggresome was found situated at the MTOC.

6.3.5 Distribution of mitochondria in cells containing aggresomes.

Electron microscopy has shown that mitochondria, electron lucent vesicles and multi-vesicular bodies are trapped at the periphery of the filamentous meshwork of vimentin around the aggresome (Johnston et al, 1998; García-Mata et al, 1999). The distribution of the mitochondria in Vero cells over expressing the GFP-250 protein chimera was studied using the Mito-Tracker Red CMXRos. Mito-Tracker Red CMXRos is a dye selectively taken up by mitochondria. Figure 6.7 shows the distribution of mitochondria in the cells. The two cells on the left did not contain aggresomes, in these cells the mitochondria were seen around the nucleus and throughout the cytoplasm extending to the periphery of the cells. In the cell expressing GFP-250 and generating an aggresome the mitochondria were no longer found throughout the cytoplasm, but had clustered to the area of the aggresome (Panel C).

6.3.6 Distribution of cytosolic chaperones in cells containing aggresomes.

Since previous studies had shown that the aggresomes contain proteins involved in the protein folding and degradation pathways (Johnston et al, 1998; García-Mata et al, 1999; Wigley et al, 1999), the distribution of three chaperone families in cells over-expressing the GFP-250 chimera was studied. The first protein that was investigated was Hdj-2, which is a member of the Hsp40 family and the human homolgue of the prokaryote DNAJ protein (Chellaiah et al, 1993). Hdj-2 is a family of cochaperones that regulate the activity of Hsp70 proteins (Cyr

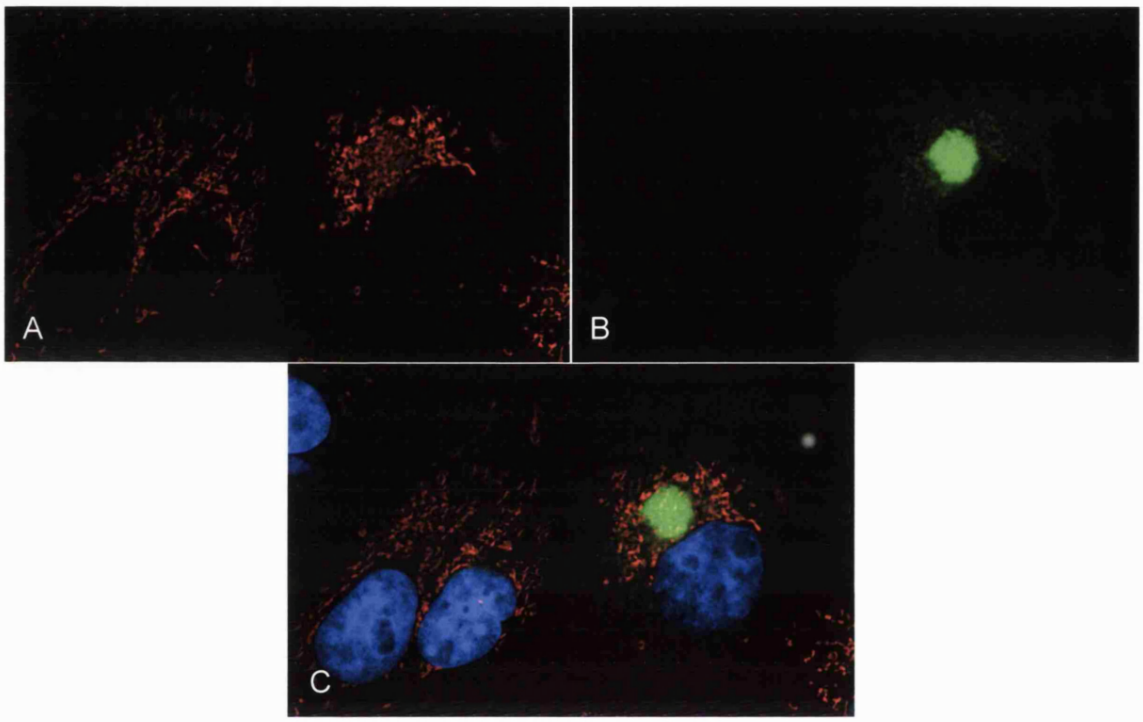

Figure 6.7: Mitochondria clustered around the GFP-250 aggresomes. Vero cells were transfected with the GFP-250 plasmid (A) and grown at 37°C for 48 hours and then incubated at 37°C for 15 minutes with 200nM Mito-Tracker Red CMXRos, a fluorescent marker for mitochondria (B). The cells were washed in PBS and fixed with 4% paraformaldehyde, permeabilised with 0.1% Triton X-100 and incubated with DAPI (blue). Cells were viewed at 60X and images captured as described in the materials and methods. The images were digitally deconvolved, using the Openlab system. GFP250, mitochondria, and DAPI (C) were digitally overlaid.

et al, 1994). Many of these chaperones are important for maintaining proteins in an unfolded state so that they can translocate through subcellular membranes or be correctly folded by the GroEL and GroES proteins (Langer et al, 1992; Feldman and Frydman, 2000). The cellular location of the Hdj-2 chaperone varies on the conditions the cells are grown in. In cells grown at 37°C Hdj-2 is located mainly to the cytoplasm with a weak staining at the nuclear membrane. The chaperone redistributes in cells heat shocked at 45°C producing intense staining of the Golgi complex, nuclear membrane and nucleolus (Davis et al, 1998). The second chaperone investigated was the constitutively expressed Hsc70 protein, a member of the Hsp70 chaperone family. The Hsp70 family are a highly conserved ubiquitous group of proteins that are involved in the prevention of aggregation of unfolded polypeptides and the disassembly of multimeric complexes (Miao et al, 1997). The final protein investigated was TCP-1, a member of the cytosolic chaperonin family. These cytosolic chaperonins have a double ring structure, ATPase activity and have a role primarily in the folding of actin and tubulin (Kubota and Willison, 1997). Vero cells were transfected with GFP-250, fixed and permeabilised, and incubated with monoclonal antibodies specific for the indicated chaperones. Panels A, C and E of figure 6.8 show the location of the GFP-250 aggresome at a perinuclear site, panels B, D and F show the distribution of Hdj-2, Hsc70 and TCP-1 chaperones respectively. The Hdj-2 protein was distributed throughout the cytoplasm of the cell, but the majority of the protein accumulated at a perinuclear location (panel B), which directly co-localised with the aggresome (panel A). The distribution of the Hsp70 protein was throughout the cytoplasm with a large quantity of the protein found in a spherical perinuclear region (panel D), which co-localised

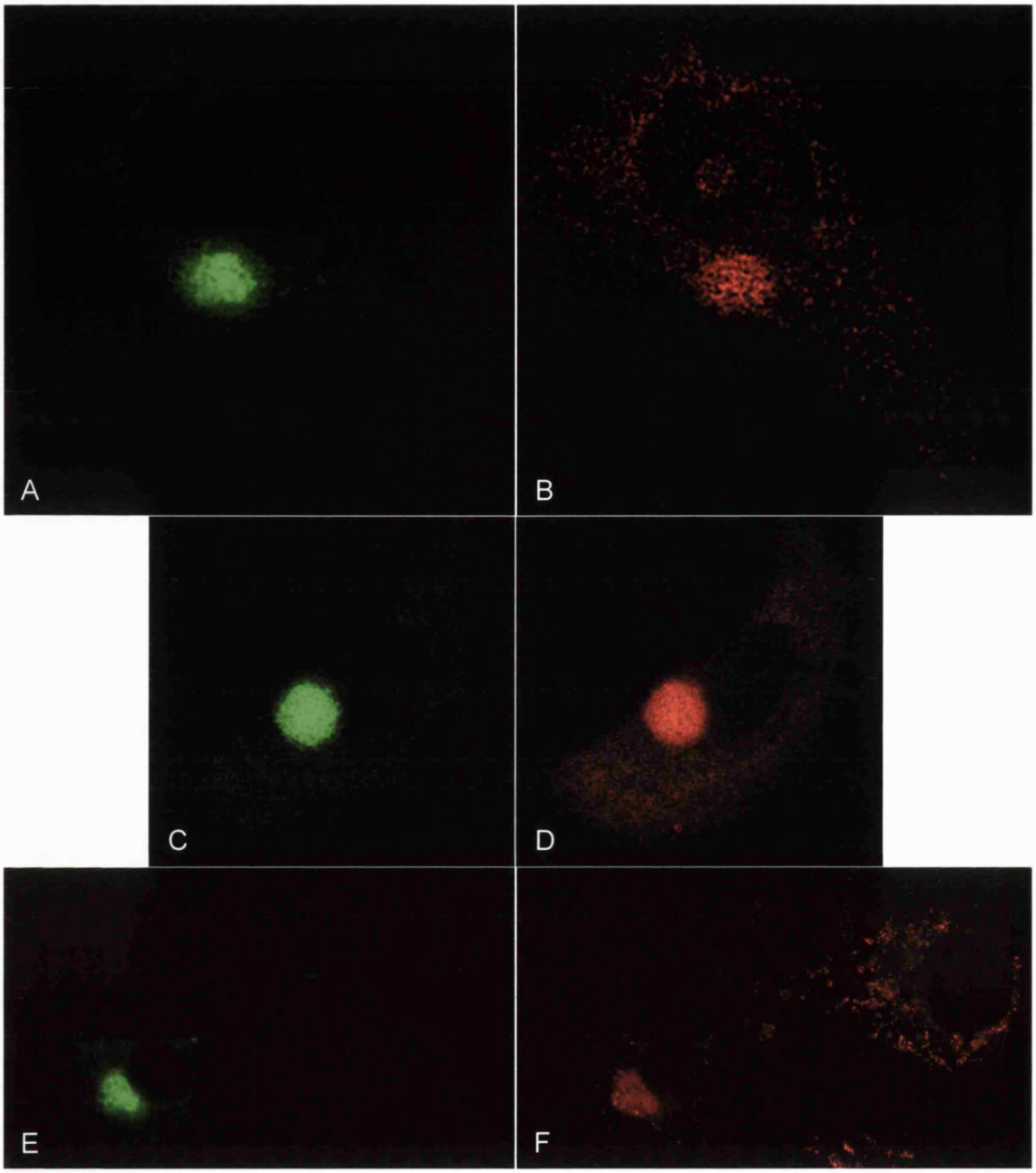

Figure 6.8: Cytosolic chaperones were co-localised with the aggresomes. Vero cells were transfected with the GFP-250 plasmid (A,C,E) and grown at 37°C for 48 hours and then fixed with ice-cold methanol, permeabilised with 0.1% Triton X-100 and incubated with either a mouse monoclonal antibody specific for Hdj-2 (B), a mouse monoclonal specific for Hsc70 (D) or a rat monoclonal specific for TCP-1 (F). The distribution of the proteins was visualised by using the Alexa Fluor 594 (red) IgG conjugates. Cells were viewed at 60X and images captured as described in the materials and methods. The images were digitally deconvolved, using the Openlab system.

directly with the aggresome (panel C). Panel F shows two cells, TCP-1 in the untransfected cell produced a diffuse cytoplasmic stain with small granule-like structures, as described by Lewis et al (1992). The cell that contained the GFP-250 aggresome (panel E), had lost the diffuse cytoplasmic stain and small granular structures of TCP-1, and instead had formed a pool of the protein at a perinuclear site (panel F) that co-localised with the aggresome. So, all three families of chaperones co-localised directly with aggresomes labelled with the GFP-250 protein chimera.

6.3.7 Distribution of ubiquitin in cells containing aggresomes.

It was shown above that aggresomes formed following proteasome inhibition contained ubiquitin. The next experiment investigated the ubiquitination of the GFP-250 aggresome formed in the absence of proteasome inhibition. Panels A and B of figure 6.9 compare the distribution of the GFP-250 chimera and ubiquitin. The subcellular distribution of ubiquitin was similar to the GFP-250 protein suggesting that the aggresomes contained ubiquitinated protein. Interestingly, García-Mata et al (1999) used immunoblot analysis to show that the GFP-250 protein was not ubiquitinated. So the fluorescence signal seen in the figure 6.9 may represent ubiquitination of other proteins present in the aggresome.

6.4 Summary of the production of aggresomes in an ASFV susceptible cell line.

The above sections have used the expression of a single subunit of the T-cell receptor and proteasome inhibition, or the overexpression of a protein

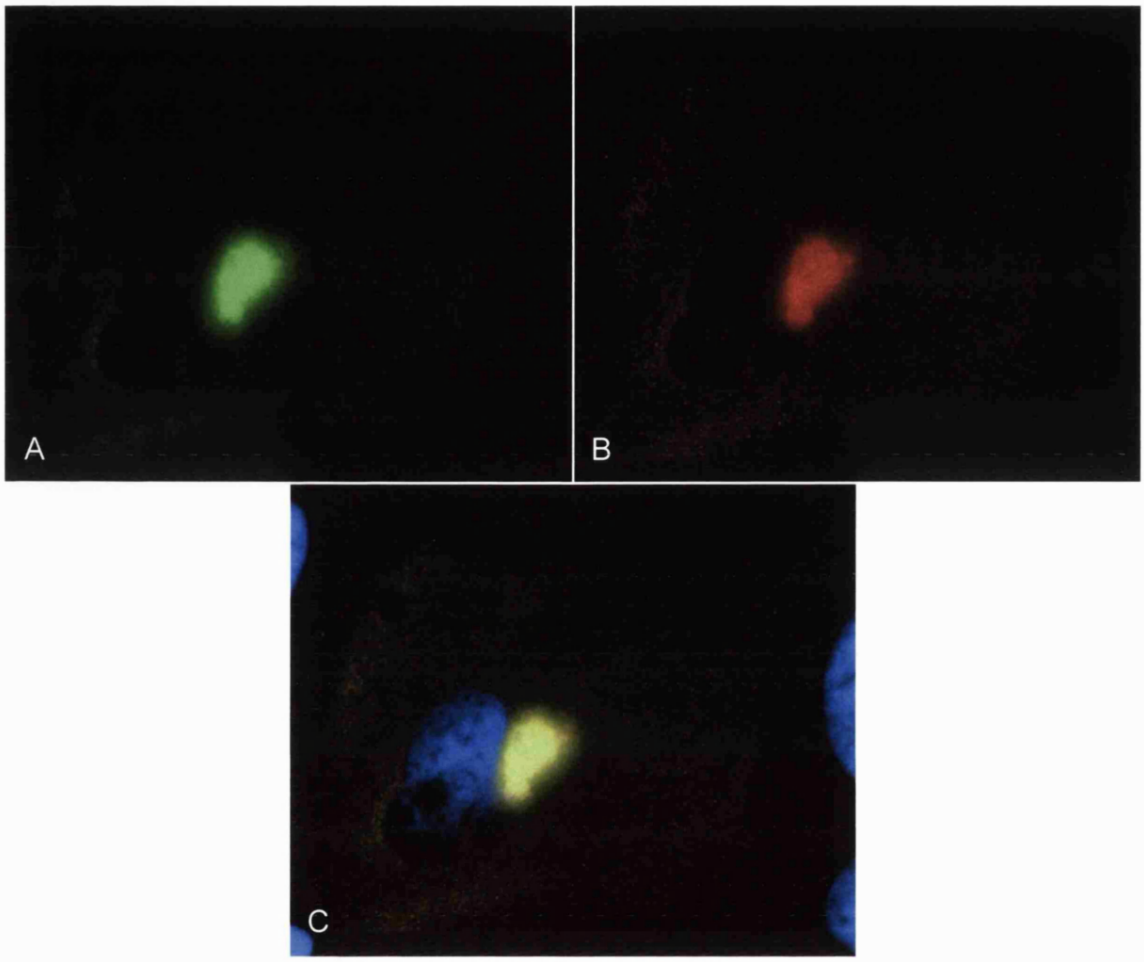

Figure 6.9: The area of the GFP-250 aggresomes was highly ubiquitinated. Vero cells were transfected with the GFP-250 plasmid (A) and grown at 37°C for 48 hours and then fixed with ice-cold methanol, permeabilised with 0.1% Triton X-100 and incubated with a rabbit antibody specific for ubiquitin (B). The distribution of the ubiquitin was visualised by using the Alexa Fluor 594 (red) IgG conjugate. Cells were viewed at 60X and images captured as described in the materials and methods. The images were digitally deconvolved, using the Openlab system. The GFP-250 aggresome, ubiquitin and cellular DNA were digitally overlaid (C).

chimera to generate aggresomes. In the first, inhibition of degradation of the δ-subunit of the T-cell receptor produced large aggresomes, which were not as well defined as those described in the literature (Johnston et al, 1998; García-Mata et al, 1999; Wigley et al, 1999). These aggresomes formed at a perinuclear location that impinged on the nucleus and consisted of a collection of small structures, most likely aggregates of the protein. The aggresome was surrounded by a cage of vimentin and also co-localised with ubiquitin.

The over expression of the GFP-250 protein chimera generated aggresomes similar to those described by García-Mata et al (1999). The aggresome was located at the MTOC, enclosed by a vimentin cage and surrounded by a cluster of mitochondria, and was enriched for host chaperones and ubiquitin.

The results showed that it was possible to generate aggresomes in cells susceptible to ASFV infection. The next stage of the investigation was to see if the ASF viral factories had similar morphological features to aggresomes.

6.5 ASFV viral factories have similar morphology to aggresomes.

6.5.1 Distribution of vimentin in ASFV infected cells.

The first experiment investigated the distribution of vimentin in Vero cells infected with BA71v. Viral factories were identified through strong staining for the viral structural protein, p34, in panels A and D of figure 6.10, while panels B and E show the distribution of vimentin. ASFV produced a striking effect on vimentin and as seen for the aggresomes, vimentin collapsed to form a ring structure, but this time surrounding the viral factories. The cells that were negative for p34, and therefore not infected with ASFV, contained long filamentous, mesh-like fibres

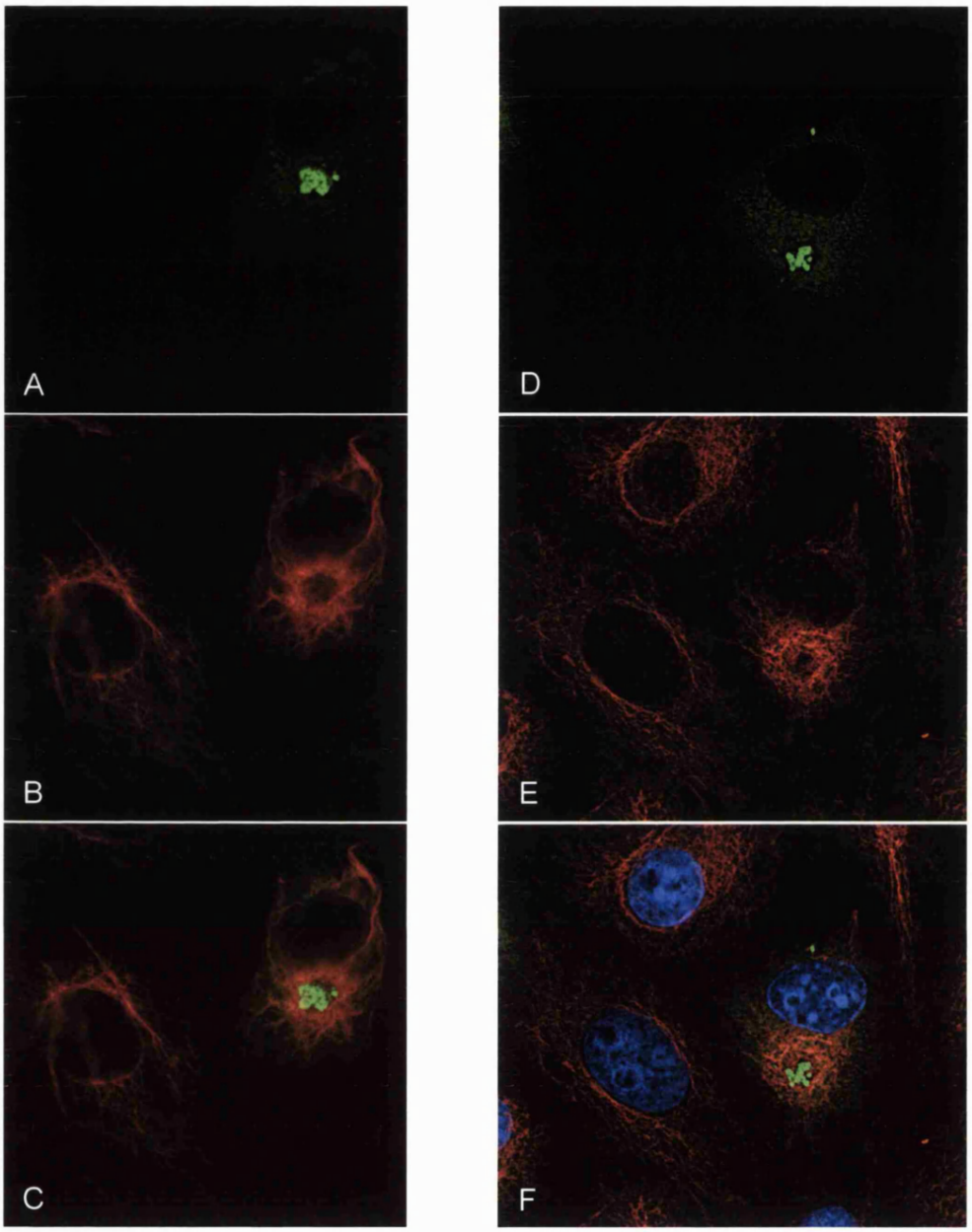

Figure 6.10: ASFV infection caused a reorganisation of vimentin. At 12 hours after infection with BA71v, Vero cells were fixed with ice-cold methanol, permeabilised with 0.1% Triton X-100 and incubated with the rabbit antibody specific for p34 (A,D) and a mouse monoclonal antibody specific for vimentin (B,E). The distribution of the proteins was visualised by using the Alexa Fluor 488 (green) anti-rabbit and 594 (red) anti-mouse IgG conjugates. The cellular and viral DNA was labelled with DAPI (blue). Cells were viewed at 60X and images captured as described in the materials and methods. The images were digitally deconvolved, using the Openlab system and p34 and vimentin (C) and DAPI (F) were digitally overlaid.

extending to the periphery of the cells. The digital overlays shown in panels C and F show that the vimentin had not only collapsed around the viral factories, but had also retracted from the periphery of infected cells. The outline of infected cells was revealed by the weak staining of the cytoplasm with the antibody specific for p34.

6.5.2 The viral factories are found in the area of the MTOC.

The next experiment compared the location of the viral factories and the MTOC. Vero cells infected for 12 hours with BA71v were fixed and permeabilised and incubated with a monoclonal antibody specific for γ-tubulin. Viral factories were again detected using the antibody raised against p34. Panel A of figure 6.11 displays the typical staining of the viral factory and cytoplasm by the antibody specific for p34, panel B shows the staining of the two centrioles of the MTOC and a faint cytoplasmic staining, and panel C is a digital merge of panels A and C with cellular and viral DNA stained with DAPI. All three panels contain an insert depicting a higher magnification view of the viral factory and MTOC. Figure 6.11 was representative of many cells viewed and clearly demonstrates that the assembly site of ASFV is located in the area of the MTOC.

6.5.3 Distribution of mitochondria in ASFV infected cells.

The distribution of mitochondria in cells infected with ASFV was explored by incubation with Mito-Tracker Red CMXRos as described above. Viral factories were visualised with the antibody specific for p34. Panels A and B of figure 6.12 compare the distribution of mitochondria and viral assembly sites in the same cells. Panel D shows an uninfected cell stained with the Mito-Tracker and DAPI

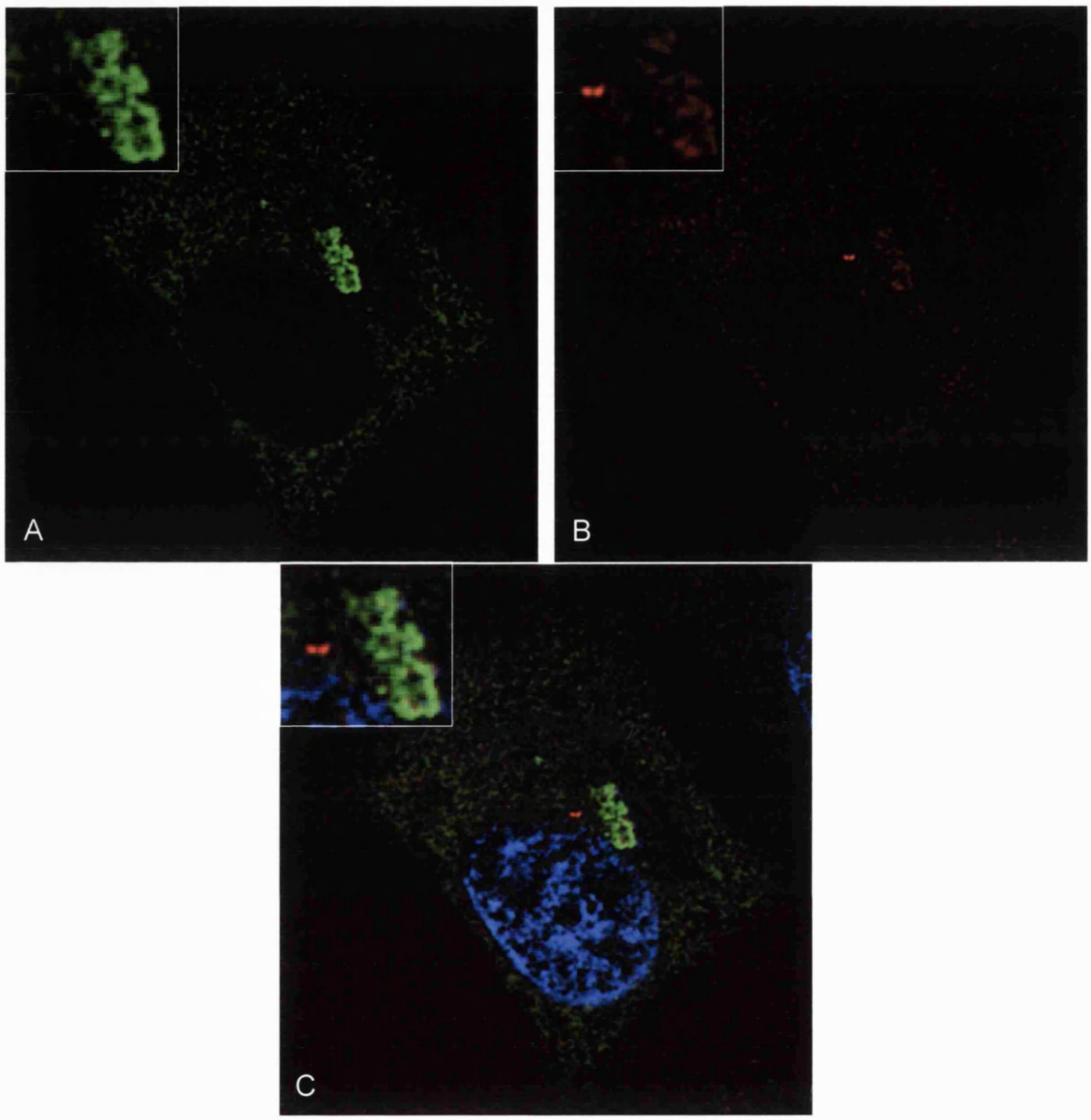

Figure 6.11: ASF viral factories were located near the MTOC. At 12 hours after infection with BA71v, Vero cells were fixed with ice-cold methanol, permeabilised with 0.1% Triton X-100 and incubated with the rabbit antibody specific for p34 (A) and a mouse monoclonal antibody specific for γ-tubulin (B). The distribution of the proteins was visualised by using the Alexa Fluor 488 (green) anti-rabbit and 594 (red) anti-mouse IgG conjugates. The cellular and viral DNA was labelled with DAPI (blue). Cells were viewed at 60X and images captured as described in the materials and methods. The images were digitally deconvolved, using the Openlab system and p34, γ-tubulin, and DAPI were digitally overlaid (C). The inserts were a digital enlargement of the viral factory and the MTOC.

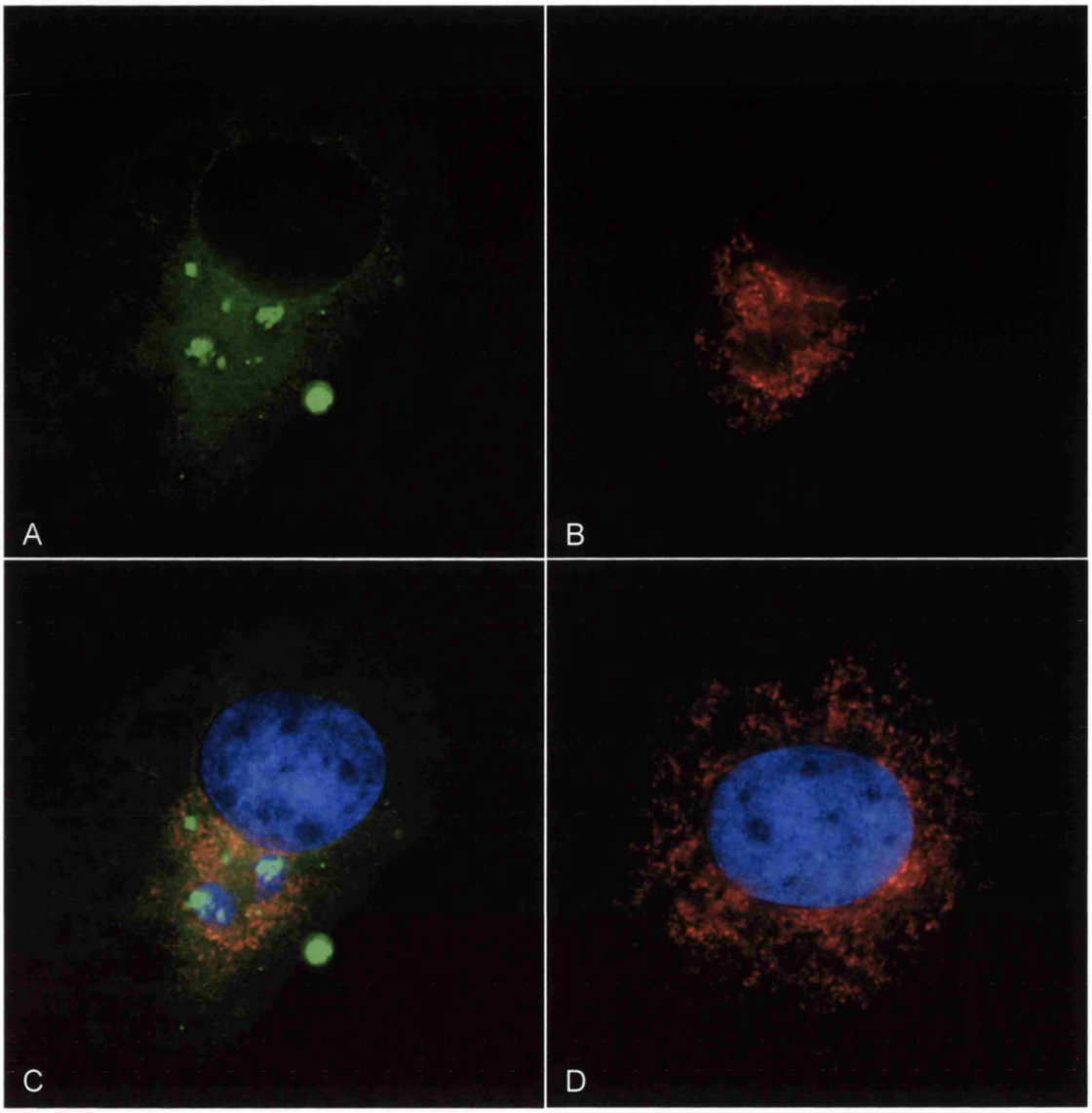

Figure 6.12: Mitochondria clustered around the viral factory. At 12 hours after infection with BA71v, Vero cells were incubated at 37°C for 15 minutes with 200nM Mito-Tracker Red chloromethyl derivatives of X rosamine, a fluorescent marker for mitochondria (B,D). The cells were washed in PBS and fixed with 4% paraformaldehyde, permeabilised with 0.1% Triton X-100 and incubated with the rabbit antibody specific for p34 (A). The distribution of the proteins was visualised using the Alexa Fluor 488 (green) anti-rabbit IgG conjugate. The cellular and viral DNA was labelled with DAPI (blue). Cells were viewed at 60X and images captured as described in the materials and methods. The images were digitally deconvolved, using the Openlab system. p34, mitochondria, and DAPI (C) were digitally overlaid and panel D shows the distribution of mitochondria and the nucleus in an uninfected cell.

for comparison. In the uninfected cell (Panel D) the mitochondria were seen throughout the cytosol radiating out from a perinuclear location. A comparison of panels A and B showed that mitochondria clustered around the viral factory, however, the digital overlay (Panel C) showed there was no direct co-localisation of the ASFV p34 structural protein with the mitochondria.

6.5.4 Distribution of cytosolic chaperones in ASFV infected cells.

The next experiments determined the distribution of chaperones in cells infected with ASFV. In each case ASFV infected Vero cells were grown at 37°C and observed 12 hours later. The cells were fixed and permeabilised and the cells were labelled with the antibody specific for p34 and the monoclonal antibodies raised against the chaperones Hdj-2, Hsp70 and TCP-1. Each image compares infected and uninfected cells Panels A, C and E on the left of figure 6.13 show cells labelled for the ASFV structural protein, p34. Panels B, D and F show cells labelled for the Hdj-2, Hsp70 and TCP-1 chaperones respectively. In each case the antibody specific for p34 strongly stained the viral factory, but surprisingly the antibodies specific for the various chaperones had very different distributions. The Hdj-2 protein (panel B) was distributed throughout the cytoplasm and had a similar stain in both uninfected and infected cells and showed no redistribution to the viral factories. The Hsp70 protein was largely cytoplasmic in uninfected cells (panel D), where as in the infected cell (top right, panel D) there was a limited redistribution to the viral factories. The chaperonin TCP-1 (panel F) produced a diffuse cytoplasmic stain with small granule-like structures throughout the cytoplasm in uninfected cells, as previously described above and by Lewis et al (1992). In the infected cell the faint cytoplasmic

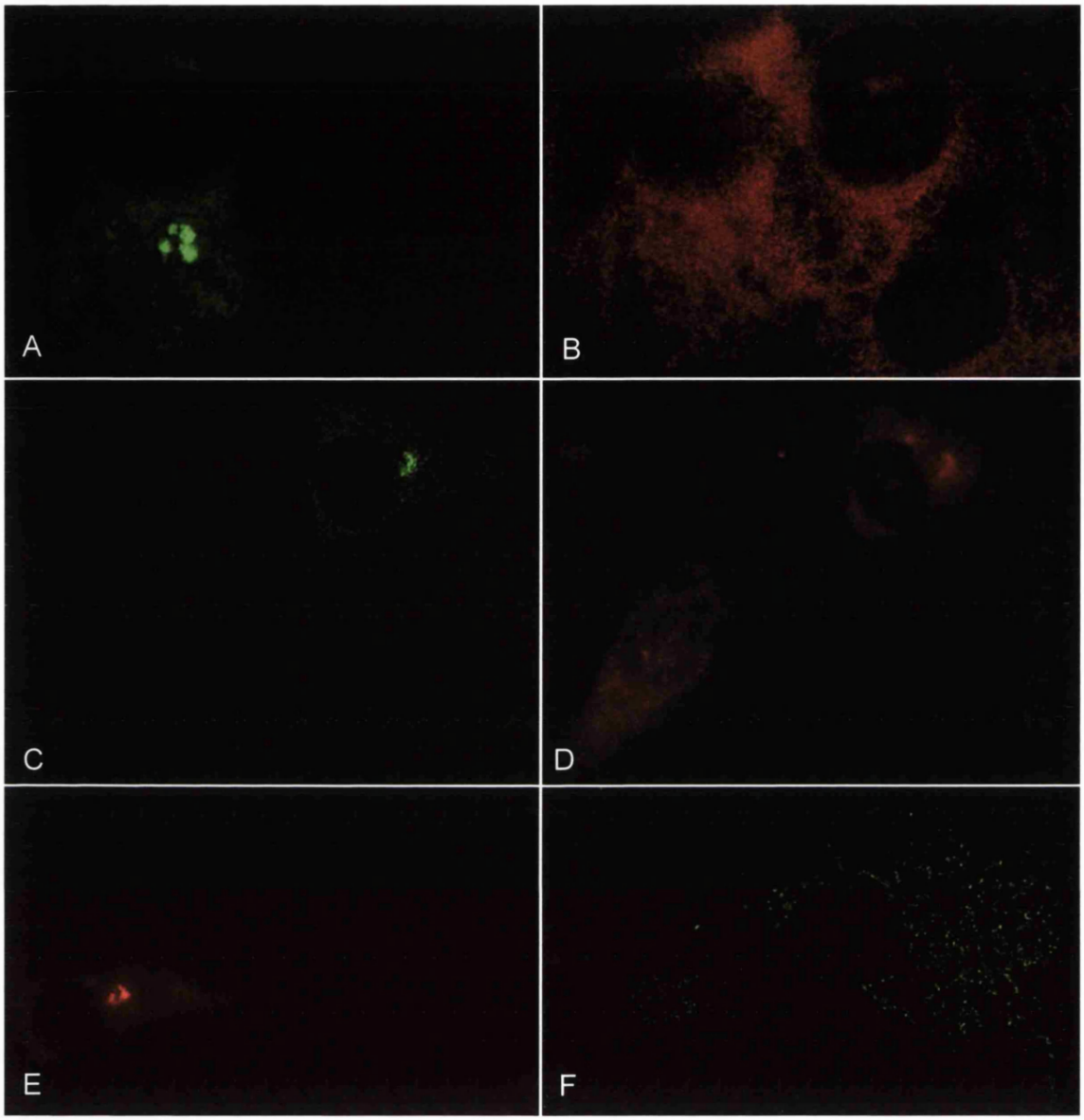

Figure 6.13: The distribution of cytosolic chaperones in infected cells. At 12 hours after infection with BA71v, Vero cells were fixed with ice-cold methanol, permeabilised with 0.1% Triton X-100 and incubated with the rabbit antibody specific for p34 (A, C, E) and either a mouse monoclonal antibody specific for Hdj-2 (B), a mouse monoclonal specific for Hsp70 (D) or a rat monoclonal specific for TCP-1 (F). The distribution of the proteins was visualised by using the Alexa Fluor 488 (green) and 594 (red) IgG conjugates. Cells were viewed at 60X and images captured as described in the materials and methods. The images were digitally deconvolved, using the Openlab system.

staining was still present, however, the small granule-like structures had redistributed to the area of the viral factory. In summary, the DNAJ homologue, Hdj-2, did not redistribute to the viral factories, where as the Hsp70 chaperone co-localised with the p34 protein in the viral factories and the chaperonin TCP-1 redistributed to a small area around the viral factory.

6.5.5 The integrity of the viral factories is dependent on the microtubule network.

Several studies have demonstrated that the microtubule network is required for the formation and integrity of aggresomes. In the next experiment nocodazole was used to disrupt microtubules in cells infected with ASFV. 10μg/ml nocodazole was added to cells 14 hours after infection, the cells were incubated for a further 2 hours and then fixed and permeabilised. Viral factories were localised using antibodies specific for p34 or p73, and microtubules were visualised using an antibody specific for α-tubulin. Panel B of figure 6.14 shows an untreated control cell containing the long filamentous fibres of the microtubule network and panel E shows the loss of fibres in cells incubated with nocodazole. The upper panels (panels A, B and C) of figure 6.14 show control cells infected with ASFV and stained with antibodies specific for p34 and α-tubulin. The factory/assembly site was compact and located over the viral DNA shown by the extranuclear DAPI staining (panel C). α-tubulin in these cells was localised to a filamentous network extending throughout the cell. The central panels (panels D, E, and F) show the effects of nocodazole. The drug caused the disassembly of microtubules (panel E) and the viral factory (panel D) and the viral DNA was less compact (panel F). The effect of nocodazole on the morphology of the viral factories was more clearly defined in the lower panels (panels G, H and I). In this

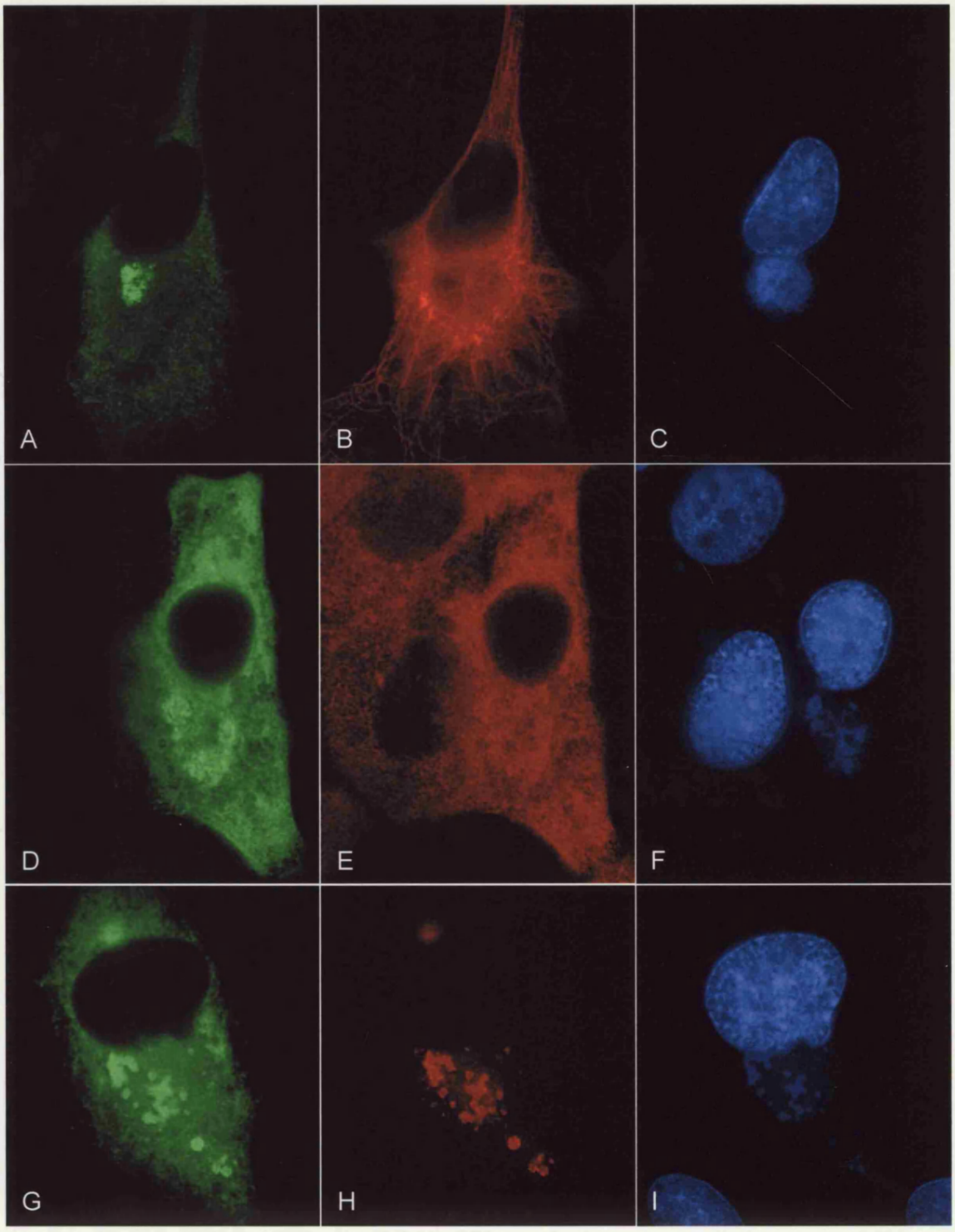

Figure 6.14: The disruption of the microtubule network affected the integrity of the viral factories. See over for figure legend

Figure 6.14 (legend): The disruption of the microtubule network affected the integrity of the viral factories. Vero cells were infected with BA71v for 14 hours and then 10μg/ml nocodazole (D-I) was added to the cells and incubated at 37°C for a further two hours, then fixed and permeabilised. Untreated cells are shown in panels A-C. The cells were then labelled with either the rabbit antibody raised against p34 (A, D) and the monoclonal mouse antibody raised against α-tubulin (B, E), or the rabbit antibody raised against p34 (G) and the mouse antibody specific for p73 (H). The proteins were visualised with the Alexa Fluor 488 (green) goat-α-rabbit and the Alexa Fluor 594 (red) goat-α-mouse IgG conjugates and the DNA was labelled with DAPI (blue) (C, F, I). Cells were viewed at 60X and images captured as described in the materials and methods. The images were digitally deconvolved using the Openlab system.

experiment the cell was stained with two different markers for viral factories, p34 in panel G, and p73 in panel H. The factory extends throughout the cytoplasm as does the viral DNA (panel I). In common with aggresomes, therefore, compact viral factory localisation was dependent on an intact microtubule network.

6.6 Summary of the comparison between aggresomes and factories.

The African swine fever viral factories shared several morphological features with aggresomes. The most striking change in cellular morphology, visualised with both the ASF viral factories and the aggresomes, was the collapse of vimentin to a mesh-like halo surrounding the viral factories or the aggresomes. The second common feature of the factories and aggresomes was their location at the microtubule organising centre. This was consistent with the observation that aggresomes and viral factories were both disrupted by nocodazole indicating a role for an intact microtubule network during their assembly in cells. Johnston et al (1998) and García-Mata et al (1999) proposed that the movement of aggregates along microtubules, in a minus end direction, would bring the particles into the area of the MTOC and be instrumental in forming the aggresomes. The experiments described here suggest a similar mechanism for the formation of viral factories. The third similarity was the clustering of mitochondria around the viral factories and aggresomes. Many of the proteins involved in protein folding and degradation pathways have a requirement for ATP, such as TCP-1 (Kubota and Willison, 1997), Hsp70 (Miao et al, 1997) and proteasomes (Varshavsky, 1997). The clustering of the mitochondria around these sites would provide ample energy for the folding and degradative pathways. It has been demonstrated recently that assembly of ASFV requires

ATP (Cobbold et al, 2000). The virus may use the microtubule/aggresome pathway to cluster mitochondria at assembly sites to provide this energy.

The major role of the aggresomes is to sequester misfolded or aggregated proteins to a subcellular location, where the cell can attempt to fold the proteins correctly or, if that fails, degrade them. The response of a cell to unfamiliar ASFV proteins may be to pass them into the aggresome pathway to attempt to fold or degrade them. This maybe beneficial to the virus as it would concentrate structural proteins at virus assembly sites. The preliminary data in figure 6.13 showed that Hsp70 and TCP-1 chaperones were found in viral factories, but the Hdj-2 chaperone showed no change in its distribution in infected cells. This was a surprising observation as the Hdj-2 chaperone, a member of the Hsp40 family, binds to Hsp70 and acts as a co-chaperone (Feldman and Frydman, 2000). In summary, the results suggest that African swine fever virus may be using aspects of the aggresome pathway to sequester viral structural proteins into a specialised subcellular location, which has a supply of energy and chaperones, which may aid with the assembly virions.

6.7 Investigation into the interaction between aggresomes and virus assembly.

6.7.1 Introduction.

The previous data in this chapter had demonstrated several similarities between aggresomes and African swine fever virus assembly sites. The next stage of the investigation was to determine the effects of producing aggresomes and viral factories in the same cells.

6.7.2 Effect of proteasome inhibition on the formation of ASF viral factories.

Inhibition of proteasomes was required for the formation of aggresomes containing TCR CD3 δ-subunit. Therefore, an initial experiment was carried out to determine the effects of the proteasome inhibitor, MG132, on the replication of the virus. Vero cells were infected for 1 hour, MG132 was added at 25μM and the cells were incubated for a further 15 hours at 37°C. The cells were fixed, permeabilised and labelled with antibodies specific for the early viral protein, vp30, and for the late structural protein, p73. Panels A and D of figure 6.15 compare the distribution of the major capsid protein, p73, in the absence or presence of the proteasome inhibitor respectively. Panels B and E show the distribution of the early viral protein, vp30, in the absence and presence of MG132, respectively. A comparison of panels B and E shows that the staining for the early viral protein was very similar, irrespective of the addition of MG132. By contrast the distribution of the late structural protein, p73, was markedly affected by MG132. The cells infected in the absence of the inhibitor show the familiar bright viral factory, decorated with individual virions, which were also found throughout the cytoplasm (panel A). In cells grown in the presence of MG132 (panel D), there was no labelling of viral factories with the antibody specific for p73. Virions were, however, seen around the edges of cell. These bright punctate spots were thought to be virions bound to the cell during the original infection that had not entered the cells. In addition to this, cells treated with MG132 and labelled with the antibody specific for p34, another late structural protein, showed no staining (data not shown). In conclusion, proteasome inhibition allows cells to be infected by ASFV, as seen by the production of the early protein vp30, but it blocks the production of late structural proteins, p73 and

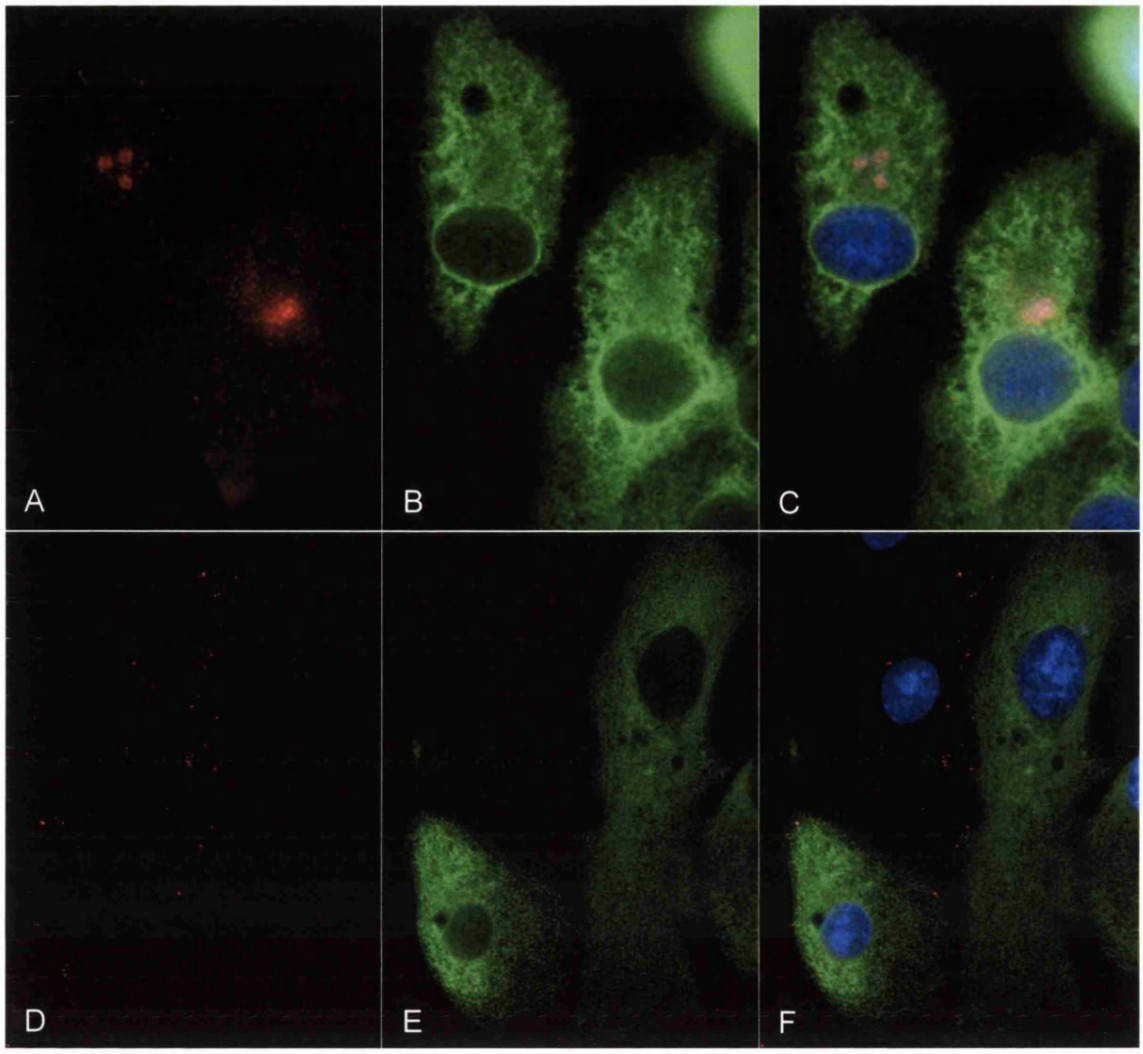

Figure 6.15: Proteasome inhibition blocked late viral protein synthesis. Vero cells were infected for 1 hour and then 25μM MG132, a potent proteasome inhibitor, was added and the cells incubated for 15 hours at 37°C. The cells were fixed with ice-cold methanol, permeabilised with 0.1% Triton X-100 and incubated with the rabbit antibody specific for p73 (A, D) and a mouse antibody specific for VP30 (B, E). The distribution of the proteins was visualised by using the Alexa Fluor 488 (green) anti-mouse and 594 (red) anti-rabbit IgG conjugates. The cellular and viral DNA was labelled with DAPI (blue). Panels A-C were grown in the absence of MG132 and panels D-F were incubated in the presence of MG132. Cells were viewed at 40X and images captured as described in the materials and methods. The images were digitally deconvolved, using the Openlab system and p73, vp30, and DAPI were digitally overlaid (C, F).

p34. There was also an absence of perinuclear DNA, suggesting a block in viral DNA replication.

6.7.3 The inhibition of proteasomes blocks late viral protein synthesis.

The above section showed by immunofluorescence that proteasome inhibition blocked the formation of viral factories, the next stage was to use metabolic labelling and immunoprecipitation to see if late protein synthesis was blocked. Vero cells were infected with BA71v and incubated with MG132 as described above. The cells were labelled for one hour with ^{35}S-methionine and -cysteine and then lysed in IPB and immunoprecipitated using antibodies specific for p73 and vp30. The first two lanes of figure 6.16 show that expression of the vp30 protein was unaffected by MG132. The second two lanes show that expression of p73 was blocked by MG132. The results show that cells treated with the proteasome inhibitor can be infected with ASFV, but that the virus cannot progress onto the synthesis of the late viral proteins. This is an interesting observation that needs further investigation, unfortunately it precludes the use of proteasome inhibition as a means of producing aggresomes in cells infected with ASFV.

6.8 Investigation into the interaction of the GFP-250 aggresome and ASF viral assembly pathways.

6.8.1 Introduction.

The previous sections demonstrated that the GFP-250 construct could be used to produce aggresomes in Vero cells without the use of inhibitors of proteasomes. The next experiment attempted to produce aggresomes in cells

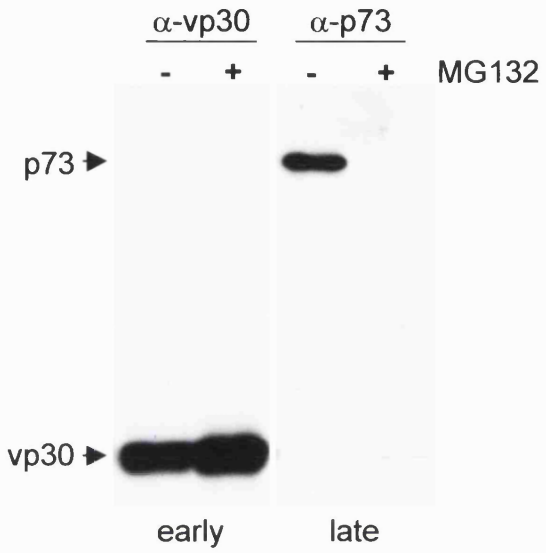

Figure 6.16: Proteasome inhibition blocked late viral protein synthesis. Vero cells were infected with BA71v for 12 hours and after the first hour of infection 25μM MG132 was added. The cells were metabolically labelled for one hour and then lysed in IPB and immunoprecipitated overnight using antibodies specific for p73 and vp30.

infected with ASFV by transfecting them with GFP-250, without the need for proteasome inhibition.

6.8.2 Aggresome formation prevents the infection of Vero cells with ASFV.

Vero cells were transfected with GFP-250 for 36 hours as described previously and then infected with BA71v for a further 12 hours. The cells were then fixed, permeabilised and then labelled with the antibody raised against the late structural protein p34. Figure 6.17 shows representative images from several experiments attempting to demonstrate GFP-250 expression and ASFV infection in the same cell. Panel A depicts two cells infected with ASFV stained with the antibody specific for p34, and shows the familiar staining of the perinuclear viral factories and a faint cytoplasmic stain. Panel B shows the same cells, one of which contains a GFP-250 aggresome. Panel C is a digital overlay of the two images with a DAPI stain. Figure 6.17 shows infected cells in close proximity to cells expressing GFP-250 and producing aggresomes, however on examination of several hundred cells, by indirect immunofluorescence, it was not possible to find cells containing both an aggresome, and late structural proteins of ASFV. In conclusion, it appears that the formation of aggresomes in the cell protects the cell from infection by African swine fever virus.

6.8.3 Late ASF viral protein expression is inhibited by the presence of aggresomes.

Transfection with the GFP-250 chimera and subsequent formation of aggresomes could either prevent cells from being infected by ASFV, or as shown for MG132, prevent late protein expression. In the next experiment these

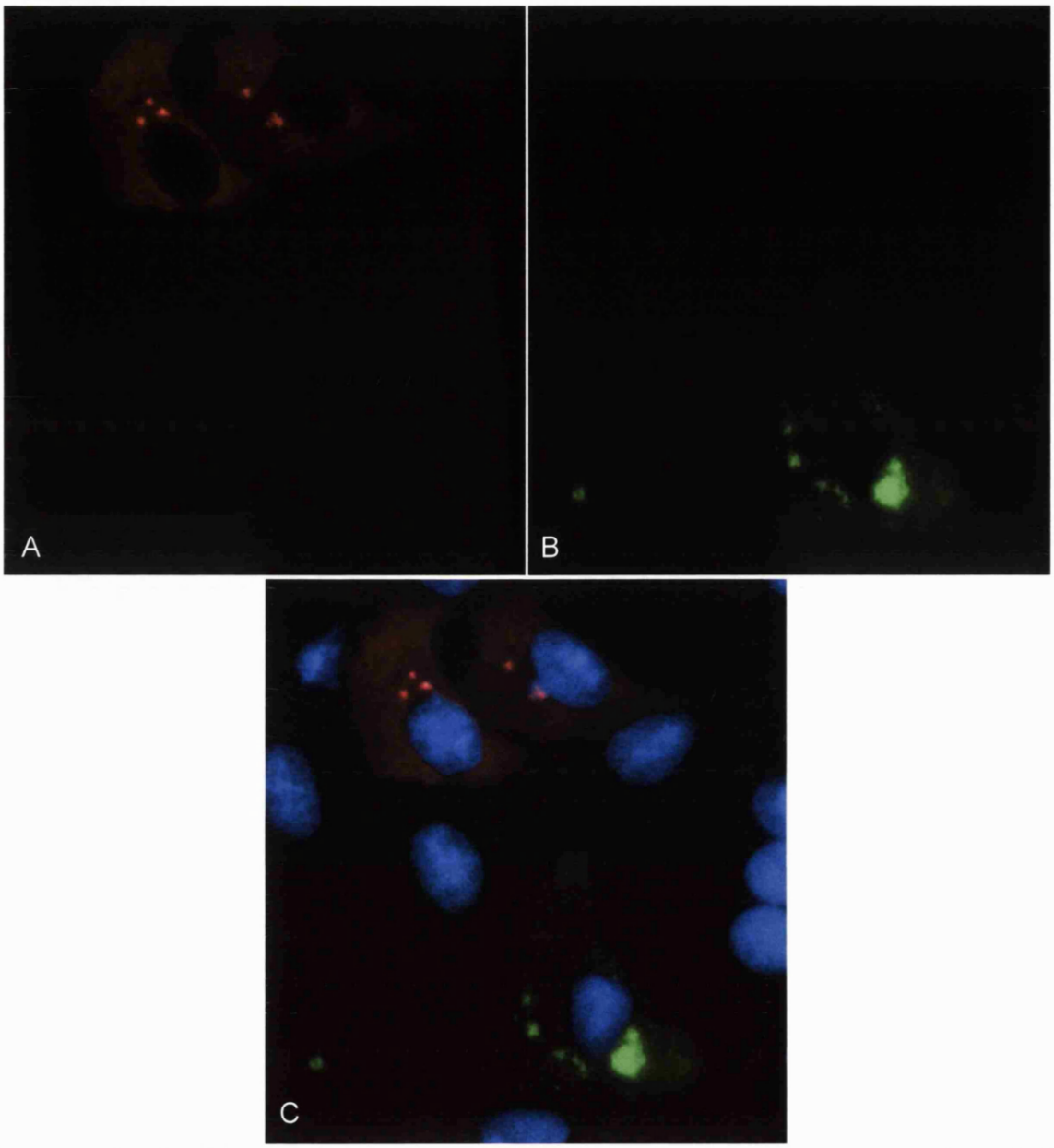

Figure 6.17: The presence of GFP-250 aggresomes prevented ASFV infection. Vero cells were transfected with the GFP-250 plasmid and grown for 36 hours at 37°C, the cells were then infected with BA71v for 12 hours. The cells were fixed with ice-cold methanol, permeabilised with 0.1% Triton X-100 and incubated with the rabbit antibody specific for p34 (A). The distribution of the protein was visualised by using the Alexa Fluor 594 (red) anti-rabbit. Panel B shows the GFP-250 distribution. The cellular and viral DNA was labelled with DAPI (blue). Cells were viewed at 60X and images captured as described in the materials and methods. The images were digitally deconvolved, using the Openlab system and p34, GFP-250, and DAPI were digitally overlaid (C).

possibilities were investigated by determining whether the early viral protein, vp30 could be produced in cells expressing GFP-250. Figure 6.18 shows the distribution of vp30 in cells transfected with the GFP-250 chimera. Panel A and D show cells that had been infected with ASFV, as revealed by the cytoplasmic staining for vp30, panel B and E show cells transfected with the GFP-250 protein chimera and panel C and F show digital overlays of the panels with a DAPI stain, respectively. Panels C and F clearly showed that there is transfection of GFP-250 and subsequent aggresome formation and ASFV infection in the same cells, suggesting that the overexpression of GFP-250 had not blocked virus infection, but somehow prevented the expression of late viral proteins.

6.8.4 Conclusion.

The studies comparing African swine fever viral factories and aggresomes have shown that they share several features. Both the viral factories and aggresomes are surrounded by a vimentin cage and mitochondria and are localised at a perinuclear site that was revealed to be at, or near, to the microtubule organising centre. The major difference between the structures of aggresomes and viral factories was their protein content. The aggresomes contained several proteins involved in the protein folding and degradation pathways, such as molecular chaperones and proteasomes, but there was little, or no evidence, for the co-localisation of these components with viral factories. This seemed to suggest that the viral factories were using the structural aspects of the aggresome pathway to form a self contained site for virus assembly, but were able to exclude cellular proteins that could inhibit virus assembly. The most surprising result was the inhibition of the expression of late structural proteins by

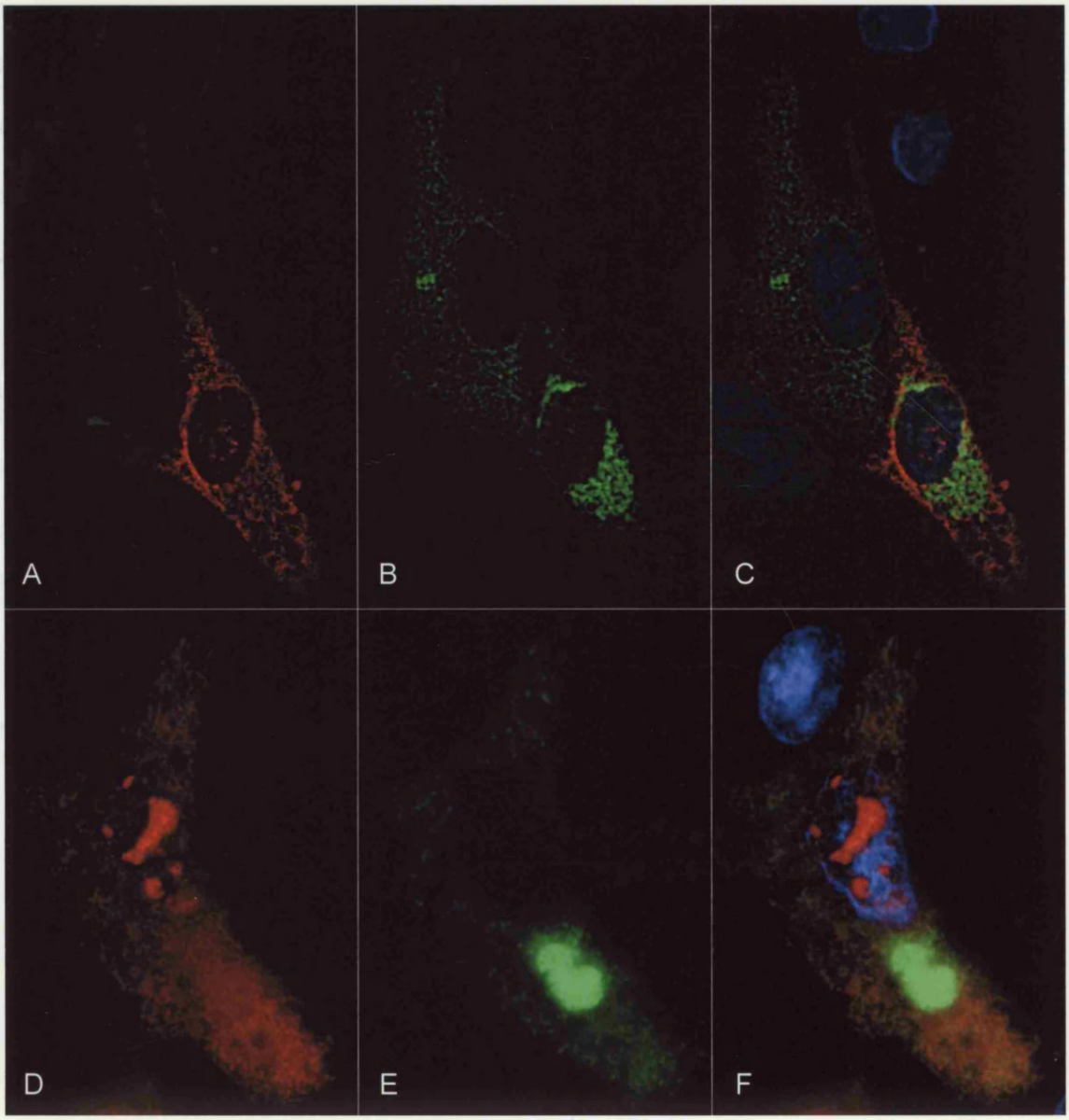

Figure 6.18: The presence of GFP-250 aggresomes prevented late viral protein synthesis. Vero cells were transfected with the GFP-250 plasmid and grown for 36 hours at 37°C, the cells were then infected with BA71v for 12 hours. The cells were fixed with ice-cold methanol, permeabilised with 0.1% Triton X-100 and incubated with the mouse antibody specific for vp30 (A, D). The distribution of the protein was visualised by using the Alexa Fluor 594 (red) anti-mouse IgG conjugate. Panel B and E shows the GFP-250 distribution. The DNA was labelled with DAPI (blue). Cells were viewed at 60X and images captured as described in the materials and methods. The images were digitally deconvolved, using the Openlab system and vp30, GFP-250, and DAPI were digitally overlaid in panels C and F.

inhibitors of proteasomes, and by the formation of aggresomes. This may be as a result of direct competition for the MTOC location as the site of assembly of the virus and aggresomes or a need for proteasomes by the virus during transition between early and late gene expression. These aspects will be discussed below. In conclusion, ASFV uses aspects of the aggresome pathway to establish viral factories at the MTOC, which can be blocked by the formation of aggresomes.

7 Discussion.

The ordered proteolytic processing of the 220kDa polyprotein of ASFV was first described by Simón-Mateo et al (1993). Figure 7.1 shows a representation of the ordered cascade producing p150, p37, p34 and p14.

Recombinant proteins and synthetic peptides were used to raise antibodies recognising p150 and p34. These recognised the polyprotein and their respective final products by Western blot analysis. Surprisingly, both antisera reacted to a ladder of proteins, which suggested more processing intermediates than described in the literature (Simón-Mateo et al, 1993). Unfortunately, these antibodies were unable to detect the final p34 protein and only very low levels of the p150 protein by immunoprecipitation analysis. The possible reasons for this will be discussed later.

7.1 The polyprotein is processed via several intermediates to the final structural proteins.

As described in sections 5 and 6 the ladder of proteins recognised by antibodies specific to p34 and p150 may indicate processing at minor Gly-Gly-X sites. It was possible to predict the size of the proteins formed by cleavage at the Gly-Gly-X sites from their amino acid composition (figures 4.3 and 5.2) and compare these to the actual molecular weights visualised by Western blot analysis. If cleavage was occurring at the 15 minor Gly-Gly-X sites, in addition to the 4 major Gly-Gly-X sites, then the antibody raised against p34 would be expected to recognise a total of 34 proteins, and the antibody specific for p150 detected a total of 16 proteins. The limitations of SDS-PAGE system made it difficult to resolve the high molecular weight proteins precisely, and as a

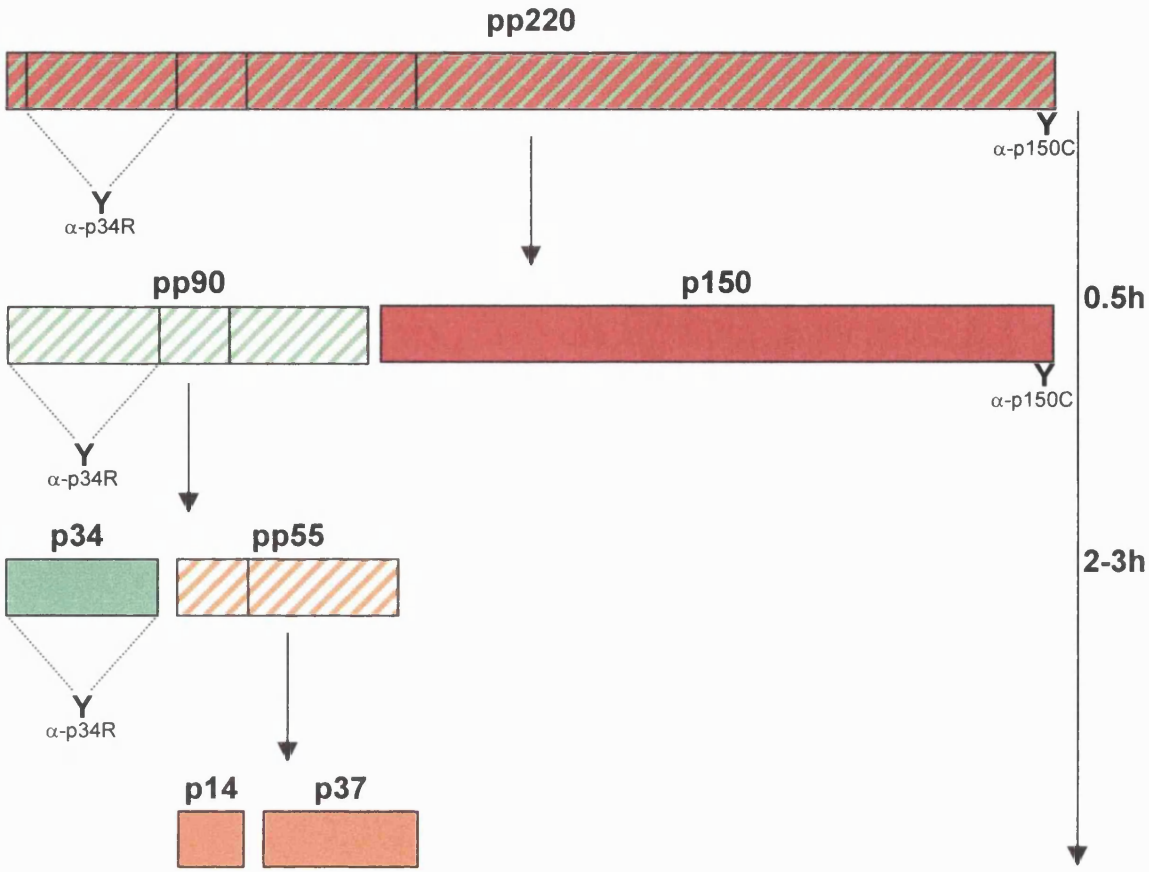

Figure 7.1: The ordered cascade of proteolytic cleavages during pp220 polyprotein processing. The ordered processing of pp220 polyprotein as described by Simón-Mateo et al (1993). The green boxes depict the proteins that would be recognised by an antibody against p34, the red boxes depict proteins that would be recognised by an antibody raised against p150 and the solid boxes represent the final proteins produced in proteolytic processing. The time of appearance of the proteins is shown on the right in hours.

result it was not possible to calculate the total number of proteins detected by the antibody specific for p34. A well-defined ladder of 17 proteins was, however, seen below 143kDa in figure 4.1. This is in agreement with the prediction from Gly-Gly-X cleavage where the antibody would be expected to detect 17 proteins with molecular weights less than 141kDa. For the antibody against p150 a ladder of 16 proteins could be visualised at 16 hours post infection (figure 5.1) as predicted.

Evidence for the use of the minor Gly-Gly-X sites, rather than non-specific proteolysis, was that the smallest proteins detected by the antibodies against p34 and p150 were predicted to be 36 and 63kDa proteins respectively, and proteins of these sizes and no smaller were seen (figures 4.1 and 5.1).

The antibody against the C-terminus of p150 was generated so that the precise location of the epitope was known and therefore the exact molecular weights of the possible fragments could be predicted. The antibody was predicted to bind 16 proteins, and 16 proteins were detected. Surprisingly, the actual molecular weights seen in figure 4.1 did not all directly correspond to the predicted molecular weights. For example, four proteins migrated as predicted at 63, 86, 122 and 136kDa (figure 7.2), whereas other proteins migrated at molecular weights that were not predicted from cleavage at Gly-Gly-X sites (69, 100 and 110kDa). In conclusion, there is substantial evidence for cleavage at minor Gly-Gly-X sites, however, due to the limited resolution of the high molecular weight proteins it was difficult to state conclusively that cleavage was occurring at all 19 Gly-Gly-X sites. Further investigations need to be undertaken to resolve the protein bands further, possibly by 2D electrophoresis. In addition,

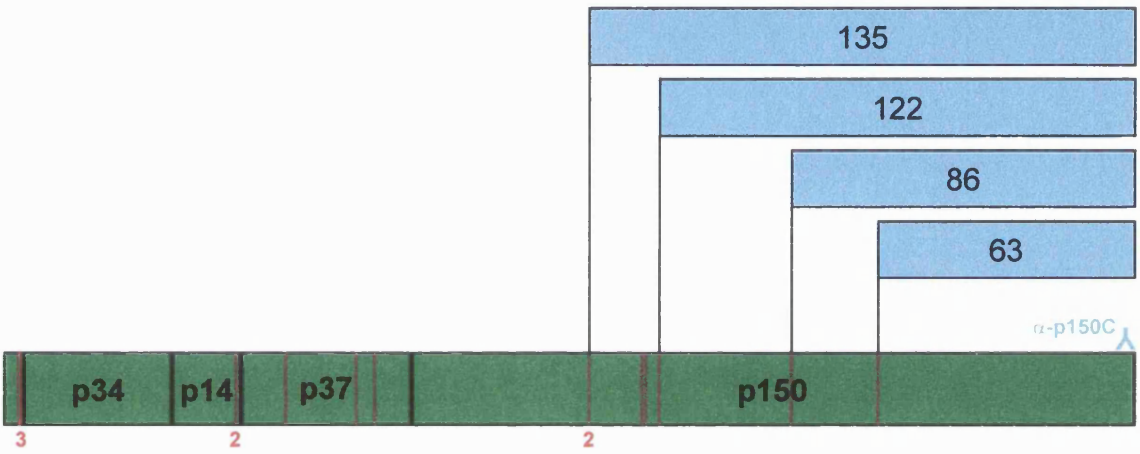

Figure 7.2: Cleavage occurs at the minor Gly-Gly-X sites. The blue boxes depict the proteins, recognised by the antibody specific for p150, that are formed by cleavage at minor Gly-Gly-X sites. The green box shows a schematic representation of pp220 showing the 19 Gly-Gly-X sites, with the solid black lines representing the major Gly-Gly-X sites and the red lines and numbers for the minor Gly-Gly-X sites. Molecular weights shown in kilodaltons.

N-terminal sequencing could be undertaken to determine the precise cleavage sites of the proteins detected by the respective antibodies.

7.2 Membrane association is important for correct processing and packaging.

As already stated, the polyprotein was processed not only into the final structural proteins, but also a large number of "intermediate" proteins. Interestingly, only the final structural proteins, p34 and p150, were located in the mature virions. This raised the question of how the virus distinguishes between the polyprotein, intermediates and final structural proteins and only packages the structural proteins?

Figure 7.3 shows a diagram depicting two possible pathways. The polyprotein is translated in the cytoplasm and a pool of the polyprotein associates with the membrane (1). Once associated with the membrane the polyprotein can either be processed to the final structural proteins (2), possibly via intermediates, and the final proteins are then selectively packaged into the virions (3). Alternatively, the polyprotein itself becomes packaged in conjunction with a protease (4), where it is then rapidly cleaved into the final structural proteins (5). For both pathways, the structural proteins then oligomerise and the mature virions are formed (6). The cytoplasmic pool of the polyprotein is randomly cleaved (7), either by a cellular or viral proteases. In addition, the membrane-associated proteins, which are either processed incorrectly or not selectively recruited to the virions, become randomly cleaved, either on the membrane (2) or they dissociate and become cleaved in the cytosol (8).

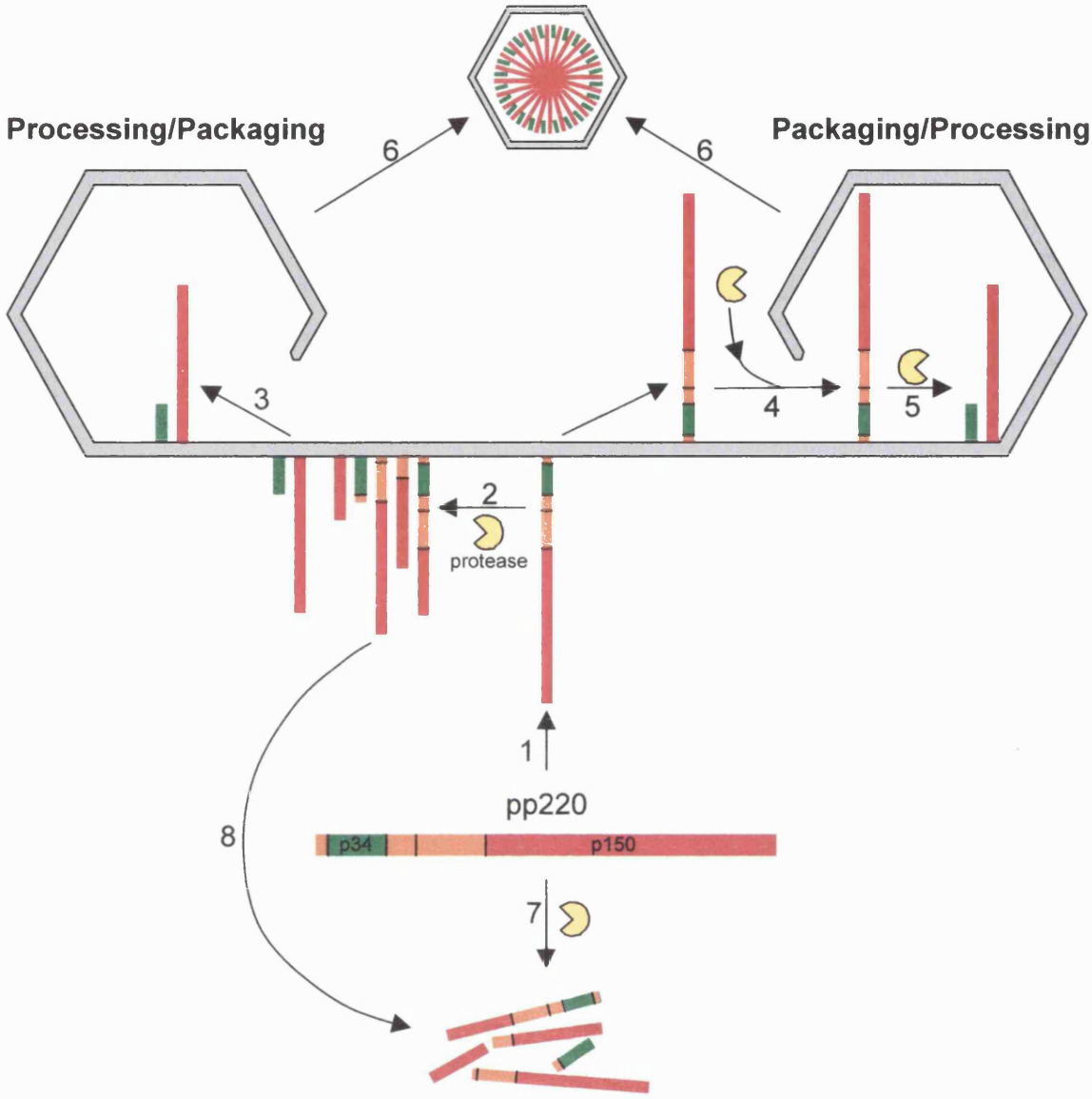

Figure 7.3: The selective recruitment and packaging of the final structural proteins. The polyprotein associates with the membrane (1), where it is either processed on the membrane to form the structural proteins (2), before they are packaged (3); or the polyprotein is packaged with a protease (4) and then rapidly processed into the final structural proteins (5). The structural proteins oligomerise and mature virions are formed (6). The cytosolic pool is randomly cleaved (7), either by a cellular or viral protease. In addition, the membrane-associated polyprotein, which fails to adopt the correct pathway, is also randomly cleaved, either on the membrane (2) or it dissociates and becomes cleaved in the cytosol (8).

Western blot analysis showed that pp220 was absent from purified virions. This argues against step 4 in the pathway where pp220 is packaged into the virions. It is possible, however, that once delivered into the assembling virion, processing of pp220 by the putative protease is rapid and the unprocessed pp220 was not, therefore, detected in the experiments. This is a possible mechanism as it is known that wrapping of virions takes approximately one hour and release from cells a further 2-3 hours (Cobbold et al, 1996). The formation of virions is therefore slow compared with the potentially fast processing of the polyprotein by a protease.

One way of distinguishing between the two pathways is to compare the levels of pp220, or the final products of processing (p150 and p34), on membranes in the presence or absence of trypsin. If there were significant pools of pp220 in virions (step 4) then this would be protected from trypsin, alternatively, if there were pools of processed p150 and p34, which were not packaged (step 2), these would be sensitive to trypsin. Both would be revealed by comparative Western blots. Figures 4.7 and 5.5 are Western blot analysis of protease protection assays, which show that only the final p34 and p150 structural protein were protected from the action of the protease. These data support the processing before packaging pathway, however if processing was rapid then the polyprotein could be packaged into assembling virions and the processing events coincide with the final wrapping events. In this case the polyprotein would be sensitive to the protease protection assay, whereas the final structural proteins would be protected. In support of this, the levels of p150 and p34 in the protected pools (figures 4.7 and 5.3) are very similar to the untreated

fractions, therefore it appears that all the membrane associated p34 and p150 was packaged.

The model in figure 7.3 and the data in figures 4.5 and 5.4 show that the membrane and cytosolic pools of protein are different. Importantly, p34 and the majority of the p150 pool were absent from the cytosolic pool suggesting that binding to the membrane, in some way, ensures the correct processing of the polyprotein. This is most easily explained if the polyprotein is processed in the virion. Here binding of pp220 to the membrane would be viewed as being essential for the packaging of pp220. Correct processing would be achieved if access of the putative viral protease to Gly-Gly-X sites was restricted by conformational constraints imposed during assembly and maturation of the virion (steps 4, 5 and 6). The way in which membrane binding would ensure correct processing, without packaging, is less easily explained. One explanation could be that membrane association is again essential for packaging, but that the packaging mechanism is selective for p150 and p34. This effectively rescues the protein from further processing (step 3). Intermediates that do not enter the virion are processed at minor Gly-Gly-X sites and eventually join the cytosolic pool (step 8). The support for this argument comes from the protease protection assays (figures 4.7 and 5.5) showing processing intermediates on the membrane, but not in enveloped virions.

In agreement with both hypotheses, the antibody raised against the p34 protein recognised a highly dense ladder of proteins in the cytosolic fraction, which ranged from ≈50kDa to over 200kDa. This large ill-defined ladder of proteins in the cytosolic fraction appeared to be formed by random proteolysis of the polyprotein, possibly by a host protease. Surprisingly, if random proteolysis

was occurring in the cytosol then this would mean that the polyprotein was being randomly cleaved and therefore lead to the formation of small proteins. As already stated the ladder ranged from ≈50kDa to over 200kDa, with the majority of the proteins having molecular weights of greater than 75kDa. So, there appeared to be inhibition of the total cleavage of the polyprotein, possibly by the aggregation of the polyprotein. Interestingly, the antibody raised against the p150 C-terminus only recognised two proteins in the cytosol, a major >250kDa protein and a minor 186kDa protein. As stated earlier, this may be due to proteolytic removal of the antibody binding site from the C-terminus of p150, therefore random proteolysis may still be happening, however the proteins produced are not recognised by the antibody specific for p150. Further investigations need to be undertaken to better define the ladders of proteins and to study the fate of the cytosolic pool of the polyprotein.

7.3 Signals leading to the correct packaging of pp220 products.

7.3.1 Myristylation.

The pp220 polyprotein has been shown to be myristylated at its N-terminus (Aguado et al, 1991; Simón-Mateo et al, 1993) and myristylation may play a role in membrane association (Grand, 1989; Schultz et al, 1988; Towler et al, 1988). As already stated, membrane association appears to be important for the correct processing and packaging of the polyprotein and the structural proteins, therefore the myristylation may play a role in the membrane association of the polyprotein. Interestingly, the proteolysis of the polyprotein resulted in the cleavage of the N-terminus and therefore the myristylation site would be removed. As a result the proteolytic products are therefore not myristylated, but

are still membrane associated. So, although the final structural proteins are not bound to the membranes through myristate, myristylation may have an important role in the targeting of the polyprotein to the membranes.

The Western blot analysis of the distribution of the polyprotein between the membrane and cytosolic fractions showed that only about 35% of the total pool of pp220 was membrane associated at steady state (figures 4.5 and 5.4). Interestingly, the pulse-chase experiments showed that there was a time-dependent association of the polyprotein with the membrane, with 60% of the pulse-labelled polyprotein becoming membrane associated after 12 hours (figures 4.15 and 5.12). Unfortunately, due to the limitations of resolving high molecular weight proteins on SDS-PAGE it was not possible to differentiate between full length polyprotein, and the polyprotein lacking the N-terminus (282 and 277kDa respectively). It is not known, therefore, if the membrane bound pool contains the N-terminal amino acids and therefore the myristylation motif.

Although myristylation involves the attachment of a hydrophobic group to the proteins and may make them more susceptible to membrane association, not all myristyl proteins are associated with membranes. Several viral proteins, important in virus assembly and structure have been shown to be myristylated and the majority associate with membranes and play a role in virus assembly and structure, however some of these proteins are found in the cytoplasm (Table 7.1; Towler at al, 1988; Grosenbach and Hruby, 1998). In conclusion, the myristyl group may anchor the polyprotein to the membrane, however the subsequent proteolysis would produce non-myristylated proteins, which may be anchored to the membrane by interaction with other membrane proteins.

Protein	Subcellular Location	Function
Murine Leukaemia Virus *gag*	Plasma membrane	Assembly/structure
Mason-Pfizer Monkey Virus *gag*	Plasma membrane	Assembly/structure
Bovine leukaemia virus *gag*	Plasma membrane	Assembly/structure
Mouse mammary tumour virus *gag*	Plasma membrane	Assembly/structure
Human T-Lymphotropic Virus Type I *gag*	Plasma membrane	Assembly/structure
HI*V gag*	Plasma membrane	Assembly/structure
HIV 3' orf	Cytoplasm, membrane?	Virus replication?
Hepatitis B Virus pre-S1	ER	Assembly/structure
SV40 Virus VP2	Nuclear	Assembly/structure
Polyoma virus VP2	Nuclear	Assembly/structure
Poliovirus VP4	Cytoplasm, ER	Assembly/structure Cell entry?
Bovine enterovivirus VP4	Cytoplasm, ER	Cell entry?
Vaccinia virus A16L	Cytoplasm	Unknown
Vaccinia virus E7R	Cytoplasm	Unknown
Vaccinia virus G9R	Unknown	Unknown
Vaccinia virus M25	IMV envelope	Assembly/structure

Table 7.1: Known viral N-myristyl proteins. Adapted form Towler et al, 1988 and Grosenbach and Hruby, 1998.

7.3.2 Protein signals.

Figure 7.4 shows four hypotheses for the possible signals required for the targeting of membrane associated proteins to the virus assembly site. The first and simplest hypothesis suggests that a single signal is required.

The next two models propose that each of the final products of pp220 contain a packaging signal. This could be the same for each protein, however, there is no evidence for a linear motif within the amino acid sequences of the proteins. The signals could therefore depend on conformation, or be different for each protein. The signals would be present on the polyprotein, and the processing intermediates. A mechanism to exclude these inappropriately processed proteins from the virions has to be proposed. In the "gate" model the packaging mechanism somehow distinguishes between final structural proteins and the intermediates. Alternatively, the signal is masked until the protein is processed correctly (model 3).

The fourth model, the sequestration model, proposes that all the proteins formed from the processing of the polyprotein enter the assembling intermediates, where the final structural proteins are anchored to their assembly sites. The remaining proteins are either ejected from the virion or become degraded. Although this report has no compelling evidence in favour of a particular hypothesis, the single signal model is the simplest as it involves the targeting of a single protein to the assembling intermediates. The published literature reports that the final structural proteins are present in the mature virions in equimolar amounts (Andrés et al, 1997). This would be better achieved using the "packaging before processing" pathway and single signal hypotheses, as one

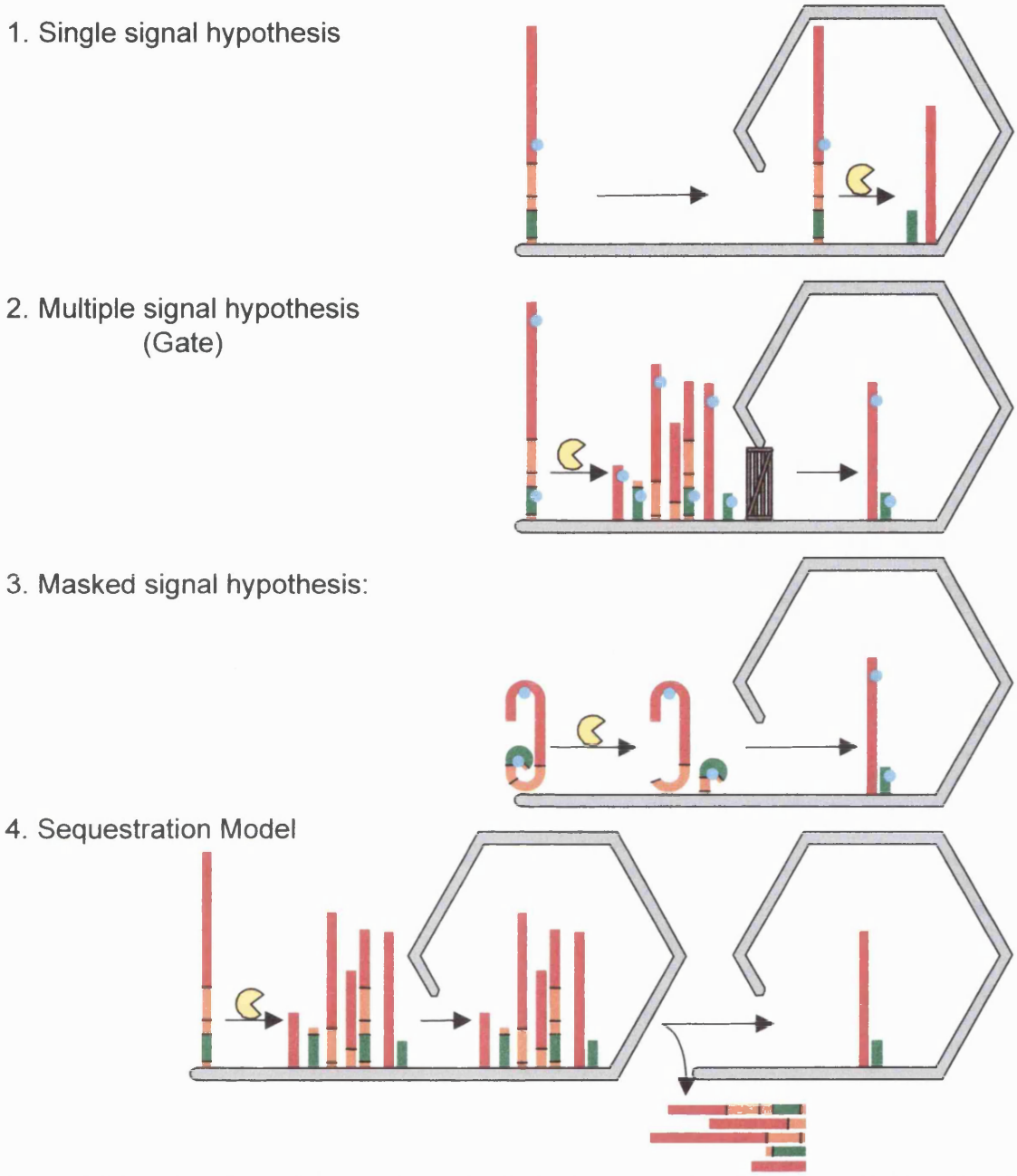

Figure 7.4: The possible signal models for the packaging of the viral proteins. 1) The single signal hypothesis suggests that the polyprotein contains a signal (blue circle) that directs the polyprotein to the packaging virions. 2) The multiple signal hypothesis proposes that the final structural proteins have signals that ensures selective packaging of the final proteins. 3) The masked signal hypothesis proposes that packaging signals are masked until correct processing. 4) The sequestration model proposes that all the proteins are sequestered to the wrapping virion, where the structural proteins are anchored to their assembly site, and the other proteins are ejected.

polyprotein would generate a 1:1:1:1 ratio of the four structural proteins in the assembling virions.

7.4 p34 and p150 form oligomeric complexes on the membranes.

This report has shown that the membrane-associated p34 and p150 proteins formed a large protein complex of over 50,000kDa. In addition, at steady state, the antibody specific for p34 detected a range of protein complexes, with sizes from 150kDa to over 50,000kDa, suggesting that the formation of the large complex was via intermediates. This was in agreement with the published literature on the assembly of the major capsid protein, p73 (Cobbold and Wileman, 1998).

Simón-Mateo et al (1993) and Andrés et al (1997) suggested that the pp220 polyprotein may have a role as a scaffolding protein in the assembly of ASFV. However the data in this report has shown that the polyprotein did not form a large complex (figures 4.8 and 5.6), characteristic of a scaffold protein. The final products of processing were incorporated into a large protein complex by the progressive oligomerisation of the proteins, as demonstrated by the presence of intermediates seen in figure 4.9A. The final proteins are also not acting as scaffolding proteins as these proteins are present in the mature virions, whereas scaffold proteins aid the assembly of the capsid and are then ejected from the capsid on entry of the DNA (Casjens and Hendrix, 1988). It appears that the products of the pp220 are involved in the assembly of capsids and/or matrix precursors on the membranes, possibly in conjunction with the major capsid protein (Cobbold and Wileman, 1998). This appears to be similar to the first identifiable step in morphogenesis of the vaccinia virus, where a protein

scaffold or matrix was seen on the membrane crescents originating from the cisternae of the ER and/or the intermediate compartment between the ER and Golgi (Sodeik et al, 1993).

Although kinetic studies were not carried out on the oligomerisation of the structural proteins, it is expected that this occurs after the packaging of the final structural proteins and occurs with similar kinetics as membrane wrapping. This is similar to the oligomerisation and wrapping of the p73 protein (Cobbold and Wileman, 1998).

7.5 The final structural proteins are located in the inner core of the virions.

Immunofluorescence analysis was undertaken to explore the subcellular distribution of the polyprotein and its products, however the antibodies failed to produce a punctate staining indicative of virions. Antibodies specific for p34 and p150 labelled an amorphous pool of proteins at the virus factory and also detected a less concentrated pool throughout the cytoplasm.

Figure 7.5 shows a model to explain the lack of labelling of virions by the antibodies. The major capsid protein, p73, has been shown to locate to both the inside and outside of the inner envelope (Cobbold and Wileman, 1998). An outer pool of p73 has also been implied by the observation that the virus can be neutralised by antibodies specific for p73 (Borca et al, 1994; Gómez-Puertas et al, 1996). Interestingly, the electron microscopy data from this report and published literature (Andrés et al, 1997) has shown that p34 and p150 were only found inside the virions, located at the inner core shell. One possibility is that the structures labelled with the antibody specific for p73 were on the exterior of the assembling intermediates and virions. Therefore, the apparent lack of binding of

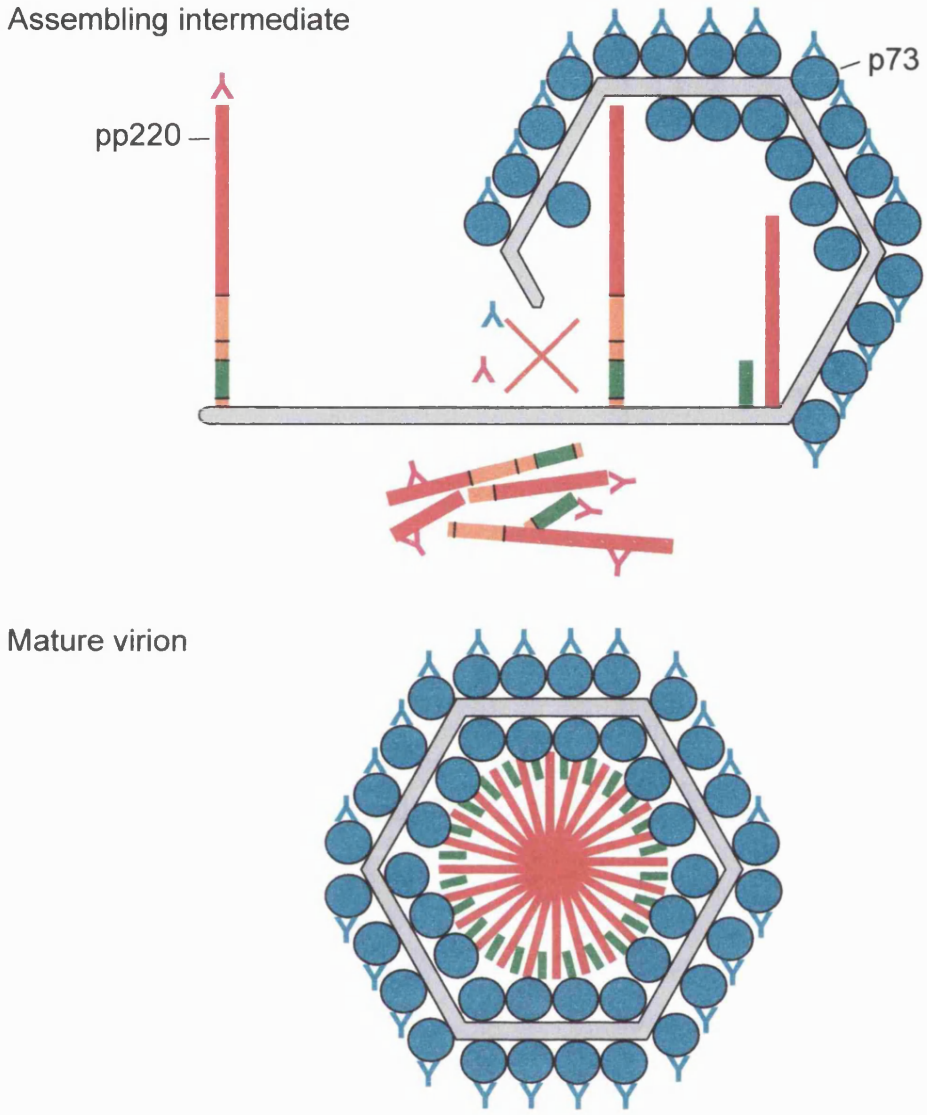

Figure 7.5: The antigenic sites of p34 and p150 are masked by packaging into the virions. The antibodies against the specific proteins (**Y**) can only label the proteins located outside the assembling intermediate and mature virions. For example, the outer capsid of p73, the unpackaged, membrane-associated pp220 proteins and the cytosolic pool of the proteins. The antibodies are unable to bind to the proteins located inside the assembling intermediate and mature virion.

the antibodies specific for p34 and p150 to virions was due to steric masking of epitopes within the interior of the assembling virions. Epitopes were revealed, however, when virions were disrupted by denaturation for Western blotting and when virions were cut during cryo-sectioning (figure 4.13). In conclusion, the polyprotein, intermediates, and structural proteins are concentrated at the virus assembly sites, however their antigenic sites appear to be blocked in assembling intermediates and mature virions, as no virus-like structures were visualised by immunofluorescence.

7.6 Loss of epitopes during packaging was also suggested from the pulse-chase immunoprecipitation experiments.

The antibodies were able to immunoprecipitate the polyprotein, however there were difficulties in detecting the final structural proteins. On examination of infected cell lysates, both antibodies showed a slight decrease in the levels of the polyprotein after 8 hours. The decrease in the levels of the polyprotein was expected as it was gradually processed into its final products, however it seems that only a small pool of the polyprotein was susceptible to proteolysis.

The antibodies specific for p34 and p150 proteins detected a small amount of the polyprotein after the initial labelling, however after 2 hours the levels increased considerably. This may be possible due to a large conformational change at 2 hours, followed by proteolysis of a small fraction of the total pool of polyprotein. The final structural proteins were then rapidly incorporated into large protein complexes, which masked the antibody epitopes. Figure 7.6 shows a schematic representation of this model explaining the increase in levels of the polyprotein and the inability of the antibodies to recognise the final products.

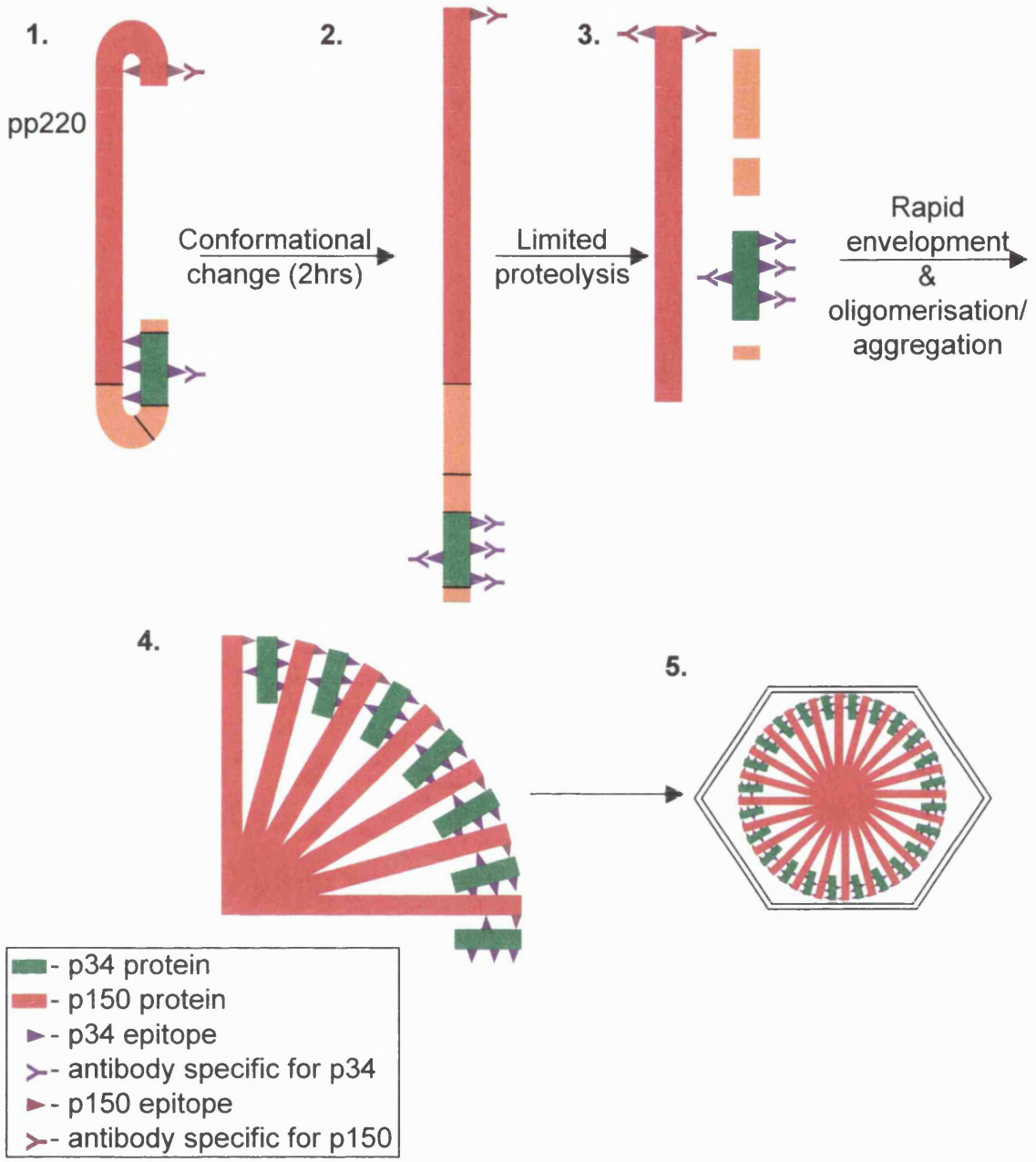

Figure 7.6: Schematic representation of the masking of antigenic sites.

1. Following synthesis, the polyprotein is held in a conformation that masks some of the p34 and p150 epitopes. 2. After 2 hours the polyprotein undergoes a conformational change, resulting in the unmasking of the epitopes. 3. A small fraction of the polyprotein undergoes proteolysis to produce the final structural proteins. 4&5. The structural proteins rapidly associate with themselves and possibly other viral proteins to form either large oligomers or aggregates, masking the epitopes. This may occur in parallel with envelopment of the structural proteins.

Several experiments were undertaken in an attempt to immunoprecipitate the final structural proteins, however none of the experiments described below revealed the structural proteins. Firstly, more rigorous lysis buffers were used. These included the use of different detergents, such as Brij-35, NP-40, sodium deoxycholate, digitonin and SDS, and varying other components of the lysis buffer, such as iodoacetamide and DTT, at varying concentrations. These were followed by more severe cell lysis protocols, such as 1% SDS followed by sonication and boiling before dilution with the immunoprecipitation buffer and immunoprecipitated. One possibility was that the large oligomers were not dissociating in the immunoprecipitation buffers and were being pelleted with the nuclei and cell debris during the preclear stage. To investigate this the pellet was resuspended in 1% SDS, sonicated and boiled and then diluted in IPB and immunoprecipitated.

The final structural proteins were successfully immunoprecipitated by Simón-Mateo et al (1993), so their protocol was followed precisely, however the antibodies used in this investigation were unable to detect p150 or p34.

This report and others have shown that the final products were associated with the inner core shell and therefore may be tightly associated with the DNA, therefore the lysed cells were treated with DNAse in an attempt to release the final structural proteins. In addition, the labelling and chase periods were varied from minutes to hours, to explore the possibility that the initial experiments may have missed the processing event. Surprisingly, all the various conditions and protocols above failed to bring about the immunoprecipitation of the final structural proteins. The reason for this is currently unknown and needs further investigation. In conclusion, the kinetic studies have shown that a large pool of

the polyprotein was made, of which a small fraction was proteolytically processed after 2 hours. The inability to detect the final proteins suggests that they may rapidly form protein complexes, hence masking the epitopes. The delay in processing suggests that the proteolytic processing may play a temporal role in the assembly of ASFV.

8 Discussion.

8.1 Generation of aggresomes.

The term aggresome was first proposed by Johnston et al (1998) to describe a microtubule dependent pathway able to sequester misfolded proteins close to the MTOC, where they became enclosed in a vimentin cage. The published immunofluorescence images of aggresomes show a striking similarity to African swine fever virus assembly sites. The aim of the second part of this project was to see if there was a relationship between aggresome assembly and the assembly of ASFV replication sites. Aggresomes were formed in cells permissive for ASFV infection either by blocking the degradation of the CD3 δ-chain expressed in CHO cells, or by the overexpression of a GFP-p115 chimera (GFP-250) in Vero cells.

8.1.1 Characteristics of aggresomes labelled with the TCR CD3 δ-subunit.

Misfolded proteins retained in the endoplasmic reticulum (ER) pass across the ER membrane into the cytosol, where they are degraded by proteasomes (reviewed in Bonifacino and Weissman, 1998). The best studied substrates for this pathway are the mutants of CFTR, especially ΔF508, (Jensen et al, 1995; Ward et al, 1995) and single chains of the TCR CD3 complex expressed alone in cells (Bonifacino and Klausner, 1994; Huppa and Ploegh, 1997; Yu et al, 1997; Yang et al, 1998). In this study the characteristics of aggresomes formed by blocking degradation of the TCR CD3 δ-subunit were compared with published work describing aggresomes sequestering the mutant CFTR protein (Johnston et al, 1998; García-Mata et al, 1999). As recorded for the CFTR protein, the aggresomes generated with the δ-subunit were perinuclear in location, where

they distorted the nucleus and appeared to contain small aggregates. The most dramatic feature of aggresome formation was the rearrangement of the intermediate filament, vimentin, into a mesh-like cage surrounding the aggresome. In this study a similar cage of vimentin surrounded the aggresomes generated from the δ-subunit.

The study also demonstrated that aggresomes containing TCR CD3 δ-chain were highly ubiquitinated. These results were in agreement with the initial work of Johnston et al (1998) and consistent with the proposal that multi-ubiquitination is the signal for degradation of the CFTR by proteasomes (Ward et al, 1995). Recent work (Yang et al, 1998) has shown that the CD3 δ-subunit is ubiquitinated prior to degradation. The present study did not show, however, that the CD3 δ-subunit in aggresomes was ubiquitinated. The signal could be associated with other proteins present in the aggresome.

Inhibition of TCR CD3 δ-subunit degradation was a successful means of producing aggresomes in cells, unfortunately they were not ideal for further investigation. The aggresomes were very large, often taking up the majority of the cytoplasm, and were very difficult to image, due to the cells rounding up, suggesting that the proteasome inhibitor, MG132, was toxic to the cells. An alternative means of producing aggresomes was therefore investigated.

8.1.2 Overexpression of GFP-250 produced aggresomes in Vero cells.

Aggresomes can be generated in cells without the use of potentially toxic proteasome inhibitors through the over expression of a GFP-250 protein chimera (García-Mata et al; 1999). This strategy was used to generate aggresomes in Vero cells susceptible to ASFV infection. These aggresomes were more

compact than those formed using the TCR CD3 δ-chain and were surrounded by better-defined vimentin cages. The compact nature of the structures allowed the orientation of aggresomes with respect to the MTOC and mitochondria to be determined. In agreement with previous studies aggresomes located to the MTOC within clustered mitochondria.

Aggresomes containing the GFP-250 chimera have also been shown to recruit four different cytosolic chaperones, Hdj-1, Hdj-2, Hsc70 and TCP-1 (García-Mata et al, 1999). This was confirmed, in part, in this study showing that the cytosolic chaperones Hdj-2, Hsc70 and TCP-1 were concentrated within the GFP-250 aggresomes. One difference between this study and the published work of García-Mata et al (1999) was the presence of ubiquitin in the aggresomes. They showed that GFP-250 containing aggresomes were not ubiquitinated, therefore the ubiquitin seen in the aggresomes, shown in figure 6.9, may be associated with other proteins located in the aggresome.

In conclusion, it was possible to generate aggresomes in ASFV susceptible cells using the over-expression of the GFP-250 protein chimera.

8.2 The structural and morphological features of ASF viral factories.

The next experiments compared the structural and morphological features of ASFV assembly sites with those determined above for aggresomes. Vimentin filaments collapsed to form a cage-like structure around the viral factory, similar to the cages seen around aggresomes. The ASF viral factories have long been characterised as being perinuclear (Breese and DeBoer, 1966; Vigario et al, 1967; Moulton and Coggins, 1968; Moura-Nunes et al, 1975; Pan et al, 1980), but this investigation refined this description and showed that the viral factories

were in fact pericentriolar. However, the ASFV assembly sites were localised near the MTOC, where as the aggresomes formed directly at the centrioles. This report demonstrated a requirement for an intact microtubule network for the formation and integrity of the assembly sites at a pericentriolar location, suggesting a role for the MTOC. This report also demonstrated that the mitochondria clustered around the viral factories, in a similar manner to the aggresomes.

There were differences between ASFV assembly sites and aggresomes in the distribution of cytosolic chaperones. The Hsp70 chaperone was found at the viral factories and TCP-1 clustered around the viral factories, but the Hdj-2 chaperone showed no change in its cellular location in infected cells. The significance of this observation will be discussed later.

In conclusion, the viral factories of ASFV shared several features with aggresomes. It was possible therefore that ASFV used the aggresome pathway to generate assembly sites.

8.3 ASFV utilises the aggresome pathway for virus assembly.

The study into the common features of aggresomes and ASFV assembly sites led to the following hypothesis:

"ASFV utilises the aggresome pathway to concentrate structural and accessory proteins in a subcellular structure, which has an established transport system, a concentrated supply of energy, and cytosolic machinery to aid in the correct assembly of the virus" (figure 8.1).

For viruses, such as the rotaviruses, bunyaviruses and orthomyxoviruses assembly is focused at the ER, Golgi and plasma membrane respectively, by

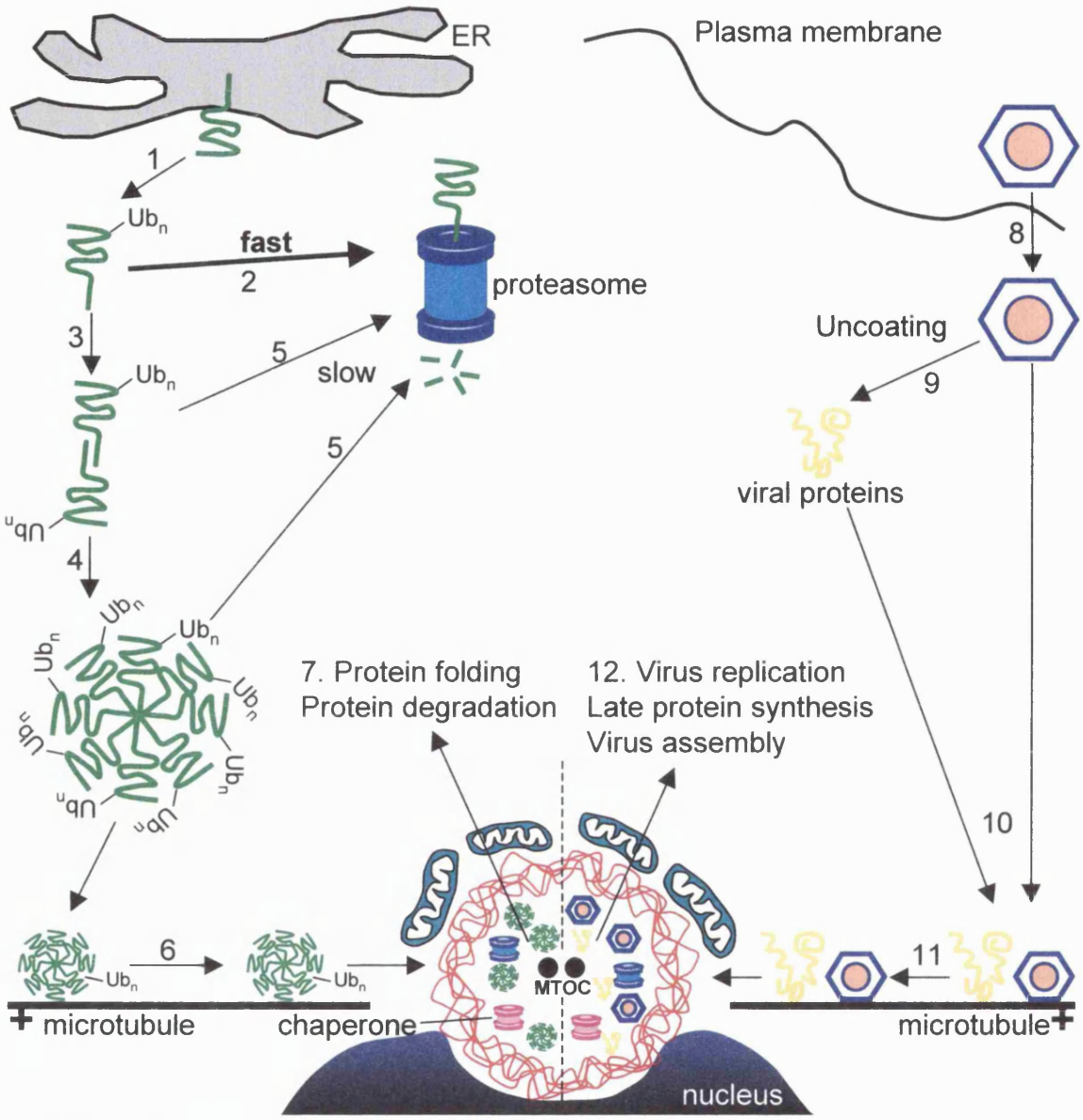

Figure 8.1: The aggresome and ASFV assembly pathways. Misfolded ER proteins are dislocated from the membrane and become ubiquitinated (1), where they can be rapidly degraded by cytosolic proteasomes (2) or aggregate (3,4). The aggregates are difficult to unfold, and as a result are likely to be slowly degraded by the proteasomes (5). Misfolded, aggregated protein is transported to the MTOC by MT, where it becomes surrounded by collapsed vimentin and clustered mitochondria (6), the aggregates are then correctly folded or degraded (7). ASFV enters the cell (8) and may uncoat and early proteins are translated (9). The virions and/or viral proteins associate with the MT (10) and are transported to the MTOC and establish an assembly site, surrounded by vimentin and mitochondria (11). The assembly site is the location for virus replication, late protein synthesis and assembly (12).

envelope proteins with specific targeting sequences. The herpesviruses and adenoviruses use the nucleus as a site for assembly (reviewed in Stephens and Compans, 1988; Pettersson, 1991; Griffiths and Rottier, 1992; Doerfler, 1994), and are targeted to the nucleus by nuclear localisation signals on viral proteins (reviewed in Greber and Kasamatsu (1996) and Kasamatsu and Nakanishi (1998)). For ASFV, iridoviruses and poxviruses, assembly is concentrated in cytoplasmic viral factories (Breese and DeBoer, 1966; Fenner, 1976; Fenner et al, 1989), which are the sites of DNA replication. In these cases, rather than using an existing cellular structure, such as the ER, Golgi or nucleus, a new subcellular structure is assembled. Strikingly, the cell creates a similar structure when stressed with high quantities of misfolded or unusual protein. The entry and subsequent replication of ASFV in the cytoplasm would lead to the production of a large concentration of viral proteins, which would be unfamiliar to the cell, and therefore may result in the initiation of the aggresome pathway.

This study has shown that ASFV uses many of the characteristic features of the aggresome pathway in its assembly. The next sections aim to discuss the role of these characteristics in the aggresome and ASFV assembly pathways.

8.3.1 Role of vimentin cages.

Aggresomes cause the collapse of the vimentin network to form a cage-like structure around misfolded proteins. This structure effectively forms a new subcellular site that sequesters aggregated or misfolded proteins, where they can be folded or degraded. Vimentin is a type III intermediate filament that is a major component of the cytoskeleton and is thought to play a role in cell integrity (reviewed in Steinert and Roop (1988) and Fuchs and Weber (1994)). The

vimentin network has been shown to be a dynamic structure, which requires the interactions of the intermediate filaments with microtubules and microfilaments (Yoon et al, 1998). In support of this, vimentin collapse has been described for cells incubated with microtubule-disrupting agents. These structures were described as juxtanuclear caps (Starger and Goldman, 1977) or whorls (Franke et al, 1978) of vimentin, but were different from the vimentin cages seen surrounding the aggresomes, and were less ordered. The assembly and disassembly (collapse) of the vimentin network appears to be highly regulated. In 1998, Prahlad et al showed that the assembly of the vimentin network required the movement of intermediate precursors along microtubules, whereas the rearrangement of vimentin during the cell cycle appeared to be regulated by site specific phosphorylation (Inagaki et al, 1987), initiated by cell cycle-regulated kinases including Cdc2 (Chou et al, 1990), Rho kinase (Goto et al, 1998) and RhoA-binding kinaseα (Sin et al, 1998). This suggests that vimentin collapse induced by the formation of aggresomes is not a random event caused by the high levels of aggregated proteins or disruption of the cytoskeleton. It appears that the presence of misfolded, aggregated proteins in the cells initiates a signalling pathway that results in the collapse of vimentin and the formation of the aggresomes. This report clearly demonstrated that vimentin collapsed around viral factories and the collapse may be as a result of the high concentration of viral proteins initiating the aggresome pathway and therefore vimentin collapse, as described above. Alternatively, the virus may have direct effects on vimentin assembly.

8.3.2 Role of microtubule network.

The aggresomes have been shown to be pericentriolar and have a requirement for an intact microtubule network and dynein/dynactin motors (Johnston et al, 1998; García-Mata et al, 1999) for the movement of aggregates to the aggresome, so its location at the MTOC is ideally situated. The above section has described the important interactions between the microtubule and vimentin network, so the microtubules may be important for the movement of the collapsing vimentin to the MTOC. In support of this, Wigley et al (1999) suggested that the centrosome may act as a scaffold for the aggresomes and Zieve et al (1980) described the collapse of vimentin around the centrioles during mitosis. This evidence suggests that the centrioles, and hence the MTOC, may act as a structure around which the aggresomes can form. The localisation of ASFV at a pericentriolar location would have similar benefits and allow the virus to utilise the microtubule network transport system of the aggresome pathway to recruit viral and cytosolic proteins required for ASFV assembly. This report has shown a requirement for the microtubule network for the formation and integrity of the viral factories and Carvalho et al (1988) and Alves de Matos and Carvalho (1993) showed the movement of virions from the viral factories to the periphery of the cell also required microtubules. Although this report has shown that the microtubule transport mechanism was employed by ASFV, the actual method of movement along microtubules was not demonstrated and therefore ASFV may use a different mechanism to aggresomes. Aggresomes require dynein/dynactin-associated motors for the movement of protein aggregates. One experiment to elucidate the use of the aggresome transport system in ASFV assembly would be to use the over expression of the p50/dynamitin component of the dynactin

complex to inhibit the dynein/dynactin-associated minus-end motors (Echeverri et al, 1996; Burkhardt et al, 1997; Presley et al, 1997; García-Mata et al, 1999) in ASFV infected cells. This may demonstrate that the viral proteins and/or virions move to the MTOC by the same method as the aggregates to aggresomes.

8.3.3 Role of mitochondria.

One aspect of the aggresome pathway is the induction of mitochondrial clustering around the aggresome. It is possible that the aggresomes require an energy supply to power protein folding and protein degradation. The aggresomes have been shown to contain many proteins involved in protein folding and degradation, for example, Hsp70, Hsp90, Hsc70, Hdj-1, Hdj-2, TCP1, the 20S proteasome, PA700 and PA28 (700 and 180kDa proteasome activator complexes) and ubiquitin. The processes involved in folding and degradation have an obligate requirement for ATP. It is possible that ASFV assembly sites would also require a source of energy for the replication and assembly of the virus. ASFV encodes the enzymes required for the replication of the viral DNA and RNA, such as an α-like DNA polymerase (Rodríguez et al, 1993; Martins et al, 1994), an ATP dependent DNA ligase (Hammond et al, 1992; Yáñez and Viñuela, 1993) and a DNA dependent RNA polymerase (Kuznar et al, 1980), all of which require ATP. Cobbold et al (2000) demonstrated a requirement for ATP in the wrapping of the virus by the endoplasmic reticulum in the viral factories. The clustering of mitochondria would facilitate the supply of energy to assembly sites.

8.3.4 Role of chaperones and proteasomes.

The major function of the aggresome is to sequester misfolded proteins in an attempt to fold them, or otherwise degrade them. Consequently, aggresomes contain high concentrations of chaperones and proteasomes. This report investigated the distribution of three chaperones from the Hsp40, Hsp70 and chaperonin families (Hdj-2, Hsp70 and TCP-1 respectively) in the presence of viral factories and showed that the viral factories had differing effects on their distribution in the cells. The presence of cytosolic chaperones would be beneficial to ASFV as replication and assembly occurs in the cytoplasm and the chaperones would protect newly translated proteins from possible misfolding and aggregation. The presence of the degradative machinery may also be advantageous to ASFV, in order to degrade incorrectly folded proteins and waste products of virus assembly, and therefore prevent an overload of unwanted proteins at the assembly site. In addition to this, the proteasome may play an important role in the transition from early to late DNA replication. In 1998, Everett et al described a viral activator of the herpes simplex virus type 1 (HSV-1), Vmw110, that requires proteasome activity to reactivate and enter the lytic cycle of the virus. They showed that inhibition of the proteasomes with MG132 blocked viral infection at the immediate-early stage (reviewed in Everett, 1999). The control of the expression of late viral genes of ASFV is poorly understood, however the control of expression using the ubiquitin-proteasome pathway may be a possible control mechanism. In support of this, this report showed that the inhibition of proteasomes blocked late viral synthesis, also Hingamp et al (1992, 1995) described an ubiquitin-conjugating (UBC) enzyme (UBCv1) encoded for by the ASFV genome, which may play a role in the onset of late gene expression

and also in the targeting of ASFV waste products to the proteasome. In addition Bulimo (1999) showed that the UBCv1 gene was an essential gene whose level and timing of expression are important in the viability of ASFV. Further work needs to be undertaken to explore the association of ASFV with molecular chaperones and also the proteins involved in the degradative pathways, such as the 20S proteasome and its activators.

8.4 The interactions of the aggresome and ASFV assembly pathways.

In an attempt to produce aggresomes and viral factories in the same cell CHO cells expressing the TCR CD3 δ-subunit in conjunction with proteasome inhibition were infected with ASFV. Surprisingly, the cells could be infected by ASF, however late structural protein synthesis and viral factory formation were blocked. This raised the question as to whether late viral protein synthesis required proteasome activity, or whether aggresomes disrupted virus replication. While these observations were interesting, the experiment showed that it would not be possible to produce virus assembly sites in cells containing aggresomes generated from the inhibition of degradation of the TCR CD3 δ-chain.

Fortunately, over expression of the GFP-250 protein chimera in cells provided a means of producing aggresomes without the requirement of proteasome inhibition. The results showed that cells containing aggresomes could be infected with ASFV, but again late viral protein expression and viral factory formation were prevented. Therefore, it appears that virus replication was inhibited in cells containing aggresomes. This suggests that there may be competition for some or all of the features of the aggresome pathway by ASFV.

8.5 Is there competition between aggresome and ASFV assembly pathways?

This question relates to how ASFV assembly sites are formed. There are two main areas for competition between the two pathways; the first is the actual movement of the virions or viral proteins and subsequent formation of the assembly sites, and the second is the replication and assembly of the virus at the aggresome. For the uptake of ASFV, the virions or viral proteins may be passively recruited into the aggresome pathway, due to the fact that the main role of aggresomes is to sequester abundantly expressed, unusual proteins to a subcellular location (Sanchez et al, 2000). On reaching the site of the aggresome the virus could then begin DNA replication, confident of an aggresome-mediated supply of viral proteins from the cytosol. However, this study showed that aggresomes, whether formed in the presence or absence of a proteasome inhibitor, blocked the formation of viral factories and the production of late viral proteins. This suggests that the passive recruitment of virions or viral proteins was not occurring and that there maybe some competition between ASFV assembly and aggresome pathways. Secondly, if the aggresome pathway has a role in the uptake and movement of ASFV to the assembly site then this would suggest that the aggresome pathway was present before virus entry. However, the published literature suggests that the aggresome pathway is only initiated in response to excess misfolded, aggregated proteins. Therefore, it seems that the competition occurs between the pathways for the elements involved in the formation of the assembly site.

Although the data show that aggresomes prevent the formation of the viral factories, the "hijacking" of the aggresome pathway may still be a possible

mechanism for the generation of assembly sites. In all the experiments described the formation of the aggresomes was always initiated before ASFV infection. Therefore, rather than ASFV initiating the formation of the aggresome pathway to generate assembly sites, the virus has to compete against an established aggresome for the cellular proteins and machinery involved.

The common features shared by the two pathways and therefore potential sites for competition are the microtubule network, the MTOC, the intermediate filament vimentin, mitochondria and possibly the chaperones and proteasomes. As already stated, García-Mata et al (1999) showed that the aggregated proteins move to the aggresome on microtubules, using the dynein/dynactin motors. The use of nocodazole showed that the microtubule network was important for the formation and integrity of the assembly sites and therefore viral proteins may migrate in a similar fashion to the aggregated proteins. Therefore, there may be direct competition for binding to the dynein/dynactin motors on the microtubules.

The second common feature is the association of both the aggresome and viral assembly sites with the microtubule organising centre. As already stated the MTOC may have a role as a scaffold for the formation of the aggresomes and this report and others (Johnston et al, 1998; García-Mata et al, 1999) demonstrated that the aggresomes were located at the MTOC. However, this report also showed that while viral factories were pericentriolar they did not directly locate at the MTOC, which might suggest that there is no direct competition for the MTOC, but for the pericentriolar area.

The collapse of vimentin, one of the more dramatic morphological changes involved in both pathways, is an ideal candidate for competition. The collapse of vimentin is controlled by phosphorylation. So, if the aggresomes have initiated

the phosphorylation of vimentin and its subsequent collapse before ASFV assembly sites are formed, then the virus will probably be unable to acquire a vimentin cage to enclose the viral factories. This would mean that the virus would have no established subcellular location to concentrate viral proteins and begin late viral gene expression. A possible method to investigate the inhibition of viral factory formation by the early collapse of vimentin would be to artificially collapse vimentin during various stages of ASFV infection. One possible method to induce the collapse of vimentin was described by Gyoeva and Gelfand (1991), who showed that collapse could be induced by microinjection of antibodies against intermediate filaments.

The mitochondria, chaperones and possibly the degradative machinery may be an important requirement for ASFV assembly and aggresomes, however it is unlikely that there will be direct competition for these components. The prevention of the formation of ASFV assembly sites appears to be a result of competition between the structural aspects of the aggresomes, and therefore in the actual formation of the ASFV assembly sites. If assembly sites were prevented from forming then there would be no late DNA replication, late protein synthesis or virus assembly and therefore no role for the mitochondria, chaperones and degradative machinery. The competition for these components would only be important once a factory had formed and the data in this report was unable to show factories in cells with aggresomes. In conclusion, ASFV uses many aspects of the aggresome pathway, but the presence of aggresomes blocks the establishment of viral factories, whether this is by direct or competitive inhibition needs to be investigated further.

8.6 Do viruses manipulate the aggresome pathway in general?

The published literature provides several examples of viruses that appear to utilise aspects of the aggresome pathway for their replication and assembly. This section attempts to review this literature.

8.6.1 Viral manipulation of vimentin.

Interestingly, several viruses have been shown to interact with the intermediate filaments, resulting in the collapse of the vimentin. Examples include, reoviruses (Sharpe et al, 1982), Frog virus 3 (Murti and Goorha, 1983), adenovirus (White and Cipriani, 1989), vaccinia virus (Leão Ferreira et al, 1994), human immunodeficiency virus type 1 (Karczewski and Strebel, 1996), influenza A virus (Arcangeletti et al, 1997) and Theiler's virus (Nédellec et al, 1998).

8.6.1.1 Expression of viral proteins causes the collapse of vimentin.

Several publications show that expression of single viral proteins leads to the collapse of vimentin. The E1B 19kDa viral protein of adenoviruses associates with and disrupts the organisation of the vimentin network, which collapses to a juxtanuclear position and disrupts the nuclear lamin protein (White and Cipriani, 1989). The immunofluorescence images are similar to those seen for aggresomes, with the collapsed vimentin and the distortion of the nuclear envelope. Interestingly, there is no increase in the phosphorylation of collapsed vimentin (White and Cipriani, 1989), the mechanism for vimentin collapse around aggresomes suggested by Johnston et al (1998). The HIV-1 Vif protein aggregates in cells and co-localises with collapsed vimentin at a perinuclear location (Karczewski and Strebel, 1996). Surprisingly, they reported that the

vimentin collapse was only associated with the expression of Vif, and not with the expression of other HIV-1 proteins, suggesting a specific interaction between Vif and vimentin. It is difficult to determine whether vimentin collapse is caused by protein aggregation or results from the function of the viral protein. Now that more is known concerning aggresomes, these questions can be answered in the future.

8.6.1.2 Viruses that cause the collapse of vimentin.

Several viruses cause the collapse of vimentin around viral inclusions or assembly sites. Vimentin filaments and mitochondria are reported to surround viral inclusions in cells infected with reovirus (Sharpe et al, 1982). In 1988, Zhonghe et al described the collapse of vimentin around vaccinia virus viral factories in the cytoplasm, and suggested that the vimentin had a role as support for the factories. It was later shown that there was increased phosphorylation of vimentin filaments in vaccinia infected cells (Leão Ferreira et al, 1994). This supports the suggestion of Johnston et al (1998) that phosphorylation leads to the collapse of vimentin. Theiler's virus, a murine encephalomyelitis virus, was shown to collapse vimentin to form shell-like structures around viral inclusions (Nédellec et al, 1998). Finally, vimentin cages form around the assembly sites of the iridovirus frog virus 3 (FV3). This is significant because ASFV was originally classified as an iridovirus and is structurally related to FV3 (Carrascosa et al, 1984; Arzuza et al, 1992). Murti and Goorha (1983) showed that as the FV3 assembly sites formed, vimentin delimited the sites and remained around factories throughout infection. Further work on the characterisation of vimentin collapse and FV3 assembly sites showed that there was a 4-fold increase in

phosphorylation of vimentin in cells infected with FV3 and this phosphorylation preceded the reorganisation of vimentin (Chen et al, 1986). This implies that the collapse of vimentin is controlled by phosphorylation, and the phosphorylation may be induced by the virus. In 1988, Murti et al used the disruption of microtubules and the injection of anti-vimentin antibodies to artificially disrupt the vimentin network prior to FV3 infection. They showed that the collapsed vimentin was unable to reorganise around the viral assembly sites, the assembly sites that formed were aberrant and there was a significant reduction in the number of mature virions present. So, the work of Murti and colleagues has shown that an intact vimentin network was required for FV3 replication and assembly, and this may be regulated by phosphorylation.

8.6.2 Virus induced clustering of mitochondria.

Both the aggresomes and the ASFV assembly sites have been shown to cluster mitochondria, which are thought to supply the energy for the protein folding/degradative machinery or the assembly of ASFV. Several groups have described the clustering of mitochondria in response to viral proteins. As already stated above Sharpe et al (1982) demonstrated that reovirus viral inclusions were enclosed in a vimentin cage, which in turn was surrounded by mitochondria. Also the mitochondria were shown to migrate to a perinuclear region in the cytoplasm of herpes simplex virus (HSV) infected cells, where they co-localised with the tegument proteins of the virus (Murata et al, 2000). Mitochondrial clustering or aggregation has also been shown in response to the hepatitis B virus X protein (Takada et al, 1999) and in liver cells of AIDS patients (Radovanovic et al, 1999). Some of the published literature has implied that the clustering of the

mitochondria was linked to cell death, often in a response to viral infection (Green and Reed, 1998; Takada et al, 1999), however clustering of mitochondria around ASFV factories was suggested as a source of energy, not as a role in cell death. In support of this Murata et al (2000) showed that the clustered mitochondria, around the HSV tegument proteins, maintained their function until at least the middle stage of infection. So, the mitochondria around the viral factories and aggresomes may supply energy at early stages of viral replication and aggresome formation, but further investigation needs to be undertaken to explore the possibility that late in infection or aggresome function the mitochondria may have a role in cell death.

8.6.3 Viral movement on microtubules and MTOC association.

Aggresomes and ASFV assembly sites form at a pericentriolar location and have been shown to have a need for the intact microtubule network. The reoviruses, herpes simplex virus 1 and adenoviruses have all been shown to move to the cellular nucleus on microtubules (Georgi et al, 1990; Sodeik et al, 1997; Suomalainen et al, 1999). In addition to this, HSV-1 has been shown, by electron microscopy, to be associated with dynein (Sodeik et al, 1997) and the overexpression of p50/dynamitin severely reduced the minus end-directed migration of the adenovirus (Suomalainen et al, 1999). This demonstrates the movement of viruses along microtubules to the MTOC, using dynein-dependent minus end-directed motors, is similar to the movement of protein aggregates to the aggresomes. The tegument and envelope proteins of human cytomegalovirus were shown to co-localise in a stable compartment at the MTOC and this area was described as the site of tegumentation and envelopment and

therefore a cytoplasmic assembly site (Sanchez et al, 2000). The published data is encouraging support for the proposal that ASFV moves to the MTOC, using the dynein-dependent minus end-directed motors and that the MTOC acts as a scaffold for the formation of assembly sites.

8.6.4 Viral interaction with cellular folding and degradative machinery.

The use of cellular chaperones has been shown for several viruses, many of which use the ER localised chaperones, such as BiP, calnexin and calreticulin, as these viruses use the secretory pathway for virus assembly. Examples of these viruses are influenza (Tatu et al, 1995; Hebert et al, 1996), hepatitis B virus (Prange et al, 1999), sindbis virus (Mulvey and Brown, 1995), rabies virus (Gaudin, 1997), and hepatitis C virus (Choukhi et al, 1998). This report has shown that ASFV may use molecular chaperones to assist in the replication and assembly of the virus. The tobacco mosaic virus (TMV) has been shown to use the cytosolic chaperones, GrpE and GroEL/GroES, for the correct folding of its coat protein (Hwang et al, 1998). Human papillomavirus uses Hsp70 and Hsp40 chaperones to facilitate viral DNA replication (Liu et al, 1998), and SV40 uses Hsc70 chaperone to promote efficient viral DNA replication (Cambell et al, 1997). Interestingly the large T antigen of SV40 promotes the efficient viral DNA replication as it contains a DNAJ/Hsp40 chaperone domain that interacts with Hsc70 (Cambell et al, 1997). As already stated the Hsp70 chaperone was found at ASFV viral factories, but its co-chaperone (Hdj-2) was not, therefore ASFV may use a similar strategy as SV40 and contain a DNAJ/Hsp40 domain or encode a viral DNAJ/Hsp40 to interact with Hsp70.

As previously stated, one of the main functions of aggresomes is the degradation of misfolded, aggregated proteins by the 20S proteasome. This report has not shown that ASFV assembly sites contained proteasomes, but published literature has shown that ASFV encodes a ubiquitin conjugating enzyme and ASF virions contain ubiquitinated proteins (Hingamp et al, 1992, 1995). In addition, this report has shown that proteasome inhibition blocks the production of late viral proteins, suggesting a role for the proteasome in virus replication. The hepatitis B virus X protein and, as already stated, the herpes simplex virus type 1 (HSV-1) Vmw110 protein have been shown to interact with proteasomes (Hu et al, 1999; Everett et al, 1998). In both cases the proteasome is important in the replication and assembly of the respective viruses. In conclusion, the presence of the proteasomes at the ASFV assembly site may be beneficial for ASFV replication and assembly.

8.7 Conclusion.

This report and the published literature provide strong evidence for ASFV using the aggresome pathway to form viral assembly sites. The evidence suggests that ASFV competes for the components of the pathway and is unable to form viral factories if aggresomes have formed. It appears that ASFV assembly site formation is dependent on a normal cytoskeleton, which it can manipulate to form the assembly sites. In conclusion, the hypothesis "ASFV utilises the aggresome pathway to concentrate structural and accessory proteins in a subcellular structure, which has an established transport system, a concentrated supply of energy, and cytosolic machinery to aid in the correct assembly of the virus" seems to be correct.

9. References

Acharya, R., E. Fry, D. Stuart, G. Fox, D. Rowlands, and F. Brown. 1989. The 3-dimensional structure of foot and mouth disease virus At 2.9-Å Resolution. Nature. **337:**709-716.

Afonso, C. L., C. Alcaraz, A. Brun, M. D. Sussman, D. V. Onisk, J. M. Escribano, and D. L. Rock. 1992. Characterization of p30, a highly antigenic membrane and secreted protein of African swine fever virus. Virology. **189:**368-373.

Aguado, B., E. Viñuela, and A. Alcamí. 1991. African swine fever virus fatty acid acylated proteins. Virology. **185:**942-945.

Alb, J. G., M. A. Kearns, and V. A. Bankaitis. 1996. Phospholipid metabolism and membrane dynamics. Current Opinion in Cell Biology. **8:**534-541.

Alcamí, A., A. L. Carrascosa, and E. Viñuela. 1989a. The entry of African swine fever virus into Vero cells. Virology. **171:**68-75.

Alcamí, A., A. L. Carrascosa, and E. Viñuela. 1989b. Saturable binding sites mediate the entry of African swine fever virus into Vero cells. Virology. **168:**393-398.

Alcamí, A., A. Angulo, C. López-Otín, M. Muñoz, J. M. P. Freije, A. L.

Carrascosa, and E. Viñuela. 1992. Amino acid sequence and structural properties of protein p12, an African swine fever virus attachment protein. Journal of Virology. **66:**3860-3868.

Alcaraz, C., A. Brun, F. Ruiz-Gonzalvo, and J. M. Escribano. 1992. Cell culture propagation modifies the African swine fever virus replication phenotype in macrophages and generates viral subpopulations differing in protein p54. Virus Research. **23:**173-182.

Almazán, F., J. M. Rodríguez, A. Angulo, E. Viñuela, and J. F. Rodríguez. 1993. Transcriptional mapping of a late gene coding for the p12 attachment protein of African swine fever virus. Journal of Virology. **67:**553-556.

Alves de Matos, A. P., and Z. G. Carvalho. 1993. African swine fever virus interaction with microtubules. Biology of the Cell. **78:**229-234.

Amann, E., J. Brosius, and M. Ptashne. 1983. Vectors bearing a hybrid *trp-lac* promoter useful for regulated expression of cloned genes in *Escherichia coli*. Gene. **25:**167-178.

Andrés, G., C. Simón-Mateo, and E. Viñuela. 1993. Characterisation of two African swine fever virus 220-kDa proteins: a precursor of the major structural protein p150 and an oligomer of phosphoprotein p32. Virology. **194:**284-293.

Andrés, G., C. Simón-Mateo, and E. Viñuela. 1997. Assembly of African swine

fever virus: role of polyprotein pp220. Journal of Virology. **71:**2331-2341.

Andrés, G., R. García-Escudero, C. Simón-Mateo, and E. Viñuela. 1998. African swine fever virus is enveloped by a two-membraned collapsed cisterna derived from the endoplasmic reticulum. Journal of Virology. **72:**8988-9001.

Angulo, A., E. Viñuela, and A. Alcamí. 1993. Inhibition of African swine fever virus binding and infectivity by purified recombinant virus attachment protein p12. Journal of Virology. **67:**5463-5471.

Arcangeletti, M. C., F. Pinardi, S. Missorini, F. De Conto, G. Conti, P. Portincasa, K. Scherrer, and C. Chezzi. 1997. Modification of cytoskeleton and prosome networks in relation to protein synthesis in influenza A virus-infected LLC-MK2 cells. Virus Research. **51:**19-34.

Arzuza, O., A. Urzainqui, J. R. Díaz-Ruiz, and E. Tabarés. 1992. Morphogenesis of African swine fever virus in monkey kidney cells after reversible inhibition of replication by cycloheximide. Archives Of Virology. **124:**343-354.

Barros, M. F., C. V. Cunha, and J. V. Costa. 1986. Single-stranded deoxyribonucleic acid nuclease induced by African swine fever virus and associated to the virion. Virology. **155:**183-191.

Blasco, R., M. Agüero, J. M. Almendral, and E. Viñuela. 1989. Variable and

constant regions in African swine fever virus DNA. Virology. **168:**330-338.

Bonifacino, J. S., C. K. Suzuki, J. Lippincott-Schwartz, A. M. Weissman, and R. D. Klausner. 1989. Pre-Golgi degradation of newly synthesized T-cell antigen receptor chains: intrinsic sensitivity and the role of subunit assembly. Journal of Cell Biology. **109:**73-83.

Bonifacino, J. S., P. Cosson, and R. D. Klausner. 1990. Colocalized transmembrane determinants for ER degradation and subunit assembly explain the intracellular fate of TCR chains. Cell. **63:**503-513.

Bonifacino, J. S., and R. D. Klausner. 1994. Degradation of proteins retained in the endoplasmic reticulin. *In* A. Ciechanover and A. L. Schwartz (ed.), Modern cell biology: cellular proteolytic systems. Wiley-Liss, New York. pp137-160.

Bonifacino, J. S., and A. M. Weissman. 1998. Ubiquitin and the control of protein fate in the secretory and endocytic pathways. Annual Review of Cell and Developmental Biology. **14:**19-57.

Borca, M. V., P. Irusta, C. Carrillo, C. L. Afonso, T. Burrage, and D. L. Rock. 1994. African swine fever virus structural protein p72 contains a conformational neutralising epitope. Virology. **201:**413-418.

Borca, M. V., P. M. Irusta, G. F. Kutish, C. Carrillo, C. L. Afonso, T. Burrage, J. G. Neilan, and D. L. Rock. 1996. A structural DNA binding protein of African

swine fever virus with similarity to bacterial histone-like proteins. Archives of Virology. **141:**301-313.

Breese, S. S., and C. J. DeBoer. 1966. Electron microscope observations of African swine fever virus in tissue culture cells. Virology. **28:**420-428.

Breese, S. S., and C. J. DeBoer. 1967. Chemical structure of African swine fever virus investigated by electron microscopy. Journal of General Virology. **1:**251-251.

Breese, S. S., and I. C. Pan. 1978. Electron microscopic observation of African swine fever virus development in Vero cells. Journal of General Virology. **40:**499-502.

Brookes, S. M., L. K. Dixon, and R. M. E. Parkhouse. 1996. Assembly of African swine fever virus: quantitative ultrastructural analysis *in vitro* and *in vivo*. Virology. **224:**84-92.

Bulimo, W. D. 1999. The role of UBCv1 enzyme of African swine fever virus. A thesis submitted to the University of Hertfordshire for the degree of Doctor of Philosophy. 227pp.

Burkhardt, J. K., C. J. Echeverri, T. Nilsson, and R. B. Vallee. 1997. Overexpression of the dynamitin (p50) subunit of the dynactin complex disrupts dynein-dependent maintenance of membrane organelle distribution. Journal of

Cell Biology. **139:**469-484.

Cairns, J. 1960. The initiation of vaccinia infection. Virology. **11:**603-623.

Camacho, A., and E. Viñuela. 1991. Protein p22 of African swine fever virus: An early structural protein that is incorporated into the membrane of infected cells. Virology. **181:**251-257.

Campbell, K. S., K. P. Mullane, I. A. Aksoy, H. Stubdal, J. Zalvide, J. M. Pipas, P. A. Silver, T. M. Roberts, B. S. Schaffhausen, and J. A. DeCaprio. 1997. DnaJ/hsp40 chaperone domain of SV40 large T antigen promotes efficient viral DNA replication. Genes & Development. **11:**1098-1110.

Carrascosa, J. L., J. M. Carazo, A. L. Carrascosa, N. García, A. Santisteban, and E. Viñuela. 1984. General morphology and capsid fine structure of African swine fever virus particles. Virology. **132:**160-172.

Carrascosa, A. L., M. Delval, J. F. Santaren, and E. Viñuela. 1985. Purification and properties of African swine fever virus. Journal of Virology. **54:**337-344.

Carrascosa, J. L., P. González, A. L. Carrascosa, B. Garciá-Barreno, L. Enjuanes, and E. Viñuela. 1986. Localization of structural proteins in African swine fever virus particles by immunoelectron microscopy. Journal of Virology. **58:**377-384.

Carrascosa, A. L., I. Saastre, P. Gonzalez, and E. Viñuela. 1993. Localization of the African swine fever virus attachment protein-p12 in the virus particle by immunoelectron microscopy. Virology. **193:**460-465.

Carvalho, Z. G., A. P. Alves de Matos, and C. Rodrigues-Pousada. 1988. Association of African swine fever virus with the cytoskeleton. Virus Research. **11:**175-192.

Casjens, S., and R. Hendrix. 1988. Control mechanisms is dsDNA bacteriophage assembly. 15-91. *In* R. Calendar (ed.), The Bacteriophages, vol. 1. Plenum Press, New York. pp15-91.

Casjens, S. 1997. Principles of virion structure, function, and assembly. p. 3-37. *In* W. Chiu and R. M. Burnett and R. L. Garcea (ed.), Structural biology of viruses. Oxford University Press, Oxford. pp3-37.

Chellaiah, A., A. Davis, and T. Mohanakumar. 1993. Cloning of a unique human homologue of the *Escherichia coli* DnaJ heat shock protein. Biochimica et Biophysica Acta. **1174:**111-113.

Chen, M., R. Goorha, and K. G. Murti. 1986. Interaction of frog virus-3 with the cytomatrix. IV. Phosphorylation of vimentin precedes the reorganisation of intermediate filaments around the virus assembly sites. Journal of General Virology. **67:**915-922.

Cheng, S. H., R. J. Gregory, J. Marshall, S. Paul, D. W. Souza, G. A. White, C. R. O'Riordan, and A. E. Smith. 1990. Defective intracellular transport and processing of CFTR is the molecular basis of most cystic fibrosis. Cell. **63:**827-834.

Chou, Y. H., J. R. Bischoff, D. Beach, and R. D. Goldman. 1990. Intermediate filament reorganisation during mitosis is mediated by p34cdc2 phosphorylation of vimentin. Cell. **62:**1063-1071.

Choukhi, A., S. Ung, C. Wychowski, and J. Dubuisson. 1998. Involvement of endoplasmic reticulum chaperones in the folding of hepatitis C virus glycoproteins. Journal of Virology. **72:**3851-3858.

Cistué, C., and E. Tabarés. 1992. Expression *in vivo* and *in vitro* of the major structural protein (VP73) of African swine fever virus. Archives of Virology. **123:**111-124.

Cobbold, C., J. T. Whittle, and T. Wileman. 1996. Involvement of the endoplasmic reticulum in the assembly and envelopment of African swine fever virus. Journal of Virology. **70:**8382-8390.

Cobbold, C., and T. Wileman. 1998. The major structural protein of African swine fever virus, p73, is packaged into large structures, indicative of viral capsid or matrix precursors, on the endoplasmic reticulum. Journal of Virology. **72:**5215-5223.

Cobbold, C., S. M. Brookes, and T. Wileman. 2000. Biochemical requirements of virus wrapping by the endoplasmic reticulum: Involvement of ATP and endoplasmic reticulum calcium store during envelopment of African swine fever virus. Journal of Virology. **74:**2151-2160.

Coffin, J. M. 1996. *Retroviridae*: the viruses and their replication. *In* B. N. Fields et al (ed.), Virology, (Third edition), vol. 2. Lippincott-Raven, Philadelphia. pp1767-1847.

Costa, J. V. 1990. African swine fever virus. *In* G. Darai (ed.), Molecular biology of iridoviruses. Kluwer Academic, Boston, MA. pp247-270.

Cudmore, S., P. Cossart, G. Griffiths, and M. Way. 1995. Actin-based motility of vaccinia virus. Nature. **378:**636-638.

Cunha, C. V., and J. V. Costa. 1992. Induction of ribonucleotide reductase activity in cells infected with African swine fever virus. Virology. **187:**73-83.

Cyr, D. M., T. Langer, and M. G. Douglas. 1994. DnaJ-like proteins: molecular chaperones and specific regulators of Hsp70. Trends in Biochemical Sciences. **19:**176-181.

Dales, S., and E. H. Mossbach. 1968. Vaccinia as a model for membrane biogenesis. Virology. **35:**564-583.

Davies, D. R. 1990. The structure and function of the aspartic proteinases. Annual Review of Biophysics and Biophysical Chemistry. **19:**189-215.

Davis, A. R., Y. G. Alevy, A. Cheliaiah, M. T. Quinn, and T. Mohanakumar. 1998. Characterization of HDJ-2, a human 40kD heat shock protein. International Journal of Biochemistry & Cell Biology. **30:**1203-1221.

de la Vega, I., A. González, R. Blasco, V. Calvo, and E. Viñuela. 1994. Nucleotide-sequence and variability of the inverted terminal repetitions of African swine fever virus DNA. Virology. **201:**152-156.

Dixon, L. K., P. J. Wilkinson, K. J. Sumption, and F. Ekue. 1990. Diversity of the African swine fever virus genome. *In* G. Darai (ed.), Molecular Biology of Iridoviruses. Kluwer Academic Publishers, Boston. pp281-295.

Dixon, L. K., D. Rock, and E. Viñuela. 1995. African swine fever-like viruses. Archives of Virology. (Supplement 10):92-94.

Doerfler, W. 1994. Adenoviruses: molecular biology. *In* R. G. Webster and A. Granoff (eds.), Encyclopaedia of virology, vol. 1. Academic Press, London. pp8-14.

Dougherty, W. G., and B. L. Semler. 1993. Expression of virus encoded proteinases: functional and structural similarities with cellular enzymes.

Microbiological Reviews. **57:**781-822.

Echeverri, C. J., B. M. Paschal, K. T. Vaughan, and R. B. Vallee. 1996. Molecular characterisation of the 50-kD subunit of dynactin reveals function for the complex in chromosome alignment and spindle organisation during mitosis. Journal of Cell Biology. **132:**617-633.

Enjuanes, L., A. L. Carrascosa, and E. Viñuela. 1976. Isolation and properties of the DNA of African swine fever (ASF) virus. Journal of General Virology. **32:**479-492.

Escribano, J. M., and E. Tabarés. 1987. Proteins specified by African swine fever virus. 5. Identification of immediate early, early and late proteins. Archives of Virology. **92:**221-232.

Esteves, A., M. I. Marques, and J. V. Costa. 1986. Two-dimensional analysis of African swine fever virus proteins and proteins induced in infected cells. Virology. **152:**192-206.

Esteves, A., G. Ribeiro, and J. V. Costa. 1987. DNA-binding proteins specified by African swine fever virus. Virology. **161:**403-409.

Everett, R. D., A. Orr, and C. M. Preston. 1998. A viral activator of gene expression functions via the ubiquitin-proteasome pathway. EMBO Journal. **17:**7161-7169.

Everett, R. D. 1999. A surprising role for the proteasome in the regulation of herpesvirus infection. Trends in Biochemical Sciences. **24:**293-295.

Feldman, D. E., and J. Frydman. 2000. Protein folding *in vivo*: the importance of molecular chaperones. Current Opinion in Structural Biology. **10:**26-33.

Fenner, F. 1976. Classification and nomenclature of viruses: second report of the international committee on taxonomy of viruses. S. Karger, Basel. 115pp.

Fenner, F., R. Wittek, and K. R. Dumbell. 1989. The orthopoxviruses. Academic Press, London. 432pp.

Franke, W. W., E. Schmid, M. Osborn, and K. Weber. 1978. Different intermediate-sized filaments distinguished by immunofluorescence microscopy. Proceedings of the National Academy of Sciences. **75:**5034-5038.

Freimuth, P., and C. W. Anderson. 1993. Human adenovirus serotype 12 virion precursors Pmu and PVI are cleaved at amino terminal and carboxy terminal sites that conform to the adenovirus 2 endoproteinase cleavage consensus sequence. Virology. **193:**348-355.

Fuchs, E., and K. Weber. 1994. Intermediate filaments: structure, dynamics, function and disease. Annual Review of Biochemistry. **63:**345-382.

García-Beato, R., M. L. Salas, E. Viñuela, and J. Salas. 1992. Role of the host cell nucleus in the replication of African swine fever virus DNA. Virology. **188:**637-649.

García-Mata, R., Z. Bebök, E. J. Sorscher, and E. S. Sztul. 1999. Characterisation and dynamics of aggresome formation by a cytosolic GFP-chimera. Journal of Cell Biology. **146:**1239-1254.

Gaudin, Y. 1997. Folding of rabies virus glycoprotein: epitope acquisition and interaction with endoplasmic reticulum chaperones. Journal of Virology. **71:**3742-3750.

Georgi, A., C. Mottolahartshorn, A. Warner, B. Fields, and L. B. Chen. 1990. Detection of individual fluorescently labeled reovirions in living cells. Proceedings of the National Academy of Sciences. **87:**6579-6583.

Geraldes, A., and M. L. Valdeira. 1985. Effect of chloroquine on African swine fever virus infection. Journal of General Virology. **66:**1145-1148.

Gershon, A. A., D. L. Sherman, Z. L. Zhu, C. A. Gabel, R. T. Ambron, and M. D. Gershon. 1994. Intracellular transport of newly synthesized varicella-zoster virus- final envelopment in the trans Golgi network. Journal of Virology. **68:**6372-6390.

Gómez-Puertas, P., F. Rodriguez, J. M. Oviedo, F. Ramiro-Ibáñez, F. Ruiz-

Gonzalvo, C. Alonso, and J. M. Escribano. 1996. Neutralising antibodies to different proteins of African swine fever virus inhibit both virus attachment and internalisation. Journal of Virology. **70:**5689-5694.

González, A., A. Talavera, J. M. Almendral, and E. Viñuela. 1986. Hairpin loop structure of African swine fever virus DNA. Nucleic Acids Research. **14:**6835-6844.

Goorha, R., and A. Granoff. 1979. Icosahedral cytoplasmic deoxyviruses. *In* H. Fraenkel-Contrat and R.R. Wagner (ed.), Newly characterised vertebrate viruses (Comprehensive Virology 14). pp347-399.

Goto, H., H. Kosako, K. Tanabe, M. Yanagida, M. Sakurai, M. Amano, K. Kaibuchi, and M. Inagaki. 1998. Phosphorylation of vimentin by Rho-associated kinase at a unique amino-terminal site that is specifically phosphorylated during cytokinesis. Journal of Biological Chemistry. **273:**11728-11736.

Gouet, P., J. M. Diprose, J. M. Grimes, R. Malby, J. N. Burroughs, S. Zientara, D. I. Stuart, and P. P. C. Mertens. 1999. The highly ordered double-stranded RNA genome of bluetongue virus revealed by crystallography. Cell. **97:**481-490.

Grand, R. J. A. 1989. Acylation of viral and eukaryotic proteins. Biochemical Journal. **258:**625-638.

Greber, U. F., and H. Kasamatsu. 1996. Nuclear targeting of SV40 and adenovirus. Trends in Cell Biology. **6:**189-195.

Green, D. R., and J. C. Reed. 1998. Mitochondria and apoptosis. Science. **281:**1309-1312.

Griffiths, G., and P. Rottier. 1992. Cell biology of viruses that assemble along the biosynthetic pathway. Seminars in Cell Biology. **3:**367-381.

Grimes, J. M., J. N. Burroughs, P. Gouet, J. M. Diprose, R. Malby, S. Zientara, P. P. C. Mertens, and D. I. Stuart. 1998. The atomic structure of the bluetongue virus core. Nature. **395:**470-478.

Grosenbach, D. W., and D. E. Hruby. 1998. Biology of vaccinia virus acylproteins. Frontiers in Bioscience. **3:**354-364.

Gyoeva, F. K., and V. I. Gelfand. 1991. Coalignment of vimentin intermediate filaments with microtubules depends on kinesin. Nature. **353:**445-448.

Hames, B. D. 1990. Molecular mass estimation. In Hames, B.D. and Rickwood, D. (eds) Gel electrophoresis of proteins. A practical approach. Oxford University Press, Oxford. pp16-21,

Hammond, J. M., S. M. Kerr, G. L. Smith, and L. K. Dixon. 1992. An African swine fever virus gene with homology to DNA ligases. Nucleic Acids Research.

20:2667-2671.

Hannan, C., L. H. Raptis, C. V. Dery, and J. Weber. 1983. Biological and structural studies with an adenovirus type 2 temperature sensitive mutant defective for uncoating. Intervirology. **19:**213-223.

Hebert, D. N., B. Foellmer, and A. Helenius. 1996. Calnexin and calreticulin promote folding, delay oligomerisation and suppress degradation of influenza hemagglutinin in microsomes. EMBO Journal. **15:**2961-2968.

Hellen, C. U. T., H. G. Kräusslich, and E. Wimmer. 1989. Proteolytic processing of polyproteins in the replication of RNA viruses. Biochemistry. **28:**9881-9890.

Hellen, C. U. T., and E. Wimmer. 1992. Maturation of poliovirus capsid proteins. Virology. **187:**391-397.

Hellen, C. U. T., and E. Wimmer. 1992b. The role of proteolytic processing in the morphogenesis of virus particles. Experientia. **48:**201-215.

Henderson, L. E., H. C. Krutzsch, and S. Oroszlan. 1983. Myristyl amino terminal acylation of murine retrovirus proteins: an unusual post-translational protein modification. Proceedings of the National Academy of Sciences. **80:**339-343.

Hingamp, P. M., J. E. Arnold, R. J. Mayer, and L. K. Dixon. 1992. A ubiquitin conjugating enzyme encoded by African swine fever virus. EMBO Journal. **11:**361-366.

Hingamp, P. M., M. L. Leyland, J. Webb, S. Twigger, R. J. Mayer, and L. K. Dixon. 1995. Characterisation of a ubiquitinated protein which is externally located in African swine fever virions. Journal of Virology. **69:**1785-1793.

Hu, Z. Y., Z. S. Zhang, E. Doo, O. Coux, A. L. Goldberg, and T. J. Liang. 1999. Hepatitis B virus X protein is both a substrate and a potential inhibitor of the proteasome complex. Journal of Virology. **73:**7231-7240.

Huppa, J. B., and H. L. Ploegh. 1997. The α chain of the T cell antigen receptor is degraded in the cytosol. Immunity. **7:**113-122.

Hwang, D. J., N. E. Tumer, and T. M. A. Wilson. 1998. Chaperone protein GrpE and the GroEL/GroES complex promote the correct folding of tobacco mosaic virus coat protein for ribonucleocapsid assembly *in vivo*. Archives of Virology. **143:**2203-2214.

Inagaki, M., Y. Nishi, K. Nishizawa, M. Matsuyama, and C. Sato. 1987. Site-specific phosphorylation induces disassembly of vimentin filaments *in vitro*. Nature. **328:**649-652.

Jensen, T. J., M. A. Loo, S. Pind, D. B. Williams, A. L. Goldberg, and J. R.

Riordan. 1995. Multiple proteolytic systems, including the proteasome, contribute to CFTR processing. Cell. **83:**129-135.

Johnston, J. A., C. L. Ward, and R. R. Kopito. 1998. Aggresomes: a cellular response to misfolded proteins. Journal of Cell Biology. **143:**1883-1898.

Jore, J., B. De Geus, R. J. Jackson, P. H. Pouwels, and B. E. Enger-Valk. 1988. Poliovirus protein 3CD is the active protease for processing of the precursor protein P1 *in vitro*. Journal of General Virology. **69:**1627-1636.

Karczewski, M. K., and K. Strebel. 1996. Cytoskeleton association and virion incorporation of the human immunodeficiency virus type 1 Vif protein. Journal of Virology. **70:**494-507.

Kasamatsu, H., and A. Nakanishi. 1998. How do animal DNA viruses get to the nucleus? Annual Review of Microbiology. **52:**627-686.

Katz, E., and B. Moss. 1970. Formation of a vaccinia virus structural polypeptide from a higher molecular weight precursor: inhibition by Rifampicin. Proceedings of the National Academy of Sciences. **66:**677-684.

Kozak, M. 1983. Comparison of initiation of protein-synthesis in prokaryotes, eukaryotes, and organelles. Microbiological Reviews. **47:**1-45.

Kräusslich, H. G., and E. Wimmer. 1988. Viral proteinases. Annual Review of

Biochemistry. **57:**701-754.

Kubota, H., and K. Willison. 1997. Cytosolic chaperonins- an overview. *In* M. Gething (ed.), Guidebook to molecular chaperones and protein folding catalysts. Sambrook & Tooze publication at Oxford University Press, Oxford. pp207-211.

Kuznar, J., M. L. Salas, and E. Viñuela. 1980. DNA-dependent RNA polymerase in African swine fever virus. Virology. **101:**169-175.

Langer, T., C. Lu, H. Echols, J. Flanagan, M. K. Hayer, and F. U. Hartl. 1992. Successive action of DnaK, DnaJ and GroEL along the pathway of chaperone-mediated protein folding. Nature. **356:**683-689.

Lawson, M. A., and B. L. Semler. 1990. Picornavirus protein processing-enzymes, substrates, and genetic regulation. *In* V.R. Racaniello (ed.), Picornaviruses (Current Topics in Microbiology and Immunology 161). Springer-Verlag, Berlin. pp49-87.

Leão Ferreira, R. L., N. Moussatche, and V. M. Neto. 1994. Rearrangement of intermediate filament network of BHK-21 cells infected with vaccinia virus. Archives of Virology. **138:**273-285.

Lewis, V. A., G. M. Hynes, Z. Dong, H. Saibil, and K. Willison. 1992. T-complex polypeptide-1 is a subunit of a heteromeric particle in the eukaryotic cytosol. Nature. **358:**249-252.

Liang, Y. K., G. Akusjarvi, P. Alestrom, U. Pettersson, M. Tremblay, and J. Weber. 1983. Genetic Identification of an Endoproteinase Encoded by the Adenovirus Genome. Journal of Molecular Biology. **167:**217-222.

Liu, F. Y., and B. Roizman. 1991. The herpes simplex virus-1 gene encoding a protease also contains within its coding domain the gene encoding the more abundant substrate. Journal of Virology. **65:**5149-5156.

Liu, J. S., S. R. Kuo, A. M. Makhov, D. M. Cyr, J. D. Griffith, T. R. Broker, and L. T. Chow. 1998. Human Hsp70 and Hsp40 chaperone proteins facilitate human papillomavirus-11 E1 protein binding to the origin and stimulate cell-free DNA replication. Journal of Biological Chemistry. **273:**30704-30712.

López-Otín, C., C. Simon, E. Méndez, and E. Viñuela. 1988. Mapping and sequence of the gene encoding protein p37, a major structural protein of African swine fever virus. Virus Genes. **1:**291-303.

López-Otín, C., C. Simón-Mateo, L. Martinez, and E. Viñuela. 1989. Gly-Gly-X, a novel consensus sequence for the proteolytic processing of viral and cellular proteins. Journal of Biological Chemistry. **264:**9107-9110.

López-Otín, C., J. M. P. Freije, F. Parra, E. Méndez, and E. Viñuela. 1990. Mapping and sequence of the gene coding for protein p72, the major capsid protein of African swine fever virus. Virology. **175:**477-484.

Mangel, W. F., W. J. McGrath, D. L. Toledo, and C. W. Anderson. 1993. Viral DNA and a viral peptide can act as cofactors of adenovirus virion proteinase activity. Nature. **361:**274-275.

Mangel, W. F., D. L. Toledo, J. Z. Ding, R. M. Sweet, and W. J. McGrath. 1997. Temporal and spatial control of the adenovirus proteinase by both a peptide and the viral DNA. Trends in Biochemical Sciences. **22:**393-398.

Manolios, N., J. S. Bonifacino, and R. D. Klausner. 1990. Transmembrane helical interactions and the assembly of the T-cell receptor complex. Science. **249:**274-277.

Mao, J., T. N. Tham, G. A. Gentry, A. Aubertin, and V. G. Chinchar. 1996. Cloning, sequence analysis, and expression of the major capsid protein of the Iridovirus frog virus 3. Virology. **216:**431-436.

Makarov, V. V., M. S. Malakhova, and N. A. Vlasov. 1991. Reaction of African swine fever virus with antibodies and causes of lack of neutralization. Soviet Agricultural Science. **12:**26-30.

Martinez-Pomares, L., C. Simón-Mateo, C. López-Otín, and E. Viñuela. 1997. Characterization of the African swine fever virus structural protein p14.5: a DNA binding protein. Virology. **229:**201-211.

Martins, A., G. Ribeiro, M. I. Marques, and J. V. Costa. 1994. Genetic identification and nucleotide-sequence of the DNA-polymerase gene of African swine fever virus. Nucleic Acids Research. **22:**208-213.

Mathews, R. E. F. 1982. Classification and nomenclature of viruses. Intervirology. **17:**1-199.

Mebus, C. A. 1988. African swine fever. *In* K. Maramorosch and F. A. Murphy and A. J. Shatkin (ed.), Advances in Virus Research, vol. 35. Academic Press Inc, San Diego. pp 251-269.

Miao, B., J. Davis, and E. Craig. 1997. The Hsp70 family- an overview. *In* M. Gething (ed.), Guidebook to molecular chaperones and protein folding catalysts. Sambrook & Tooze publication at Oxford University Press, Oxford. pp3-13.

Mirza, A., and J. Weber. 1980. Infectivity and uncoating of adenovirus cores. Intervirology. **13:**307-311.

Montgomery, R. E. 1921. One form of swine fever occurring in British East Africa (Kenya colony). Journal of Comparative Pathology. **34:**159-191 and 243-262.

Moulton, J., and L. Coggins. 1968. Synthesis and cytopathogenesis of African swine fever virus in porcine cell cultures. American Journal of Veterinary Research. **29:**219-232.

Moura Nunes J, F., D. Vigario J, and M. Terrinha A. 1975. Ultrastructural study of African swine fever virus replication in cultures of swine bone marrow cells. Archives of Virology. **49:**59-66.

Mulvey, M., and D. T. Brown. 1995. Involvement of the molecular chaperone BiP in maturation of Sindbis virus envelope glycoproteins. Journal of Virology. **69:**1621-1627.

Muñoz, M., J. M. P. Freije, M. L. Salas, E. Viñuela, and C. López-Otín. 1993. Structure and expression in *Escherichia coli* of the gene coding for protein p10 of African swine fever virus. Archives of Virology. **130:**93-107.

Murata, T., F. Goshima, T. Daikoku, K. Inagaki-Ohara, H. Takakuwa, K. Kato, and Y. Nishiyama. 2000. Mitochondrial distribution and function in herpes simplex virus-infected cells. Journal of General Virology. **81:**401-406.

Murti, K. G., and R. Goorha. 1983. Interaction of frog virus-3 with the cytoskeleton. I. Altered organisation of microtubules, intermediate filaments, and microfilaments. Journal of Cell Biology. **96:**1248-1257.

Murti, K. G., R. Goorha, and M. W. Klymkowsky. 1988. A functional role for intermediate filaments in the formation of frog virus-3 assembly sites. Virology. **162:**264-269.

Nakamura, N., M. Lowe, T. P. Levine, C. Rabouille, and G. Warren. 1997. The

vesicle docking protein p115 binds GM130, a *cis*-Golgi matrix protein, in a mitotically regulated manner. Cell. **89:**445-455.

Nédellec, P., P. Vicart, C. Laurent-Winter, C. Martinat, M. C. Prévost, and M. Brahic. 1998. Interaction of Theiler's virus with intermediate filaments of infected cells. Journal of Virology. **72:**9553-9560.

Neilan, J. G., Z. Lu, G. F. Kutish, M. D. Sussman, P. C. Roberts, T. Yozawa, and D. L. Rock. 1993. An African swine fever virus gene with similarity to bacterial DNA binding proteins, bacterial integration host factors, and the *Bacillus* phage SPO1 transcription factor, TF1. Nucleic Acids Research. **21:**1496-1496.

Ortín, J., and E. Viñuela. 1977. Requirement of the cell nucleus for African swine fever virus replication in Vero cells. Journal of Virology. **21:**902-905.

Ortín, J., L. Enjuanes, and E. Viñuela. 1979. Cross-links in African swine fever virus DNA. Journal of Virology. **31:**579-583.

Palmenberg, A. C. 1990. Proteolytic processing of picornaviral polyprotein. Annual Review of Microbiology. **44:**603-623.

Pan, I., M. Shimizu, and W. R. Hess. 1980. Replication of African swine fever virus in cell culture. American Journal of Veterinary Research. **41:**1357-1367.

Pessano, S., H. Oettgen, A. K. Bhan, and C. Terhorst. 1985. The T3/T-cell

receptor complex: antigenic distinction between the two 20-kD T3 (T3-δ and T3-ε) subunits. EMBO Journal. **4:**337-344.

Pettersson, R. F. 1991. Protein localization and virus assembly at intracellular membranes. *In* R.W. Compans (ed.), Protein traffic in eukaryotic cells: selected reviews (Current topics in Microbiology and Immunology 170). Springer-Verlag, Berlin. pp67-106.

Plowright, W. 1977. Vector transmission of African swine fever virus. *In* B. Leiss (ed.), Hog cholera/classical swine fever and African swine fever: A seminar in the EEC programme of co-ordination of research on swine fever and a FAO/EEC expert's consultation of the eradication of classical and African swine fever, held in Hanover, September 6-11, 1976. Commission of the European Communities, Luxembourg. pp575-587.

Plowright, W. 1981. African swine fever. *In* J. W. Davis and L. H. Karstad and D. O. Trainer (ed.), Infectious diseases of wild animals. Iowa State University Press, Iowa. pp178-190.

Plowright, W. 1984. African swine fever. *In* G. Wilson and A. Miles and M. T. Parker (ed.), Topley and Wilsons Principles of bacteriology and immunity. Vol. 4. Edward Arnold, London. pp538-554.

Polatnick, J., and W. R. Hess. 1970. Altered thymidine kinase activity in cultured cells inoculated with African swine fever. American Journal of Veterinary

Research. **31:**1609-1613.

Polatnick, J., and W. R. Hess. 1972. Increased deoxyribonucleic acid polymerase activity in African swine fever virus-infected culture cells. Archiv fur die Gesamte Virusforschung. **38:**383-385.

Prahlad, V., M. Yoon, R. D. Moir, R. D. Vale, and R. D. Goldman. 1998. Rapid movements of vimentin on microtubule tracks: kinesin-dependent assembly of intermediate filament networks. Journal of Cell Biology. **143:**159-170.

Prange, R., M. Werr, and H. Löffler-Mary. 1999. Chaperones involved in hepatitis B virus morphogenesis. Biological Chemistry. **380:**305-314.

Presley, J. F., N. B. Cole, T. A. Schroer, K. Hirschberg, K. J. M. Zaal, and J. Lippincott-Schwartz. 1997. ER-to-Golgi transport visualised in living cells. Nature. **389:**81-85.

Radovanovic, J., V. Todorovic, I. Boricic, M. Jankovic-Hladni, and A. Korac. 1999. Comparative ultrastructural studies on mitochondrial pathology in the liver of AIDS patients: clusters of mitochondria, protuberances, "minimitochondria," vacuoles, and virus-like particles. Ultrastructural Pathology. **23:**19-24.

Rashid Bhatti, A., and J. Weber. 1979. Protease of adenovirus type 2. Journal of Biological Chemistry. **254:**12265-12268.

Riordan, J. R., J. M. Rommens, B. S. Kerem, N. Alon, R. Rozmahel, Z. Grzelczak, J. Zielenski, S. Lok, N. Plavsic, J. L. Chou, M. L. Drumm, M. C. Iannuzzi, F. S. Collins, and L. C. Tsui. 1989. Identification of the cystic fibrosis gene: cloning and characterization of complementary DNA. Science. **245:**1066-1072.

Rodriguez, J. M., R. J. Yáñez, J. F. Rodriguez, E. Viñuela, and M. L. Salas. 1993. The DNA polymerase-encoding gene of African swine fever virus-sequence and transcriptional analysis. Gene. **136:**103-110.

Rodríguez, F., C. Alcaraz, A. Eiras, R. J. Yáñez, J. M. Rodríguez, C. Alonso, J. F. Rodríguez, and J. M. Escribano. 1994. Characterization and molecular basis of heterogeneity of the African swine fever virus envelope protein p54. Journal of Virology. **68:**7244-7252.

Rojo, G., M. Chamorro, M. L. Salas, E. Viñuela, J. M. Cuezva, and J. Salas. 1998. Migration of mitochondria to viral assembly sites in African swine fever virus-infected cells. Journal of Virology. **72:**7583-7588.

Rojo, G., R. Garcia-Beato, E. Viñuela, M. L. Salas, and J. Salas. 1999. Replication of African swine fever virus DNA in infected cells. Virology. **257:**524-536.

Rosevear, E. R., M. McReynolds, and R. D. Goldman. 1990. Dynamic properties of intermediate filaments- disassembly and reassembly during mitosis

in baby hamster kidney cells. Cell Motility and the Cytoskeleton. **17:**150-166.

Rouiller, I., S. M. Brookes, A. D. Hyatt, M. Windsor, and T. Wileman. 1998. African swine fever virus is wrapped by the endoplasmic reticulum. Journal of Virology. **72:**2373-2387.

Rueckert, R. R. 1996. *Picornaviridae*: the viruses and their replication. *In* B. N. Fields et al (ed.), Virology, (Third edition), vol. 1. Lippincott-Raven, Philadelphia. pp609-654.

Ryan, M. D., and M. Flint. 1997. Virus-encoded proteinases of the picornavirus super-group. Journal of General Virology. **78:**699-723.

Ryan, M. D., S. Monaghan, and M. Flint. 1998. Virus-encoded proteinases of the Flaviviridae. Journal of General Virology. **79:**947-959.

Salas, M. L., J. Kuznar, and E. Viñuela. 1981. Polyadenylation, methylation, and capping of the RNA synthesized *in vitro* by African swine fever virus. Virology. **113:**484-491.

Sanchez, V., K. D. Greis, E. Sztul, and W. J. Britt. 2000. Accumulation of virion tegument and envelope proteins in a stable cytoplasmic compartment during human cytomegalovirus replication: characterisation of a potential site of virus assembly. Journal of Virology. **74:**975-986.

Sanz, A., B. Garciá-Barreno, M. L. Nogal, E. Viñuela, and L. Enjuanes. 1985. Monoclonal antibodies specific for African swine fever virus proteins. Journal of Virology. **54:**199-206.

Schlesinger, S., and M. J. Schlesinger. 1996. *Togaviridae*: the viruses and their replication, *In* B. N. Fields et al (ed.), Virology, (Third edition), vol. 1. Lippincott-Raven, Philadelphia. pp825-841.

Schloer, G. M. 1985. Polypeptides and structure of African swine fever virus. Virus Research. **3:**295-310.

Schmelz, M., B. Sodeik, M. Ericsson, E. J. Wolffe, H. Shida, G. Hiller, and G. Griffiths. 1994. Assembly of vaccinia virus: the second wrapping cisterna is derived from the trans Golgi network. Journal of Virology. **68:**130-147.

Schultz, A. M., L. E. Henderson, and S. Oroszlan. 1988. Fatty acylation of proteins. Annual Review of Cell Biology. **4:**611-647.

Sharpe, A. H., L. B. Chen, and B. N. Fields. 1982. The interaction of mammalian reoviruses with the cytoskeleton of monkey kidney CV-1 cells. Virology. **120:**399-411.

Shenk, T. 1996. *Adenoviridae*: the viruses and their replication. *In* B. N. Fields et al (ed.), Virology, (Third edition), vol. 2. Lippincott-Raven, Philadelphia. pp2111-2148.

Simón-Mateo, C., G. Andrés, and E. Viñuela. 1993. Polyprotein processing in African swine fever virus: a novel gene expression strategy for a DNA virus. EMBO Journal. **12:**2977-2987.

Simón-Mateo, C., J. M. P. Freije, G. Andrés, C. López-Otín, and E. Viñuela. 1995. Mapping and sequence of the gene encoding protein p17, a major African swine fever virus structural protein. Virology. **206:**1140-1144.

Simón-Mateo, C., G. Andrés, F. Almazán, and E. Viñuela. 1997. Proteolytic processing in African swine fever virus: evidence for a new structural polyprotein, pp62. Journal of Virology. **71:**5799-5804.

Sin, W. C., X. Q. Chen, T. Leung, and L. Lim. 1998. RhoA-binding kinase α translocation is facilitated by the collapse of the vimentin intermediate filament network. Molecular and Cellular Biology. **18:**6325-6339.

Sodeik, B., R. W. Doms, M. Ericsson, G. Hiller, C. E. Machamer, W. van 't Hof, G. van Meer, B. Moss, and G. Griffiths. 1993. Assembly of vaccinia virus: role of the intermediate compartment between the endoplasmic reticulum and the Golgi stacks. Journal of Cell Biology. **121:**521-541.

Sodeik, B., M. W. Ebersold, and A. Helenius. 1997. Microtubule-mediated transport of incoming herpes simplex virus 1 capsids to the nucleus. Journal of Cell Biology. **136:**1007-1021.

Starger, J. M., and R. D. Goldman. 1977. Isolation and preliminary characterization of 10-nm filaments from baby hamster kidney (BHK-21) cells. Proceedings of the National Academy of Sciences. **74:**2422-2426.

Steinert, P. M., and D. R. Roop. 1988. Molecular and cellular biology of intermediate filaments. Annual Review of Biochemistry. **57:**593-625.

Stephens, E. B., and R. W. Compans. 1988. Assembly of animal viruses at cellular membranes. Annual Review of Microbiology. **42:**489-516.

Sun, H. C., S. C. Jacobs, G. L. Smith, L. K. Dixon, and R. M. E. Parkhouse. 1995. African swine fever virus gene j13L encodes a 25-27kDa virion protein with variable numbers of amino-acid repeats. Journal of General Virology. **76:**1117-1127.

Suomalainen, M., M. Y. Nakano, S. Keller, K. Boucke, R. P. Stidwill, and U. F. Geber. 1999. Microtubule-dependent plus- and minus end-directed motilities are competing processes for nuclear targeting of adenovirus. Journal of Cell Biology. **144:**657-672.

Tabares, E., J. Martinez, F. Ruiz Gonzalvo, and C. Sanchez-Botija. 1980. Proteins specified by African swine fever virus. II. Analysis of proteins in infected cells and antigenic properties. Archives of Virology. **66:**119-132.

Takada, S., Y. Shirakata, N. Kaneniwa, and K. Koike. 1999. Association of hepatitis B virus X protein with mitochondria causes mitochondrial aggregation at the nuclear periphery, leading to cell death. Oncogene. **18:**6965-6973.

Tatu, U., C. Hammond, and A. Helenius. 1995. Folding and oligomerization of influenza hemagglutinin in the ER and the intermediate compartment. EMBO Journal. **14:**1340-1348.

Thomas, P. J., P. Shenbagamurthi, J. Sondek, J. M. Hullihen, and P. L. Pedersen. 1992. The cystic fibrosis transmembrane conductance regulator. Effects of the most common cystic fibrosis-causing mutation on the secondary structure and stability of a synthetic peptide. Journal of Biological Chemistry. **267:**5727-5730.

Tihanyi, K., M. Bourbonniere, A. Houde, C. Rancourt, and J. M. Weber. 1993. Isolation and properties of adenovirus type-2 proteinase. Journal of Biological Chemistry. **268:**1780-1785.

Tooze, J., M. Hollinshead, B. Reis, K. Radsak, and H. Kern. 1993. Progeny vaccinia and human cytomegalovirus particles utilize early endosomal cisternae for their envelopes. European Journal of Cell Biology. **60:**163-178.

Towler, D. A., J. I. Gordon, S. P. Adams, and L. Glaser. 1988. The biology and enzymology of eukaryotic protein acylation. Annual Review of Biochemistry. **57:**69-99.

Toyoda, H., M. J. H. Nicklin, M. G. Murray, C. W. Anderson, J. J. Dunn, F. W. Studier, and E. Wimmer. 1986. A second virus-encoded proteinase involved in proteolytic processing of poliovirus polyprotein. Cell. **45:**761-770.

Urzainqui, A., E. Tabarés, and L. Carrasco. 1987. Proteins synthesized in African swine fever virus-infected cells analyzed by two-dimensional gel electrophoresis. Virology. **160:**286-291.

Valdeira, M. L., and A. Geraldes. 1985. Morphological study on the entry of African swine fever virus into cells. Biology of the Cell. **55:**35-40.

van Meer, G. 1993. Transport and sorting of membrane lipids. Current Opinion in Cell Biology. **5:**661-673.

Varshavsky, A. 1997. The ubiquitin system. Trends in Biochemical Sciences. **22:**383-387.

Vigario, J. D., E. Relvas, F. P. Ferraz, J. M. Ribeiro, and C. G. Pereira. 1967. Identification and Localization of genetic material of African swine fever virus by autoradiography. Virology. **33:**173-175.

Viñuela, E. 1985. African swine fever virus. *In* D.B. Willis (ed.), Iridoviridae (Current Topics in Microbiology and Immunology 116). Springer-Verlag, Berlin. pp151-170.

Viñuela, E. 1987. Molecular biology of African swine fever virus. *In* Y. Becker (ed.), African swine fever (Developments in Veterinary Virology). Martinus Nijhof Publishing, Boston. pp31-39.

Vogt, V. M. 1996. Proteolytic processing and particle maturation. *In* H.G. Krausslich (ed.), Morphogenesis and maturation of retroviruses (Current Topics in Microbiology and Immunology 214). Springer-Verlag, Berlin. pp95-131.

Ward, C. L., S. Omura, and R. R. Kopito. 1995. Degradation of CFTR by the ubiquitin-proteasome pathway. Cell. **83:**121-127.

Waters, M. G., D. O. Clary, and J. E. Rothman. 1992. A novel 115-kD peripheral membrane protein is required for intercisternal transport in the Golgi stack. Journal of Cell Biology. **118:**1015-1026.

Weber, J. 1976. Genetic analysis of adenovirus type 2. III. Temperature sensitivity of processing of viral proteins. Journal of Virology. **17:**462-471.

Weissman, A. M. 1994. The T-cell antigen receptor- a multisubunit signalling complex. Chemical Immunology. **59:**1-18.

Wellink, J., and A. van Kammen. 1988. Proteases involved in the processing of viral polyproteins. Archives Of Virology. **98:**1-26.

Welsh, M. J., and A. E. Smith. 1993. Molecular mechanisms of CFTR chloride channel dysfunction in cystic fibrosis. Cell. **73:**1251-1254.

Whealy, M. E., J. P. Card, R. P. Meade, A. K. Robbins, and L. W. Enquist. 1991. Effect of brefeldin A on alphaherpesvirus membrane protein glycosylation and virus egress. Journal of Virology. **65:**1066-1081.

White, E., and R. Cipriani. 1989. Specific disruption of intermediate filaments and the nuclear lamina by the 19-kDa product of the adenovirus E1B oncogene. Proceedings of the National Academy of Sciences. **86:**9886-9890.

Wigley, W. C., R. P. Fabunmi, M. Goo Lee, C. R. Marino, S. Muallem, G. N. DeMartino, and P. J. Thomas. 1999. Dynamic association of proteasomal machinery with the centrosome. Journal of Cell Biology. **145:**481-490.

Wileman, T., G. R. Carson, M. Concino, A. Ahmed, and C. Terhorst. 1990. The γ and ε subunits of the CD3 complex inhibit pre-Golgi degradation of newly synthesized T cell antigen receptors. Journal of Cell Biology. **110:**973-986.

Wileman, T., L. P. Kane, J. Young, G. R. Carson, and C. Terhorst. 1993. Associations between subunit ectodomains promote T cell antigen receptor assembly and protect against degradation in the ER. Journal of Cell Biology. **122:**67-78.

Wilkinson, P. J., and R. C. Wardley. 1978. The replication of African swine

fever virus in endothelial cells. British Veterinary Journal. **134:**280-283.

Wilkinson, P. J. 1989. African swine fever. *In* M. B. Pensaert (ed.), Virus infections of porcines. Elsevier, Amsterdam. pp17-35.

Willison, K. R., K. Dudley, and J. Potter. 1986. Molecular cloning and sequence analysis of a haploid expressed gene encoding T-complex polypeptide-1. Cell. **44:**727-738.

Willison, K., V. Lewis, K. S. Zuckerman, J. Cordell, C. Dean, K. Miller, M. F. Lyon, and M. Marsh. 1989. The T-Complex Polypeptide-1 (TCP-1) is Associated with the Cytoplasmic Aspect of Golgi Membranes. Cell. **57:**621-632.

Yáñez, R. J., and E. Viñuela. 1993. African swine fever virus encodes a DNA ligase. Virology. **193:**531-536.

Yáñez, R. J., J. M. Rodríguez, M. L. Nogal, L. Yuste, C. Enríquez, J. F. Rodriguez, and E. Viñuela. 1995. Analysis of the complete nucleotide sequence of African swine fever virus. Virology. **208:**249-278.

Yang, M., S. Õmura, J. S. Bonifacino, and A. M. Weissman. 1998. Novel aspects of degradation of T cell receptor subunits from the endoplasmic reticulum (ER) in T cells: importance of oligosaccharide processing, ubiquitination, and proteasome-dependent removal from ER membranes. Journal of Experimental Medicine. **187:**835-846.

Yoon, M., R. D. Moir, V. Prahlad, and R. D. Goldman. 1998. Motile properties of vimentin intermediate filament networks in living cells. Journal of Cell Biology. **143:**147-157.

Ypma-Wong, M. F., P. G. Dewalt, V. H. Johnson, J. G. Lamb, and B. L. Semler. 1988. Protein 3CD is the major poliovirus proteinase responsible for cleavage of the P1 capsid precursor. Virology. **166:**265-270.

Yu, H., G. Kaung, S. Kobayashi, and R. R. Kopito. 1997. Cytosolic degradation of T-cell receptor α chains by the proteasome. Journal of Biological Chemistry. **272:**20800-20804.

Zhonghe, Z., G. Krochmalnic, and S. Penman. 1988. The association of vaccinia virus with intermediate filament. Scientia Sinica (Series B). **31:**28-32.

Zhu, Z. L., M. D. Gershon, Y. Hao, R. T. Ambron, C. A. Gabel, and A. A. Gershon. 1995. Envelopment of varicella-zoster virus- targeting of viral glycoproteins to the trans Golgi network. Journal of Virology. **69:**7951-7959.

Zieve, G. W., S. R. Heidemann, and J. R. McIntosh. 1980. Isolation and partial characterisation of a cage of filaments that surrounds the mammalian mitotic spindle. Journal of Cell Biology. **87:**160-169.